

CLEO PACIFIC RIM 2018

July 29 - August 3, 2018 | Hong Kong Convention and Exhibition Centre | HONG KONG



THE HONG KONG
POLYTECHNIC UNIVERSITY
香港理工大學



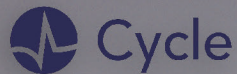
Diamond Sponsor



Gold Sponsors



Exhibitors



www.cleopr2018.org/

CLEO
PACIFIC RIM
2018

Conference Schedule

	Sunday 29 July	Monday 30 July	Tuesday 31 July	Wednesday 1 August	Thursday 2 August	Friday 3 August	Venue
Registration	14:00-17:00 ¹	08:00-18:00 ²	08:00-18:00 ²	08:00-18:00 ²	08:00-18:00 ²	08:00-12:00 ²	1. Room AG206, The Hong Kong Polytechnic University 2. Room S221 Foyer, HKCEC
Lab Tours	14:00-17:00					14:00-17:00	The Hong Kong Polytechnic University
Workshops		08:30-12:30 14:00-18:00					Room S222-S228, HKCEC
Welcome Reception		18:30-20:00					DiVino Patio, Shop 11, 1/F, Causeway Centre, No. 28 Harbour Road, Wanchai
Opening and Plenary Session			08:30-12:30				Convention Hall, HKCEC
Technical Sessions			14:00-18:00 ^{3,4}	08:30-18:00 ^{3,4}	08:30-18:00 ^{3,4}	08:30-12:00 ³	3. Room S223-S228, HKCEC 4. Room S423-S428, HKCEC
Poster Session				14:00-15:30			Room S421, HKCEC
Conference Reception and Banquet				18:00-22:00			Convention Hall, HKCEC
Post-deadline Papers					18:30-20:30		Room S421, HKCEC

Note:

All time reflect Hong Kong time. Please check with conference organizer during conference for schedule Changes and updates.

Pacific Rim Conference on Lasers and Electro-Optics (CLEO-PR) 2018

29 July–3 August, 2018

Hong Kong Convention and Exhibition Centre, Hong Kong

Table of Contents

Welcome Message	2
Committees	3
General Information.....	7
Conference Highlights	9
Workshops.....	11
Conference Directory	17
Agenda of Sessions.....	23
Technical Program	28
Key to Authors and Presiders.....	93

Welcome to Hong Kong and to the Pacific Rim Conference on Lasers and Electro-Optics (CLEO-PR) 2018

Welcome to Hong Kong and to the Pacific Rim Conference on Lasers and Electro-Optics 2018.

It is our great pleasure to invite you to participate in the Pacific Rim Conference on Lasers and Electro-Optics (CLEO-PR) 2018 and share the latest discoveries and news in photonics science, technology and innovations from leading companies, universities and research laboratories throughout the world. CLEO-PR is now one of the largest conferences in the Asia-Pacific region on photonics and relevant technologies.

The CLEO-PR technical conference features a full suite of plenary, invited, and contributed talks given by international academic and industrial researchers who are leaders in their respective fields. The conference this year will feature the following topics: Solid State, Fiber, and Other Laser Sources; Ultrafast and Nonlinear Phenomena; Infrared and Terahertz Technologies and Applications; High Power, High Energy Lasers; Laser Processing and Innovative Applications; Optical Metrology; Quantum Optics, Atomic Physics and Quantum Information; Micro and Nanophotonics; Optical communication systems and networks; Optical Fiber and Waveguide Technologies; Semiconductor and Integrated Optical Devices; Silicon Photonics; Optical Signal Processing; Advanced 2D Materials for Photonics; Biophotonics and Applications; Plasmonics and Metamaterials; Optical Sensors and Systems; Imaging, Display and Storage Technologies; and Microwave Photonics.

With a conference program of broad scope and of the highest technical quality, CLEO-PR provides an ideal venue to keep up with new research directions and an opportunity to meet and interact with the researchers who are leading these advances. We have 792 papers scheduled, including 152 invited and 20 tutorial presentations made by many of the world's most prominent researchers from academia and industry. We thank all the contributors and authors for making CLEO-PR a truly unique, outstanding global event.

Our conference highlight is the Plenary Session scheduled on the morning of Tuesday, July 31. We will have four outstanding, distinguished speakers: Professor Kerry J. Vahala from California Institute of Technology, USA will present on High-Q Physics on-a-Chip for Integrated Optical Time Standards and Frequency Synthesizers; Professor Qihuang Gong from Peking University, China will give a talk on Light Manipulating and Detecting at Micro/Nano-Scale; Professor Bahram Jalali from University of California, Los Angeles, USA will present on Time Stretch and its Applications in Nonlinear Dynamics, Biomedicine, and Computational Imaging; Professor Susumu Noda from Kyoto University, Japan will discuss High-Power and High-Beam Quality Photonic-Crystal Lasers.

In addition to the regular technical sessions, twelve workshops will also be held on Monday, July 30. These workshops will be held free of charge to conference registrants. We would like to thank the workshop organizers and speakers for the excellent program.

Best Student Paper Awards sponsored by OSA will be given to students who are first authors and presenters of exceptional contributed talks. The selection will be made by the subcommittees during the conference. Awards will be presented during the Banquet on Wednesday, August 1. The poster-only session will also be held on 14:00 –15:30, Wednesday, August 1. This is a good chance for you to meet with the authors and discuss technical issues in-depth. Best poster awards sponsored by OSA and selected by conference delegates will be given as well.

In addition to the technical program, we have prepared a rich social program to facilitate meeting and networking with colleagues from all over the world. A conference reception will be held in the evening of Monday, July 30. In the evening of Wednesday, August 1, we will hold a Banquet for conference registrants in the Hong Kong Convention and Exhibition Centre. It is an enormous task to organize a conference and it is impossible to succeed without the dedicated efforts of

many supporters and volunteers. We are indebted to the entire Technical Program Committee led by Hwa-Yaw Tam, Changyuan Yu and Feng Li from The Hong Kong Polytechnic University, and the Subcommittee co-chairs who have worked persistently throughout the whole year to invite speakers, solicit and review papers, organize the technical sessions which results in the excellent technical program. We also thank the local organizing committee led by Chao Lu and Alan Pak Tao Lau from The Hong Kong Polytechnic University, and the staffs and volunteers of the professional societies (especially OSA) organizing and sponsoring the event.

General Chairs



Ping-kong Alexander Wai

The Hong Kong Polytechnic University, Hong Kong



Limin Tong

Zhejiang University, China

Committees

Honorary Chair:

Perry Shum, Nanyang Technological Univ., Singapore

General Chairs:

Ping-kong Alexander Wai, The Hong Kong Polytechnic Univ., Hong Kong SAR

Limin Tong, Zhejiang Univ., China

Technical Program Committee Chairs:

Hwa-Yaw Tam, The Hong Kong Polytechnic Univ., Hong Kong SAR

Changyuan Yu, The Hong Kong Polytechnic Univ., Hong Kong SAR

Feng Li, The Hong Kong Polytechnic Univ., Hong Kong SAR

Technical Program Subcommittee

Co-Chairs and Members

C1. Solid State, Fiber, and Other Laser Sources

Sze Set, Tokyo Univ., Japan (co-chair)

Luming Zhao, Jiangsu Normal Univ., China (co-chair)

Anting Wang, Univ. of Science and Technology of China, China (co-chair)

Chengbo Mou, Shanghai Univ., China (co-chair)

Andrey Komarov, Inst. of Automation and Electrometry, Siberian Branch of the Russian Academy of Sciences, Russia

Zhipei Sun, Aalto Univ., Finland

Zhengqian Luo, Xiamen Univ., China

Xiaoshi Zhang, Kmlabs Inc., USA

Guoqing Chang, DESY-CFEL, Germany

Meng Zhang, Beihang Univ., China

Jungwon Kim, Korea Advanced Inst. of Science and Technology (KAIST), South Korea

William Renninger, Univ. of Rochester, USA

C2. Ultrafast and Nonlinear Phenomena

Anna Peacock, Univ. of Southampton, UK (co-chair)

Jingzhen Li, Shenzhen Univ., China (co-chair)

Jinhui Yuan, Beijing Univ. of Posts and Telecommunications, China (co-chair)

Roberto Morandotti, INRS, Canada (co-chair)

Frederique Vanholsbeeck, Univ. of Auckland, New Zealand

Zhigang Chen, San Francisco State Univ., USA

Günter Steinmeyer, Max-Born-Inst. for Nonlinear Optics and Short Pulse Spectroscopy, Germany

Michael Kues, Glasgow Univ., UK

Mercedeh Khajavikhan, CREOL, Univ. of Central Florida, USA

Lin Zhang, Tianjin Univ., China

Miro Erkintalo, The Univ. of Auckland, New Zealand

Sergei K. Turitsyn, Aston Univ., UK

Shixiang Xu, Shenzhen Univ., China

Peijun Yao, Univ. of Science and Technology of China, China

C3. Infrared and Terahertz Technologies and Applications

Qijie Wang, Nanyang Technological Univ., Singapore (co-chair)

Sai Tak Chu, City Univ. of Hong Kong, Hong Kong SAR (co-chair)

Mo Li, Univ. of Minnesota, USA (co-chair)

Stuart Jackson, Macquarie Univ., Australia (co-chair)

Marco Peccianti, Univ. of Sussex, UK

Matteo Clerici, Univ. of Glasgow, UK

Luca Razzari, Énergie Matériaux Télécommunications Research Centre, Canada

Juejun Hu, MIT, USA

Joey Talgahder, Univ. of Minnesota, USA

Xianshu Luo, Inst. of Microelectronics, Singapore

Yu Luo, Nanyang Technological Univ., Singapore

Bin Zhang, Sun Yat-sen Univ., China

C4. High Power, High Energy Lasers

David Lancaster, Univ. of Southern Australia, Australia (co-chair)

Xia Yu, SIMTech, Singapore (co-chair)

Zhan Sui, Shanghai Inst. of Laser Plasma, CAEP, China (co-chair)

Wanguo Zheng, Laser Fusion Research Center China Academy of Engineering Physics, China

Yuxin Leng, State Key Laboratory of High Field Laser Physics in SIOM, China

Seongwoo Yoo, Nanyang Technological Univ., Singapore

Wenn Jing Lai, Tamasek Laboratory, Singapore

Rich Mildren, Macquarie Univ., Australia

Mark Dubinskiy, U.S. Army Research Laboratory, USA

Pu Wang, Beijing Univ. of Technology, China

Shibin Jiang, AdValue Photonics Inc., USA

C5. Laser Processing and Innovative Applications

Minghui Hong, National Univ. of Singapore, Singapore (co-chair)

Lei Su, Queen Mary Univ. of London, UK (co-chair)

Ming Tang, Huazhong Univ. of Science and Technology, China (co-chair)

Hongyu Zheng, SIMTech A*STAR, Singapore (co-chair)

Martin Wegener, Karlsruhe Inst. of Technology, Germany

Yongfeng Lu, Univ. of Nebraska-Lincoln, USA

Jeng Ywan Jeng, National Taiwan Univ. of Science and Technology, Taiwan

Xiangang Luo, Inst. of Optics and Electronics, Chinese Academy of Science, China

Yingchun Guan, Beihang Univ., China

Baohua Jia, Swinburne Univ. of Technology, Australia

Kan Wu, Shanghai Jiaotong Univ., China

Jiajing Tu, Univ. of Science and Technology Beijing, China

C6. Optical Metrology

Kenneth Kin-Yip Wong, The Univ. of Hong Kong, Hong Kong SAR (co-chair)

Xiaoxiao Xue, Tsinghua Univ., China (co-chair)

Xiaoguang Zhang, Beijing Univ. of Posts and Telecommunications, China (co-chair)

Chao Wang, Univ. of Kent, UK (co-chair)

Alessia Pasquazi, Univ. of Sussex, UK

Victor Torres-Company, Chalmers Univ., Sweden

Zheng Zheng, Beihang Univ., China

Ju Han Lee, Univ. of Seoul, South Korea

Periklis Petropoulos, Univ. of Southampton, UK

Richard Leach, Univ. of Nottingham, UK

Hongxia Zhang, Tianjin Univ., China

Jinlong Yu, Tianjin Univ., China

Adonis Bogris, Technological Educational Inst. of Athens, Greece

C7. Quantum Optics, Atomic Physics and Quantum Information

Nelson Sze Chun Chan, City Univ. of Hong Kong, Hong Kong SAR (co-chair)

Fangwen Sun, Univ. of Science and Technology of China, China (co-chair)

Yunfeng Xiao, Peking Univ., China (co-chair)

Christophe Couteau, Univ. of Technology of Troyes, France (co-chair)

Xiulai Xu, Inst. of Physics, CAS, China

Yong-Chun Liu, Tsinghua Univ., China

Jinshi Xu, Univ. of Science and Technology of China, China

Weibo Gao, Nanyang Technological Univ., Singapore

Lucia Caspani, Univ. of Strathclyde, UK

Guofeng Zhang, The Hong Kong Polytechnic Univ., Hong Kong SAR

David Wilkowski, Univ. of Nice - NTU Singapore, Singapore

Leong Chuang Kwek, National Univ. of Singapore, Singapore

Alberto Bramati, Laboratoire Kastler Brossel, France

C8. Micro and Nanophotonics

Andrew Wing-On Poon, The Hong Kong Univ. of Science and Technology, Hong Kong SAR (co-chair)

Xuming Zhang, The Hong Kong Polytechnic Univ., Hong Kong SAR (co-chair)

Xiangping Li, Jinan Univ., China (co-chair)

Xiaofeng Li, Soochow Univ., China (co-chair)

Dragomir Neshev, Australian National Univ., Australia

Vincenzo Giannini, Imperial College London, UK

Hui Liu, Nanjing Univ., China

Patrick Guo-Qiang Lo, IME A*STAR, Singapore

Joyce Poon, Univ. of Toronto, Canada

Tarik Bourouina, Université Paris-Sud, France

Yi Yang, Wuhan Univ., China

Ningmu Zou, AMD, USA

C9. Optical Communication Systems and Networks

Calvin Chun-Kit Chan, The Chinese Univ. of Hong Kong, Hong Kong SAR (co-chair)

Hoon Kim, KAIST, South Korea (co-chair)

Xian Zhou, Univ. of Science and Technology Beijing, China (co-chair)

Shanguo Huang, Beijing Univ. of Posts and Telecommunications, China (co-chair)

Min Zhang, Beijing Univ. of Posts and Telecom, China

Jian Zhao, National Tyndall Inst., Ireland

Hwan Seok Chung, Electronics and Telecommunications Research Inst. (ETRI), South Korea

Koji Igarashi, Osaka Univ., Japan

Gangxiang Shen, Soochow Univ., China

Kai Ming Feng, National Tsinghua Univ., Taiwan

Zhixin Liu, Univ. College London, UK

Elaine Wong, Univ. of Melbourne, Australia

Bingli Guo, Beijing Univ. of Posts and Telecom, China

C10. Optical Fiber and Waveguide Technologies

Kin-Seng Chiang, City Univ. of Hong Kong, Hong Kong SAR (co-chair)

Guiyao Zhou, South China Normal Univ., China (co-chair)

Lei Wei, Nanyang Technological Univ., Singapore (co-chair)

Zhaohui Li, Sun Yat-Sen Univ., China (co-chair)

Hung-Chun Chang, National Taiwan Univ., Taiwan

Qing Liu, Institut of Microelectronics, A*STAR, Singapore

Simon Fleming, Univ. of Sydney, Australia

Morten Ibsen, Univ. of Southampton, UK

Tao Zhu, Chongqing Univ., China

Guangming Tao, Huazhong Univ. of Science and Technology, China

Yange Liu, Nankai Univ., China

Xingwen Yi, Univ. of Electronic Science and Technology of China, China

C11. Semiconductor and Integrated Optical Devices

Kei May Lau, The Hong Kong Univ. of Science and Technology, Hong Kong SAR (co-chair)

Daohua Zhang, Nanyang Technological Univ., Singapore (co-chair)

Siyuan Yu, Sun Yat-sen Univ., China (co-chair)

Liang Wang, Univ. of Science and Technology of China, China (co-chair)

Marc Sorel, Glasgow Univ., UK

Yunjiang Jin, A*STAR IMRE, Singapore

Guanshi Qin, Jilin Univ., China

Kevin Williams, Eindhoven Technical Univ., Netherlands

Siming Chen, Univ. College London (UCL), UK

Xinlun Cai, Sun Yat-sen Univ., China

Dries Van Thourhout, Ghent Univ., Germany

Pengfei Wang, Shenzhen Univ., China

Tao Lu, Univ. of Victoria, Canada

Yiyang Xie, Beijing Univ. of Technology, China

C12. Silicon Photonics

Hon Ki Tsang, The Chinese Univ. of Hong Kong, Hong Kong (co-chair)

Minghao Qi, Purdue Univ., USA (co-chair)

Daoxin Dai, Zhejiang Univ., China (co-chair)

Kensuke Ogawa, Fujikura, Japan (co-chair)

Di Liang, HP Lab, USA

Ke Xu, Harbin Institute of Technology (Shenzhen), China

Zongfu Yu, Univ. of Wisconsin, USA

Mingbin Yu, Shanghai Inst. of Microsystem and Information Technology, China

Ching Eng Png, Inst. of High Performance Computing, Singapore

Kangping Zhong, Macom Technology Solutions, China

Xingjun Wang, Peking Univ., China

Xuhan Guo, Shanghai Jiao Tong Univ., China

Andy Knights, McMaster Univ., Canada

William Whelan-Curtin, Univ. of St Andrews, Ireland

Harold Chong, Univ. of Southampton, UK

C13. Optical Signal Processing

Chester Shu, The Chinese Univ. of Hong Kong, Hong Kong SAR (co-chair)

Guifang Li, Univ. of Central Florida, USA (co-chair)

Lilin Yi, Shanghai Jiao Tong Univ., China (co-chair)

Lawrence Chen, McGill Univ., Canada (co-chair)

Nan-Kuang Chen, National United Univ., Taiwan

Gabriella Cincotti, Roma Tre Univ., Italy

Bill Corcoran, Monash Univ., Australia

Giampiero Contestabile, Scuola Superiore Sant'Anna, Italy

Xiaojie Guo, Jinan Univ., China

Yong Liu, Univ. of Electronic Science and Technology of China, China

Bob Norwood, Univ. of Arizona, USA

Francesca Parmigiani, Univ. of Southampton, UK

Paul Prucnal, Princeton Univ., USA

Thomas Schneider, TU Braunschweig, Germany

Jian Wang, Huazhong Univ. of Science and Technology, China

Lianshan Yan, Southwest Jiaotong Univ., China

Deepa Venkitesh, Indian Inst. of Technology Madras, India

Qunbi Zhuge, Ciena Corp, Canada

Limin Xiao, Fudan Univ. China

C14. Advanced 2D Materials for Photonics

Dingyuan Tang, Nanyang Technological Univ., Singapore (co-chair)

Qiaoliang Bao, Monash Univ., Australia (co-chair)

Han Zhang, Shenzhen Univ., China (co-chair)

Yuen Hong Tsang, The Hong Kong Polytechnic Univ., Hong Kong SAR (co-chair)

Lain Jong Li, King Abdullah Univ. of Science and Technology, Saudi Arabia

Amos Martinez, Univ. of Tokyo, Japan

Grzegorz Sobon, Wroclaw Univ. of Technology, Poland

Kai Zhang, Suzhou Inst. of Nano-Tech and Nano-bionics (SINANO), CAS, China

Chao-kuei Lee, National Sun Yat-Sen Univ., Taiwan

Rainer Hillenbrand, CIC nanoGUNE and EHU/UPV, Spain

Jian-Bin Xu, The Chinese Univ. of Hong Kong, China

Nicolae C. Panoiu, Univ. College London, UK

Jianhua Hao, The Hong Kong Polytechnic Univ., Hong Kong SAR

Yang Chai, The Hong Kong Polytechnic Univ., Hong Kong SAR

C15. Biophotonics and Applications

Mike Somekh, The Hong Kong Polytechnic Univ., Hong Kong SAR (co-chair)

Yu Chen, Univ. of Maryland in College Park, USA (co-chair)

Tuan Guo, Jinan Univ., China (co-chair)

Nanguang Chen, National Univ. of Singapore, Singapore (co-chair)

Daqing Piao, Oklahoma State Univ., USA

Baohong Yuan, Univ. of Texas, USA

Chao Zhou, Lehigh Univ., USA

Jonathan Liu, Univ. of Washington, USA

Zhiwei Huang, National Univ. of Singapore, Singapore

Jacques Albert, Carleton Univ., Canada

Christophe Caucheteur, Univ. of Mons, Belgium

Xudong Fan, Univ. of Michigan, USA

Aaron H.P. Ho, The Chinese Univ. of Hong Kong, Hong Kong SAR

C16. Plasmonics and Metamaterials

John Pendry, Imperial College, UK (co-chair)

Federico Capasso, Harvard University, USA (co-chair)

Yu Luo, Nanyang Technological Univ., Singapore (co-chair)

Pei Wang, Univ. of Science and Technology of China, China (co-chair)

Dangyuan Lei, The Hong Kong Polytechnic Univ., Hong Kong SAR (co-chair)

Tao Li, Nanjing Univ., China

Zheyu Fang, Peking University, China

Changjun Min, Shenzhen Univ., China

Guixin Li, Southern Univ. of Science and Technology, China

Cheng-Wei Qiu, National Univ. of Singapore, Singapore

Kannatassen Appavoo, The Univ. of Alabama at Birmingham, USA

Mohsen Rahmani, Australian National Univ., Australia

Valentina Krachmalnicoff, Institut Langevin, ESPCI Paris, CNRS, France

C17. Optical Sensors and Systems

Baiou Guan, Jinan Univ., China (co-chair)

Qiang Wu, Northumbria Univ., UK (co-chair)

Liang Wang, The Chinese Univ. of HK, Hong Kong SAR (co-chair)

Liyang Shao, Southern Univ. of Science and Technology, China (co-chair)

Yongkang Dong, Harbin Inst. of Technology, China

Mable Fok, Univ. of Georgia, USA

Zhenzhou Cheng, Univ. of Tokyo, Japan

Xinyu Fan, Shanghai Jiaotong Univ., China

Fei Xu, Nanjing Univ., China

Tommy Chan, Queensland Univ. of Technology, Australia

Serhiy Korposh, Univ. of Nottingham, UK

Yiping Wang, Shenzhen Univ., China

Tomasz Nasilowski, InPhoTech, Poland

Xinyong Dong, China Jiliang Univ., China

C18. Imaging, Display and Storage Technologies

Kevin Tsia, The Hong Kong Univ., Hong Kong SAR (co-chair)

Wen Chen, The Hong Kong Polytechnic Univ., Hong Kong SAR (co-chair)

Xinzhu Sang, Beijing Univ. of Posts and Telecommunications, China (co-chair)

Lixin Xu, Univ. of Science and Technology of China, China (co-chair)

Xudong Chen, National Univ. of Singapore, Singapore

Guohai Situ, Shanghai Inst. of Optics and Fine Mechanics, Chinese Academy of Sciences, China

Cuong Dang, Nanyang Technological Univ., Singapore

Kemao Qian, Nanyang Technological Univ., Singapore

Liangcai Cao, Tsinghua Univ., China

Hongwei Chen, Tsinghua Univ., China

YongKeun Park, Korea Advanced Inst. of Science and Technology (KAIST), South Korea

Quan Liu, Nanyang Technological Univ., Singapore

C19. Microwave Photonics

Shilong Pan, Nanjing Univ. of Aeronautics and Astronautics, China (co-chair)

Xinhuan Feng, Jinan Univ., China (co-chair)

Kun Xu, Beijing Univ. of Posts and Telecommunications, China (co-chair)

Yifei Li, Univ. of Massachusetts Dartmouth, USA (co-chair)

David Marpaung, Univ. of Sydney, Australia

Jianji Dong, Huazhong Univ. of Science and Technology, China

Xihua Zou, Southwest Jiaotong Univ., China

Jonathan Klamkin, UCSB, ECE department, USA

Edward Ackerman, Photonic System Inc., USA

Yanne K. Chembo, FEMTO-ST Inst., France

Hossein-Zadeh Mani, Univ. of New Mexico, USA

Fabien Bretenaker, French National Centre for Scientific Research, France

Atsushi Kanno, NICT, Japan

Special Session and Workshop Committee Chairs

Chao Lu, The Hong Kong Polytechnic Univ., Hong Kong SAR

Aping Zhang, The Hong Kong Polytechnic Univ., Hong Kong SAR

Local Organizing Committee chairs

Chao Lu, The Hong Kong Polytechnic Univ., Hong Kong SAR (Chair)

Alan Pak Tao Lau, The Hong Kong Polytechnic Univ., Hong Kong SAR (Chair)

Kenneth Kin-Yip Wong, The Univ. of Hong Kong, Hong Kong SAR (Co-Chair)

Nelson Sze Chun Chan, City Univ. of Hong Kong, Hong Kong SAR (Co-Chair)

Andrew Poon, The Hong Kong Univ. of Science and Technology, Hong Kong SAR (Co-Chair)

Xuming Zhang, The Hong Kong Polytechnic Univ., Hong Kong SAR (Co-Chair)

Local Arrangement Committee

Feng Li, Jinhui Yuan,
Chao Shang, Xian Zhou,
Nan Guo, Zhe Kang,
Yin Xu, Jiajing Tu,
Zhengyong Liu, Jiahao Huo,
Kun Zhu, Tao Gui,
Dongmei Huang, Xianting Zhang,
Zhiyong Zhao, Chao Jin,
Fengze Tan, Biwei Wang,
Xin Cheng,

The Hong Kong Polytechnic Univ., Hong Kong SAR

Steering Committee

ByoungHo Lee, Seoul National Univ., South Korea (chair)

Shanti Bhattacharya, IIT Madras, India

Woo-Young Choi, Yonsei Univ., South Korea

Benjamin Eggleton, Univ. of Sydney, Australia

Fumio Futami, Tamagawa Univ., Japan

John Harvey, Southern Photonics and Univ. of Auckland,
Australia

Akihiko Kasukawa, Furukawa Electric, Japan

Alan Pak Tao Lau, The Hong Kong Polytechnic Univ.,
Hong Kong SAR

Gong-Ru Lin, National Taiwan Univ., Taiwan

Xu Liu, Zhejiang Univ., China

Chang Hee Nam, Gwangju Inst. of Science and
Technology, South Korea

Takashige Omatsu, Chiba Univ., Japan

Perry Shum, Nanyang Technological Univ., Singapore

Jian-Jun He, Zhejiang Univ., China (Ex-Officio Member)

Hao-chung Kuo, National Chiao-Tung Univ., Taiwan (Ex-
Officio Member)

General Information

Conference Venue: Hong Kong Convention and Exhibition Centre (HKCEC), Hong Kong
Address: No. 1 Expo Drive, Wanchai, Hong Kong



The conference will take place in the HKCEC which is a major landmark located in the heart of Hong Kong on Victoria Harbour. Its vast curtain of glass and 40,000 square-meter aluminum roof is sculpted to echo a seabird soaring in flight. The HKCEC has been awarded 'Best Convention and Exhibition Centre in Asia' 13 times by the industry-leading CEI Asia magazine.

Accessibility

The HKCEC is easily accessible from MTR (metro system in Hong Kong) Wanchai Station, or Wanchai Ferry Pier. It is about a 10-minute walk from the MTR station or ferry pier.

From Hong Kong International Airport to HKCEC

By Bus: Take bus at Airport Ground Transport Center by

- (1) A12 --> [Immigration Tower] (Stop No. 7) --- walk ~10 mins --> HKCEC (~80 mins, HK\$45);
- (2) A11 --> [Fleming Road, Hennessy Road] (Stop No. 10) --- walk ~15 mins --> HKCEC (~90 mins, HK\$40);

By MTR: By Airport Express line from Airport station to Hong Kong station and switch at Central station to Wanchai station (~40 mins, HK\$115)

By Taxi: (~45 mins, ~40 km via Western Harbour Tunnel, ~HK\$360 including WHT Toll)

From Lo Wu/Fu Tian Port of Shenzhen to HKCEC

By MTR: East Rail Line from Lo Wu/Lok Ma Chau to Kowloon Tong, change to Kwun Tong Line (Direction: Whampoa), then change to Tsuen Wan Line (Direction: Central) at Mong Kok, then change to Island Line (Direction: Chai Wan) at Admiralty to Wan Chai. (~70 mins, HK\$51).

The HKCEC is directly connected to two world class hotels: The Grand Hyatt Hong Kong and the Renaissance Harbour View Hotel.

Registration

Registration Hours and Location:

14:00–17:00	Sunday, 29 July	Room AG206, The Hong Kong Polytechnic Univ.
08:00–18:00	Monday - Friday, 30 July - 3 August	S221 Foyer, HKCEC

Speaker Preparation

All oral presenters should check in at the preview room or corresponding session room at least thirty minutes prior to their scheduled talk to upload and check their presentation. **No shows of the oral presentation will be reported to Conference management and these papers will not be published.**

Poster Session

Time: 14:00–15:30, Wednesday August 1
Venue: S421, HKCEC

Over 150 posters will be displayed during CLEO-PR 2018. The poster session is designed to provide an opportunity for selected papers to be presented in greater visual detail and facilitate vivid discussions with attendees. Authors are expected to remain in the vicinity of the bulletin board for the duration of the poster session to answer questions.

Poster Preparation

Authors should prepare their poster before the poster session starts. The poster must not exceed the boundaries of the display board and **A0** size is recommended. **Authors are required to be standing by their poster** for the duration of poster session to answer questions and further discuss their work with attendees. **No shows will be reported to Conference management and these papers will not be published.**

Poster Board Size – 2.0m (Height) X 0.95m (Width) Set-up Time – 10:00 on Wednesday, 1 August

Tear-down Time – 16:00 on Wednesday, 1 August

Exhibition

The CLEO PR Exhibition is open to all attendees. Location: S221, HKCEC

Exhibition Hours:

08:30–18:00	31 July – 2 August
-------------	--------------------

Conference Materials

CLEO PR 2018 Technical Digest will be provided in a USB drive and not available in print form. The CLEO PR 2018 Technical Digest material is composed of the 2-page summaries of invited and accepted contributed papers. The Technical Digest material is included with a technical conference registration and can be found in your registration bag.

The Digest will be available on OSA Publishing's Digital Library (<https://www.osapublishing.org/>) and IEEE Xplore Digital Library (<http://www.ieee.org/web/publications/xplore/>) after the conference. IEEE Xplore Digital Library and OSA Publishing's Digital Library are archived and indexed by INSPEC and EI Compendex, where it will be available to the international research community.

Social Activities

Welcome Reception

The CLEO Pacific Rim 2018 welcome reception will be held on 30 July, 2018.

Location: *Divino Patio, Shop 11, 1/F, Causeway Centre, No. 28 Harbour Road, Wanchai*

Time: 18:30–20:00, Monday, 30 July, 2018

Conference Reception and Banquet

The CLEO Pacific Rim 2018 Banquet will be held in the Convention Hall of the Hong Kong Convention and Exhibition Centre on Wednesday August 1. The Best Paper Awards, OSA Best Student Paper Awards and Best Poster Awards will be presented at the banquet.

Location: *Convention Hall, HKCEC*

Time: 18:00–22:00, Wednesday, 1 August, 2018

Visit Program

Visit program will be organized to the Photonics Research Centre, The Hong Kong Polytechnic Univ. on both 29 July and 3 August, 2018

Gathering point: *AG206, The Hong Kong Polytechnic Univ., Hung Hom, Kowloon*

Time: 14:00–17:00, Sunday, 29 July, 2018

Gathering point: *CD634, The Hong Kong Polytechnic Univ., Hung Hom, Kowloon*

Time: 14:00–17:00, Friday, 3 August, 2018

Conference Highlights

Plenary Session

Time: 8:30–12:30, Tuesday, 31 July

Venue: Convention Hall, HKCEC

Topic: High-Q Physics on-a-Chip for Integrated Optical Time Standards and Frequency Synthesizers

08:55–09:40



Professor Kerry J. Vahala
California Inst. of Technology, USA

Biography:

Professor Kerry J. Vahala is the Jenkins Professor and Professor of Applied Physics at Caltech. He has pioneered the study of nonlinear optics in high-Q optical micro resonators. In the course of this work, his research group has invented optical resonators that hold

the record for highest optical Q on a semiconductor chip. They have applied these devices to study a wide range of nonlinear phenomena including the first demonstration of parametric oscillation and cascaded four-wave mixing in a micro cavity - the central regeneration mechanisms for frequency micro combs. His research has also led to the demonstration of dynamic backaction, a long-anticipated interaction of mechanics and optics mediated by radiation pressure that is responsible for opto-mechanical cooling and recent realizations of mechanical amplification by stimulated phonon emission. Professor Vahala was involved in the early effort to develop quantum-well lasers for optical communications and received the IEEE Sarnoff Award for his research on quantum-well laser dynamics. He has also received an Alexander von Humboldt Award for his work on ultra-high-Q optical microcavities, a NASA achievement award for application of frequency combs to exoplanet detection and is a fellow of the IEEE, the IEEE Photonics Society and the Optical Society of America.

Abstract:

Communication systems leverage the respective strengths of optics and electronics to convey high-bandwidth signals over great distances. These systems were enabled by a revolution

in low-optical-loss dielectric fiber, complex integrated circuits as well as devices that link together the optical and electrical worlds. Today, another revolution is leveraging the advantages of optics and electronics in new ways. At its center is the laser frequency comb which provides a coherent link between these two worlds. Significantly, because the link is also bidirectional, performance attributes previously unique to electronics and optics can be shared. The end result has been transformative for time keeping, frequency metrology, precision spectroscopy, microwave-generation, ranging and other technologies. Even more recently, low-optical-loss dielectrics, now in the form of high-Q optical resonators, are enabling the miniaturization of frequency combs. These new 'microcombs' can be integrated with electronics and other optical components to potentially create systems on-a-chip. I will briefly overview the history and elements of frequency combs as well as the physics of the new microcombs. Application of the microcombs for spectroscopy and LIDAR will be discussed. Finally, efforts underway to develop integrated optical clocks and integrated optical frequency synthesizers using the microcomb element are described.

Topic: Light Manipulating and Detecting at Micro/Nano-Scale

09:40–10:25



Professor Qihuang Gong
Peking Univ., China

Biography:

Professor Qihuang Gong is the Academician of Chinese Academy of Science and member of the world academy of sciences. He is the Founding Director of the Inst. of Modern Optics, Peking Univ.. He also serves as the Vice President of Peking Univ.. In addition, Prof. Gong

serves as Director of Academic committee of the State Key Laboratory for Artificial Microstructure and Mesoscopic Physics. His current research interests are in ultrafast optics and spectroscopy, nonlinear optics, and mesoscopic optical devices for applications in optical information processing and communication. Prof. Gong has received numerous awards,

including The State Natural Science Award (2nd -Class), the Beijing City Science and Technology Award (1st -Class), the Science and Technology Award (1st-Class) of Ministry of Education. He serves as the President of the Chinese Optical Society, Vice President of the Chinese Physical Society. He is the Standing Committee member of China Association for Science and Technology. Prof. Gong is the vice chair for ICO (International Commission for Optics) and vice chair for IUPAP C17.

Abstract:

Micro/nano scale light manipulating can be realized by using nano/mico photonic structures. Using photonic crystal made of the composite materials with large and fast third-order optical nonlinearity, ultrafast and low threshold all-optical switching was demonstrated. Based on tunable Fano resonance or PIT of metallic nanostructures, ultrafast modulations on light transmission were also demonstrated. Moreover, highly sensitive optical sensor were experimentally demonstrated using microcavity and SPP devices.

Topic: Time Stretch and its Applications in Nonlinear Dynamics, Biomedicine, and Computational Imaging

11:00–11:45



Professor Bahram Jalali
Univ. of California, Los Angeles, USA

Biography:

Bahram Jalali is the Director of the Photonics Laboratory, the Northrop-Grumman Endowed Chair and Professor of Electrical and Computer Engineering at UCLA with joint appointments in Biomedical Engineering, California Nano-Systems Inst. (CNSI) and Department of

Surgery at the UCLA School of Medicine. He received his Ph.D. in Applied Physics from Columbia Univ. in 1989 and was with the Physics Research Division of Bell Laboratories in Murray Hill, New Jersey until 1992 before joining UCLA. He is a Fellow of IEEE, the Optical Society of America (OSA), the American Physical Society (APS), American Inst. for Medical and Biological Engineering (AIMBE), and SPIE.

He is the recipient of the R.W. Wood Prize from OSA, Aaron Kressel Award from IEEE, and IET Achievement Medal, and the Pioneer in Technology Award from the Society of Brain Mapping & Therapeutics. He was the Founder and CEO of Cognet Microsystems, a company acquired by Intel in 2001. He was elected into the Scientific American Top 50 and MIT Technology Review Magazine Top 10 in 2005.

Abstract:

Measurements of non-repetitive and rare signals that occur on short timescales requires fast real-time measurements that exceed the speed, precision, and record length of digitizers. Time-stretch is an optical hardware accelerator that overcomes the speed limitations of photodetectors and electronic digitizers and enables ultrafast single-shot spectroscopy, imaging and other measurements at refresh rates reaching billions of frames per second with continuous recording spanning trillions of consecutive frames. The technology has opened a new frontier in measurement science and has led to discovery of several new scientific phenomena in nonlinear optics, laser dynamics and diagnostics of relativistic electron beams. It has also created a new class of instruments that have been integrated with artificial intelligence for sensing and biomedical diagnostics. We review the fundamental principles and applications of time stretch including a spin-off technology known as the phase stretch transform, a new computational imaging algorithm that is emerging as the best edge and texture feature extractor for digital images.

Topic: High-Power and High-Beam Quality Photonic-Crystal Lasers

11:45–12:30



Professor Susumu Noda
Kyoto Univ., Japan

Biograph:

Susumu Noda received B.S., M.S., and Ph.D. degrees from Kyoto Univ., Kyoto, Japan, in 1982, 1984, and 1991, respectively, all in electronics. In 2006, he received an honorary degree from Gent Univ., Gent, Belgium. Currently he is a full Professor with the Department of Electronic Science and Engineering and a

director of Photonics and Electronics Science and Engineering Center (PESEC), Kyoto Univ.. His research interest covers physics and applications of photonic nanostructures based

on photonic crystals. He received various awards, including the IBM Science Award (2000), the Japan Society of Applied Physics Achievement Award on Quantum Electronics (2005), Optical Society of America Joseph Fraunhofer Award/Robert M. Burley Prize (2006), 1st the Japan Society of Applied Physics Fellow (2007), The Commendation for Science and Technology by the Minister of Education, Culture, Sports, Science and Technology (2009), the IEEE Nanotechnology Pioneer Award (2009), The Reo-Esaki Award (2009), Medal with Purple Ribbon (2014), and the Japan Society of Applied Physics Outstanding Achievement Award (2015).

Abstract:

Achieving high-power and high-beam-quality (namely, high-brightness) semiconductor lasers is important for various applications including direct-laser processing and light detection and ranging (LiDAR) for next-generation smart production and mobility. Although semiconductor lasers with various kinds of resonators have been developed, the usefulness of these lasers has been limited by their low brightness, which is more than one order of magnitude smaller than those of existing gas and fiber/disk lasers. The key challenge in realizing high brightness is to increase the output power while maintaining a good beam quality indicated by a low M^2 value. Here, we describe photonic crystal lasers have a potential to enable such a high-brightness operation. Very recently, 10W output power with $M^2 \sim 2$ has been successfully achieved. We believe that these photonic-crystal lasers will allow compact, affordable semiconductor lasers to rival large-scale gas and fiber/disk ones in the future.

OSA Best Student Paper Awards

CLEO-PR 2018 is pleased to announce that this year's Best Student Paper Awards will be sponsored by OSA. There will be 5 recipients.

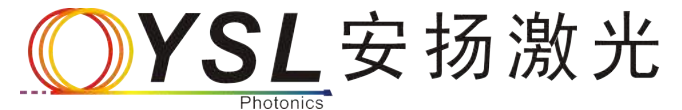
To be eligible for the award, a student must be the first author of the paper and declare his/her student candidature during online submission; and the student must give the presentation at the conference by himself/herself. The selection will be made by the subcommittees during the conference. The prize will be awarded at the conference banquet at Wednesday August 1.

Best Paper Awards

The selection will be made by the TPC chairs and subcommittee chairs during the conference. The awards will be granted at the conference banquet in the evening of Wednesday August 1.

YSL Photonics Best Poster Awards

CLEO-PR 2018 is pleased to announce that the best poster awards will be sponsored by YSL Photonics. The selection will be based on the voting of conference delegates. The prize will be awarded at the Conference Banquet at Wednesday August 1.



Workshops

Workshop 1: Artificial Intelligence in Photonics

Time: 08:30–12:35, 30 July

Venue: Room S223, HKCEC

Organizers:



Bahram Jalali
The University of
California, Los Angeles



Lei Zhang
The Hong Kong
Polytechnic University

Invited Speakers:

08:30–08:55 **Aydogan Ozcan**, *University of California, Los Angeles, USA*

Topic: Machine Learning Enabled Computational Imaging and Sensing for Point-of-Care Medicine and Global Health

08:55–09:20 **Andrew Laine**, *Columbia University, USA*

Topic: Quantitative imaging in classification of lung disease

09:20–09:45 **Lei Zhang**, *The Hong Kong Polytechnic University, Hong Kong SAR*

Topic: Super-Resolution of Nano-scale Particles with A Single Frame Wide-Field Microscopy

09:45–10:10 **Robert Huber**, *Universität zu Lübeck / Institut für Biomedizinische Optik, Germany*

Topic: Towards artificial intelligence for bionic imaging in advanced endo-microscopy

10:30–10:55 **David Brady**, *Duke University, USA*

Topic: Compressive Sampling and Artificial Neural Networks for Array Cameras

10:55–11:20 **YongKeun Park**, *Korea Advanced Institute of Science and Technology, South Korea*

Topic: Rapid and label-free detection of anthrax spores using quantitative phase imaging and deep learning

11:20–11:45 **Alan Pak Tao Lau**, *The Hong Kong Polytechnic University, Hong Kong SAR, China*

Topic: Machine Learning Techniques for Optical Communications and Networks

11:45–12:10 **Muneeb Khalid**, *Alazar Technologies Inc., Canada*

Topic: Data acquisition and direct graphic memory access for high throughput GPU-based processing

12:10–12:35 **Sifeng He**, *University of California, Los Angeles, USA*

Topic: Computationally-efficient and Hallucination-free Medical Image Super Resolution

Workshop 2: Optical Microscopy and Super-Resolution Imaging

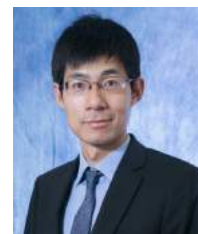
Time: 08:30–12:15, 30 July

Venue: Room S224, HKCEC

Organizers:



Xu Liu
Zhejiang University



Renjie Zhou
The Chinese University of
Hong Kong

Invited Speakers:

08:30–08:55 **Peter So**, *Massachusetts Institute of Technology, USA*

Topic: High Throughput, High Content Neurobiological Imaging

08:55–09:20 **Guoan Zheng**, *University of Connecticut, USA*

Topic: Fourier Ptychographic Imaging and a Machine-learning Approach

09:20–09:45 **Yongkeun Park**, *Korea Advanced Institute of Science and Technology, South Korea*

Topic: Holotomography for Non-invasive Label-free 3D Imaging of Live Cells and Tissues

09:45–10:10 **Gabriel Popescu**, *University of Illinois at Urbana-Champaign, USA*

Topic: Quantitative Histopathology of Stained Tissues using Color Spatial Light Interference (cSLIM)

10:30–10:55 **Zhuyuan Wang**, *Southeast University, China*

Topic: Single Molecule Localization Imaging and SERS Detection of Exosomes for Cancer Diagnosis

10:55–11:20 **Kimani Toussaint**, *University of Illinois at Urbana-Champaign, USA*

Topic: Polarimetric-Based Quantitative Second-Harmonic Generation Microscopy

11:20–11:45 **Cuifang Kuang**, *Zhejiang University, China*

Topic: Super-resolution Volume Imaging based on Multi-angle TIRF Microscopy

11:45–12:15 **Panel discussion**

Workshop 3: Advanced Laser Micro-Nanofabrication for Photonics

Time: 14:00–18:00, 30 July
Venue: Room S222, HKCEC

Organizers:



Hong-Bo Sun
Tsinghua University



Saulius Juodkazis
Swinburne University of
Technology



A. Ping Zhang
The Hong Kong Polytechnic University

Invited Speakers:

14:00–14:25 **Andrei Rode**, *Australian National University, Australia*

Topic: Material modification at Megabar pressures with ultrashort microjoule pulses

14:25–14:50 **Kwang-Sup Lee**, *Hannam University, South Korea*

Topic: Diverse applications of 3D nano/micro-structures fabricated by two-photon photolithography

14:50–15:15 **Feng Chen**, *Shandong University, China*

Topic: Femtosecond laser writing of nonlinear optical waveguides

15:15–15:40 **Yoshiaki Nishijima**, *Yokohama National University, Japan*

Topic: Sub-micron plasmonic metasurfaces for mid infrared sensing application

16:00–16:25 **David Moss**, *Swinburne University of Technology, Australia*

Topic: Microcombs for photonic microwave and RF devices

16:25–16:50 **Vygantas Mizeikis**, *Shizuoka University, Japan*

Topic: Fabrication of optical field concentrator structures using direct laser write technique

16:50–17:15 **Qi-Dai Chen**, *Jilin University, China*

Topic: Micro-optics elements fabricated by femtosecond laser direct writing

17:15–17:40 **F. Ömer Ilday**, *Bilkent University, Turkey*

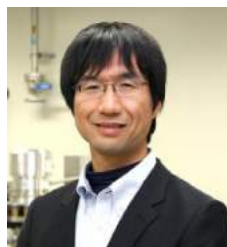
Topic: Ultrafast laser-controlled, nonlinear feedback-driven self-organization of nanostructures

17:40–18:00 **Panel discussion**

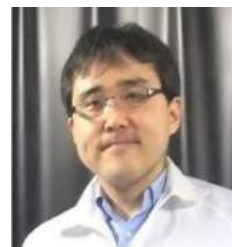
Workshop 4: Advanced THz Devices and Systems

Time: 08:30–12:30, 30 July
Venue: Room S225, HKCEC

Organizers:



Yukio Kawano
Tokyo Institute of
Technology



Shinichi Watanabe
Keio University

Invited Speakers:

08:30–09:00 **Christoph Lange**, *University of Regensburg, Germany*

Topic: Nonlinear subcycle THz quantum dynamics of electronic charges and spins

09:00–09:30 **Hyunsoo Yang**, *National University of Singapore, Singapore*

Topic: Advancing terahertz technology using spintronics

09:30–10:00 **Manfred Helm**, *Helmholtz-Zentrum Dresden-Rossendorf, Germany*

Topic: THz relaxation dynamics and nonlinear optics in graphene

10:30–11:00 **Jérôme Faist**, *ETH Zurich, Switzerland*

Topic: Terahertz Quantum Cascade Lasers: single mode operation and frequency combs

11:00–11:30 **Takayuki Watanabe**, *Tohoku University, Japan*

Topic: Broadband terahertz light emission and lasing operation in current-injection distributed-feedback dual-gate graphene-channel field-effect transistor

11:30–12:00 **Ya Zhang**, *The University of Tokyo, Japan*

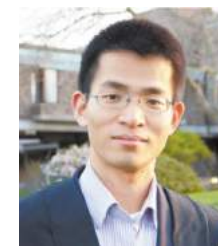
Topic: Novel thermomechanical terahertz detection by using fundamental and coupled modes in doubly clamped MEMS beam resonators

12:00–12:30 **Panel discussion**

Workshop 5: Photonic Quantum Computing

Time: 08:30–12:30, 30 July
Venue: Room S226, HKCEC

Organizers:



Chao-Yang Lu
University of Science and
Technology of China



Sven Hoefling
University of Wurzburg

Invited Speakers:

08:30–08:55 **Satoshi Iwamoto**, *The University of Tokyo, Japan*

Topic: Advances in quantum dot cavity quantum electrodynamics using photonic crystal nanocavities

08:55–09:20 **Niels Gregersen**, *Technical University of Denmark, Denmark*

Topic: Designing single-photon sources: towards unity

09:20–09:45 **Fabio Sciarrino**, *Sapienza Università di Roma, Italy*

Topic: Machine learning for processing and certification of photonic quantum information

09:45–10:10 **Anthony Laing**, *University of Bristol, UK*

Topic: Photonic simulations of molecular quantum dynamics

10:30–10:55 **Leonardo Midolo**, *University of Copenhagen, Denmark*

Topic: Quantum photonic circuits with semiconductor quantum dots

10:55–11:20 **Wenfu Zhang**, *Xi'an Institute of Optics and Precision Mechanics, CAS, China*

Topic: Silicon-based high-index-contrast waveguides for nonlinear optics and quantum photonics

11:20–11:45 **Daniel Riedel**, *University of Basel, Switzerland*

Topic: Deterministic enhancement of coherent photon generation from a nitrogen-vacancy centre in ultrapure diamond

11:45–12:10 **John O'Hara**, *University of Sheffield, UK*

Topic: High Purcell factor generation of indistinguishable on-chip single photons

12:10–12:30 **Yuanzhao Yao**, *National Institute for Materials Science, Japan*

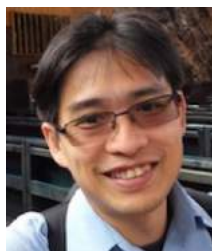
Topic: Excitonic aharonov-bohm effect in ring-shaped semiconductor nanostructures

Workshop 6: Topology and Novel Symmetry in Optics

Time: 08:30–12:15, 30 July

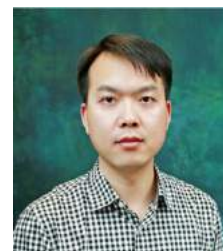
Venue: Room S227, HKCEC

Organizers:



Jensen T. H. Li

The Hong Kong University of Science and Technology



Danguan Lei

The Hong Kong Polytechnic University

Invited Speakers:

08:30–08:55 **Nicholas X. Fang**, *Massachusetts Institute of Technology, USA*

Topic: Collective Behaviors of 2D Plasmon-Polaritons: From Topological States to Emission Engineering

08:55–09:20 **Yidong Chong**, *Nanyang Technological University, Singapore*

Topic: Magneto-optical Dirac cones

09:20–09:45 **Namkyoo Park**, *Seoul National University, Korea*

Topic: Symmetries in Optical Hamiltonians for Isospectrality

09:45–10:10 **Jianwen Dong**, *Sun Yat-Sen University, China*

Topic: All-dielectric valley photonic crystals: Paving the way to topological nanophotonics

10:30–10:55 **Baile Zhang**, *Nanyang Technological University, Singapore*

Topic: Spin-valley locking and topological phase transition in photonic crystals

10:55–11:20 **Qinghai Song**, *Harbin Institute of Technology, China*

Topic: Microlasers around exceptional points and their applications

11:20–11:45 **Haitao Jiang**, *Tongji University, China*

Topic: Experimental demonstration of the robust edge states in a split-ring-resonator chain

11:45–12:15 **Panel discussion**

Workshop 7: Optical Resonators: Fundamentals and Applications

Time: 14:00–17:45, 30 July

Venue: Room S223, HKCEC

Organizers:



Lan Yang

Washington University in St. Louis



Sile Nic Chormaic

Okinawa Institute of Science and Technology Graduate

Invited Speakers:

14:00–14:25 **Kyungwon An**, *Seoul National University, South Korea*

Topic: Coherent thresholdless lasing by single-atom super-radiance

14:25–14:50 **Tal Carmon**, *Technion – Israel Institute of Technology, Israel*

Topic: Flying nano-couplers make an irreversible index of refraction

14:50–15:15 **Chunhua Dong**, *University of Science and Technology of China, China*

Topic: Optomechanically induced non-reciprocity

15:15–15:40 **Pascal Del'Haye**, *National Physical Laboratory in Teddington, UK*

Topic: Spontaneous symmetry breaking and optically induced nonreciprocity of counter propagating light in microresonators

16:00–16:25 **Takasumi Tanabe**, *Keio University, Japan*
Topic: Brillouin lasing in a coupled toroid microcavities system

16:25–16:50 **Yun-Feng Xiao**, *Peking University, China*
Topic: Ultra-high-Q asymmetric microcavity optics and photonics

16:50–17:15 **Andrew Poon**, *The Hong Kong University of Science and Technology, Hong Kong SAR*
Topic: Integrated microdisk lasers and nonlinear light sources on a silicon chip

17:15–17:45 **Panel discussion**

Workshop 8: Microstructured Optical Fibers and Applications

Time: 14:00–18:00, 30 July
Venue: Room S224, HKCEC

Organizers:



Wei Jin
The Hong Kong Polytechnic University



Yingying Wang
Beijing University of Technology

Invited Speakers:

14:00–14:25 **Jonathan Knight**, *University of Bath, UK*
Topic: Hollow optical fibres: What do we add by taking away the core?

14:25–14:50 **Xin Jiang**, *Max Planck Institute for the Science of Light, Germany*
Topic: Soft-glass micro-/nano-structured fibres

14:50–15:15 **Wei Ding**, *Institute of Physics, CAS, China*
Topic: Confinement loss in hollow-core negative curvature fiber

15:15–15:40 **Tristan Kremp**, *OFS laboratory, USA*
Topic: Improved Design and Fabrication of Low Loss Single Mode Photonic Bandgap Hollow Core Fibers

16:00–16:25 **Markus Schmidt**, *Leibniz Institute of Photonic Technology, Germany*
Topic: Optofluidic microstructured fibers: a tool to detect freely diffusing nanoobjects

16:25–16:50 **John Travers**, *Heriot-watt university, UK*
Topic: Nonlinear optics in gas-filled microstructured fibres

16:50–17:15 **Tijmen G. Euser**, *University of Cambridge, UK*
Topic: Optofluidic hollow-core photonic crystal fiber

17:15–17:40 **Wei Jin**, *The Hong Kong Polytechnic University, Hong Kong SAR*
Topic: Photonic crystal fiber gas sensors

17:40–18:00 **Panel discussion**

Workshop 9: Tailored Complex Optical Fields: from Twisted Light to Structured Light

Time: 08:30–18:00, 30 July
Venue: Room S228, HKCEC

Organizers:



Jian Wang
Huazhong University of Science and Technology



Andrew Forbes
University of the Witwatersrand



Siddharth Ramachandran
Boston University

Invited Speakers:

08:30–09:00 **Federico Capasso**, *Harvard University, USA*
Topic: J-plates for spin to total angular momentum conversion and complex structured light generation

09:00–09:30 **Siddharth Ramachandran**, *Boston University, USA*
Topic: Opto-mechanical interactions with OAM states

09:30–10:00 **Andrew Forbes**, *University of the Witwatersrand, South Africa*
Topic: Ghost imaging with structured photons

10:30–11:00 **Cornelia Denz**, *University of Muenster, Germany*
Topic: Tailored vectorial light landscapes pioneer applications in nanophotonics and quantum optics

11:00–11:30 **Yangjian Cai**, *Soochow University, China*
Topic: Manipulating the spatial coherence of vortex beam and orbital angular moment measurement

11:30–12:00 **Takashige Omatsu**, *Chiba University, Japan*
Topic: Wavelength-versatile vortex parametric sources

12:00–12:30 **Mo Mojahedi**, *University of Toronto, Canada*
Topic: Longitudinally structured light and its applications

14:00–14:30 **Qiwen Zhan**, *University of Shanghai for Science and Technology, China; University of Dayton, USA*
Topic: Complex optical fields: recent advances and future perspectives

14:30–15:00 **Filippo Romanato**, *University of Padova, Italy*
Topic: iMux: integrated device for orbital angular momentum mode division multiplexing

15:00–15:30 **Bora Ung**, *Université du Québec, Canada*
Topic: Annular beams: their generation and transmission in optical fibers

16:00–16:30 **Xiaocong Yuan**, *Shenzhen University, China*
Topic: Singular optical beam multiplexing communication for next generation high performance computing

16:30–17:00 **Alan Willner**, *University of Southern California, USA*
Topic: Some practical issues with free-space OAM-based optical communications

17:00–17:30 **Jian Wang**, *Huazhong University of Science and Technology, China*

Topic: Structured light communications: advances and perspectives

17:30–18:00 **Panel discussion**

Workshop 10: Visible Light Communications

Time: 14:00–17:20, 30 July

Venue: Room S225, HKCEC

Organizers:



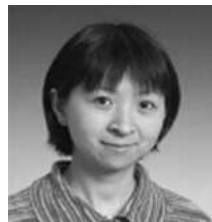
Nan Chi
Fudan University



Shinichiro Haruyama
Keio University



Boon Ooi
King Abdullah University of Science and Technology



Haiyan Ou
Technical University of Denmark



Steve Hranilovic
McMaster University

Tutorial Speaker:

14:00–14:45 **Boon S. Ooi**, *King Abdullah University of Science and Technology, Saudi Arabia*

Topic: Visible Light Communication: Devices and Systems

Invited Speakers:

14:45–15:15 **Takaya YAMAZATO**, *Nagoya University, Japan*
Topic: Overview of image-sensor communication

15:15–15:45 **Gong-Ru Lin**, *National Taiwan University, Taiwan, R.O.C.*

Topic: Visible Light Communication for White-Light and Underwater Applications

16:00–16:20 **Anthony E. Kelly**, *University of Glasgow, UK*
Topic: InGaN/GaN Laser Diodes for Visible Light Communications and Beyond

16:20–16:40 **Jaafar M. H. Elmirghani**, *University of Leeds, UK*
Topic: VLC Systems with CGHs

16:40–17:00 **Jin Xu**, *Zhejiang University, China*
Topic: Practical Considerations on Underwater Wireless Optical Communication

17:00–17:20 **Panel discussion**

Workshop 11: Advanced Laser Display

Time: 14:00–18:00, 30 July

Venue: Room S226, HKCEC

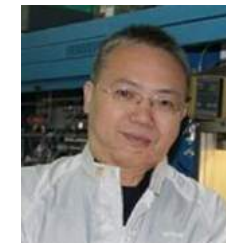
Organizers:



Lixin Xu
University of Science and Technology of China



Yong Bi
Technical Institute of Physics and Chemistry, CAS



Degang Zhao
Institute of Semiconductors, CAS

Invited Speakers:

14:00–14:30 **Yong Bi**, *Technical Institute of Physics and Chemistry, CAS, China*
Topic: High Efficiency and Compact Lasers Modules for Laser

14:30–15:00 **Degang Zhao**, *Institute of Semiconductors, CAS, China*
Topic: Performance improvement of GaN-based laser diodes by considering the residual carbon impurities and modulating the device structure

15:00–15:30 **Fushan Li**, *Fuzhou University, China*
Topic: Quantum dot light-emitting display technology

16:00–16:30 **Lixin Xu**, *University of Science and Technology of China, China*
Topic: Laser display: theory and technology

16:30–17:00 **Wenjiang Shen**, *Suzhou Institute of Nano-tech and Nano-bionics, CAS, China*

Topic: MEMS 2D scanning micromirror for Laser Display

17:00–17:30 **Zhaomin Tong**, *Shanxi University, China*

Topic: Methods for Laser Speckle Reduction in Projection Displays

17:30–18:00 **Panel discussion**

16:30–17:00 **Guojia Fang**, *Wuhan University, China*

Topic: Enhanced performance of perovskite solar cells with electron transport layer of SnO₂ quantum dots

17:00–17:30 **Xuming Zhang**, *The Hong Kong Polytechnic University, Hong Kong SAR*

Topic: Microfluidics for photoenzymatic CO₂ conversion using solar energy

17:30–18:00 **Panel discussion**

Workshop 12: Solar Energy Materials and Devices

Time: 14:00–18:00, 30 July

Venue: Room S227, HKCEC

Organizers:



Feng Yan

*The Hong Kong
Polytechnic University*



Gang Li

*The Hong Kong
Polytechnic University*

Invited Speakers:

14:00–14:30 **Peng Wang**, *Zhejiang University, China*

Topic: Organic dye-sensitized solar cells

14:30–15:00 **Baoquan Sun**, *Soochow University, China*

Topic: Nanostructured silicon used for integrating energy harvesting device

15:00–15:30 **Tae-Dong Kim**, *Hannam University, Republic of Korea*

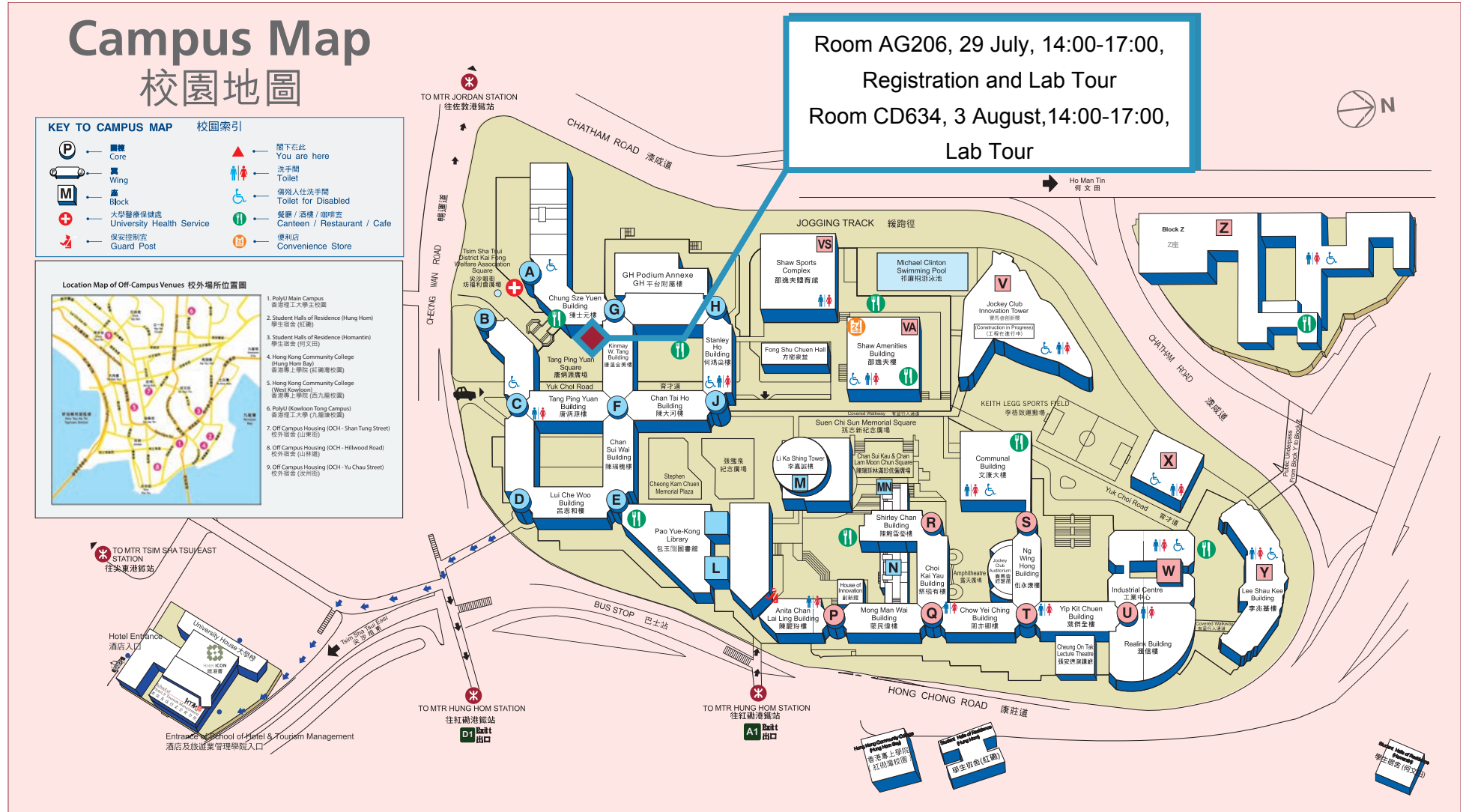
Topic: Enhanced photovoltaic performance of polymeric solar cells through side-chain engineering

16:00–16:30 **Jun Liu**, *Changchun Institute of Applied Chemistry, CAS, China*

Topic: n-Type polymer semiconductors containing boron-nitrogen coordination bond and their application in all polymer solar cells

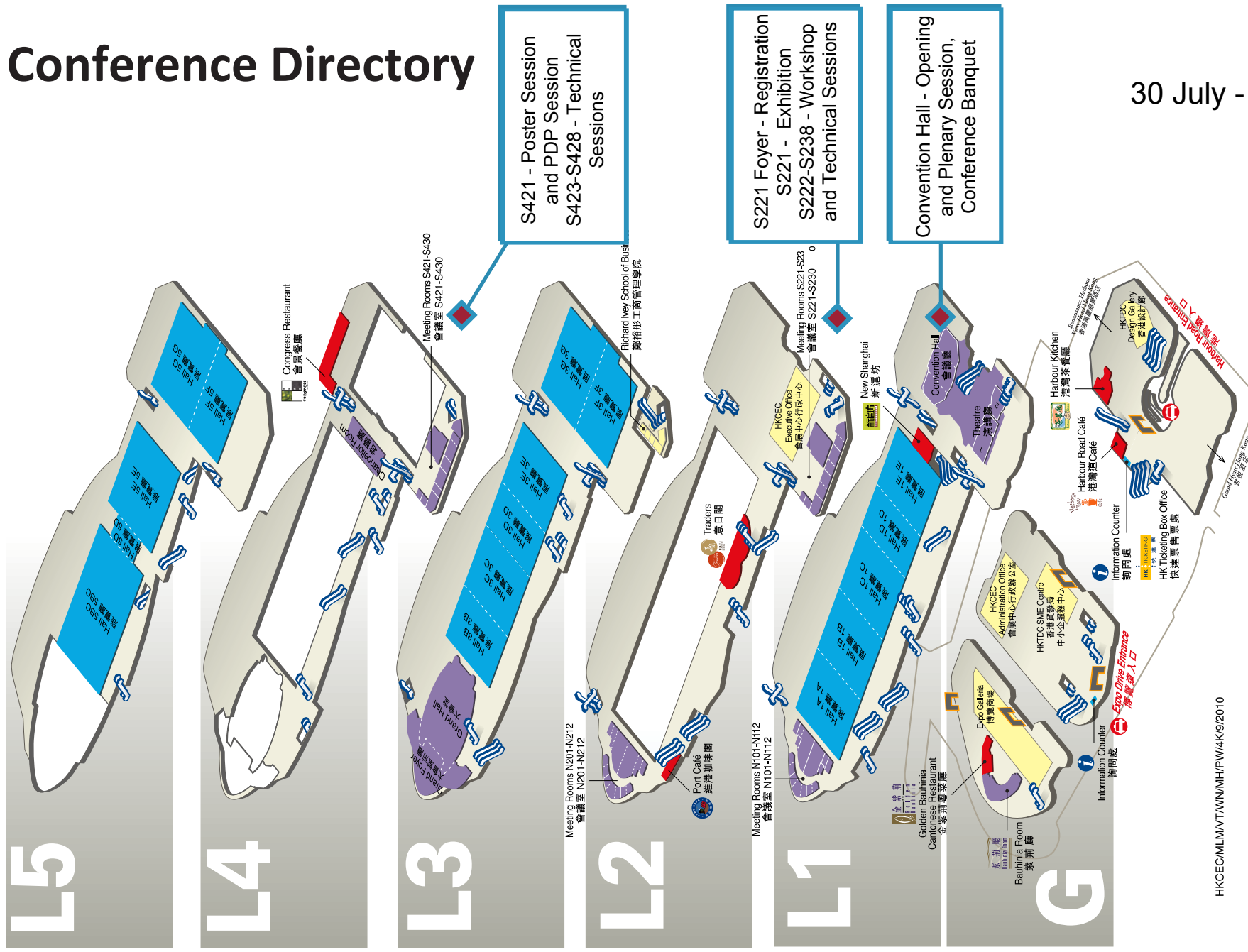
Conference Directory

29 July and 3 August



Conference Directory

30 July - 3 August

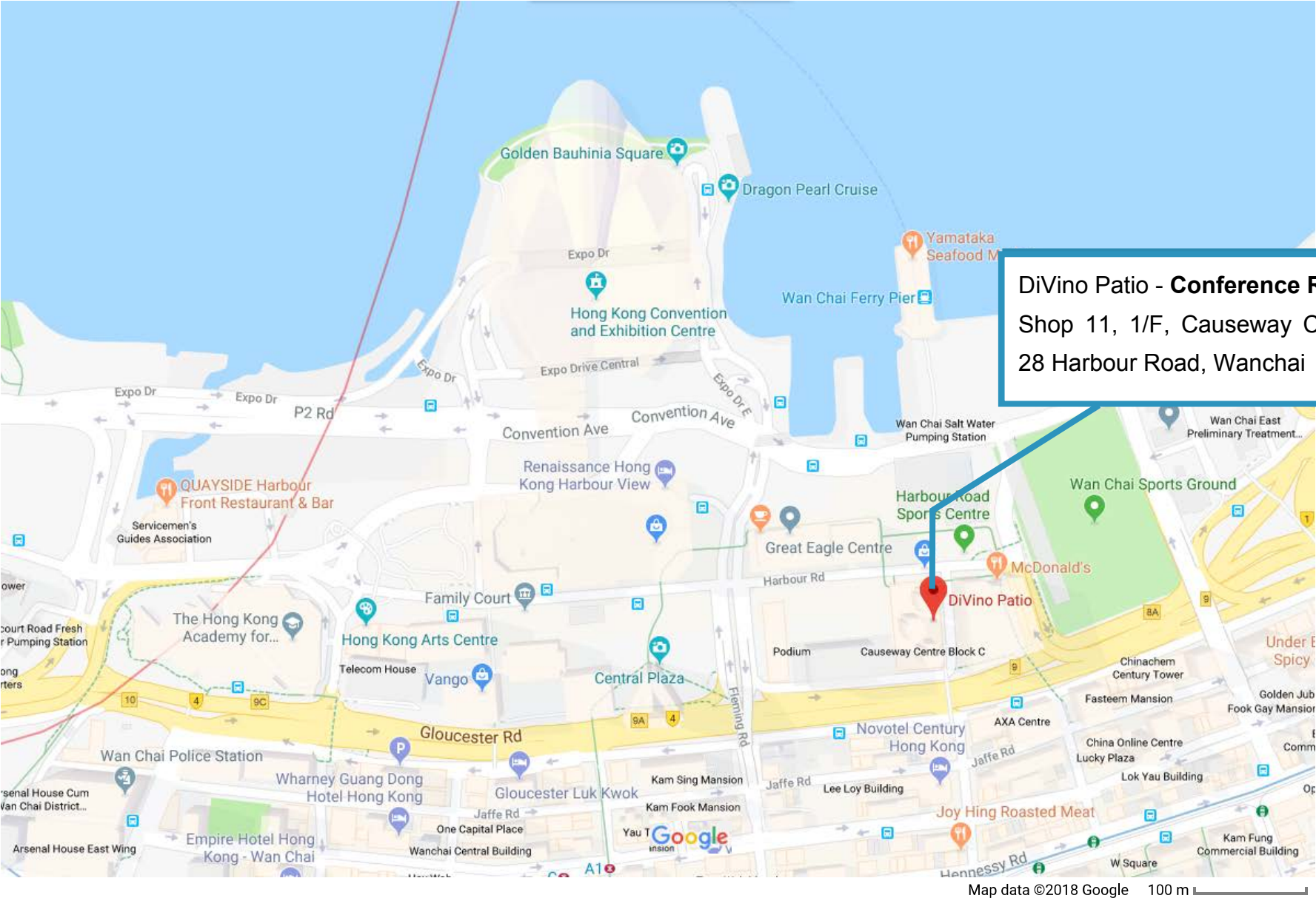


HKCEC/MLM/VTWN/HPW/4K/9/2010

Expo Drive Hall, Car Parks & Loading Facilities
博覽道展廳、停車場及卸貨設施

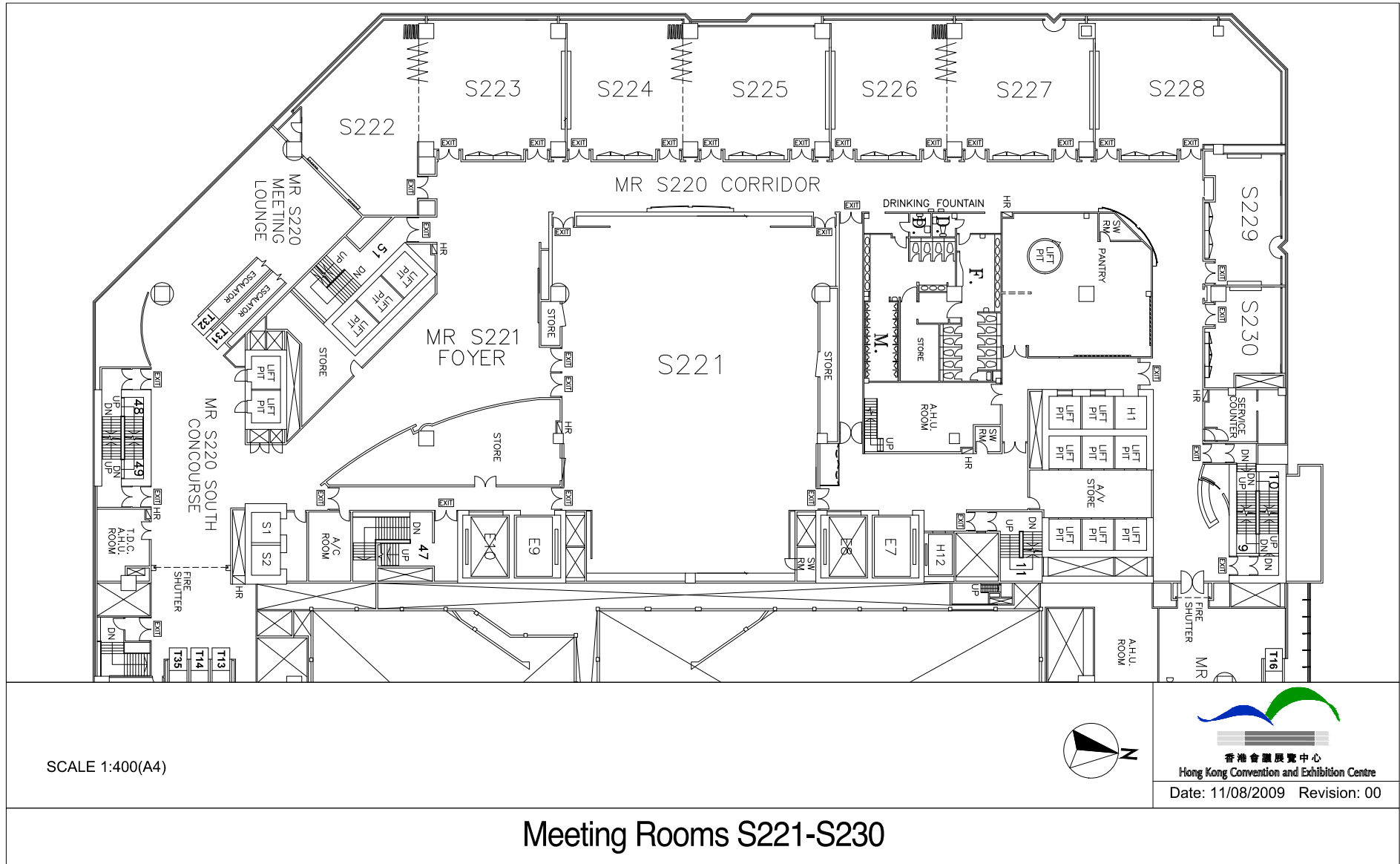
HKCEC Elevation Plan 香港會議展覽中心立視圖

Conference Directory

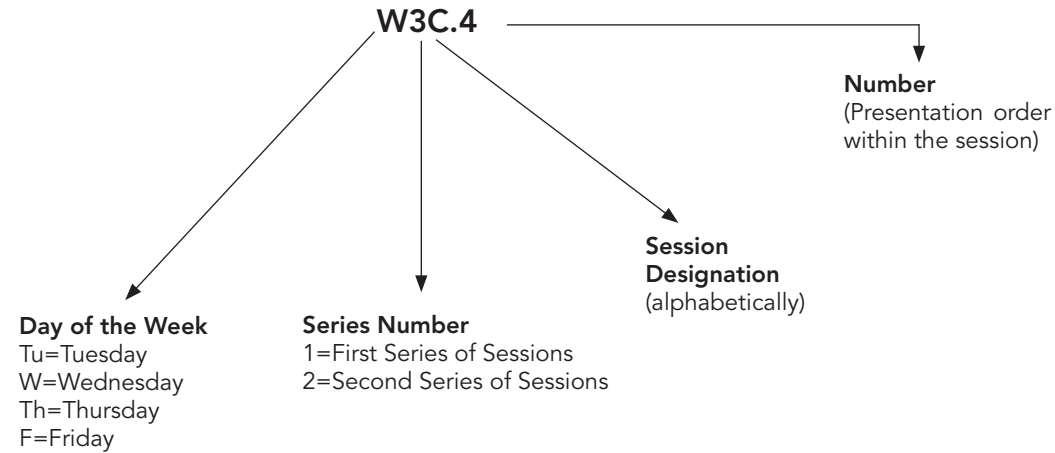


DiVino Patio - Conference Reception
Shop 11, 1/F, Causeway Centre, No. 28 Harbour Road, Wanchai

Conference Directory



Explanation of Session Codes



The first letter of the code designates the day of the week (Tu= Tuesday, W = Wednesday, Th =Thursday, F= Friday). The second element indicates the session series in that day (for instance, 1 would denote the first parallel sessions in that day). The third element continues alphabetically through a series of parallel sessions. The lettering then restarts with each new series. The number on the end of the code (separated from the session code with a period) signals the position of the talk within the session (first, second, third, etc.). For example, a presentation coded W3C.4 indicates that this paper is being presented on Wednesday (W) in the third series of sessions (3), and is the third parallel session (C) in that series and the fourth paper (4) presented in that session.

Invited papers are noted with **Invited**

Plenary papers are noted with **Plenary**

Tutorial papers are noted with **Tutorial**

Agenda of Sessions — Sunday, 29 July

14:00–18:00 Registration, AG206 of The Hong Kong Polytechnic University

Monday, 30 July

	Room S222	Room S223	Room S224	Room S225	Room S226	Room S227	Room S228
08:00–18:00	Registration, S221 Foyer of HKCEC						
08:30–10:00		Workshop 1: Artificial Intelligence in Photonics Session I	Workshop 2: Optical Microscopy and Super-Resolution Imaging Session I	Workshop 4: Advanced THz Devices and Systems Session I	Workshop 5: Photonic Quantum Computing Session I	Workshop 6: Topology and Novel Symmetry in Optics Session I	Workshop 9: Tailored Complex Optical Fields: From Twisted Light to Structured Light Session I
10:00–10:30	Coffee Break						
10:30–12:30		Workshop 1: Artificial Intelligence in Photonics Session II	Workshop 2: Optical Microscopy and Super-Resolution Imaging Session II	Workshop 4: Advanced THz Devices and Systems Session II	Workshop 5: Photonic Quantum Computing Session II	Workshop 6: Topology and Novel Symmetry in Optics Session II	Workshop 9: Tailored Complex Optical Fields: From Twisted Light to Structured Light Session II
12:30–14:00	Lunch						
14:00–15:30	Workshop 3: Advanced Laser Micro-Nanofabrication for Photonics Session I	Workshop 7: Optical Resonators: Fundamentals and Applications Session I	Workshop 8: Microstructured Optical Fibers and Applications Session I	Workshop 10: Visible Light Communications Session I	Workshop 11: Advanced Laser Display Session I	Workshop 12: Solar Energy Materials and Devices Session I	Workshop 9: Tailored Complex Optical Fields: From Twisted Light to Structured Light Session III
15:30–16:00	Coffee Break						
16:00–18:00	Workshop 3: Advanced Laser Micro-Nanofabrication for Photonics Session II	Workshop 7: Optical Resonators: Fundamentals and Applications Session II	Workshop 8: Microstructured Optical Fibers and Applications Session II	Workshop 10: Visible Light Communications Session II	Workshop 11: Advanced Laser Display Session II	Workshop 12: Solar Energy Materials and Devices Session II	Workshop 9: Tailored Complex Optical Fields: From Twisted Lights to Structured Light Session IV
18:30–20:00	Welcome Reception, Divino Patio, Shop 11, 1/F, Causeway Centre, No. 28 Harbour Road, Wanchai						

Agenda of Sessions — Tuesday, 31 July

	Room S223	Room S224	Room S225	Room S226	Room S227	Room S228	Room S423	Room S424	Room S425	Room S426	Room S427	Room S428
08:00–18:00	Registration, S221 Foyer of HKCEC											
08:30–12:30	Tu1A • Plenary Session, Convention Hall, HKCEC											
12:30–14:00	Lunch											
14:00–15:30	Tu2A • Light Sources and Optical Fields	Tu2B • Mode-locked and Ultrafast Lasers	Tu2C • Infrared and Terahertz Metamaterials and Detectors	Tu2D • Time-frequency Signal Analysis and Processing	Tu2E • Special Fibers I	Tu2F • Novel Measurement Methods I	Tu2G • Quantum Optomechanics	Tu2H • Optical Filtering	Tu2I • High-Speed Optical Transmission	Tu2J • Advances in Plasmonics and Metamaterials	Tu2K • Biophotonics and Applications I	Tu2L • Fiber Devices & Sensing I
15:30–16:00	Coffee Break											
16:00–18:00	Tu3A • Ultrafast Fiber Laser Sources	Tu3B • Nonlinear Optical Sources	Tu3C • Infrared and Terahertz Microscopy and Nanoscopy and Their Applications	Tu3D • Nonlinear Wave Mixing and Applications	Tu3E • Waveguide Devices I	Tu3F • Novel Measurement Methods II	Tu3G • Atom-photon Interaction	Tu3H • Optical Microcavities	Tu3I • Fiber Technologies and Applications	Tu3J • Nonlinear Plasmonics and Metamaterials	Tu3K • Biophotonics and Applications II	Tu3L • Laser Applications and Technologies

Agenda of Sessions — Wednesday, 1 August

	Room S223	Room S224	Room S225	Room S226	Room S227	Room S228	Room S423	Room S424	Room S425	Room S426	Room S427	Room S428
08:00–18:00	Registration, S221 Foyer of HKCEC											
08:30–10:00	W1A • Power Scaling of Lasers	W1B • Nonlinear Optics in Microresonators	W1C • Infrared Fibers & Materials and Their Applications (ends at 09:45)	W1D • Machine Learning and Neural Networks in Photonics	W1E • Laser Additive Manufacturing	W1F • Silicon Hybrid Integration	W1G • High Power Fiber Laser	W1H • Optical Metasurfaces I	W1I • Advanced Signal Modulation	W1J • Integrated Sources I	W1K • Biophotonics and Applications III	W1L • Integrated Microwave Photonics I
10:00–10:30	Coffee Break											
10:30–12:30	W2A • Advanced Laser Sources I	W2B • Nonlinear Dynamics in Waveguides and Harmonic Generation	W2C • Infrared Ultrafast Subcycle Subwavelength Photonics	W2D • Optical Signal Processing Based on Integrated Devices	W2E • Ultrafast Laser Machining and Processing	W2F • Optical Devices for Precision Measurements	W2G • Quantum Information Processing I	W2H • Optical Metasurfaces II	W2I • Fiber-Wireless Systems and PONs	W2J • Integrated Sources II	W2K • Biophotonics and Applications IV	W2L • Interferometers & Applications
12:30–14:00	Lunch											
14:00–15:30	W3A • Poster Session, S421, HKCEC											
15:30–16:00	Coffee Break 16:00–18:00											
W4A •	Advanced Light Sources II	W4B • Nonlinear Nanophotonics and Waveguides	W4C • Infrared and Terahertz Materials and Light Sources for High Performance Applications	W4D • Integrated Nanophotonic Devices	W4E • Fiber Devices I	W4F • Dual-comb Spectroscopy and its Applications	W4G • Holographic Technologies	W4H • Integrated Photonics	W4I • Optical Signal Characterization	W4J • Integrated Devices for Communications	W4K • Biophotonics and Applications V	W4L • Fiber Devices & Sensing II
18:00–22:00	Conference Reception and Banquet, Convention Hall, HKCEC											

Agenda of Sessions — Thursday, 2 August

	Room S223	Room S224	Room S225	Room S226	Room S227	Room S228	Room S423	Room S424	Room S425	Room S426	Room S427	Room S428
08:00–18:00	Registration, S221 Foyer of HKCEC											
08:30–10:00	Th1A • Novel Laser Sources I	Th1B • Nonlinear Spectroscopy and Imaging	Th1C • Frequency Control and Measurement for Optical Metrology	Th1D • Quantum Information Processing II	Th1E • Fiber Devices II	Th1F • Metamaterials and Meta-devices	Th1G • 2D Nonlinear Materials	Th1H • Nanostructures for Optoelectronic Applications	Th1I • Probabilistic Signal Shaping	Th1J • Silicon Photonics Devices	Th1K • Display Technologies	Th1L • Waveguides and Sensors
10:00–10:30	Coffee Break											
10:30–12:30	Th2A • Novel Laser Sources II	Th2B • Solitons and Temporal Wave Guiding, and Frequency Comb	Th2C • Integrated Optical Devices for Switching Multiplexing and Signal Processing	Th2D • High Energy Laser	Th2E • Special Fibers II	Th2F • Plasmonics Metasurfaces (ends at 13:15)	Th2G • 2D Materials for Mode Locking and Nonlinear Photonics	Th2H • Light-matter Interactions in Micro/nano-structures	Th2I • Polarization Effects and Optical Networking	Th2J • Advanced Modulators	Th2K • Imaging Technologies	Th2L • Distributed Fiber Sensing
12:30–14:00	Lunch											
14:00–15:30	Th3A • Vectorial Light Sources	Th3B • High-field Technologies	Th3C • Germinum Modulators and Ge Photonics	Th3D • Power Scaling and Plasmonics	Th3E • Waveguide Devices II	Th3F • Integrated Microwave Photonics II	Th3G • Structured 2D Surfaces	Th3H • Entanglement and Squeezed States I	Th3I • Signal Processing for Optical Transmsision	Th3J • 2D and Metamaterial	Th3K • Microscopy	Th3L • Novel Fiber Structures
15:30–16:00	Coffee Break											
16:00–18:00	Th4A • Characteristics of shortpulse lasers	Th4B • Nonlinear Optical Technologies	Th4C • Novel Laser System and its Applications	Th4D • High Power CW Lasers and Coherent Combining	Th4E • Plasmon-enhanced Spectroscopies and Imaging	Th4F • Radio Over Fiber and Optical Wireless Communication	Th4G • 2D Photonics Devices	Th4H • Novel Photonic Structures	Th4I • Optical Access Technologies	Th4J • Entanglement and Squeezed States II	Th4K • Imaging and Applications	Th4L • Optical Fiber Gratings, Sensors & Technology
18:30–20:30	Post Deadline Papers, S421, HKCEC											

Agenda of Sessions — Friday, 3 August

	Room S223	Room S224	Room S225	Room S226	Room S227	Room S228
08:00–18:00	Registration, S221 Foyer of HKCEC					
08:30–10:00	F1A • Mid infrared lightsource	F1B • Fiber Devices III	F1C • Emerging Technologies in Microwave Photonics	F1D • Entanglement and Squeezed States III	F1E • Optical Fiber Sensing & Microfluidics	F1F • Related Technologies and Applications for Imaging, Display and Storage
10:00–10:30	Coffee Break					
10:30–12:30	F2A • Laser Comb Technologies	F2B • Novel Plasmonics Nanostructures and Phenomena	F2C • Photonic Microwave Generation, Processing and Measurement	F2D • Optical Technologies for Communications	F2E • Laser Dynamics	F2F • Technologies and Approaches for Optical Transmission and Processing
12:30–14:00	Lunch					
14:00	Afternoon Tours					

Convention Hall

08:30–12:30

Tu1A • Plenary Session and Welcome Remarks

Welcoming remarks by General Chair Professor Ping-kong Alexander Wai and OSA President Professor Ian Walmsley

Tu1A.1 • 08:55

High-Q Physics on-a-Chip for Integrated Optical Time Standards and Frequency Synthesizers, Kerry J. Vahala¹; ¹California Institute of Technology, USA. Communication systems leverage the respective strengths of optics and electronics to convey high-bandwidth signals over great distances. These systems were enabled by a revolution in low-optical-loss dielectric fiber, complex integrated circuits as well as devices that link together the optical and electrical worlds. Today, another revolution is leveraging the advantages of optics and electronics in new ways. At its center is the laser frequency comb which provides a coherent link between these two worlds. Significantly, because the link is also bidirectional, performance attributes previously unique to electronics and optics can be shared. The end result has been transformative for time keeping, frequency metrology, precision spectroscopy, microwave-generation, ranging and other technologies. Even more recently, low-optical-loss dielectrics, now in the form of high-Q optical resonators, are enabling the miniaturization of frequency combs. These new 'microcombs' can be integrated with electronics and other optical components to potentially create systems on-a-chip. I will briefly overview the history and elements of frequency combs as well as the physics of the new microcombs. Application of the microcombs for spectroscopy and LIDAR will be discussed. Finally, efforts underway to develop integrated optical clocks and integrated optical frequency synthesizers using the microcomb element are described.

Tu1A.2 • 09:40

Light Manipulating and Detecting at Micro/Nano-Scale, Qihuang Gong¹; ¹Peking University, China. Micro/nano scale light manipulating can be realized by using nano/mico photonic structures. Using photonic crystal made of the composite materials with large and fast third-order optical nonlinearity, ultrafast and low threshold all-optical switching was demonstrated.

Tu1A.3 • 11:00

Time Stretch and its Applications in Nonlinear Dynamics, Biomedicine, and Computational Imaging, Bahram Jalali¹; ¹University of California, Los Angeles, USA. Measurements of non-repetitive and rare signals that occur on short timescales requires fast real-time measurements that exceed the speed, precision, and record length of digitizers. Time-stretch is an optical hardware accelerator that overcomes the speed limitations of photodetectors and electronic digitizers and enables ultrafast single-shot spectroscopy, imaging and other measurements at refresh rates reaching billions of frames per second with continuous recording spanning trillions of consecutive frames. The technology has opened a new frontier in measurement science and has led to discovery of several new scientific phenomena in nonlinear optics, laser dynamics and diagnostics of relativistic electron beams. It has also created a new class of instruments that have been integrated with artificial intelligence for sensing and biomedical diagnostics. We review the fundamental principles and applications of time stretch including a spin-off technology known as the phase stretch transform, a new computational imaging algorithm that is emerging as the best edge and texture feature extractor for digital images.

Tu1A.4 • 11:45

High-Power and High-Beam Quality Photonic-Crystal Lasers, Susumu Noda¹; ¹Kyoto University, Japan. I would like to describe coherent lasing oscillation of photonic-crystal lasers with advanced double-hole structures over areas of 300 - 1000µm diameters and the formation of high-quality beams (M2 < 2) whose output power exceeds 10W at room temperature. These results promise to bring the benefits of semiconductor lasers to high-power applications including material processing and laser ranging (i.e., LiDAR et al).

12:30–14:00 Lunch

Room S223

Room S224

Room S225

Room S226

Room S227

Room S228

These concurrent sessions are grouped across two pages. Please review both pages for complete session information.

14:00–15:30

Tu2A • Light Sources and Optical Fields

Presider: Andrey Komarov; Inst. of Automation and Electrometry, Russia

Tu2A.1 • 14:00 **Tutorial**

The Breakthroughs and Challenges in Mid-infrared Fibre Source Development, Stuart D. Jackson¹; ¹Macquarie Univ., Australia. The development of mid-infrared fibre sources of light is reaching new levels of power, efficiency and wavelength coverage. In this tutorial I will briefly review the major achievements that have resulted in the record performance and I will outline the challenges and opportunities ahead.

14:00–15:30

Tu2B • Mode-locked and Ultrafast Lasers

Presider: Frederique Vanholsbeeck; Univ. of Auckland, New Zealand

Tu2B.1 • 14:00 **Invited**

Polarization Dynamics in Ultrafast Thulium Fiber Lasers, Ahmet E. Kosman¹, Michelle Y. Sander¹; ¹Boston Univ., USA. Polarization dynamics in soliton mode-locked femtosecond thulium fiber lasers are presented that can lead to pulse modulation. A dual output pulse train with orthogonally polarized interlaced pulses is discussed.

14:00–15:30

Tu2C • Infrared and Terahertz Metamaterials and Detectors

Presider: Daniel Mittleman; Brown Univ., USA

Tu2C.1 • 14:00 **Invited**

Terahertz and Infrared Electromagnetic Metasurfaces, Willie J. Padilla¹; ¹Duke Univ., USA. Abstract not available.

14:00–15:30

Tu2D • Time-frequency Signal Analysis and Processing

Presider: Deepa Venkitesh; Indian Inst. of Technology, Madras, India

Tu2D.1 • 14:00

Compressing the dynamic range and statistics of optical signals, Yunshan Jiang¹, Bahram Jalali¹; ¹Univ. of California Los Angeles, China. We describe a new concept in photonics in which the dynamic range and signal's statistical distribution is optically engineered. We discuss how it improves light detection and means to implement it.

14:00–15:30

Tu2E • Special Fibers I

Presider: Kin Chiang; City Univ. of Hong Kong, Hong Kong

Tu2E.1 • 14:00 **Tutorial**

Recent Developments in Photonic Crystal Fibres, Philip S. Russell¹; ¹Max-Planck-Inst Physik des Lichts, Germany. Recent PCF developments include optoacoustic high harmonic mode-locking of fibre lasers, twist-induced guidance in coreless PCF, "swimming" microparticle lasers in liquid-filled PCF and ultrashort wavelength-tunable DUV and VUV pulses from gas-filled hollow-core PCF.

14:00–15:30

Tu2F • Novel Measurement Methods I

Presider: Zhichao Luo; South China Normal Univ., China

Tu2F.1 • 14:00 **Invited**

Extreme Imaging for Large-scale single-cell Analysis, Keisuke Goda¹, Cheng Lei¹; ¹Univ. of Tokyo, Japan. I present an ultrafast molecular imaging technology combined with artificial intelligence on a microfluidic platform for large-scale single-cell analysis. It rapidly provides information-rich images of numerous single cells, enabling us to exploit cellular heterogeneity.

Room S223

Room S224

Room S225

Room S226

Room S227

Room S228

These concurrent sessions are grouped across two pages. Please review both pages for complete session information.

Tu2A • Light Sources and Optical Fields—Continued

Tu2B • Mode-locked and Ultrafast Lasers—Continued

Tu2C • Infrared and Terahertz Metamaterials and Detectors—Continued

Tu2D • Time-frequency Signal Analysis and Processing—Continued

Tu2E • Special Fibers I—Continued

Tu2F • Novel Measurement Methods I—Continued

Tu2B.2 • 14:30

Passive mode-locking of a diode-pumped Nd laser based on cascaded second-order nonlinearity, How-Wei Liu¹, Shou-Tai Lin¹, Chun-Hui Huang¹; ¹Feng Chia Univ., Taiwan. A diode-pumped mode-locking Nd:YVO₄/YVO₄ laser via positive cascaded second-order Kerr lens effects at 1064 nm was demonstrated. The measured average power, pulse repetition rate and pulse duration are 1.3 W, 186 MHz and 2.8 ps, respectively.

Tu2B.3 • 14:45

Asynchronous mode-locking and FM oscillation transition in a 10 GHz hybrid mode-locked fiber laser, Cheng-Jih Luo¹, Yen-Chia Juan¹, Yinchieh Lai¹; ¹Dept. of Photonics, National Chiao Tung Univ., Taiwan. By studying an asynchronously mode-locked (ASM) fiber laser, we experimentally find that the laser directly transits from the ASM state into the FM oscillation state when the modulation frequency detuning is increased beyond a threshold.

Tu2C.2 • 14:30 Invited

Metamaterials and Metallic Hole Arrays Coupled to Short Wave Infrared Intersubband Transitions in the GaN/AlN Based Quantum Cascade Structures, Gad Bahir¹; ¹Dept. of Electrical Engineering, Technion-Israel Inst. of Technology, Israel. We present the design, realization and characterization of optical coupling between intersubband transitions within a GaN/AlN based quantum cascade detector structure and planar metamaterials nano-antennas or metal hole arrays (MHA) in the near-infrared spectral range.

Tu2D.2 • 14:15

Temporal differential manipulation of optical frequency chirp, Lei Zhang¹, Xin Dong¹, Liao Chen¹, Xi Zhou¹, Chi Zhang¹, Xinliang Zhang¹; ¹Wuhan National Lab for Optoelectronics, China. We propose and demonstrate the temporal differential manipulation of optical frequency chirp based on interference and cross-phase modulation. It realizes the dispersion order reduction, and enhances the flexibility of the dispersive time-stretch technique.

Tu2D.3 • 14:30

Temporal Shack-Hartman wavefront sensor for large temporal phase dynamics recovery, Chen Zheng¹, Liao Chen¹, Xi Zhou¹, Lei Zhang¹, Chi Zhang¹, Xinliang Zhang¹; ¹Wuhan National Lab for Optoelectronics, China. We propose and simulate a temporal Shack-Hartman wavefront sensor based on time-lenses array, which is capable of retrieving the temporal phase information with large dynamics. It is a complementary scheme for the coherent detection technique.

Tu2D.4 • 14:45

Real-time spectral analysis based on time-lens enhanced dispersive Fourier transform, Yuan Wei¹, Bowen Li¹, Pingping Feng¹, Kenneth Kin-Yip Wong¹; ¹Univ. of Hong Kong, Hong Kong. Time-lens enhanced dispersive Fourier transform (TE-DFT) is demonstrated for real-time spectral analysis in the continuous-wave regime. Flexible frame rate, 0.03-nm resolution and -32.2-dBm detection sensitivity can be achieved across 36-nm range limited only by amplifier.

Tu2F.2 • 14:30

Direct spatially resolved snapshot polarimetric phase extraction by using an imaging PolarCam, Dahi Abdelsalam^{1,2}, Vamara Dembele², Inho Choi², Madhan P. Jayakumar², Sukhyun Choi², Junho Kim², Daesuk Kim²; ¹National Inst. of Standards, Egypt; ²Optical Engineering, Division of Mechanical System Engineering, Chonbuk National Univ., Korea. We extract Stokes vectors and 3D phase of a transmissive anisotropic object by a novel polar interferometric system. PolarCam employing a micro polarizer array is used to capture four inline interferograms in single shot.

Tu2F.3 • 14:45

A frequency to voltage converter with ultra-low residual phase noise, Lulu Yan^{1,2}, Yanyan Zhang^{1,2}, Zhaoyang Tai^{1,2}, Pan Zhang¹, Ru Yuan¹, Shougang Zhang^{1,2}, Haifeng Jiang^{1,2}; ¹National Time Service Center, China; ²School of Astronomy and Space Science, Univ. of Chinese Academy of Science, China. We report on the process of residual noise suppression in a frequency to voltage converter based on a frequency difference multiplication method, for measuring frequency noise of ultra-stable laser. The double sideband frequency noise is lower than -40 dB Hz²/Hz in a bandwidth from 3 Hz to 100 kHz.

These concurrent sessions are grouped across two pages. Please review both pages for complete session information.

Tu2G • Quantum Optomechanics—Continued

Tu2H • Optical Filtering—Continued

Tu2I • High-Speed Optical Transmission—Continued

Tu2J • Advances in Plasmonics and Metamaterials—Continued

Tu2K • Biophotonics and Applications I—Continued

Tu2L • Fiber Devices & Sensing I—Continued

Tu2H.2 • 14:30

High-Extinction-Ratio Optical Filters Based on High-Order Silicon Microring Resonators, Renyou Ge¹, Xinlun Cai¹; ¹*Sun Yat-sen Univ., China*. We designed and fabricated coupled-resonator optical waveguide filters on silicon platform with insertion loss ~ 1.5 dB, and obtained extinction ratio of > 70 dB for 7th filters by thermally tuning resonances of each ring.

Tu2H.3 • 14:45

Multi-wavelength tunable filter based on chirped phase-shift grating on Lithium Niobate, Yuan Yao¹, Ailing Zhang¹, Zhengrong Tong¹; ¹*Tianjin Univ. of Technology, China*. Multi-wavelength tunable filter based on chirped phase-shift grating on Lithium Niobate (LN) is proposed. The wavelengths of the filter are linearly tuned and the number of wavelength is determined by the number of electrode pairs.

Tu2I.2 • 14:30

On the Hardware Complexity of Kramers-Kronig Receiver, Tianwai Bo¹, Rui Deng², Jing He², Hoon Kim¹; ¹*School of Electrical Engineering, Korea Advanced Inst. of Science and Technology (KAIST), Korea*; ²*College of Computer Science and Electronic Engineering, Hunan Univ., China*. The analysis on the hardware complexity of Kramers-Kronig (KK) receiver shows that, compared with the conventional KK receiver, the recently proposed receiver without digital upsampling saves the number of adders, multipliers, and memory by 80%.

Tu2I.3 • 14:45

Comparison for 100 Gb/s PDM-DD Short Reach Optical Communication System Transmission Performance with PAM4, CAP16 and DMT, Jiahao Huo^{1,2}, Xian Zhou^{1,2}, Kangping Zhong³, Jiajing Tu^{1,2}, Wei Huangfu¹, Jinhui Yuan², Keping Long¹, Changyuan Yu², Alan Lau⁴, Chao Lu²; ¹*Beijing Engineering and Technology Research Center for Convergence Networks and Ubiquitous Services, Univ. of Science and Technology Beijing, China*; ²*Dept. of Electronic and Information Engineering, The Hong Kong Polytechnic Univ., Hong Kong*; ³*Macom Technology Solutions, China*; ⁴*Dept. of Electrical Engineering, The Hong Kong Polytechnic Univ., Hong Kong*. A promising way to significantly meet the demands of short reach systems is polarization division multiplexing with direct detection (PDM-DD). In this paper, we compare three advanced modulation formats performance on PDM-DD system.

Tu2L.2 • 14:30

Enhanced Sensitivity of Hetero-core Structure SPR Temperature Sensor Based on Local Microstructures, Wenjie Zhu¹, Qing Huang¹, Yong Wang¹, Elfed Lewis², Minghong Yang¹; ¹*National Engineering Laboratory for Fiber Optics Sensing Technology, Wuhan Univ. of Technology, China*; ²*Optical Fibre Sensors Research Centre, Univ. of Limerick, Ireland*. Femtosecond laser micromachining system was used to manufacture microstructures on hetero-core structure SPR sensor to enhance the temperature sensitivity of the conventional one. The temperature sensitivity of the proposed sensor has increased 30.2%.

Tu2L.3 • 14:45

Fiber optic plasmonic sensor utilizing carbon nanotubes based surface imprinted matrix for the sensing of dopamine, Anisha Pathak¹, Banshi D. Gupta¹; ¹*IIT Delhi, India*. A fiber optic dopamine sensor is realized utilizing surface imprinted carbon nanotube platform and surface plasmon resonance technique. The sensor possesses dynamic range of 0-150 μ M and detection limit of 2.1 μ M.

These concurrent sessions are grouped across two pages. Please review both pages for complete session information.

Tu2A • Light Sources and Optical Fields—Continued

Tu2A.2 • 15:00 **Invited**

Complex Optical Fields: Fundamentals and Applications, Qiwen Zhan^{1,2}, ¹Univ. of Dayton, USA; ²Univ. of Shanghai for Science and Technology, China. Complex optical fields with spatially structured field distributions within the cross section have drawn significant attention recently. This paper intends to review the latest developments and applications of this emerging field of optics.

Tu2B • Mode-locked and Ultrafast Lasers—Continued

Tu2B.4 • 15:00

All-optical multi-parameter regulations for ultrafast fiber laser, Yu Long Cao^{1,2}, Lei Gao^{1,2}, Tao Zhu^{1,2}, Yujia Li^{1,2}, ¹Chongqing Univ., China; ²Key Laboratory of Optoelectronic Technology & Systems, China. We employ all-optical devices with precise controllable spectra bandwidths and wavelengths into an ultrafast fiber laser cavity, durations and wavelengths of pulses can be all-optically tuned with sensitivities of 470 fs/mW and 2.9 pm/mW, separately.

Tu2B.5 • 15:15

78-fs Pulses from a SWCNTs Mode-Locked Tm:CLNGG Disordered Garnet Crystal Laser, Yicheng Wang¹, Zhongben Pan^{1,2}, Yongguang Zhao^{1,3}, Ji Bae⁴, Sun Choi⁴, Fabian Rotermund⁴, Josep Serres⁵, Xavier Mateos⁵, Haohai Yu⁶, Huaijin Zhang⁶, Mark Mero¹, Uwe Griebner¹, Valentin Petrov¹, ¹Max Born Inst., Germany; ²Inst. of Chemical Materials, China; ³Jiangsu Normal Univ., China; ⁴KAIST, Korea; ⁵Universitat Rovira i Virgili, Spain; ⁶Shandong Univ., China. We report on a Tm:CLNGG laser passively mode-locked by single-walled carbon nanotubes (SWCNTs) at 2017 nm, generating 78-fs pulses with an average output power of 54 mW at a repetition rate of 86 MHz.

Tu2C • Infrared and Terahertz Metamaterials and Detectors—Continued

Tu2C.3 • 15:00

All-Dielectric Terahertz Half-Wave Plate with Antireflection Layer, Jianchen Zi¹, Quan Xu¹, Qiu Wang¹, Chunxiu Tian², Yanfeng Li¹, Xixiang Zhang², Jiaguang Han¹, Weili Zhang^{1,3}, ¹Tianjin Univ., China; ²King Abdullah Univ. of Science and Technology, Saudi Arabia; ³Oklahoma State Univ., USA. We present an all-dielectric terahertz half-wave plate with an antireflection layer. The device is made of pure silicon, and can realize cross polarization conversion with almost 100% conversion rate and 90% of transmission at the operating frequency.

Tu2C.4 • 15:15

Frequency Comb Generation in Terahertz Quantum Cascade Lasers, Hua Li¹, Chang Wang¹, Wenjian Wan¹, Ziping Li¹, Zhiyong Tan¹, Juncheng Cao¹, ¹Shanghai Inst. of Microsystem and In, China. We report the fast detection of terahertz light generated from an electrically-pump terahertz quantum cascade laser lasing at 4.2 THz by terahertz quantum well photodetector. It is demonstrated that the terahertz quantum well photodetector can extract the terahertz light modulated with frequency as high as 6.2 GHz.

Tu2D • Time-frequency Signal Analysis and Processing—Continued

Tu2D.5 • 15:00

Ultrafast optical tomography using Raman-assisted temporal magnification, Sheng Wang^{1,2}, Lingxiao Yang¹, Chi Zhang², Bowen Li¹, Kenneth Kin-Yip Wong¹, ¹Dept. of Electrical and Electronic Engineering, The Univ. of Hong Kong, Hong Kong; ²Wuhan National Laboratory for Optoelectronics, Huazhong Univ. of Science and Technology, China. The sensitivity of temporal magnified tomography is further enhanced using Raman-assisted temporal magnification. Tomographic imaging of a cm-thick phantom has been demonstrated at 78-dB sensitivity and 86.7- μ m resolution with an A-scan rate of 44 MHz.

Tu2D.6 • 15:15

Realtime Comb-Assisted Discrete Fourier Transform Processor, Huan Hu¹, Vahid Ataie¹, Yauheni Myslivets¹, Stojan Radic¹, ¹UCSD, USA. For the first time we present an optical comb-assisted 60-point DFT engine operating in real-time at 12×10^7 coefficients per second. The engine is used to demodulate an 8-PPM signal using its DFT coefficients.

Tu2E • Special Fibers I—Continued

Tu2E.2 • 15:00

Low loss large bandwidth seven-cell hollow core photonic bandgap fiber at 1 μ m spectral range, Xin Zhang¹, Shoufei Gao¹, Yingying Wang¹, Pu Wang¹, ¹Inst. of Laser Engineering, Beijing Univ. of Technology, China. We report a seven-cell hollow-core photonic bandgap fiber with loss of 26.7 dB/km at 1090 nm and bandwidth over 255 nm, ideal for creating all-fiber device for strong light-matter interaction type of applications.

Tu2E.3 • 15:15

Hollow Core Fibers for Optical pumped Fiber Gas Laser, Changming Xia¹, Zicheng Sheng¹, Haixia Fan¹, Jiantao Liu¹, Zhiyun Hou¹, Guiyao Zhou¹, ¹South China Normal Univ., China. We report optical properties and fabrication of hollow core fibers in our lab for optical pumped fiber gas laser. A width transmission window in near infrared spectral region is obtained in octagram hollow core fiber.

Tu2F • Novel Measurement Methods I—Continued

Tu2F.4 • 15:00

Improvement of Frequency Accuracy of Spatially-resolved Spectroscopy / Tomographic Spectroscopy, Shohei Gunji¹, Tatsutoshi Shioda¹, ¹Saitama Univ., Japan. Novel calibration method for tomographic spectroscopy with high-depth resolution is proposed. Measured depth resolution has been achieved to 1.1 μ m, and the frequency accuracy was improved from 10.6 THz to 0.8 THz by calibration.

Tu2F.5 • 15:15

High-speed Optical Frequency Comb Analyzer with Single-detection Technique for Ultrafast Waveform Measurement, Leona Yuda¹, Tatsutoshi Shioda¹, ¹Saitama Univ., Japan. Ultrafast-phase spectrum analyzer for 25 GHz \times 45 lines frequency comb has been developed with novel optical delay-circuit system and single detector. It can be applied to single-shot optical waveform measurement system with femto-second time-resolution.

15:30–16:00 Coffee Break

These concurrent sessions are grouped across two pages. Please review both pages for complete session information.

Tu2G • Quantum Optomechanics—Continued

Tu2G.2 • 15:00

Cavity Enhanced Raman Heterodyne Spectroscopy in Er:YSO for Microwave to Optical Signal Conversion, Xavier Fernandez-Gonzalvo¹, Sebastian P. Horvath¹, Yu-Hui Chen¹, Jevon J. Longdell¹; ¹Univ. of Otago, New Zealand. The quantum efficiency of the microwave to optical frequency conversion process at the heart of Raman heterodyne spectroscopy was improved by four orders of magnitude by resonant enhancement of the pump and signal optical fields.

Tu2G.3 • 15:15

Cavity-free scheme for conditional π phase shift between two traveling single photons, Keyu Xia^{1,2}, Mattias Johnsson², Peter L. Knight², Jason Twamley²; ¹Nanjing Univ., China; ²Macquarie Univ., Australia; ³Imperial College, UK. Using four-wave mixing in a 1D medium, we present a scheme without using cavities for achieving a conditional π phase shift between two traveling single photons. Our proposal provides a way for cavity-free quantum information processing.

Tu2H • Optical Filtering—Continued

Tu2H.4 • 15:00

Temperature and optical feedback sensitivity of the relative intensity noise of epitaxial quantum dot lasers on Ge, Yue-Guang Zhou¹, Chun-Fang Cao², Jin-Yi Yan², Qian Gong², Cheng Wang¹; ¹ShanghaiTech Univ., China; ²Shanghai Inst. of Microsystem and Information Technology, China. This work demonstrates that the relative intensity noise of Ge-based epitaxial InAs quantum dot lasers are weakly sensitive to the temperature, while it is more sensitive to the optical feedback at higher bias currents.

Tu2H.5 • 15:15

Design of GaInAs/InP membrane p-i-n photodiode with back-end distributed-Bragg-reflector (DBR), Xu Zheng¹, Zhichen Gu¹, Tomohiro Amemiya¹, Nobuhiko Nishiyama¹, Shigehisa Arai¹; ¹Tokyo Inst. of Technology, Japan. A GaInAs/InP membrane p-i-n photodiode integrated with a back end DBR was investigated under the back reflection of -30dB. As the result, it was found that the 3dB bandwidth of 17 GHz can be obtained with the device length of 12 μ m. These are approximately 3 times faster and 1/3 times smaller than those of a similar PD without the back end DBR.

Tu2I • High-Speed Optical Transmission—Continued

Tu2I.4 • 15:00

100Gb/s/ λ Optical Fiber Transmission Based on High Speed DAC in SiGe Technology, Weizhong Li^{2,1}, Lei Zhou³, Ming Luo¹, Daojun Xue¹, Xiang Li¹; ¹State Key Laboratory of Optical Communication Technologies and Networks, Wuhan Research Inst. of Posts & Telecommunications, China; ²Wuhan National Laboratory for Optoelectronics, Huazhong Univ. of Science and Technology, China; ³Inst. of Microelectronics of Chinese Academy of Science, China. This paper presents multi-level pulse amplitude modulation (PAM) optical fiber transmission based on 32-GS/s 6-bit digital to analog converter fabricated by 0.18 μ m SiGe technology. The 32GBd PAM-4/8/16 signals are successfully transmitted over 2-km fiber.

Tu2I.5 • 15:15

Longest-ever unrepeatable transmission over 713.2km of 2.5 Gb/s with a span loss in excess of 111dB, Jian Xu¹, Jiekui Yu¹, Qianggao Hu¹, Hongyan Zhou^{3,4}, Ming Li¹, Liyan Huang¹, Fusheng Zheng², Weihua Li², Li Deng², Lei Zhang³, Honghai Wang³, Jie Luo³, Tao Zeng³, Lingheng Meng⁵; ¹Accelink Technologies Co. Ltd, China; ²State Grid Information and Telecommunication Branch, China; ³State Key Laboratory of Optical Fiber and Cable Manufacturing Technology, China; ⁴Yangtze Optical Fiber and Cable Company, China; ⁵State Key Laboratory of Optical Communication Technologies and Networks, China. Longest-ever unrepeatable transmission over 713.2km for 2.5G and 665.7km for 10G is achieved by employing 2.5G PM-BPSK, 10G PM-QPSK, optimized ROPAs structure and ultra low loss & large effective area fiber link.

Tu2J • Advances in Plasmonics and Metamaterials—Continued

Tu2J.2 • 15:00

Plasmonic Computing of Spatial Differentiation, Tengfeng Zhu¹, Yihan Zhou¹, Yijie Lou¹, Hui Ye², Min Qiu², Shanhuai Fan², Zhichao Ruan^{1,2}; ¹Dept. of Physics, Zhejiang Univ., China; ²College of Optical Engineering, State Key Laboratory of Modern Optical Instrumentation, Zhejiang Univ., China; ³Dept. of Electrical Engineering, Gintzong Laboratory, Stanford Univ., USA. We show that the interference effects associated with surface plasmon excitations at a metal-dielectric interface can perform spatial differentiation. Utilizing it, we experimentally demonstrate edge detection of images without any Fourier lens. This work points to a simple yet powerful mechanism for optical analog computing at the nanoscale.

Tu2J.3 • 15:15

Strong Emission Enhancement in All-Dielectric High-Q Fano Metasurface, Xingzhi Qiu¹, Shuai Yuan¹, Jinsong Xia¹; ¹Huazhong Univ of Science and Technology, China. A high-Q Fano metasurface by breaking structural symmetry is proposed and over three orders emission enhancement of embedded Ge quantum dots is experimentally demonstrated in the metasurface. The lineshape of photoluminescence is typically Fano-like, the origin of Fano resonance and strong emission enhancement are analyzed in detail.

Tu2K • Biophotonics and Applications I—Continued

Tu2K.2 • 15:00 **Invited**

Optical Micro Imaging Technologies for Biomedicine, Xingde Li¹; ¹Biomedical Engineering, Johns Hopkins Univ., USA. We present recent developments of (1) a super-achromatic monolithic OCT microprobe for intraluminal imaging of tissue microanatomies and (2) a scanning fiber-optic nonlinear endomicroscope for in vivo imaging of tissue histology. Representative applications will also be discussed.

Tu2L • Fiber Devices & Sensing I—Continued

Tu2L.4 • 15:00

Refractive index measurement based on disturbance to RF conversion function in a fiber OFC cavity, Ryo Oe^{1,2}, Kosuke Nagai¹, Takeo Minamikawa^{1,2}, Shuji Taue³, Hideki Fukano³, Yoshiaki Nakajima^{4,2}, Kaoru Minoshima^{4,2}, Takeshi Yasui^{1,2}; ¹Tokushima Univ., Japan; ²JST, ERATO MINOSHIMA IOS, Japan; ³Okayama Univ., Japan; ⁴Univ. Electro-Commun, Japan. We demonstrate refractive index (RI) measurement of water/ethanol mixture based on disturbance to RF conversion in fiber comb cavity including multi-mode interference fiber sensor. We attached RI resolution of 4.3×10^{-6} and RI accuracy of 5.4×10^{-5} .

Tu2L.5 • 15:15

Static and dynamic strain sensing over 3.5 kHz with fiber-based optical frequency comb cavity, Takeo Minamikawa^{1,2}, Takashi Masuoka^{1,2}, Takashi Ogura¹, Kyuki Shibuya^{1,2}, Yoshiaki Nakajima^{3,2}, Yoshihisa Yamaoka⁴, Kaoru Minoshima^{3,2}, Takeshi Yasui^{1,2}; ¹Tokushima Univ., Japan; ²ERATO Intelligent Optical Synthesizer Project, Japan; ³The Univ. of Electro-Communications, Japan; ⁴Saga Univ., Japan. We proposed a novel static and dynamic strain sensor employing an optical-frequency-comb. We realized strain sensing from 8.7 n ϵ to 500 $\mu\epsilon$ over the strain frequencies of 3.5 kHz.

15:30–16:00 Coffee Break

Room S223

Room S224

Room S225

Room S226

Room S227

Room S228

These concurrent sessions are grouped across two pages. Please review both pages for complete session information.

16:00–18:00

Tu3A • Ultrafast Fiber Laser Sources

Presider: Chengbo Mou; Shanghai Univ., China

Tu3A.1 • 16:00 **Invited**

High Energy Ultrafast Fiber Lasers Based on Coherent Pulse Stacking Amplification, Almantas Galvanauskas¹; ¹Univ. of Michigan, USA. Coherent pulse stacking amplification extends ultrashort pulse energies from a fiber amplifier by approximately two orders of magnitude compared to CPA, and can lead to compact coherently-combined laser systems with TW-peak and kW-average powers.

Tu3A.2 • 16:30

Development of a Spaceborne Fiber-based Laser MOPA Transmitter, Anthony W. Yu¹, Mark A. Stephen¹, Jeffrey R. Chen¹, Kenji Numata¹, Stewart T. Wu¹, Brayler Gonzalez¹, Lawrence I. Han¹, Molly E. Fahey¹, Michael R. Rodriguez², Graham R. Allan², James B. Abshire¹, Jeffrey W. Nicholson³, Anand Hariharan³, William A. Mamakos⁴, Brian R. Bean⁵; ¹NASA Goddard Space Flight Center, USA; ²Science Systems and Applications, Inc., USA; ³OFS Fitel LLC, USA; ⁴Design Interface Inc, USA; ⁵Sobosoft LLC, USA. NASA is developing a lidar instrument to measure the atmospheric carbon dioxide (CO₂) column concentrations from space. We will discuss the development effort of a space-qualified fiber-based master oscillator power amplifier laser for this instrument.

16:00–18:00

Tu3B • Nonlinear Optical Sources

Presider: Michelle Sander; Boston Univ., USA

Tu3B.1 • 16:00 **Tutorial**

Building Quantum Machines Out of Light, Ian Walmsley¹; ¹Univ. of Oxford, UK. Light has the remarkable capacity to reveal quantum features under ambient conditions, making exploration of the quantum world feasible in the laboratory and field. Further, the availability of high-quality integrated optical components makes it possible to conceive of large-scale quantum states by bringing together many different quantum light sources and manipulating them in a coherent manner and detecting them efficiently. By this route, we can envisage a scalable photonic quantum network that will facilitate the preparation of distributed quantum correlations among many light beams. This will enable a new regime of state complexity to be accessed - one for which it is impossible using classical computers to determine the structure and dynamics of the system. This is a new regime not only for scientific discovery, but also practical purpose: the same complexity of big quantum systems may be harnessed to perform tasks that are impossible using known future information processing technologies. For instance, ideal universal quantum computers may be exponentially more efficiently than classical machines for certain classes of problems, and communications may be completely secure. Photonic quantum machines will open new frontiers in quantum science and technology.

16:00–18:00

Tu3C • Infrared and Terahertz Microscopy and Nanoscopy and Their Applications

Presider: Willie Padilla; Duke Univ., USA

Tu3C.1 • 16:00 **Invited**

Advances in Ultrafast Terahertz Scanning Tunneling Microscopy, Frank A. Hegmann¹; ¹Univ. of Alberta, Canada. Terahertz scanning tunneling microscopy (THz-STM) is able to probe ultrafast dynamics on the surface of materials with simultaneous sub-nanometer spatial resolution. How THz-STM works, recent progress in THz-STM, and future directions will be discussed.

Tu3C.2 • 16:30 **Invited**

Laser Terahertz Emission Nanoscopy, Angela Pizzuto¹, Pernille Klarskov^{3,2}, Daniel M. Mittleman²; ¹Dept. of Physics, Brown Univ., USA; ²DTU Fotonik - Dept. of Photonics Engineering, Technical Univ. of Denmark, Denmark; ³Dept. of Electrical and Computer, Brown Univ., USA. We demonstrate depletion of terahertz emission from semiconductors by applying a DC bias between a substrate and an AFM probe operating in tapping mode. The depletion is strongly dependent on the probe tapping amplitude.

16:00–18:00

Tu3D • Nonlinear Wave Mixing and Applications

Presider: Chester C.T. Shu; The Chinese Univ. of Hong Kong, Hong Kong

Tu3D.1 • 16:00 **Tutorial**

Advances in Core Technologies and Wave-Mixing Techniques for Optical Signal Processing, Alan E. Willner¹; ¹Univ. of Southern California, USA. This tutorial will highlight challenges in achieving efficient, flexible, and reconfigurable optical networks. Various optical approaches that enable key functions will be discussed, including: dynamic bandwidth allocation, increasing spectral efficiency, format conversion, and phase-sensitive operations.

16:00–17:45

Tu3E • Waveguide Devices I

Presider: Paulo Dainese; Universidade Estadual de Campinas, USA

Tu3E.1 • 16:00 **Invited**

On-chip Brillouin filtering of RF and Optical Signals, Benjamin J. Eggleton¹; ¹Univ. of Sydney, Australia. In this talk I review signal processing based on the nonlinear optical process known as stimulated Brillouin scattering (SBS) for high-performance analog signal filtering for RF communications and in coherent optical communication systems for carrier amplification.

Tu3E.2 • 16:30 **Invited**

Mid-Infrared Waveguides and Applications, Xin Gai¹; ¹City Univ. of Hong Kong, Hong Kong. Mid-infrared spectroscopy attracts growing interests because of its coverage over the characteristic spectral absorption features for many molecules. This paper reviews our study in mid-infrared including material characterization, waveguide fabrication and supercontinuum for spectroscopic applications.

16:00–18:00

Tu3F • Novel Measurement Methods II

Presider: Zheng Zheng; Beihang Univ., China

Tu3F.1 • 16:00 **Invited**

Infrared On-Chip Photonics: Towards Precision Biodiagnostics, Boris Mizaiakoff¹; ¹Ulm Univ., Germany. State-of-the-art sensing platforms ideally benefit from miniaturized and integrated optical technologies providing direct access to molecule-specific information. With in-situ sensing strategies point-of-care diagnostics in medicine becoming more prevalent, in particular if labeled constituents are not required.

Tu3F.2 • 16:30

Study on remote gas sensing by photoacoustic wave detected with an optical probe, Daichi Fujii¹, Kazuhide Sato¹, Kazuyoku Tei¹, Shigeru Yamaguchi¹; ¹Tokai Univ., Japan. We report the results of remote gas detection using an optical wave microphone (OWM). It enables photoacoustic signal remotely without installing conventional microphone where acoustic wave stands. We successfully demonstrated C₂H₂ detection with OWM.

These concurrent sessions are grouped across two pages. Please review both pages for complete session information.

16:00–18:00

Tu3G • Atom-photon Interaction

Presider: Arno Rauschenbeutel; Humboldt-Universität zu Berlin, Germany

Tu3G.1 • 16:00 **Invited**

Multi-photon Quantum Boson-sampling Machines, Chaoyang Lu¹; ¹Univ of Science and Technology of China, China. We develop single-photon sources that simultaneously combines high purity, efficiency, and indistinguishability. We demonstrate entanglement among ten single photons. We construct high-performance multi-photon boson sampling machines to race against classical computers.

Tu3G.2 • 16:30 **Invited**

Atom-photon Interaction in the Strong Focusing Regime, Christian Kurtsiefer¹; ¹Dept. of Physics / Centre for Quantum Technologies, National Univ. of Singapore, Singapore. Abstract not available.

16:00–18:00

Tu3H • Optical Microcavities

Presider: Andrew Poon; Hong Kong Univ of Science & Technology, Hong Kong

Tu3H.1 • 16:00 **Tutorial**

Sensing the Nanoscale Dynamics of Proteins with Optoplasmonic Microcavities, Frank Vollmer¹; ¹Univ. of Exeter, UK. My laboratory is developing a new class of nanophotonic architectures by combining optically resonant dielectric microcavities with plasmonically resonant metal nanostructures to enable detection at the nanoscale with extraordinary sensitivity.

16:00–18:00

Tu3I • Fiber Technologies and Applications

Presider: Calvin CK Chan, The Chinese Univ. of Hong Kong, Hong Kong

Tu3I.1 • 16:00 **Tutorial**

Hollow Core Fibers: Technology and Emerging Applications, David J. Richardson¹; ¹Univ. of Southampton, UK. We describe the unique properties and latest advances in the design and fabrication of hollow core optical fibers. We then review use of the technology in important application areas including power delivery, sensing and communications.

16:00–18:00

Tu3J • Nonlinear Plasmonics and Metamaterials

Presider: Ho Wai Lee; Baylor Univ., USA

Tu3J.1 • 16:00 **Invited**

Gap-enhanced Raman Tags for Superstable and High-speed Imaging, Jian Ye¹; ¹School of Biomedical Engineering, Shanghai Jiao Tong Univ., China. Gap-enhanced Raman tags (GERTs) are favorable for off-resonance near-infrared laser excitation with reduced photothermal effect, leading to super-photostable and high-speed cell and tumor imaging. GERTs have demonstrated for intraoperative imaging of the sentinel lymph nodes and elimination of microscopic and residual tumors.

Tu3J.2 • 16:30

Selective nano-CARS microscopy with dual-wavelength nanofocused ultrafast plasmon pulses, Keita Tomita¹, Fumihiko Kannari¹; ¹Keio Univ., Japan. We demonstrate selective CARS measurements of a monolayer graphene and multi-walled carbon nanotubes (MWCNT) at the D-, G-, and 2D-bands with nanofocused SPP pulses at 800 and 440 nm using an aluminum tapered tip.

16:00–18:00

Tu3K • Biophotonics and Applications II

Presider: Tuan Guo; Jinan Univ., China

Tu3K.1 • 16:00 **Invited**

Ultrasound Detection and Imaging Using Microring Resonators and Laser Generated Focused Ultrasound, L. Jay Guo¹; ¹Univ. of Michigan, USA. Optical detection of ultrasound is based on the interaction of strain field and optical field in an optical resonator for sensitive detection. Special optical transmitters generate and focus ultrasound, targeting high-amplitude focused ultrasound for imaging and therapeutic applications.

Tu3K.2 • 16:30 **Invited**

High Spatial Resolution Fiber Optic Sensors and Their Impact in Biomedical Measurements and Diagnostic, Daniele Tosi^{1,2}, Sanzhar Korganbayev^{1,2}, Carlo Molardi¹, Emiliano Schena³, Guido Perrone⁴, Agostino Iadicicco⁵, Campopiano Stefania⁵, Salvador Sales⁶; ¹Nazarbayev Univ., Kazakhstan; ²Laboratory of Biosensors and Bioinstruments, National Laboratory Astana, Kazakhstan; ³Universita' Campus Bio-Medico di Roma, Italy; ⁴Politecnico di Torino, Italy; ⁵Parthenope Univ., Italy; ⁶Universidad Politecnica de Valencia, Spain. This work presents the recent developments on fiber optic sensing technologies having narrow spatial resolution, 0.1 mm to 10 mm. Sensors are finding emerging application in real-time monitoring of therapies and diagnostic.

16:00–18:00

Tu3L • Laser Applications and Technologies

Presider: Bo Dong; Chinese Academy of Sciences, China

Tu3L.1 • 16:00

Superfluorescent Fiber Source with Ultra-low Thermal Coefficient Operating in the Conventional Band, Hsiang Wang¹, Yeng-Hong Lu¹, Tsung-Yu Lu¹, Ren-Young Liu², Shien-Kuei Liaw¹; ¹Taiwan Tech, Taiwan; ²National Space Organization (NSPO), Taiwan. An Erbium-doped fiber-based, optical DPB pumping broadband superfluorescent fiber source is proposed and demonstrated. By using temperature compensation, the mean wavelength stability of SFS is as small as 0.67 ppm/°C over the temperature range of -26 to 65°C. The output power, 3 dB bandwidth are 9 dBm and 16.5 nm, respectively.

Tu3L.2 • 16:15

Through-Focus Scanning Optical Fluorescence Microscopy for Marine Phytoplankton Count, Jun Ho Lee¹; ¹Kongju National Univ., Korea. We propose the use of through-focus scanning fluorescence microscopy for marine phytoplankton count. We built a prototype and it was demonstrated to count the phytoplankton within 1 cc seawater with 10 μm resolution in one second.

Tu3L.3 • 16:30

Nanosecond and Femtosecond Laser Induced Breakdown Spectroscopic Studies of Coal and Ash, Hemalaxmi R.¹, Aparna N¹, N.J. Vasa¹, S Seshadri²; ¹Engineering Design, Indian Inst. of technology madras, India; ²Applied Mechanics, Indian Inst. of technology madras, India. Nanosecond and femtosecond laser Induced Breakdown Spectroscopy (ns- and fs-LIBS) were used for elemental analysis of Indian coal and ash. Emissions from C, Na, K, Al, Fe, Ca and molecular CN were identified and analyzed.

Room S223

Room S224

Room S225

Room S226

Room S227

Room S228

These concurrent sessions are grouped across two pages. Please review both pages for complete session information.

Tu3A • Ultrafast Fiber Laser Sources—Continued

Tu3A.3 • 16:45

Broadband coherence of bidirectional mode-locked Er-fiber laser with two saturable absorber mirrors, Yoshiaki Nakajima^{1,2}, Yuya Hata², Kaoru Minoshima^{1,2}; ¹Univ. of Electro-Communications, Japan; ²JST ERATO MINOSHIMA IOS Project, Japan. We evaluate broadband coherence of bidirectional mode-locked Er-fiber-laser with two saturable absorber mirrors. Signal-to-noise ratio of 35-dB at 100-kHz resolution bandwidth in beat notes between narrow linewidth single frequency laser and the output is obtained.

Tu3A.4 • 17:00

High average and peak power laser based on Yb:YAG amplifiers of advanced geometries for OPCPA pumping, Ivan Kuznetsov¹, Ivan Mukhin¹, Evgeny Perevezentsev¹, Mikhail Volkov¹, Oleg Palashov¹; ¹Inst. of Applied Physics of the RAS, Russia. High-power picosecond laser for OPCPA pumping is under development. It is composed of ytterbium fiber oscillator, Yb:YAG thin-rod preamplifiers and Yb:YAG thin-disk amplifier. 120W average power, 10mJ pulse energy with diffraction-limited beam quality is achieved.

Tu3A.5 • 17:15

Picosecond Yb-doped Alumino-phosphosilicate Fiber MOPA with >35kW Peak Power, Arindam Halder¹, Di Lin¹, Andrey Umnikov¹, N. J. Ramirez-Martinez¹, Martin Miguel¹, Pranabesh Barua¹, Shaiful Alam¹, Jayanta K. Sahu¹; ¹Univ. of Southampton, UK. We report a ps-MOPA using an efficient ytterbium-doped Al-P-SiO₂ fiber fabricated by MCVD solution-doping process, generating 35kW peak-power pulses at 1035nm with repetition-rate 1.47MHz and average power 9.1W. The optical conversion efficiency was 76%.

Tu3B • Nonlinear Optical Sources—Continued

Tu3B.2 • 17:00

100-as-level synchronized two-color source based on SPM-enabled spectral selection, Yi Hua¹, Gengji Zhou¹, Wei Liu¹, Ming Xin¹, Franz X. Kärtner¹, Guoqing Chang¹; ¹DESY, Germany. We demonstrate that SPM-enabled spectral selection (SESS) pulses exhibit 100-as-level relative timing jitter with respect to excitation pulses, which is 10 times lower than the Raman soliton pulses derived from the same source laser.

Tu3B.3 • 17:15

Efficient Visible Femtosecond Supercontinuum from an Air-Suspended-Core Microstructured Optical Fiber, Feng Han¹, Jindan Shi¹, Chengli Wei², Jonathan Hu², Xian Feng³; ¹Jiangsu Normal Univ., China; ²Baylor Univ., USA; ³Beijing Univ. of Technology, China. We report efficient visible supercontinuum (SC) generated from an air-suspended-core microstructured optical fiber. The conversion efficiency of pump-to-SC was measured to be 25.4%, while the fraction of the visible SC was as high as 67.3%.

Tu3C • Infrared and Terahertz Microscopy and Nanoscopy and Their Applications—Continued

Tu3C.3 • 17:00

Immune assay using a micro-flow channels detected by a terahertz chemical microscopy, Tatsuki Kamiya¹, Masahiro Iida¹, Kenji Sakai¹, Toshihiko Kiwa¹, Keiji Tsukada¹; ¹Graduate school of natural science and technology, Okayama Univ., Japan. We have developed a terahertz chemical microscopy (TCM) to visualize various types of chemical reactions. Here, a micro-flow channels were fabricated on a sensing plate, and measured time evolution of immune reactions using the TCM.

Tu3C.4 • 17:15

Determination of plant water status using THz radiation, Ran Li¹, Yaojie Lu², Andrew J. Lee¹; ¹Macquarie Univ., Australia; ²Hawkesbury Inst. for the Environment, Western Sydney Univ., Australia. We report the application of THz radiation, generated from a solid-state THz laser source, to the detection of water content within plant leaves, and the determination of plant health status.

Tu3D • Nonlinear Wave Mixing and Applications—Continued

Tu3D.2 • 17:00 **Invited**

Ultra-fast and Ultra-broadband Nonlinear Optical Signal Processing, Leif K. Oxenlowe¹; ¹DTU Fotonik, Denmark. Nonlinear optical effects are useful to control and manipulate large numbers of parallel optical data signals, enabling flexible networks with high spectral and energy efficiency. This talk will describe recent advances in optical signal processing.

Tu3E • Waveguide Devices I—Continued

Tu3E.3 • 17:00

Electro-optic Modulators Further than 100 Gbps, Feng Qiu¹, Shiyoshi Yokoyama¹; ¹Kyushu Univ., Japan. The continuing explosive growth of the Internet and digital storage technology is creating a growing need for high performance electro-optic modulators. Through designing optical waveguides and developing organic materials, we have realized high-performance EO modulators for future optical communication systems.

Tu3E.4 • 17:15

All-optical control of propagation loss with a graphene-embedded polymer waveguide, Zeshan Chang¹, Kin S. Chiang¹; ¹City Univ. of Hong Kong, Hong Kong. We demonstrate, theoretically and experimentally, all-optical control of propagation loss with a graphene-embedded polymer waveguide. Using a 10-mm long waveguide, we achieve 4.6-dB loss modulation for 1550-nm light with 12.4-dBm co-propagating 980-nm pump light.

Tu3F • Novel Measurement Methods II—Continued

Tu3F.3 • 16:45

Phonon Confinement by the Force of Light, Xin He¹, Christopher Baker¹, Yauhen Sachkou¹, Andreas Sawadsky¹, Stefan Forstner¹, Yasmine Sfindla¹, Warwick P. Bowen¹; ¹Univ. of Queensland, Australia. Using superfluid optomechanical system, here we show both that radiation pressure can greatly deform superfluid film, and that this generates new sound modes within the film locally, that are confined by the optical mode and interact strongly with it. This demonstrates a new form of dynamical backaction between light and mechanics.

Tu3F.4 • 17:00

A Large Helium-Neon Ring Laser Gyroscope Operating at 543 nm, Caroline Anyi¹, Jon-Paul Wells¹, Robert Thirkettle¹, Robert Hurst¹, Karl U. Schreiber²; ¹School of Physical and Chemical Sciences, Univ. of Canterbury, New Zealand; ²Technical Univ. of Munich, Germany. We report on the operation of a helium-neon based large ring laser gyroscope on the shortest wavelength neon laser transition at 543.5 nm. The 6.4 metre perimeter gyroscope unlocked on the bias provided by Earth rotation alone; exhibiting a Sagnac frequency near 133 Hz.

Tu3F.5 • 17:15

Theory of Inelastic Optical Wave Mixing Magnetometry, Lu Deng¹, Chengjie Zhu², Edward W. Hagley¹; ¹National Inst of Standards & Technology, USA; ²MOE Key Lab of Advanced Micro-Structured Materials, Tongji Univ., China. We show the presence of an energy-symmetry-based nonlinear propagation blockade on magneto-optical rotation in the widely used single-beam three-state scheme and an inelastic wavemixing scheme that removes this detrimental blockade.

These concurrent sessions are grouped across two pages. Please review both pages for complete session information.

Tu3G • Atom-photon Interaction—Continued

Tu3G.3 • 17:00

Deterministic Creation and Spins in Quantum Emitters in Atomically Thin Semiconductors, Alejandro Montblanch¹, Dhiren Kara¹, Carmen Palacios-Berraquero¹, Matteo Barbone¹, Pawel Latawiec², Marko Loncar², Andrea Ferrari¹, Mete Atatüre¹; ¹Univ. of Cambridge, UK; ²Harvard Univ., USA. We report the deterministic generation of novel single-photon emitters (SPEs) in monolayers of transition metal dichalcogenides (TMDs) by using patterned substrates, and current efforts to generate charged TMD-SPEs through electrical gating to act as qubits.

Tu3G.4 • 17:15

Synthetic spin-orbit coupling for ultracold fermions in optical lattices, Bo Song¹, Chengdong He¹, Zejian Ren¹, Elhur Hajjyev¹, Qianhang Cai¹, Gyu-Boong Jo¹; ¹The Hong Kong Univ. of Science and Technology, Hong Kong. We experimentally implement synthetic spin-orbit coupling in optical lattices with ultracold ¹⁷³Yb fermions. We engineer band topology in one- and two-dimensional lattices and investigate topological states such as symmetry-protected topological phases in this spin-orbit-coupled system.

Tu3H • Optical Microcavities—Continued

Tu3H.2 • 17:00

Exceptional Points in a Specialty Microcavity: Interplay between State-Conversion and Cavity Control Parameters, Arnab Iaha¹, Abhijit Biswas², Sayan Bhattacharjee¹, R. K. Varshney¹, Somnath Ghosh¹; ¹Indian Inst. of Technology, India; ²Inst. of Radio Physics and Electronics, India. Exploiting scattering-matrix in a gain-loss assisted optical-microcavity, interplay between asymmetric-state-conversion and cavity-control parameters around exceptional points is analyzed; where occupying a least area by coupled states during switching, maximum conversion-efficiency with minimal asymmetry is achieved.

Tu3H.3 • 17:15

Raman Lasing in a silica microdisk resonator, Xinyu Cheng¹, Jiaxin Gu¹, Longfu Xiao¹, Guanyu Li¹, Xiaoshun Jiang¹, Min Xiao¹; ¹Nanjing Univ., China. We have demonstrated a chip-based Raman laser by using a silica microdisk resonator with an intrinsic optical Q-factor of 1.5×10^7 . The achieved lasing threshold is as low as 3.9 mw with a conversion efficiency of 7.5%.

Tu3I • Fiber Technologies and Applications—Continued

Tu3I.2 • 17:00

High order cylindrical vector beams transmission in air-core photonic crystal fiber, Juncheng Fang¹; ¹Shenzhen Univ., China. We propose and demonstrate high order cylindrical vector beams transmission in air-core photonic crystal fiber. According to the numerical simulation and experiment, the mode purities of CVBs are measured as high as 67%.

Tu3I.3 • 17:15 Invited

Huge Capacity SDM Transmission and Multi-granular Optical Switching Network Technologies, Naoya Wada¹, Benjamin Puttnam¹, José M. Mendinueta¹, Hideaki Furukawa¹; ¹NICT, Japan. We describe Pb/s space-division-multiplexed transmission technologies to satisfy the ever-increasing traffic demand. We also present optical integrated network technologies capable of providing multi-granular switching capacity to allow data service diversification.

Tu3J • Nonlinear Plasmonics and Metamaterials—Continued

Tu3J.3 • 16:45

Plasmonic waveguides for nano-lasing and four-wave mixing, C. Martijn de Sterke¹, Guangyuan Li¹, Stefano Palomba¹; ¹Univ. of Sydney, Australia. We present a systematic procedure for designing plasmonic waveguides for nano-lasing and for nonlinear optics. We identify superior device designs in which an increased overlap of the field with the gain compensates for higher losses.

Tu3J.4 • 17:00

Boosted Kerr Nonlinearity in Nanoscale Slot Waveguides with Hyperbolic Claddings, Guangyuan Li^{1,2}; ¹Shenzhen Inst.s of Advanced Technology, Chinese Academy of Sciences, China; ²Biomedical Engineering Laboratory for Photoelectric Sensing Technology, China. We show that nanoscale slot waveguides clad by hyperbolic metamaterials can have higher Kerr nonlinear effects for shorter device lengths compared with the conventional metal-slot waveguides.

Tu3J.5 • 17:15

Brightening of Dark Excitons in Monolayer WS₂ Sandwiched in a Metal-film-coupled Nanocavity, Jin Liu¹, Tsz Wing Lo¹, Meng Qiu¹, Chi-hang Lam¹, Dang Yuan Lei¹; ¹Applied Physics, Hong Kong Polytechnic Univ., Hong Kong. We provide a simple method to observe the effects of dark excitons from room temperature in monolayer WS₂ by using a metal-film-coupled nanocavity.

Tu3K • Biophotonics and Applications II—Continued

Tu3K.3 • 17:00

Machine Learning Enabled Computational Imaging and Sensing for Point-of-Care Medicine and Global Health, Aydogan Ozcan¹; ¹Univ. of California Los Angeles, USA. We provide an overview of our recent work on the use of machine learning, including e.g., deep neural networks, in advancing computational imaging and sensing systems, targeting various global health and point-of-care medicine related applications.

Tu3K.4 • 17:15

Wide-view Bessel light-sheet fluorescence microscopy for high-resolution, isotropic neuron imaging, Chunyu Fang¹, Xuechun Wang¹, Yusha Li², Tingting Chu¹, Lanxin Zhu¹, Dan Zhu², Peng Fei^{1,3}; ¹School of Optical and Electronic Information, Huazhong Univ. of Sci and Tech, China; ²Britton Chance Center for Biomedical Photonics Wuhan National Laboratory for Optoelectronics Huazhong Univ. of Science and Technology, China; ³Shenzhen Huazhong Univ. of Science and Technology Research Inst., China. We develop a wide-view Bessel light-sheet fluorescence microscopy with 2 μm optical sectioning over 3 mm field of view. It achieves high-resolution, isotropic imaging of large-scale neural structures in mouse brain.

Tu3L • Laser Applications and Technologies—Continued

Tu3L.4 • 16:45

Supercontinuum Laser Based Photoacoustic Approach for Acetylene Gas Sensing, Ramya Selvaraj¹, N. J. Vasa¹, Shiva N. S. N¹; ¹Indian Inst. of Technology, Madras, India. A broadband photoacoustic gas sensor with solid etalon using supercontinuum laser for acetylene monitoring was characterized. The acetylene concentration was determined to be 330 pptv at a data acquisition time of 10 ms

Tu3L.5 • 17:00

Optical monitoring of nitrous acid (HONO) in ambient air using a continuous-wave quantum cascade laser, Xiaojuan Cui¹, Fengzhong Dong¹, Runqing Yu¹, Zhirong Zhang¹, Hua Xia¹, Pengshuai Sun¹, Luo Han¹, Weidong Chen²; ¹Anhui Inst. of Optics & Fine Mechani, China; ²Université du Littoral Côte d'Opale, France. An optical instrument based on a quantum cascade laser operating at 8 μm for measurement of atmospheric gaseous HONO was developed. Typical photochemical reactions of HONO have been observed on sunny and snowy days.

Tu3L.6 • 17:15

Linearly Optical Frequency Chirped DFB Laser with Pre-distorted Modulation Waveform for High Resolution FMCW Ranging System, Koichi Iiyama¹, Misaki Isoda¹, Atsushi Nakamoto¹; ¹Kanazawa Univ., Japan. Optical frequency chirp of a DFB laser is linearized by modifying the modulation waveform using an interference signal of an interferometer, and high spatial resolution FMCW ranging system was realized.

Room S223

Room S224

Room S225

Room S226

Room S227

Room S228

These concurrent sessions are grouped across two pages. Please review both pages for complete session information.

Tu3A • Ultrafast Fiber Laser Sources—Continued

Tu3A.6 • 17:30

Hybrid fiber MOPA-bulk amplifier system, Kota Masuda¹, Daichi Fujii¹, Yuki -. Kato¹, Shota Mizuno¹, Yukiko Harada¹, Ayumu Maruyama¹, koji isaku¹, Kazuyoku Tei¹, Shigeru Yamaguchi¹; ¹Tokai Univ., Japan. We report on a hybrid fiber MOPA + solid-state amplifier. The maximum average power from a solid-state amplifier was 10.9 W, and the maximum peak power was 1.0 MW with the spectral width of 0.07 nm.

Tu3A.7 • 17:45

Passively mode-locked Erbium-doped fiber laser using PbS quantum dots deposited on microfiber, Liyuan Liu¹, Xiaolan Sun¹, Wei Zhao¹, Chuanhang Zou¹, Qianqian Huang¹, Chengbo Mou¹, Tingyun Wang¹; ¹Key Laboratory of Specialty Fiber Optics and Optical Access Networks, Shanghai Univ., China. PbS quantum dots (QDs) deposited on microfiber as a new type of saturable absorber is demonstrated in an erbium doped fiber laser. Successfully mode locked pulses with 51.56 dB signal to noise ratio was achieved.

Tu3B • Nonlinear Optical Sources—Continued

Tu3B.4 • 17:30

Hollow-core fiber based mid-IR gas Raman laser with high peak power, Shoufei Gao¹, Ling Cao¹, Zhigang Peng¹, Xiaocong Wang¹, Yingying Wang¹, Pu Wang¹; ¹Beijing Univ. of Technology, China. We report a 2.8 μ m gas Raman laser in a methane-filled hollow-core negative-curvature fiber with average power of 113 mW, pulse energy of 113 μ J and estimated peak power of 9.5 MW.

Tu3B.5 • 17:45

Two-color-field Driven Hollow-core Fiber Compressor with Robust Inline Scheme, Yudong Yang^{1,2}, Liwei Song^{1,3}, Fabian Scheiba^{2,1}, Giulio Maria Rossi^{2,1}, Roland E. Mainz¹, Shaobo Fang¹, Giovanni Cirmi^{1,2}, Oliver D. Mücke^{1,2}, Franz Kaertner^{1,2}; ¹Deutsches Elektronen-Synchrotron DESY, Germany; ²The Hamburg Centre for Ultrafast Imaging CUI, Univ. of Hamburg, Germany; ³State Key Laboratory of High Field Laser Physics, Shanghai Inst. of Optics and Fine Mechanics, China. We present a new scheme of two-color-field driven hollow-core-fiber compression, whose \sim 1mJ output covers 300 nm to 950 nm supporting sub-cycle pulses of \sim 2.1 fs duration. The spectral phase is characterized with two-dimensional spectral shearing interferometry.

Tu3C • Infrared and Terahertz Microscopy and Nanoscopy and Their Applications—Continued

Tu3C.5 • 17:30

Evaluation of penetration of cosmetic liquid with Terahertz time-of-flight method, Taiga Morimoto¹, Taihei Kuroda¹, Kenji Sakai¹, Toshihiko Kiwa¹, Keiji Tsukada¹; ¹Okayama Univ., Japan. A terahertz time-of-flight method has been developed to evaluate penetration of cosmetic liquid. By using a face mask as the reservoir of the cosmetic liquid, the evaluation from the horny layers could be realized.

Tu3C.6 • 17:45

Development of in situ methods for battery using a THz chemical microscope, Kentaro Fujiwara¹, Yuki Akiwa¹, Kenji Sakai¹, Toshihiko Kiwa¹, Keiji Tsukada¹; ¹Okayama Univ. graduate school, Japan. It is important to measure the special deviation of electrochemical reactions on electrodes to improve the performance of batteries. Here, electrochemical measurement using THz chemical microscope with a sealed container was applied for measurements.

Tu3D • Nonlinear Wave Mixing and Applications—Continued

Tu3D.3 • 17:30

Pump correlation requirements for four wave mixing-based phase quantization schemes, Aneesh Sobhanan¹, Arjun N. Iyer¹, Aravind P. Anthur², Liam P. Barry², Deepa Venkitesh¹; ¹Indian Inst. of Technology, Madras, India; ²School of Electronic Engineering, Dublin City Univ., Ireland. We demonstrate the experimental results of phase noise measurements on the coherent addition of signal and conjugate in a four wave mixing-based two-level phase quantizer and illustrate the requirement of the anti-correlation between the pumps.

Tu3D.4 • 17:45

Polarization Insensitive Phase Conjugation Using Single-pump Four Wave Mixing in SOA, Aneesh Sobhanan¹, Lakshmi Narayanan Venkatasubramani¹, R David Koilpillai¹, Deepa Venkitesh¹; ¹Indian Inst. of Technology, Madras, India. We experimentally demonstrate the generation of polarization insensitive phase conjugate of PM-QPSK signal in both input and output ports of SOA using partially degenerate four wave mixing with pump power of only 4 dBm.

Tu3E • Waveguide Devices I—Continued

Tu3E.5 • 17:30

Broadband filtering of the fundamental mode of a few-mode waveguide with a phase-shifted long-period grating, Quandong Huang¹, Wen Wang², Wei Jin¹, Kin S. Chiang¹; ¹City Univ. of Hong Kong, Hong Kong; ²Univ. of Electronic Science and Technology of China, China. We design and fabricate a phase-shifted long-period grating in a few-mode waveguide to filter out the fundamental mode. Our experimental device shows a mode extinction ratio larger than 8 dB from 1520 to 1610 nm.

Tu3F • Novel Measurement Methods II—Continued

Tu3F.6 • 17:30

Optical interferometry with transmitted Haidinger fringes through a plane parallel plate, Choonghwan Lee¹, Ju Eun Park¹, Heejoo Choi¹, Jiung Kim¹, Myoungsik Cha¹, Jonghan Jin²; ¹Pusan National Univ., Korea; ²Korea Research Inst. of Standards and Science, Korea. Haidinger fringes can be observed when a quasi-monochromatic extended source is viewed through a plane parallel plate. We present two applications of Haidinger fringes; measurements of the thickness profiles of glass plates and laser wavelengths.

Tu3F.7 • 17:45

Infrared metrology with visible photons, Leonid A. Krivitsky¹, Anna Paterova^{1,2}, Hongzhi Yang¹, Chengwu An¹, Dmitry Kalashnikov¹; ¹Data Storage Inst., Singapore; ²Nanyang technological Univ., Singapore. We realize an infrared (IR) metrology technique, which uses only components for the visible range. It relies on nonlinear interference of correlated photons. We show its applications to IR spectroscopy, optical coherence tomography and imaging.

These concurrent sessions are grouped across two pages. Please review both pages for complete session information.

Tu3G • Atom-photon Interaction—Continued

Tu3G.5 • 17:30

Ultrathin Optical Fibers for Probing and Manipulating Neutral Atoms, Thomas Nieddu¹, Krishnapriya S. Rajasree¹, Ratnesh K. Gupta¹, Anjana Krishnadas¹, Tridib Ray¹, Jinjin Du¹, Wenfang Li¹, Sile Nic Chormaic¹, ¹Okinawa Inst of Science & Technology, Japan. We present recent work on the integration of ultrathin optical fibers into a cold ⁸⁷Rb system, for exploring multiphoton processes and the generation of Rydberg atoms near a dielectric surface.

Tu3G.6 • 17:45

Accurate Determination of the Landé g-Factors for 5s² 1S₀ and 5s5p 3P₀ States of the ⁸⁷Sr Atom, Benquan Lu^{1,2}, Yebing Wang^{1,2}, Qinfang Xu¹, Mojuan Yin¹, Hong Chang^{1,2}, ¹National Time Service Center, China; ²Univ. of Chinese Academy of Sciences, China. In the ultra-cold ⁸⁷Sr atomic system, the Zeeman shift of the clock transition was measured with the σ^+ -polarized interrogation to accurately determine the g-factors of the 5s² 1S₀ and 5s5p 3P₀ states.

Tu3H • Optical Microcavities—Continued

Tu3H.4 • 17:30

Kerr Comb Generation under Weak Dispersion Regime in High-Q Silica Microtoroids, Shun Fujii¹, Ryo Suzuki¹, Minoru Hasegawa¹, Takasumi Tanabe¹, ¹Keio Univ., Japan. We experimentally and numerically investigated Kerr comb generation under a weak dispersion regime in high-Q factor silica microtoroids. Higher-order dispersion dominates the Kerr comb at near zero dispersion wavelengths and potentially provides broadband frequency conversion.

Tu3H.5 • 17:45

Tunable Spatiotemporal Soliton Generation in Serially Coupled Dual Micro-Ring Resonators, Lingsong Hong¹, Shaohao Wang¹, Yazhen Zhang¹, Sai Tak Chu², Ping Kong A. Wai³, ¹Fuzhou Univ., China; ²City Univ. of Hong Kong, Hong Kong; ³The Hong Kong Polytechnic Univ., Hong Kong. We present an inter-ring detuning control scheme to generate spatiotemporal soliton in symmetric serially coupled dual micro-ring resonators. By using our proposed model, we numerical demonstrate tunable different orders solitons generation from identical initial state.

Tu3I • Fiber Technologies and Applications—Continued

Tu3I.4 • 17:45

Photodarkening of ytterbium-doped large-mode-area photonic crystal fiber, Yun Chen¹, Guiyao Zhou¹, Yang Xiao¹, Teng wang¹, Haixia Fan¹, Xian Wang¹, Jiantao Liu¹, Luyao Zhu¹, Mengmeng Zhu¹, Zhiyun Hou¹, ¹School of Information and Optoelectronics Science and Engineering, South China Normal Univ., China. We investigate the temporal evolution of photodarkening effect in ytterbium-doped large-mode-area photonic crystal fiber and discuss its mechanism. The results show the great influence of photodarkening on lasing properties.

Tu3J • Nonlinear Plasmonics and Metamaterials—Continued

Tu3J.6 • 17:30 **Invited**

Quantum Entanglement of Surface Plasmons, Xifeng Ren¹, Yong-Jing Cai¹, Ming Li¹, Yang Chen¹, Guang-Can Guo¹, ¹Key laboratory of quantum information, China. Here we introduce our recent works on quantum plasmonics: plasmon on-chip quantum interference, generation and propagation of plasmon entanglement and two-plasmon NOON state in a nanoscale waveguide. Our works can bridge nanophotonics and quantum optics.

Tu3K • Biophotonics and Applications II—Continued

Tu3K.5 • 17:30

Integration of photonic crystal and magnetic bead aggregation technique for fluorescence enhancement, Yang Chen¹, Ying-Bin Wang¹, Lin-Yun Su¹, Ching-Shu Fu¹, Cheng-Yeh Huang¹, Cheng-Sheng Huang¹, Wensyang Hsu¹, ¹National Chiao Tung Univ., Taiwan. We combine photonic crystal and magnetic beads aggregation enhanced fluorescence for extremely sensitive detection of biomolecules in bead-based assay format. The limit of detection for Interleukin 1 β can achieve 100 ag/ml.

Tu3K.6 • 17:45

3D super resolution microscopy in multicellular tissues, Rong Chen¹, Yuxuan Zhao¹, Yarong Wang¹, Peng Fei^{1,2}, ¹Huazhong Univ. of Sci and Tech, China; ²Shenzhen Huazhong Univ. of Science and Technology Research Inst., China. We combined Bessel light sheet microscopy with Bayesian analysis of bleaching and blinking(3B) method to achieve multicellular volumetric imaging. This technology offers low-background, 3D super resolution imaging in thick scattering tissues and organisms.

Tu3L • Laser Applications and Technologies—Continued

Tu3L.7 • 17:30

Non-uniform Optical Phased Array Optimized with Genetic Algorithm, TianHua Lin^{1,3}, Tao Chu², ¹Inst. of Semiconductors, China; ²Zhejiang Univ., China; ³Univ. of Chinese Academy of Sciences, China. An optical phased array with 32 Gaussian beam emitters was optimized with genetic algorithm. The side mode suppression deteriorates with the decrease of the beam waist radius and the increase of the steering angle.

Tu3L.8 • 17:45

Laser Architectures for Space-Based Sodium Resonance Fluorescence Lidar, Anthony W. Yu¹, Steven X. Li¹, Michael A. Krainak¹, Yingxing Bai¹, Oleg Konoplev², Molly E. Fahey¹, Kenji Numata¹, Diego Janches¹, ¹NASA Goddard Space Flight Center, USA; ²SSAI, USA. NASA GSFC is developing a space-based sodium resonance fluorescence lidar for the International Space Station (ISS). We discuss the technology, prototypes, risks and trades for two laser architectures - Raman laser and sum frequency generation.

These concurrent sessions are grouped across two pages. Please review both pages for complete session information.

08:00–18:00 Registration, S221 Foyer of HKCEC

08:30–10:00

W1A • Power Scaling of Lasers
Presider: Anting Wang; Univ. of Sci & Tech of China, China

W1A.1 • 08:30 **Invited**

Coherent Beam Combining of Fiber Lasers, Arno Klenke^{1,2}, Michael Müller¹, Henning Stark¹, Andreas Tünnermann^{1,3}, Jens Limpert^{1,2}; ¹Friedrich-Schiller-Univ. Jena, Germany; ²Helmholtz-Inst. Jena, Germany; ³Fraunhofer Inst. of Applied Optics and Precision Engineering, Germany. Coherent beam combination has been established as a performance scaling concept for laser systems to overcome limitations of a single emitter. Today, the most powerful femtosecond fiber lasers employ his technique.

W1A.2 • 09:00

Reinforcement Learning for Coherent Beam Combining, Henrik Tuennermann¹, Akira Shriakawa¹; ¹Univ. of Electro-Communications, Japan. Reinforcement learning has been shown to be capable of solving complex tasks. Here we show potential advantages and disadvantages in the context of phase control for coherent beam combining.

08:30–10:00

W1B • Nonlinear Optics in Microresonators
Presider: Kuijuan Jin; Chinese Academy of Sciences, China

W1B.1 • 08:30 **Tutorial**

Whispering-gallery-mode Resonators and Their Applications for Nonlinear Optics, Lan Yang¹; ¹Washington Univ. in St Louis, USA. I will discuss the fundamental physics, such as parity-time symmetry and exceptional points, in whispering-gallery-mode resonators, which can be used to achieve a new generation of nonlinear optical systems enabling unconventional control of light flow.

08:30–10:00

W1C • Infrared Fibers & Materials and Their Applications
Presider: Cheng Wang; Harvard Univ., USA

W1C.1 • 08:30 **Invited**

Thulium fiber lasers – the Modulation Instability and future high power scaling, Martin Richardson^{1,2}, Alex Sincore¹, Don Jin Shin¹, Justin Cook¹, Joshua Bradford¹, Nathan Bodnar¹; ¹Univ. of Central Florida, CREOL, USA; ²School of Electrical & Electronic Engineering, Nanyang Technology Univ., Singapore. A new examination of Tm fiber laser concepts and the interplay of non-linear thermal and optical effects, open promising avenues of investigation that should lead to effective power scaling of mid-IR sources in the future.

W1C.2 • 09:00 **Invited**

Nano-structured Optical Metasurfaces and Multi-material Fibers for IR Applications, Fabien Sorin¹, Tapajyoti Das Gupta¹, Wei Yan¹, Louis Martin-Monier¹, Tung Nguyen-Dang¹, Alexis G. Page¹, Yunpeng Qu¹; ¹Inst. of Materials, Ecole Polytechnique Fédérale de Lausanne (EPFL), Switzerland. We will show how controlling the fluid dynamics of glasses and polymers can result in the scalable fabrication of optical metasurfaces and multimaterial fibers. Some applications in the IR region will also be discussed

08:30–10:00

W1D • Machine Learning and Neural Networks in Photonics
Presider: Lilin Yi; Shanghai Jiao Tong Univ., China

W1D.1 • 08:30 **Invited**

Coherent Ising Machine - Optical Neural Network operating at the Quantum Limit, Yoshihisa Yamamoto^{2,1}; ¹Stanford Univ., USA; ²Japan Science and Technology Agency, Japan. We will present the basic concept, operational principle and experimental performance of a novel computing machine with the network of degenerate optical parametric oscillators. The developed machine has 2048 qubits with all-to-all connections.

W1D.2 • 09:00

Bit-Error Rate Performance on Depth of Learning in BPSK Label Processing Using Complex-Valued Neural Network, Kazumasa Ishihara¹, Hiroki Nakagawa¹, Hiroki Kishikawa¹, Nobuo Goto¹; ¹Tokushima Univ., Japan. Bit-error rate performance of the BPSK-label processing optical neural network is numerically evaluated. As a result, the noise tolerance for the incident labels is improved by reducing the learning depth for weights.

08:30–10:00

W1E • Laser Additive Manufacturing
Presider: Wei Xiong; Wuhan National Lab for Optoelectronics, China

W1E.1 • 08:30 **Invited**

Fabrication of Metal Matrix Composites by Laser Additive Manufacturing, Zhuo Li¹, Dong Liu¹, Xiangjun Tian¹, Huaming Wang¹; ¹Beihang Univ., China. Varieties of metal matrix composites were prepared by laser additive manufacturing. The stable and high energy density heat source provided by laser is suitable for the manufacture of intractable, refractory metal or metal matrix composite components.

W1E.2 • 09:00

Laser writing of nanostructures deep inside Gallium Arsenide (GaAs), Onur Tokel¹, Ahmet Turnali¹, Petro Deminskyi¹, Serim Ilday¹, F. Ömer Ilday¹; ¹Bilkent Universitesi, Turkey. Recently, we have showed a direct laser writing method that enables the first subsurface modifications and functional devices created deep inside silicon. Here, we extend the technique demonstrating the first controlled subsurface nanostructures in GaAs.

08:30–10:00

W1F • Silicon Hybrid Integration
Presider: Hon Tsang; The Chinese Univ. of Hong Kong, Hong Kong

W1F.1 • 08:30

Hot-wire CVD a-Si:H for low loss silicon photonic waveguides, Swe Z. Oo^{1,2}, Antulio Tarazona¹, Rafidah Petra², Ali Khokhar¹, Graham Reed¹, Anna C. Peacock¹, Harold M. Chong²; ¹Optoelectronics Research Centre, Univ. of Southampton, UK; ²School of Electronics and Computer Science, Univ. of Southampton, UK. We demonstrate low temperature hot-wire chemical vapor deposition of low loss a-Si:H wire waveguides. We achieved propagation loss of 0.65 dB/cm at TE polarized 1.55 μ m wavelength for waveguides deposited at 230 °C.

W1F.2 • 08:45 **Invited**

O-band InAs Quantum Dot Light Sources Monolithically Grown on Si, Shu Pan¹, Mengya Liao¹, Zizhuo Liu¹, Ying Lu¹, Victoria Cao¹, Mingchu Tang¹, Jae-Seong Park¹, Jiang Wu¹, Siming Chen¹, Alwyn Seeds¹, Huiyun Liu¹; ¹Univ. College London, UK. We discuss our recent progress made in the direct growth of 1.3 μ m InAs/GaAs quantum dot (QD) light-emitting sources on Si substrates for Si photonics.

These concurrent sessions are grouped across two pages. Please review both pages for complete session information.

08:00–18:00 Registration, S221 Foyer of HKCEC

08:30–10:00

W1G • High Power Fiber Laser
Presider: Pu Zhou; National Univ. of Defense Tech., China

W1G.1 • 08:30 **Tutorial**

High Power Fiber Lasers, Johan Nilsson¹; ¹Univ. of Southampton, UK. Abstract not available.

08:30–10:00

W1H • Optical Metasurfaces I
Presider: Xiangping Li; Jinan Univ., China

W1H.1 • 08:30 **Tutorial**

A revolution towards multitasking metasurfaces, Erez Hasman¹, Elhanan Maguid¹, Bo Wang¹, Michael Yannai¹, Arkady Faerman¹, Vladimir Kleiner¹; ¹Technion-Israel Inst. of Technology, Israel. The shared-aperture concept and the geometric phase phenomenon were incorporated within a metasurface to obtained photonic spin-control multifunctional devices. The shared-aperture metasurface platform opens a pathway to novel types of nanophotonic functionality.

08:30–10:00

W1I • Advanced Signal Modulation
Presider: Xian Zhou; Univ. of Science and Technology Beijing, China

W1I.1 • 08:30 **Invited**

High-speed Faster Than Nyquist Optical Transmission, Fan Zhang¹, Yixiao Zhu¹, Pengfei Wang¹, Chuanchuan Yang¹; ¹Peking Univ., China. Faster-than-Nyquist (FTN) signaling is discussed both theoretically and experimentally. Several schemes of FTN signal generation and reception are compared with emphasize on high-speed transmission with 16-QAM format.

W1I.2 • 09:00

Simple Propagation Model for Nonlinear Fourier Transform (NFT) based Transmission, Wenqi Zhang¹, Tony Gui², Chao Lu², Tanya Monro¹, Alan Lau², Shahrar Afshar V¹, Terence Chan¹; ¹Univ. of South Australia, Australia; ²The Hong Kong Polytechnic Univ., Hong Kong. NFT-based approach for fibre optic transmission was recently proposed, aiming at achieving rate beyond the linear capacity limit. This paper simplifies the signal propagation model and characterises the effects of noises in NFT transmissions.

08:30–10:00

W1J • Integrated Sources I
Presider: T. Wang; Univ. of Sheffield, UK

W1J.1 • 08:30 **Invited**

Circular-side Polygonal Microcavity Semiconductor Lasers, Yong-Zhen Huang^{1,2}; ¹Inst. of Semiconductors, Chinese Academy of Sciences, China; ²Univ. of Chinese Academy of Sciences, China. Stable dual-mode lasing deformed square microcavity lasers and single mode deformed hexagonal microlasers are reported, where flat-sides are replaced by circular sides for enhancing mode Q factors due to the reduction of vertex radiation loss.

W1J.2 • 09:00

Multi-channel interference widely tunable semiconductor laser with a compact and efficient shallow-deep transition, Qunan Chen¹, Chun Jiang¹, Xiang Ma¹, Qiaoyin Lu¹, Weihua Guo¹; ¹Huazhong Univ. of S&T, China. Multi-channel interference laser with a compact and efficient shallow-deep transition was fabricated, achieving around 22 mA threshold currents, > 40 nm tuning range covering C band, > 40 dB SMSRs.

08:30–10:00

W1K • Biophotonics and Applications III
Presider: Peng Xi; Peking Univ., China

W1K.1 • 08:30 **Invited**

LED-based spectrophotometry, Marco Marzan¹, Massimiliano Lucidi¹, Gabriella Cincotti¹; ¹Univ. Roma Tre, Italy. We demonstrate that accurate spectrophotometric measurements can be achieved using low-cost LED-based devices, using a geometrical-optics approach and real-time image processing.

W1K.2 • 09:00 **Invited**

Objective Assessment of Surgical Skill with fNIRS, Xavier Intes¹, Arun Nemani¹, Suvarnu De¹; ¹Rensselaer Polytechnic Inst., USA. We present an advanced optical neuroimaging methodology that can objectively and successfully classify subjects with different expertise levels associated with surgical within the framework of the Fundamentals of Laparoscopic Surgery program.

08:30–10:00

W1L • Integrated Microwave Photonics I
Presider: Ming Li; Inst. of Semiconductor, CAS, China

W1L.1 • 08:30 **Tutorial**

Integrated Photonic Circuits for Microwave Photonics, Jianping Yao¹; ¹Univ. of Ottawa, Canada. Photonic integrated circuits for microwave photonic signal generation and processing based on three materials systems are reviewed. The challenges and impact of new advances for short and long term applications in communications and information processing are discussed.

These concurrent sessions are grouped across two pages. Please review both pages for complete session information.

W1A • Power Scaling of Lasers—Continued

W1A.3 • 09:15

High power single-frequency VECSEL platform for AMO physics, Jussi-Pekka Penttinen^{1,2}, Shaun C. Burd³, Sanna Ranta¹, David T. Allcock³, Mika Mäki¹, Emmi Kantola¹, Dietrich Leibfried³, Mircea Guina^{1,2}, ¹Optoelectronics Research Centre, Tampere Univ. of Technology, Finland; ²Vexlum Ltd, Finland; ³Time and Frequency Division, Ion Storage Group, National Inst. of Standards and Technology, USA. We report high power single-frequency vertical external-cavity surface-emitting lasers (VECSELs) for applications in atomic, molecular and optical (AMO) physics. The laser platform is wavelength versatile, delivering watt-level output between 920 nm to 1260 nm in single-mode.

W1A.4 • 09:30

2.5 kW narrow linewidth fiber amplifier with white noise signal phase modulated seed, Chu Q. Chu^{1,2}, Yi Shi¹, Jing Wen¹, Lie Ouyang¹, Lei Zhao², Jianjun Wang¹, Honghuan Lin¹, Feng Jing¹, ¹China Academy of Engineering Physics, China; ²Engineering Physics, Tsinghua Univ., China. The fiber laser system with white noise signal phase modulated seed is optimized. Based on the theoretical results, a fiber laser with 54 GHz linewidth, 2.5 kW output power and near-diffraction-limited beam quality is obtained.

W1A.5 • 09:45

Power scaling, passive Q-switching and intracavity frequency doubling of blue-diode-pumped Pr³⁺:YLF laser, Shogo Fujita¹, Hiroki Tanaka¹, Fumihiko Kannari¹, ¹Keio Univ., Japan. We demonstrate a blue-diode-pumped Pr³⁺:YLF laser. The output power of 6.7 W is obtained at 640 nm. The laser is extended to passive Q-switching and its intracavity second harmonic generation with a Co²⁺:MgAl₂O₄ saturable absorber.

W1B • Nonlinear Optics in Microresonators—Continued

W1B.2 • 09:30

Inter-mode breather solitons in optical microresonators, Hairun Guo¹, Erwan Lucas¹, Martin H. Pfeiffer¹, Maxim Karpov¹, Tobias J. Kippenberg¹, ¹École polytechnique fédérale de Lausanne, Switzerland. We demonstrate a novel type of breather solitons triggered by avoided mode crossings that are ubiquitous phenomena in multi-mode optical microresonators, which was termed as intermode breather soliton.

W1B.3 • 09:45

Soliton trapping in a Kerr microresonator with orthogonally polarized dual-pumping, Ryo Suzuki¹, Shun Fujii¹, Atsuhiko Hori¹, Takasumi Tanabe¹, ¹Keio Univ., Japan. We study soliton trapping between orthogonally polarized solitons inside a microresonator by using dimensionless coupled LLEs. We reveal the trapping conditions, which depend on the FSR difference, second order dispersion, and input field.

W1C • Infrared Fibers & Materials and Their Applications—Continued

W1C.3 • 09:30

Low EML, large effective area, and high power fraction performance in THz propagation with porous core PCF, Li Xia¹, Udaya S. Rahubadde¹, Nishan Wu¹, ¹School of Optical and Electronic Information, Huazhong Univ. of Science and Technology, China. We designed a porous core PCF with tetrahedral hole for THz with specific model property and improved essential performance parameters. The fiber is feasible to build with aid of prevailing state of the art fabrication.

W1C.4 • 09:45

Withdrawn.

W1D • Machine Learning and Neural Networks in Photonics—Continued

W1D.3 • 09:15

Prediction Performance of Reservoir Computing Using a Semiconductor Laser with Double Optical Feedback, Guang-Qiong Xia¹, Yu-Shuang Hou¹, Zheng-Mao Wu¹, ¹Southwest Univ., China. A reservoir computing system is proposed, and its prediction performance is investigated numerically. The results indicate that, through optimizing parameters, prediction with Gb/s rate and normalized mean square error below 3% can be realized.

W1D.4 • 09:30 Invited

Reinforcement Learning in a Large Scale Photonic Network, Sheler Maktoobi², Louis Andreoli², Laurent Larger², Maxime Jacquot², Daniel Brunner¹, ¹CNRS - FEMTO-ST, France; ²FEMTO-ST, Univ. Bourgogne Franche-Comté, France. We experimentally create a neural network, implementing 2025 connections in parallel. We numerically validate the scheme for at least 34000 photonic neurons. We demonstrate photonic efficiently converging reinforcement learning, prediction a chaotic signal with.

W1E • Laser Additive Manufacturing—Continued

W1E.3 • 09:15 Invited

Chemical Advances for 3D Laser Nano-Printing, Christopher Barner-Kowollik^{1,2}, ¹School of Chemistry, Queensland Univ. of Technology, Australia; ²Inst. for Polymer Chemistry, Karlsruhe Inst. of Technology, Germany. The lecture will highlight the most recent chemical advances in 3D laser lithography including aspects of super resolution lithography, subtractive lithography and multi-material printing.

W1E.4 • 09:45

Performance improvement and add-on functionalities to conventional lateral-flow devices using a laser direct-write patterning technique, Collin L. Sones¹, Peijun He¹, Ioannis N. Katis¹, Robert W. Eason¹, ¹Optoelectronic Research Center, UK. We report the use of a laser direct-write technique for modification of a conventional lateral-flow device that not only enables enhanced sensitivity and limit of detection, but also allows multiplexing detection within a single device.

W1F • Silicon Hybrid Integration—Continued

W1F.3 • 09:15

C/L-band InAs QDs on CMOS compatible Ge and on-axis Si (001) platform, Ting Wang¹, Jianjun Zhang¹, ¹Inst. of Physics, CAS, China. In recent years, the growing demand for silicon based light sources has boosted the research field of III-V/IV hybrid lasers. Here, the C/L-band light emission (1.53 μm-1.63 μm) of InAs/In_{0.25}Ga_{0.75}As quantum dots (QDs) epitaxially grown on CMOS-compatible Ge and U-shape Si (001) substrates by solid-source molecular beam epitaxy (MBE) are reported.

W1F.4 • 09:30 Invited

3D Hybrid Integration for Silicon Photonics, Jonathan Klamkin¹, Bowen Song¹, ¹Electrical and Computer Engineering Department, Univ. of California Santa Barbara, USA. 3D hybrid integration for silicon photonics is based on flip-chip bonding and vertical coupling. The benefits of this approach will be discussed in comparison to other laser integration approaches.

10:00–10:30 Coffee Break

These concurrent sessions are grouped across two pages. Please review both pages for complete session information.

W1G • High Power Fiber Laser—Continued

W1G.2 • 09:30

Generation of Megawatt Peak-power Femtosecond Pulses from an Excessive-Normal-Dispersion Fiber Laser, Wu Liu¹, Jintao Fan¹, Ruoyu Liao¹, Jiahua Cui¹, Chen Xie¹, Chingyue Wang¹, Ming-lie Hu¹; ¹Tianjin Univ., China. We demonstrate a passively mode-locked fiber laser with excessive normal dispersion (END) yielding 230 nJ pulses with 69 fs dechirped duration. Numerical simulation indicates the energy scalability to over 1 μ J is possible.

W1G.3 • 09:45

Compact, 200 MW Peak Power, 1 μ m Source With All-fiber Front-End, Yizhou Liu^{2,1}, Peter Krogen³, Damian Schimpf^{2,4}, Guoqing Chang^{2,1}, Phillip Keathley³, Franz X. Kärtner³; ¹Hamburg Univ., Germany; ²DESY, Germany; ³MIT, USA; ⁴Hamburg Center for Ultrafast Imaging, Germany. We report on a 1.035- μ m, all-fiber, femtosecond chirped pulse amplifier with 55 μ J pulse energy, 1 MHz repetition rate, producing 800 ps chirped pulses. The output is compressed to 245 fs, 1.3x its transform limit.

W1H • Optical Metasurfaces I—Continued

W1H.2 • 09:30 **Invited**

Flat optics with metasurfaces, Federico Capasso¹, Yao-Wei Huang^{1,2}, Noah A. Rubin¹, Antonio Ambrosio³, Robert C. Devlin⁴, Cheng-Wei Qiu²; ¹Harvard John A. Paulson School of Engineering and Applied Sciences, Harvard Univ., USA; ²Dept. of Electrical and Computer Engineering, National Univ. of Singapore, Singapore; ³Center for Nanoscale Systems, Harvard Univ., USA; ⁴Metalenz Inc., USA. Q-plates based on liquid crystals have been widely used in quantum optics and novel communication schemes. Here a far more general spin to orbital angular momentum scheme is demonstrated based on a novel optical elements (J-plates) not limited to conjugate converted states, which are used to generate new complex structured light. By cascading J plates we show additional light manipulation functionalities.

W1I • Advanced Signal Modulation—Continued

W1I.3 • 09:15

Real-Time Single Threshold PAM-4 Demodulation Scheme, Hanlin Feng¹; ¹Shanghai Jiao Tong Univ., China. Complex three threshold decision circuit used to be a standard decoder for PAM-4 signal. We have experimentally demonstrated a novel single threshold demodulation scheme to real-time decode PAM-4 signal.

W1I.4 • 09:30

Employment of Multi-layer Neural Network for Channel Equalization in 4x50-Gb/s PAM4 Signal Transmission over 80-km SSMF, Xiaoxiao Dai¹, Xiang Li¹, Ming Luo¹; ¹State Key Laboratory of Optical Communication Technologies and Networks, China. A four-layer artificial neural network is designed for non-linearity compensation under two different system configurations. It achieved 4x50-Gb/s PAM-4 IM/DD transmission for 80-km fiber with 4dB power sensitivity improvement over conventional algorithms.

W1I.5 • 09:45

The Influence of Laser Linewidth on Optical SSB Nyquist PAM-4 and Direct-detection Transmission Systems, Jing Zhang¹, Mingyue Zhu¹, Xingwen Yi¹, Kun Qiu¹; ¹Univ of Electronic Science & Tech China, China. We study the influence of the laser linewidth on an optical SSB PAM-4 and direct-detection transmission systems at C-band by simulation and experiment. The 56-Gb/s PAM-4 signal successfully transmits over 800-km SSMF under 7% HD-FEC with 50-kHz laser linewidth

W1J • Integrated Sources I—Continued

W1J.3 • 09:15

Monolithic Integrated High-frequency, High-brightness Perovskite Quantum Dots Multicolor Photonic Sources Coupled with Hyperbolic Metamaterials, Feiliang Chen¹, Qian Li¹, Mo Li¹, Hui Zhang¹, Feng Huang¹, Shuxiao Li¹, Jian Zhang¹; ¹Microsystem & Terahertz Research Center, China. The fluorescence intensity and spontaneous emission rate of perovskite quantum dots with different emission wavelength are enhanced by monolithic hyperbolic metamaterials, which provides a powerful way for monolithic integrated high-frequency, high-brightness perovskite multi-color photonic sources

W1J.4 • 09:30

Full C+L-Band, Mode-hop-free Wavelength Tunable Laser Diode with a Linewidth of 8 kHz and a RIN of -130 dB/Hz, Keisuke Kasai¹, Masataka Nakazawa¹, Yasunori Tomomatsu², Takashi Endo²; ¹Tohoku Univ., Japan; ²Koshin Kogaku Co., Ltd, Japan. We demonstrate a wavelength tunable laser diode with a linewidth of less than 8 kHz and a RIN below -130 dB/Hz. The oscillation wavelength can be tuned over the full C+L-band (90-nm) without mode hopping.

W1J.5 • 09:45

Tunable Single-Mode Half-Wave Coupled Laser Using Two Back-to-Back Corner-Connected TIR Reflectors, Jia Guo¹, Xiaolu Liao¹, Jian-Jun He¹; ¹College of Optical Science and Engineering, Zhejiang Univ., China. We report the design concept and experimental results of a tunable half-wave coupled-cavity laser using two back-to-back corner-connected total internal reflection reflectors. A wide tuning range of 26.4nm is achieved with 40dB SMSR.

W1K • Biophotonics and Applications III—Continued

W1K.3 • 09:30

Isotropic super-resolution imaging of thick samples with multi-view sub-voxel-resolved light-sheet microscopy, Junyu Ping¹, Fang Zhao¹, Sa Liu¹, Yusha Li², Dan Zhu², Peng Fei^{1,3}; ¹School of Optical and Electronic Information Huazhong Univ. of Science and Technology, China; ²Britton Chance Center for Biomedical Photonics Wuhan National Laboratory for Optoelectronics Huazhong Univ. of Science and Technology, China; ³Shenzhen Huazhong Univ. of Science and Technology Research Inst., China. We present a multi-view super-resolved light-sheet fluorescence microscopy to enable high-throughput 3-D reconstruction of thick-and-scattering samples, with deteriorated signals recovered and isotropic super-resolution achieved.

W1K.4 • 09:45

A multiscale optical coherence tomography for skin imaging in vivo, Xiaojun Yu¹, Chi Hu¹, Qianshan Ding¹, Ganggang Mu³, Yunchao Deng³, Honggang Yu³, Linbo Liu²; ¹Northwestern Polytechnical Univ., China; ²School of Electrical and Electronic Engineering, Nanyang Technological Univ., Singapore; ³Dept. of Gastroenterology, Remin Hospital of Wuhan Univ., Wuhan., China. We report a multiscale optical coherence tomography (OCT) system that is capable of providing three-dimensional (3D) human skin imaging in vivo both cellular-level resolution mode and large area scanning mode.

W1L • Integrated Microwave Photonics I—Continued

W1L.2 • 09:30 **Invited**

Monolithic and Heterogeneous Microwave/Millimeter-wave Photonic Integrated Circuits, Guillermo Carpintero¹, Robinson Guzmán¹, Mu-Chieh Lo¹, Muhsin Ali¹, Alberto Zarzuelo Garcia¹, Luis Enrique García-Muñoz¹, Daniel Segovia¹, David De Felipe², Norbert Keil²; ¹Universidad Carlos III de Madrid, Spain; ²Photonics Components Dept., Fraunhofer Heinrich Hertz Inst., Germany. Among the photonic techniques to generate RF signals, optical heterodyning is preferred for wide frequency tuning. It combines two single wavelength laser sources, which behave as uncorrelated sources, affecting the stability of the generated signal. Two integration approaches are investigated, monolithic InP and heterogeneous In/Polymer.

10:00–10:30 Coffee Break

Room S223

Room S224

Room S225

Room S226

Room S227

Room S228

These concurrent sessions are grouped across two pages. Please review both pages for complete session information.

10:30–12:30
W2A • Advanced Laser Sources I
Presider: Sze Set; Univ. of Tokyo, Japan

W2A.1 • 10:30 **Invited**
High-Energy VUV Generation in Gas-Filled Hollow Capillary Fibers, John C. Travers¹, Teodora Grigorova¹, Federico Belli¹, ¹Heriot-Watt Univ., UK. We show that soliton dynamics scale to millijoule energies in simple hollow capillary fibers. We numerically model sub-femtosecond pulse self-compression, and experimentally demonstrate high-brightness multiple- μ J-scale ultraviolet (115-330 nm) pulse generation.

W2A.2 • 11:00
Multiple Wavelength Mode-Locked Laser with Control of Temperature Gradient for Sixth Harmonic Generation, Aleksej Rodin^{1,2}, Andrejus Michailovas^{1,2}, ¹Center for Physical Sciences and Technology, Lithuania; ²Ekspla Ltd, Lithuania. Fundamental 1342 nm radiation of mode-locked Nd:Vanadate laser was converted to 224 nm wavelength with an average power of ~ 1 W by control of temperature gradient applied to BBO crystal. The laser also provides 1342 nm, 671 nm and 447 nm output with an average power of 10 W, 6 W and 4 W at 300 kHz.

10:30–12:30
W2B • Nonlinear Dynamics in Waveguides and Harmonic Generation
Presider: Lan Yang; Washington Univ. in St Louis, USA

W2B.1 • 10:30 **Invited**
Evolution of Structural Distortion in BiFeO₃ Thin Films and the phase transition in BaTiO₃ Probed by Second-harmonic Generation, Kuijuan Jin¹, ¹Chinese Academy of Sciences, China. We report an initial state determined phase transition in barium titanate and the phase transition in BaTiO₃ by applying second harmonic generation technology and piezo-response force microscopy.

W2B.2 • 11:00
Light Emission Redistribution Owing to Nonlinearity in ITO/LiNbO₃, Jingwen Zhang¹, Dewang Huo¹, Chao Wang¹, Hua Zhao¹, ¹Harbin Inst. of Technology, China. UV and short wave visible emission enhancement was observed from indium-tin-oxide coated y-cut Fe:LiNbO₃, suggesting nonlinearity plays a role due to interface plasmon polaritons were excited in electrostatic modified nanometric layer of free electron gas.

10:30–12:30
W2C • Infrared Ultrafast Subcycle Subwavelength Photonics
Presider: Martin Richardson; Univ. of Central Florida, CREOL, USA

W2C.1 • 10:30 **Tutorial**
Subcycle Quantum Physics, Alfred Leitenstorfer¹, ¹Univ. of Konstanz, Germany. Operating out of a time-domain perspective provides new insights into the quantum physics of light and matter. Important ingredients include access to extreme nonequilibrium states and a lack of energy conservation on subcycle timescales.

10:30–12:30
W2D • Optical Signal Processing Based on Integrated Devices
Presider: Jian Wang; Huazhong Univ of Science and Technology, China

W2D.1 • 10:30 **Invited**
Optical Signal Processing in Silicon-Based Integrated Devices, Cosimo Lacava¹, Thalia Dominguez Bucio¹, Ali Khokhar¹, Francesca Parmigiani¹, Frederic Gardes¹, David J. Richardson¹, Marc Sorel², Periklis Petropoulos¹, ¹Univ. of Southampton, UK; ²Univ. of Glasgow, UK. We discuss the latest progress on the development of all-optical signal processing devices in Si-based platform. We discuss the realization of intra and inter-modal wavelength-converters by using our internally developed si-rich-silicon nitride platform.

W2D.2 • 11:00 **Invited**
An ISI-aware Design Process for SIP Modulators, Leslie Rusch¹, Hassan Sepehrian¹, Jiachuan Lin¹, Wei Shi¹, ¹Universite Laval, Canada. Maximizing the bit rate of optical components implies operation in a bandwidth limited regime where communications are vulnerable to intersymbol interference. We provide guidelines for the design of modulators to mitigate this impairment.

10:30–12:30
W2E • Ultra-fast Laser Machining and Processing
Presider: Christopher Barner-Kowollik; Queensland Univ. of Technology, Australia

W2E.1 • 10:30 **Invited**
Femtosecond Laser LIPSS of Copper: Modeling and Experimental Comparison, Chung-Wei Cheng¹, Chin-Lun Chang¹, Jinn-Kuen Chen², ¹National Chiao Tung Univ., Taiwan; ²Univ. of Missouri, USA. The numerical values of FLPISS on copper obtained through our proposed method were in fairly good agreement with the experimental data from different femtosecond laser pulses, e.g. 1030 nm and 515 nm.

W2E.2 • 11:00 **Invited**
Picosecond laser filamentation in sapphire for precision machining, Lingfei Ji¹, ¹Beijing Univ. of Technology, China. Picosecond laser filamentation in sapphire for precision machining were studied. The unique ability to create targeted filament traces in the material with high refractive index and provide fine cut structures based on the nonlinear effect was presented.

10:30–12:30
W2F • Optical Devices for Precision Measurements
Presider: Kenneth Kin-Yip Wong; Univ. of Hong Kong, Hong Kong

W2F.1 • 10:30 **Invited**
Microresonator Soliton Frequency Combs, Tobias J. Kippenberg¹, Hairun Guo¹, Martin H. Pfeiffer¹, John Jost¹, Erwan Lucas¹, Maxim Karpov¹, Junqiu Liu¹, Miles Anderson¹, Arslan Raja¹, Bahareh Ghadiani¹, Anton Lukashchuk¹, Wenle Weng¹, Romain Bouchand¹, Jia-Jung Ho¹, Michael Geiselmann¹, ¹IPHYs, Ecole Polytechnique Federale de Lausanne, Switzerland. Microresonator frequency combs provide access to compact, photonic-integrated optical comb with large mode spacing operating in a soliton regime. We will discuss the physics of such solitons and their applications in telecommunication and distance measurements.

W2F.2 • 11:00
High-Resolution Spectroscopy using A Tunable Dissipative Kerr Soliton Microcomb, Yong Geng¹, Heng Zhou¹, Baojian Wu¹, Kun Qiu¹, ¹Univ of Electronic Science & Tech China, China. We demonstrate interval-free frequency comb spectroscopy using a tunable dissipative Kerr soliton microcomb, and 5 MHz spectral resolution is achieved—the highest ever reported for Kerr comb based spectroscopy measurements.

These concurrent sessions are grouped across two pages. Please review both pages for complete session information.

10:30–12:30
W2G • Quantum Information Processing I
Presider: Shengwang Du; Hong Kong Univ of Science & Technology, Hong Kong

W2G.1 • 10:30 **Invited**

Seeing a Single Atom Where It Is Not, Gabriel Araneda³, Stefan Walsler¹, Yves Colombe³, Daniel Higginbottom^{3,4}, Jürgen Volz², Rainer Blatt³, Arno Rauschenbeutel^{1,2}; ¹Atominstytut, TU Wien, Austria; ²Institut für Physik, Humboldt-Universität zu Berlin, Germany; ³Institut für Experimentalphysik, Universität Innsbruck, Austria; ⁴Centre for Quantum Computation and Communication Technology, The Australian National Univ., Australia. We demonstrate that spin-orbit coupling of light can lead to fundamental wavelength-scale errors in optical precision localization of sub-wavelength scale emitters using far-field optical imaging techniques. The effect occurs even for perfect, aberration-free imaging.

W2G.2 • 11:00

Generation, storage and processing of photons in a multimode quantum memory, Michal Parniak¹, Mateusz Mazelanik¹, Adam Leszczynski¹, Michal Dabrowski¹, Michal Lipka¹, Wojciech Wasilewski¹; ¹Univ. of Warsaw, Poland. A quantum memory based on a cold atomic ensemble is demonstrated to process collective excitations in thousands of modes. Efficient photon coupling together with versatile manipulation techniques pave the way towards a universal photonic switch.

10:30–12:30
W2H • Optical Metasurfaces II
Presider: Xiangping Li; Jinan Univ., China

W2H.1 • 10:30 **Invited**

New Nano-photonics Based on vdW Materials, Antonio Ambrosio¹, Michele Tamagnone², Kundan Chaudhary², Luis A. Jauregui³, Philip Kim³, William Wilson¹, Federico Capasso²; ¹Center for Nanoscale Systems, Harvard Univ., USA; ²Harvard John A. Paulson School of Engineering and Applied Sciences, USA; ³Dept. of Physics, Harvard Univ., USA. We study ultra-confined polaritonic modes supported by thin micro- and nano-devices made of hexagonal boron nitride flakes. We image these modes using new optical scanning probes microscopy techniques. These results open new avenues for nano-photonics as a way to achieve extreme light confinement at the nanoscale.

W2H.2 • 11:00 **Invited**

Tailored Structural Disorder in Optical Metasurfaces, Dennis Arslan¹, Stefan Fasold¹, Aso Rahimzadegan², Trideep Kawde¹, Sebastian Linss¹, Najmeh Abbasirad¹, Matthias Falkner¹, Manuel Decker^{1,3}, Carsten Rockstuhl^{2,4}, Thomas Pertsch¹, Isabelle Staude¹; ¹Institute of Applied Physics, Friedrich-Schiller-Univ. Jena, Germany; ²Inst. of Theoretical Solid State Physics, Karlsruhe Inst. of Technology, Germany; ³Nonlinear Physics Centre, The Australian National Univ., Australia; ⁴Inst. of Nanotechnology, Karlsruhe Inst. of Technology, Germany. We experimentally realize various optical metasurfaces with tailored rotational and positional disorder, and demonstrate their ability to support pure circular dichroism and to tune the intensity of the transmitted light almost independently from its phase.

10:30–12:30
W2I • Fiber-Wireless Systems and PONs
Presider: Tianwai Bo; KAIST, Korea

W2I.1 • 10:30 **Invited**

Low-latency Optical Networks for 5G Wireless, Xiang J. Liu¹, Ning Deng²; ¹Futurewei Technologies, Inc., USA; ²Huawei Technologies, China. We review recent advances in the evolution of optical networks to better address the demands of 5G wireless systems by providing high-bandwidth and low-latency connectivity. Particularly, the evolution of optical cross connect and optical transport network will be discussed.

W2I.2 • 11:00 **Invited**

Demonstration of Real-time 100Gb/s Multilane-based PON System with Low Latency DBA, Kwang Ok Kim¹, KyeongHwan Doo¹, HanHyub Lee¹, SeungHwan Kim¹, Hwan Seok Chung¹; ¹Electronics & Telecomm Res. Inst, Korea. We report multilane-based real-time 100G-PON with dynamic channel bonding and low-latency DBA. Packet throughput of 80-Gb/s in downstream and 32-Gb/s in upstream with multi-speed ONUs on the distance 20-km and a 1:16 splitter are also demonstrated.

10:30–12:30
W2J • Integrated Sources II
Presider: Yong-Zhen Huang; Chinese Academy of Sciences, China

W2J.1 • 10:30 **Invited**

Electrically Injected Hybrid III-Nitride/Organic White LEDs with Non-radiative Energy Transfer, T Wang¹; ¹Univ. of Sheffield, UK. An electrically injected hybrid organic/inorganic III-nitride white LEDs with a micro-hole array structure has been reported. The novel hybrid LED geometry enables the nonradiative energy transfer process with high efficiency while retaining excellent electrical characteristics.

W2J.2 • 11:00

Widely tunable high power sampled-grating MOPA system emitting around 970 nm, Mahmoud Tawfiq¹, Hans Wenzel¹, Olaf Brox¹, Pietro Della Casa¹, Andrea Knigge¹, Markus Weyers¹, Bernd Sumpf¹, Günther Tränkle¹; ¹Ferdinand-Braun Inst., Germany. A high power widely tunable master oscillator power amplifier (MOPA) laser system will be presented, emitting between 962.0 nm - 985.5 nm, with an output power in the watt range.

10:30–12:30
W2K • Biophotonics and Applications IV
Presider: Chao Zhou; Lehigh Univ., USA

W2K.1 • 10:30 **Invited**

In vivo and Label-free Detection of Circulating Melanoma Cells by Photoacoustic Flow Cytometry, Xunbin Wei¹, Bobo Gu¹; ¹Shanghai JiaoTong Univ., China. A new in vivo photoacoustic flow cytometry was proposed and demonstrated for in vivo, label-free, non-invasive and real-time detection of circulating melanoma cells with high absorption coefficient of near-infrared light in the tumor-bearing mouse model.

W2K.2 • 11:00 **Invited**

Jones Matrix Tomography - Principle, Implementation, and Application, Yoshiaki Yasuno¹; ¹Univ. of Tsukuba, Japan. This presentation describes basic principle and applications of Jones matrix optical coherence tomography (JM-OCT), which simultaneously visualizes scattering, polarization, and flow property of living tissue.

10:30–12:30
W2L • Interferometers & Applications
Presider: Yunqi Liu; Shanghai Univ., China

W2L.1 • 10:30 **Invited**

Dual Cladding Modes Fiber Interferometer and its Application in Fiber Sensor, Bo Dong¹; ¹Xi'an Inst. of Optics and Precision Mechanics, CAS, China. Dual cladding modes fiber interferometer is based on the interferences between the core mode and two cladding modes. Here its principle and application for dual parameters measurement are presented.

W2L.2 • 11:00 **Invited**

Investigation on Temperature Sensitivities of Microfiber Mach-Zehnder Interferometers, Young-Geun Han¹; ¹Hanyang Univ., Korea. Abstract not available.

Room S223

Room S224

Room S225

Room S226

Room S227

Room S228

These concurrent sessions are grouped across two pages. Please review both pages for complete session information.

W2A • Advanced Laser Sources I—Continued

W2A.3 • 11:15

Passively mode-locked erbium-doped fiber laser with PbS colloidal quantum dots as saturable absorber, Wei Zhao¹, Xiaolan Sun¹, Bin Zhou¹, Qianqian Huang¹, Chuanhang Zou¹, Tianxing Wang¹, Chengbo Mou¹, Tingyun Wang¹, Alan Kost²; ¹Key Laboratory of Specialty Fiber Optics and Optical Access Networks, Shanghai Univ., China; ²Optical Sciences Center, Univ. of Arizona, USA. We have demonstrated a passively mode-locked erbium-doped fiber laser using colloidal PbS quantum dots (QDs) thin film as saturable absorbers (SAs). As the pump power up to 34.1 mW, we can observe the mode-locked pulse with the duration of 2.86 ns.

W2A.4 • 11:30

870fs, 448kHz pulses from an all-PM Yb-doped fiber laser with a nonlinear amplifying loop mirror, Guanyu Liu¹, Aimin Wang¹, Zhigang Zhang¹; ¹Peking Univ., China. We demonstrate a mode locked long all-polarization maintaining fiber laser with a nonlinear amplifying loop mirror. 870 fs pulse is obtained at the repetition rate of 448 kHz.

W2A.5 • 11:45

LD pumped Nd:GdNbO₄ crystal laser operating at 926 nm, Jing Gao^{1,2}, Changlei Li^{2,1}, Wenming Yao^{1,2}; ¹Chinese Academy of Sciences, China; ²Univ. of Science & Technology of China, China. We present a 926 nm laser based on quasi-three-level transition of a novel Nd:GdNbO₄ crystal. The slope efficiency with respect to absorbed pump power is estimated to be 47.7%.

W2B • Nonlinear Dynamics in Waveguides and Harmonic Generation—Continued

W2B.3 • 11:15

Quasi-phase-matching sinusoidally-tapered waveguides for third-order parametric interactions, Mohammed F. Saleh¹; ¹Heriot Watt Univ., UK. I show how periodically-tapered waveguides can be employed as efficient quasi-phase-matching schemes for four-wave mixing parametric processes in third-order nonlinear materials. Enhancing third-harmonic generation in sinusoidally-tapered fibres has been thoroughly investigated, as an example.

W2B.4 • 11:30

Efficient four-wave mixing using CMOS-compatible ultra-silicon-rich nitride photonic crystal waveguides, Ezgi Sahin^{1,2}, Kelvin J. Ooi¹, Ju Won Choi¹, Doris K. T. Ng³, C. E. Png², Dawn T. Tan¹; ¹Singapore Univ. of Technology and Design, Singapore; ²Dept. of Electronics and Photonics, Inst. of High Performance Computing, Agency for Science, Technology and Research (A*STAR), Singapore; ³Data Storage Inst., Agency for Science, Technology and Research, Singapore. Continuous wave four-wave mixing (FWM) in ultra-silicon-rich nitride photonic crystal waveguides (PhCWs) is demonstrated using low coupled pump powers. A conversion efficiency of -37 dB was observed using a 776 μm long PhCW.

W2B.5 • 11:45

Enhanced Third Harmonic Generation in a Silicon Photonic Crystal Slab, Guoxun Ban¹, Chaobiao Zhou¹, Shiyu Li¹, Yi Wang¹; ¹Wuhan National Laboratory for Optoelectronics, Huazhong Univ. of Science and Technology, China. Applying the Fano resonance in a Si photonic crystal slab, enhanced third harmonic generation (THG) has been experimentally demonstrated and the conversion efficiency is about 160 times larger than that of bulk silicon.

W2C • Infrared Ultrafast Subcycle Subwavelength Photonics—Continued

W2C.2 • 11:30

Invited

Terahertz Generation and Acceleration, Franz X. Kärtner¹; ¹Deutsches Elektronen-Synchrotron, Germany. Recent theoretical and experimental results on laser based high-energy single-cycle and multi-cycle Terahertz generation and its use for electron acceleration are discussed.

W2D • Optical Signal Processing Based on Integrated Devices—Continued

W2D.3 • 11:30

Invited

Hybrid Photonics using Foundry-Fabricated Silicon and Thin-Film Lithium Niobate, Shayan Mookherjee¹; ¹Univ. of California San Diego, USA. Thin-film lithium niobate (LN) is integrated with a silicon photonics pilot-line foundry platform, using large-area oxide bonding, and without etching or sawing LN. A Mach-Zehnder electrooptic modulator with >100 GHz 3-dB electrical bandwidth is shown.

W2E • Ultra-fast Laser Machining and Processing—Continued

W2E.3 • 11:30

Invited

Ultrafast Laser Induced Assembly of One-dimensional Nanomaterials, Wei Xiong¹, Y. Liu², J. Long¹, C.C.F. Lu¹, Huan Liu¹; ¹Wuhan National Laboratory for Optoelectronics, Huazhong Univ of Science and Technology, China; ²Dept. of Electrical and Computer Engineering, Univ. of Nebraska-Lincoln, USA. Ultrafast laser induced assembly of one-dimensional metallic and semi-conducting nanomaterials with high spatial resolution will be introduced. The user-defined nanomaterial assembly technique brings multiple benefits to the 3D micro/nanofabrication and functional device fabrication.

W2F • Optical Devices for Precision Measurements—Continued

W2F.3 • 11:15

A High-Speed-Controllable Fiber Comb Using a Compact Optical-Bench System, Yu Asahina^{1,2}, Yuko Yamada^{1,2}, Yusuke Hisai^{1,2}, Kazumichi Yoshii^{1,2}, Feng-Lei Hong^{1,2}; ¹Yokohama National Univ., Japan; ²JST, ERATO, MINOSHIMA Intelligent Optical Synthesizer Project, Japan. We developed a mode-locked Er fiber laser containing a small optical bench. The electro-optic modulator on the bench is used to control the repetition frequency at a high speed together with a piezoelectric transducer.

W2F.4 • 11:30

Invited

Integrated Modelocked Comb Lasers for Spectroscopy, Bart Kuyken¹; ¹Ghent Univ., INTEC, Belgium. Abstract not available.

These concurrent sessions are grouped across two pages. Please review both pages for complete session information.

W2G • Quantum Information Processing I—Continued

W2G.3 • 11:15

Two-Step Frequency Conversion for Connecting Distant Quantum Memories, Tamura Shuhei¹, Kohei Ikeda¹, Kotaro Okamura², Kazumichi Yoshii¹, Feng-Lei Hong¹, Tomoyuki Horikiri¹, Hideo Kosaka¹; ¹*Yokohama National Univ., Japan*; ²*Kanagawa Univ., Japan*. We demonstrate a two-step frequency conversion process (from 637.2 nm to the telecommunication wavelength and back). Signal-to-noise ratio is estimated to be sufficient for connecting nitrogen-vacancy centers in diamond based quantum repeater.

W2G.4 • 11:30

Direct quantum process tomography via sequential weak measurements, Yosep Kim¹, Yong-Su Kim², Sang-Yun Lee², Sang-Wook Han², Sung Moon², Yoon-Ho Kim¹, Young-Wook Cho²; ¹*POSTECH, Korea*; ²*KIST, Korea*. We demonstrate measurement of the sequential weak value of two incompatible observables by making use of two-photon quantum interference. We also demonstrate direct quantum process tomography of a qubit channel using the sequential weak value.

W2G.5 • 11:45

Demonstration of controlled-phase gate for time-bin qubits, Hsin Pin Lo¹, Takuya Ikuta¹, Nobuyuki Matsuda¹, Toshimori Honjo¹, Hiroki Takesue¹; ¹*NTT Basic Research Laboratories, Japan*. We demonstrate a controlled-phase (C-Phase) gate for the time-bin qubits using a 2x2 optical switch as a time-dependent beam splitter. We confirmed that independent time-bin qubits were entangled through the C-Phase gate.

W2H • Optical Metasurfaces II—Continued

W2H.3 • 11:30 **Invited**

Meta-device for Photonics in Demand, Din Ping P. Tsai¹; ¹*Academia Sinica, Taiwan*. Metasurfaces composed of artificial nano-structures attract huge interests due to their ability on controlling the electromagnetic phase and amplitude at subwavelength scale. Several metasurface based novel components for photonic applications are included in this talk.

W2I • Fiber-Wireless Systems and PONs—Continued

W2I.3 • 11:30

A Bidirectional Fiber-FSO/Wireless Convergence, Yong-Nian Chen¹, You-Ruei Wu¹, Zhen-Han Wang¹, Chung-Wei Su¹, Chung-Yi Li¹, Hai-Han Lu¹; ¹*National Taipei Univ. of Technology, Taiwan*. A bidirectional fiber-FSO/wireless convergence is proposed and demonstrated. One optical sideband (γ -polarization) is transmitted to effectively reduce fiber dispersion due to a span of 40-km SMF and distortion due to the beating among multiple sidebands.

W2I.4 • 11:45

Hybrid Optical Wired/Coherent-Wireless OFDM Access Networks with Baseband Signal Modulation and Envelop-Detection Down-Conversion, Chao-Wei Chen¹, Wen-Huang Chen¹, Hao-Hsiang Chang¹; ¹*National Chiao Tung Univ., Taiwan*. We propose hybrid optical wired/wireless access networks integrating fixed/mobile system. Tradeoff between strong carrier of EML modulation and nonlinearity is investigated. Hybrid access is achieved by employing commercial EML, envelop-detection down-conversion, and Volterra compensation.

W2J • Integrated Sources II—Continued

W2J.3 • 11:15

Optic Field Manipulation by Generation of Cylindrically Polarized Beams with Silicon Metasurface, Huiwen Luo¹, Liang Wang¹, Tianyang Zang¹, Yong Wang¹, Yonghua Lu¹, Pei Wang¹; ¹*Univ. of Sci and Tech of China, China*. We demonstrated that amplitude ratio of anisotropic transmittance is very important to determine how much input optical field remains in the generated vector optical field after metasurface.

W2J.4 • 11:30

An Integrated Composite Cavity Laser Switchable Between Single and Multi-Mode Operations, Mu-Chieh Lo¹, Robinson Guzmán¹, Guillermo Carpintero¹; ¹*Universidad Carlos III de Madrid, Spain*. An InP coupled cavity laser developed in a generic foundry is presented. Two active/passive ring cavities with different lengths constitute the Vernier-assisted versatile architecture. Single wavelength with >30 nm tunability and >30 dB extinction ratio and multimode operations with >300 GHz spacing are obtained.

W2J.5 • 11:45

Evolution of Junction Temperature and Heating Effects in UV AlGaIn Nanowires LEDs, Davide Priante¹, Rami Elafandy¹, Aditya Prabhawara¹, Bilal Janjua¹, Chao Zhao¹, Malleswararao Tangi¹, Mohd Sharizal Alias¹, Yazeed Alaskar², Abdulrahman Albadr², Ahmed Alyamani², Tien Khee Ng¹, Boon Ooi¹; ¹*King Abdullah Univ of Sci & Technology, Saudi Arabia*; ²*King Abdulaziz City for Science and Technology, Saudi Arabia*. We show reduced junction temperature and heat dissipation in AlGaIn nanowires LEDs on a metal substrate compared to devices on a silicon substrate by employing the forward-voltage and peak-shift methods.

W2K • Biophotonics and Applications IV—Continued

W2K.3 • 11:30

High Speed Optical Frequency Sweeper using Super Continuum Pulses and Optical Filters, Yuzo Yoshikuni¹, Hikari Shirasaki¹, Keiji Kuroda¹; ¹*Kitasato Univ., Japan*. A novel high speed optical sweeper is proposed and fabricated using super continuum optical pulses and time of flight technique. Combination of optical filters and optical delay lines successfully generate the frequency sweep light from a single pseudo-white light pulse.

W2K.4 • 11:45

Ultrasound-Tagged Chemiluminescence Tomography in Turbid Media, Masaki Kobayashi¹, Torai Iwasa¹; ¹*Tohoku Inst. of Technology, Japan*. Ultrasound assisted hybrid technique for optical imaging being available for biomedical tomography is proposed. We have developed a tomographic imaging system, based on the effect of ultrasonic enhancement of chemiluminescence, and demonstrated the tomographic imaging of a CL probe in dense light-scattering media with mm resolution.

W2L • Interferometers & Applications—Continued

W2L.3 • 11:30

Spaceborne Laser Transmitter for the Laser Interferometer Space Antenna (LISA) Mission, Anthony W. Yu¹, Kenji Numata¹, Hua Jiao¹, Scott A. Merritt¹, Frankie Micalizzi¹, Molly E. Fahey¹, Jordan B. Camp¹, Michael A. Krainak¹; ¹*NASA Goddard Space Flight Center, USA*. NASA is developing a highly stable, robust and reliable master oscillator power amplifier laser transmitter. We will discuss our technology development and progress on a spaceborne laser transmitter for the LISA mission.

W2L.4 • 11:45

Broadband Spectral Chirped Fabry-Perot Interferometer Based on Tapered Microfiber Bragg Grating, Yuan Cao¹, Zhong Lu¹, Peng Xiao¹, Xudong Wang¹, Yang Ran¹, Xinhuan Feng¹, Bai-Ou Guan¹; ¹*Inst. of Photonics Technology, Jinan Univ., China*. A compact Fabry-Perot (F-P) interferometer with chirped spectral characteristics based on microfiber Bragg grating is theoretically discussed and experimentally implemented. The interferometer has flat reflective and its bandwidth is 20 nm.

Room S223

Room S224

Room S225

Room S226

Room S227

Room S228

These concurrent sessions are grouped across two pages. Please review both pages for complete session information.

W2A • Advanced Laser Sources I—Continued

W2A.6 • 12:00
Different Lasing Modes from H⁺-Implantation-Defined Coherently Coupled VCSEL Arrays, Guanzhong Pan¹, Chen Xu¹, Yiyang Xie¹, Yibo Dong¹, Hongda Chen², ¹Beijing Univ. of Technology, China; ²Inst. of Semiconductor, Chinese Academy of Sciences, China. Different lasing modes including in-phase modes, out-of-phase modes and special mixture modes are obtained from H⁺-implantation-defined coherently coupled VCSEL arrays by engineering the interelement spacings between elements. The simulated far-field patterns match the experiments well.

W2A.7 • 12:15
A Tunable Single-longitudinal-mode Fiber Laser based on erbium-doped, peanut-shape fiber structure interferometer, Minling Du¹, Hongdan Wan¹, Jie Wang¹, Zuxing Zhang¹; ¹Nanjing Univ. of Posts&telecomm, China. We propose a fiber laser using erbium-doped fiber peanut-shape structure interferometer as the mode-selector for achieving single-longitudinal-mode and wavelength-tunable operation. The fiber laser has a 3 dB bandwidth of about 0.015 nm

W2B • Nonlinear Dynamics in Waveguides and Harmonic Generation—Continued

W2B.6 • 12:00
Enhanced third harmonic generation in organic multilayers, Myoungsik Cha¹, Jiung Kim¹, Pavan Kumar¹, Heejoo Choi², Kyungjo Kim², Nasser Peyghambarian²; ¹Pusan National Univ., Korea; ²Univ. of Arizona, USA. We demonstrate quasi-phase-matched third harmonic generation in organic multilayer films. The phase shift between the fundamental and the generated third harmonic light was compensated by alternately coated layers of a passive UV curable polymer material.

W2B.7 • 12:15
Phase control of high-order harmonics (HHG) in noble gas mixture by phase matching and interference effects, Lifeng Wang¹, Weiming Zhu¹, Qiangdong Ran¹, Hao Li¹, Ying Zhang¹; ¹SIMTech, Singapore. We experimentally observe strong modulation of HHG spectrum in gas mixture. Calculation results show phase of harmonics are contributed by phase-matching and interference effects, resulting in strong spectrum modulation and may benefit tunable XUV generation.

W2C • Infrared Ultrafast Subcycle Subwavelength Photonics—Continued

W2C.3 • 12:00
Terahertz Generation in PPLN by Pulse Recycling with Quartz Out-coupler, Lu Wang^{1,2}, Arya Fallahi¹, Koustuban Ravi^{1,3}, Franz Kaertner¹; ¹CFEL - DESY, Germany; ²Hamburg Univ., Germany; ³Research Laboratory of Electronics and the Dept. of Electrical Engineering and Computer Science, Massachusetts Inst. of Technology (MIT), USA. Multi-cycle terahertz generation using two consecutive PPLN crystals with designed quartz coupler is proposed. Our simulation suggests that pump pulse recycling with dispersion compensation can lead to higher terahertz conversion efficiency.

W2C.4 • 12:15
Direct Measurement of the Phase Coherence of Comb Sources, Luigi Consolino¹, Saverio Bartalini^{1,2}, Francesco Cappelli¹, Giulio Campo¹, Iacopo Galli^{1,2}, Davide Mazzotti^{1,2}, Pablo Cancio^{1,2}, Giacomo Scalari³, Jerome Faist³, Paolo De Natale^{1,2}; ¹CNR - INO, Italy; ²ppqSense Srl, Italy; ³ETH, Switzerland. We report on a novel and general method capable of measuring the coherence and the time evolution of the phases of laser comb modes. Applications to Near-IR, Mid-IR and Far-IR (THz) comb sources are presented.

W2D • Optical Signal Processing Based on Integrated Devices—Continued

W2D.4 • 12:00
Four channel 48Gbps Multicasting in a Coupled Si Ring Resonator with Tunable Channel Spacing, Awanish Pandey¹, Shankar K. Selvaraja¹; ¹Indian Inst. of Science, India. Wavelength multicasting in a quadruple resonance-split coupled cavity system is proposed and experimentally demonstrated. Bit error free performance at 12Gbps/channel is reported with aggregate data rate of 48Gbps with tunable channel spacing of 100GHz.

W2D.5 • 12:15
Tunable and Selective Wavelength Converter for 40Gbit/s Signals Employing Cascaded Second-Order Nonlinearity in Quasi-Phase Matched Lithium Niobate, Yutaka Fukuchi¹; ¹Dept. of Electrical Engineering, Tokyo Univ. of Science, Japan. We report a tunable and selective wavelength converter using a 5cm-long quasi-phase-matched lithium niobate waveguide. The conversion efficiency is ~10dB. The device is attractive for channel-by-channel wavelength conversion in 100GHz-spaced 40Gbit/s dense wavelength-division multiplexed systems.

W2E • Ultra-fast Laser Machining and Processing—Continued

W2E.4 • 12:00
 This paper has been withdrawn.

W2E.5 • 12:15
Fabrication of Carbide Nanoparticles by Femtosecond Laser Ablation of Silicon and Molybdenum in Hexane, Shusaku Terakawa¹, Toru Asaka¹, Fumihiro Itoigawa¹, Xi YU¹, Masaaki Sudo², Shingo Ono¹; ¹Nagoya Inst. of Technology, Japan; ²IMRA America Inc., Japan. Carbide nanoparticles are used in various applications. However, conventional fabrication methods are tend to be complicated and several steps are needed until fabrication. In this work, we report a simple method to fabricate carbide nanoparticles by femtosecond laser ablation in hexane.

W2F • Optical Devices for Precision Measurements—Continued

W2F.5 • 12:00
Simple method to lock an optical frequency comb to an ultra-stable laser without an RF signal generator, Kenya Hitomi¹, Atsushi Ishizawa², Kenichi Hitachi², Tadashi Nishikawa¹, Hideki Gotoh², Tetsuomi Sogawa², Kazutaka Hara¹; ¹Tokyo Denki Univ., Japan; ²NTT Basic Research Laboratories, Japan. We achieved a simple method for stabilizing an optical frequency comb (OFC). The OFC with our method is very stable and its stability does not depend on the stability of RF signal generators.

W2F.6 • 12:15
Sub-Hz Spectral Purity Transfer at the 10-18 level based on optical frequency comb, Pu Zou¹, Michele Giunta^{1,2}, Wolfgang Hänsel¹, Matthias Lezius¹, Marc Fischer¹, Ronald Holzwarth^{1,2}; ¹Menlo Systems GmbH, Germany; ²Max Planck Inst. of Quantum Optics, Germany. We report on a Er:fiber-based optical frequency comb transferring the stability of ultra-stable lasers from 194THz to 429THz. Sub-Hz level transfer to a fiber-delivered 698.44nm output port for future Strontium QPN-limited lattice clocks is demonstrated.

12:30–14:00 Lunch

These concurrent sessions are grouped across two pages. Please review both pages for complete session information.

W2G • Quantum Information Processing I—Continued

W2G.6 • 12:00

Experimental demonstration of superconducting nanowire single-photon detectors integrated with current reservoirs, Yuhao Cheng¹, Xiaoming Chi¹, Chao Gu¹, Kai Zou¹, Julien Zichi², Shufan Chen¹, Haiyi Liu¹, Val Zwiller², Xiaolong Hu¹; ¹Tianjin Univ., China; ²Royal Inst. of Technology (KTH), Sweden. We experimentally demonstrate the superconducting nanowire single-photon detectors integrated with current reservoirs that function as low-noise pre-amplifiers to increase the signal-to-noise ratio of detectors' outputs.

W2G.7 • 12:15

All optical actively tunable quantum signal de-multiplexer based on sum frequency generation, Zhi-Yuan Zhou¹, Yin-Hai Li¹, BaoSen Shi¹; ¹Univ. of Science and Technology of China, China. An actively tunable quantum signal de-multiplexer for multi-channel energy-time entangled state based on sum frequency generation is reported. Such device can de-multiplex any signal frequency and preserves entanglement after up-conversion.

W2H • Optical Metasurfaces II—Continued

W2H.4 • 12:00

Displacement-targeted metasurfaces for dispersionless and full phase and polarization control, Zi-Lan Deng¹, Junhong Deng², Guixin Li², Xiangping Li¹; ¹Jinan Univ., China; ²Southern Univ. of Science and Technology, China. We propose a novel metasurface designs by exploiting displacements instead of the size and shape between adjacent meta-atoms, leading to dispersionless and full phase and polarization control of arbitrary wavefronts.

W2H.5 • 12:15

Laser printing aluminium plasmonic metasurface hologram, Yinan Zhang¹, Liu Shi¹, shouyi Xie², Yudong Lu¹, Dejiào Hu¹, Zilan Deng¹, Xiangping Li¹; ¹Jinan Univ., China; ²The Univ. of New South Wales, Australia. We demonstrate a laser-printed metasurface hologram through the photothermal reshaping of the aluminium nanorods. Size reshaping and consequent phase modulation can be precisely controlled by the pulsed laser induced transient heat effect.

W2I • Fiber-Wireless Systems and PONs—Continued

W2I.5 • 12:00

A Cost-effective and Imbalance-insensitive 112G bit/s PM-16QAM Coherent PON Downstream Scheme, Huan Chen¹, Tao Yang¹, Xue Chen¹, Xiao Luo¹; ¹Beijing Univ of Posts & Telecom, China. We propose a cost-effective coherent PON downstream transmission scheme which not only shows high receiver sensitivity but also eliminates orthogonal imbalance inherently. Simulation and experimental results demonstrate its potentiality in next generation optical access network.

W2I.6 • 12:15

Orthogonal Matching Pursuit based Sparse Nonlinear Equalization for 40-Gb/s/wave-length Long-Reach PON, Junwei Zhang¹, Changjian Guo², Jie Liu¹, Xiong Wu¹, Alan Lau³, Chao Lu², Siyuan Yu^{1,4}; ¹School of Electronics and Information Technology, Sun Yat-Sen Univ., China; ²Dept. of Electronic and Information Engineering, The Hong Kong Polytechnic Univ., China; ³Dept. of Electrical Engineering, The Hong Kong Polytechnic Univ., China; ⁴Merchant Venturers School of Engineering, Univ. of Bristol, UK. We propose to use an orthogonal matching pursuit based sparse nonlinear equalization (OMP-SNE) for 40-Gbit/s OFDM-IM-DD long-reach PON over 60-km SSMF. Compared with conventional NE, the number of coefficients utilizing OMP-SNE is reduced by 63%.

W2J • Integrated Sources II—Continued

W2J.6 • 12:00

Novel Hybrid Micro Light-emitting Diodes with Increasing Color-Conversion Technical by Non-Radiative Energy Transfer, Sung-Wen Huang Chen¹, Zhen-You Liao¹, Yi-Yuan Chen¹, Tzu-Neng Lin³, Po-Tsung Lee¹, An-Jye Tzou^{1,2}, Hao-Chung Kuo¹; ¹National Chiao Tung Univ., Taiwan; ²National Nano Device Laboratories, Taiwan; ³Chung Yuan Christian Univ., Taiwan. Hybrid quantum dots m-LEDs promise a high color-conversion efficiency regarding the non-radiative energy transfer effect. The new approach enables a novel manufacturing method of the full-color m-display.

W2J.7 • 12:15

GaAs/AlGaAs tunable laser using Fabry-Perot filters based on half-wave coupled lossy deep etched trenches, Xin Chen¹, Jian-Jun He¹; ¹Centre for Integrated Optoelectronics, State Key Laboratory of Modern Optical Instrumentation, College of Optical Science and Engineering, Zhejiang Univ., China. We present a GaAs/AlGaAs tunable laser based on three cascaded Fabry-Perot cavities coupled by two half-wave lossy deep etched trenches. The laser exhibits good performance in lasing threshold, side-mode suppression ratio and wavelength tuning range.

W2K • Biophotonics and Applications IV—Continued

W2K.5 • 12:00

Towards spatially more efficient wavefront optical focusing with a binary-amplitude modulator, Huanhao Li¹, Puxiang Lai¹, Zhipeng Yu¹, Tianting Zhong¹, Zihao Li¹; ¹The Hong Kong Polytechnic Univ., Hong Kong. Optical wavefront shaping aims to focus light beyond the optical diffusion limit within scattering media. How to spatially enable better focusing, however, has been largely undefined. This study reports our latest effort in this regard.

W2K.6 • 12:15

OCT Endoscopic probe based on six circular arrayed two-axis MEMS, Site Luo¹, Dan Wang¹, Hao Liu², Guoxin Li², Hui Zhao³, Huikai Xie^{4,5}, Qiao Chen⁵, Yabing Liu⁵, Li Huo¹; ¹Tsinghua Univ., China; ²Dept. of General Surgery, Nanfang Hospital, Southern Medical Univ., China; ³Foshan Optomedic Technologies Co., Ltd, China; ⁴Univ. of Florida, USA; ⁵Wuxi WiO Technologies Co. Ltd., China. We present a novel circumferential scan endoscopic OCT probe by circular arrayed six MEMS mirrors and collimators with a diameter of 12 mm and a length of 25 mm.

W2L • Interferometers & Applications—Continued

W2L.5 • 12:00

Fiber optic non-wearable respiratory monitoring based on in-line modal interferometer, Ying Shen^{1,3}, Wei Xu², Na Zhang², Shanhong You¹, Changyuan Yu^{3,4}, Cheungchuen Yu²; ¹Soochow Univ., China; ²Anlight Optoelectronic Technology Inc, China; ³National Univ. of Singapore (Suzhou) Research Inst., China; ⁴Dept. of Electronic and Information Engineering, The Hong Kong Polytechnic Univ., China. A real-time non-wearable respiratory monitoring system based on single-mode-fiber-multimode-fiber-single-mode-fiber (SMS) with core-offset splicing is demonstrated and experimentally validated. Both the inhalation and exhalation activities can be detected within a wide respiratory frequency range.

W2L.6 • 12:15

A Design of Double-ring Sensor Based on Heat-tuned Mach-Zehnder Interferometer, Qiongchan Shao¹; ¹Zhejiang Univ., China. We utilize a heat-tuned Mach-Zehnder Interferometer Fourier transform spectrometer to retrieve the transmission spectrum of cascaded double-ring sensor. The sensor and spectrometer are integrated on one chip, providing a low-cost scheme for biochemical sensing.

12:30–14:00 Lunch

Room S421

14:00–15:30

W3A • Poster Session

W3A.1

Nonlinear Reflectance of Planar Plasmonic Nanostructure, Rui Xu¹, Zhonghui Nie¹, Shuchao Qin¹, Yao Li¹, Shining Zhu², Fengqiu Wang¹; ¹School of Electronic Science and Engineering, Nanjing Univ., China; ²School of Physics, Nanjing Univ., China. We reveal nonlinear reflectance of a planar plasmonic film with nanoaperture arrays. We further demonstrate that the nonlinear response of the plasmonic nanostructures can be effectively controlled by structural parameters.

W3A.2

Hybrid Quantum Dots /Photonic Crystal Color Tunable Light Emitting Diodes, Chiranjeevi Krishnan¹, Thomas Mercier¹, Zeeshan Ahmed¹, Kang-yuan Lee², Jih-Kai Huang², Chung-Hsiang Lin², Martin Charlton¹; ¹Univ. of Southampton, UK; ²Luxtaltek, Taiwan. We demonstrate spectrally tunable hybrid photonic crystal Quantum Dots (QDs) LEDs. QDs are embedded into photonic crystals of GaN/InGaN LED for efficient color conversion. Color tunable LED has individually addressable LED module.

W3A.3

Optomechanical oscillation in the lithium niobate photonic crystal nanocavity, Haowei Jiang^{1,2}, Hanxiao Liang², Rui Luo², Xianfeng Chen¹, Yuping Chen¹, Qiang Lin²; ¹Shanghai Jiao Tong Univ., China; ²Univ. of Rochester, USA. Nonlinear optomechanical oscillations are observed in the lithium niobate photonic crystal nanocavity. High harmonic oscillations up to 14th order are achieved, which may function as a mechanical frequency comb.

W3A.4

Strong MoS₂ Photoluminescence on Graphene for Coupling with Silica Microcavity, Rammaru Ishida¹, Takasumi Tanabe¹; ¹Keio Univ., Japan. We transferred monolayer MoS₂ to various substrates and evaluated its optical property by photoluminescence intensity. The study revealed that a graphene substrate is adequate when using MoS₂ as a cavity-QED material.

W3A.5

A single GaAs nanowire self-powered photodetector with Au-graphene Schottky electrodes, Yanbin Luo¹, Xin Yan¹, Xia Zhang¹, Yao Wu¹, Li Bang¹, Qichao Lu¹, Xiaomin Ren¹; ¹Beijing Univ. of Posts and Telecomm, China. A single GaAs nanowire self-powered photodetector with Au/graphene Schottky electrodes is demonstrated. The device exhibits excellent photoelectric properties, showing a strong possibility for future integrated nano-optoelectronic systems.

W3A.6

Multipolar properties of guide resonances, Yi Xu¹, Yuan He¹, Tianhua Feng¹, Andrey E. Miroshnichenko²; ¹Jinan Univ., China; ²Univ. of New South Wales, Univ. of New South Wales, Australia. We study the multipolar nature of guide resonance in photonic crystal waveguide which is consisted of periodic Mie type resonators. By reconstructed the guide resonance utilizing the induced multipole moments in one unit cell, we reveal the important roles of multipole modes play in the high-Q resonances.

W3A.7

Optically Pumped Lasing in Cesium Lead Bromide Perovskite Square-shaped Microplatelets, Zi-Wei Huang¹, Li-Juan Lin¹, Hsu-Cheng Hsu¹; ¹Dept. of Photonics, NCKU, Taiwan. Single-crystal We used CVD method to synthesize all-inorganic CsPbBr₃ microcrystal perovskite microplatelets were fabricated to realize lasing at room temperature on mica substrate. Upon optical excitation, whispering-gallery-mode (WGM) lasing is was achieved at RT with low threshold (~2.8 mW) and high quality factor (~30001).

W3A.8

On chip quantum dot based phosphor for efficient and tunable color conversion, Thomas M. Mercier¹, Chiranjeevi Krishnan¹, Martin Charlton¹; ¹Univ. of Southampton, UK. CdS_{1-x}/ZnS (core/shell) quantum dots were used in combination with band-pass filters to convert blue light emitted from InGaN/GaN LEDs to different wavelengths. We present results to show this approach is a promising way of achieving tunable color conversion.

W3A.9

Excitation Bessel beams designed for high resolution and wide-field live imaging, Jing Wen¹, Shiliang Liu¹, Binbin Yu¹, Dawei Zhang¹; ¹Engineering Research Center of Optical Instrument and System, Ministry of Education and Shanghai Key Lab of Modern Optical System, Univ. of Shanghai for Science and Technology, China. We explore generating subwavelength non-diffracting Bessel beams with long focal depths by means of custom-designed metasurfaces. The excitation approach can achieve live imaging with a high axial resolution and an ultra-wide field of view.

W3A.10

Imaging Theory of Vectorial Optical Near Field Based on Reciprocity of Electromagnetism, Lin Sun¹, Benfeng Bai¹, Tong Cui¹, Jia Wang¹; ¹Dept. of Precision Instrument, Tsinghua Univ., China. By using multipolar decomposition in the reciprocity of electromagnetism for near-field optics, a novel multipolar Hamiltonian model is developed to guide the design of functional nearfield probes and analyze the probe-field interaction.

W3A.11

Optical Power Amplification via TE Resonant Optical Tunneling in Asymmetric, Metal-Dielectric, Single Barrier Potential System, Yin-Jung Chang¹, Yu-Huan Chen²; ¹National Central Univ., Taiwan; ²Taiwan Semiconductor Manufacturing Company Limited, Taiwan. We show that, when properly configured, it is possible to have field and power amplification via unbound-state-enabled TE resonant optical tunneling through a two-dimensional, asymmetric, single-barrier potential system with metal.

W3A.12

Single-mode VCSEL for Nearly 100-Gbit/s QAM-OFDM transmission over 100-m OM4 multi-mode fiber, Hsuan-Yun Kao¹, Cheng-Yi Huang¹, Chun-Yen Peng¹, Cheng-Ting Tsai¹, Huai-Yung Wang¹, Shan-Fong Leong¹, Hao-Chung Kuo², Chao-Hsin Wu¹, Gong-Ru. Lin¹; ¹National Taiwan Univ., Taiwan; ²National Chiao Tung Univ., Taiwan. A 850-nm single-mode VCSEL with 3-dB bandwidth of 22.1 GHz enables 16-QAM OFDM transmission at nearly 100 Gbit/s over 100-m-long OM4 MMF link is demonstrated over 100-m-long OM4 MMF with BER of 3.5×10^{-3} .

W3A.13

Direct Detection for Polarization Multiplexing 100-Gb/s Signal Based on 7-Core Fiber Transmission, Xu Zhang¹, Cai Li², Xiang Li², Ming Luo²; ¹Wuhan National Laboratory for Optoelectronics, China; ²Wuhan Research Inst. of Posts and Telecom, China. We demonstrated a novel direct detection system for polarization multiplexing signal receiving based on 7-core fiber transmission. A 100-Gb/s signal transmit over 10-km with only 1.6 dB OSNR penalty compared with conventional coherent detection.

W3A.14

Simultaneous Measurement of Mode Dependent Loss and Differential Modal Group Delay in FMFs with OTDR, Feng Liu¹, Guijun Hu¹, Cuiguang Chen¹, Weicheng Chen¹, Congcong Song¹; ¹Jilin Univ., China. A new method for measuring mode dependent loss and differential modal group delay in FMFs is proposed and experimentally demonstrated that uses OTDR technique. This technique allows simultaneous measurement of MDL and DMGD in a 9.8 km-long FMF.

W3A.15

Real-Time 4×28Gb/s Transmission Over 110-km SMF Based on Dispersion Compensation and Wavelength Selective Switch, Quan You^{1,2}, Xiang Li², Ming Luo², Liyan Huang²; ¹Wuhan National Laboratory for Optoelectronics, China; ²State Key Lab of optic communication, Wuhan research Inst. of post and telecommunication, China; ³Accelink Technologies Company, Ltd., China. We experimentally demonstrate real-time 4×28-Gb/s transmission over 110 km single mode fiber. Chromatic dispersion pre-compensation and post-compensation are achieved by dispersion compensation fiber and wavelength selective switch, which is also used for wavelength division multiplexing.

W3A.16

Analytical fiber transfer function with XPM-induced process in N-channel coherent WDM transmission systems, Wataru Imajuku¹, Kuni-hiko Mori², Mitsunori Fukutoku²; ¹Kindai Univ., Japan; ²NTT Network Innovation Labs., Japan. This paper derives analytical fiber transfer function of XPM-induced optical noise in N-channel coherent WDM transmission systems by small signal approximation. The results provide analytical conditions to avoid the XPM-induced modulation instability for the first time.

W3A.17

XPM-induced phase noise mitigation by gain saturated parametric amplifiers, Wataru Imajuku¹, Kuni-hiko Mori², Mitsunori Fukutoku²; ¹Kindai Univ., Japan; ²NTT Network Innovation Labs., Japan. This paper proposes the improvement of signal-to-noise ratio by gain saturated PPLN amplifiers in n-channel coherent WDM fiber transmission systems. For this purpose, we develop semi-analytical scheme to estimate the signal-to-noise ratio including the XPM-induced phase noise.

W3A.18

Nonlinear Spurs Caused by EDFA in Analog Photonic Links, Shanhong Guan¹, Yitang Dai¹, Qizhuang Cen¹, Feifei Yin¹, Kun Xu¹; ¹Beijing Univ. of Posts and Telecommunication, China. In analog photonic links, we find the nonlinearity caused by input power fluctuations in EDFA. We theoretically analyzed the characteristics of the nonlinear spur and experimentally demonstrated that these characteristics are consistent with the theory.

W3A.19

Polarization tracking for Stokes-vector modulation formats using Kalman filter, Qian Xiang¹, Yanfu Yang¹, Juntao Cao¹, Qun Zhang¹, Yong Yao¹; ¹Harbin Inst. of Technology, China. A novel polarization tracking algorithm based on Kalman filter for Stokes-vector modulation formats are proposed. Compared with reported algorithms, the proposed scheme with optimal Q value shows fast polarization tracking capability and quick convergence.

W3A.20

Robust Multiband Frequency-tuning Algorithm for Cascaded ROADMs Filtering, Takahiro Kodama¹, Masanori Hanawa¹; ¹Yamanashi Univ., Japan. Frequency tuning for digital multiband 400G transmission over ROADMs system has been demonstrated. The long-term frequency tuning was evaluated through emulation model of laser frequency drift, and performance degradation can maintain less than 0.2 dB.

W3A.21

Accurate Channel Approximation Using Perspective Projection for a CamCom Link, Muhammad Asim Atta¹, Amine Bermak^{1,2}; ¹HKUST, Hong Kong; ²College of Science and Engineering, Hamad Bin Khalifa Univ., Qatar. This work presents channel approximation for a camera communication (CamCom) link using perspective projection model with complete intrinsic parameterization. The accuracy of the model is demonstrated by exploiting spatial separation characteristics of the output image.

W3A.22

Investigation of power allocation in ADO-OFDM based visible light communication system, Wei Liu¹, Haozhe Chen¹, Junjie Ding¹, Hao Wu¹, Mingrui Yang¹, Shihang Bian¹, Xiang Li², Wu Liu², Shanhong You¹, Honglong Cao¹, Minglai Zhou¹, Jianling Hu¹; ¹Soochow university, China; ²State Key Laboratory of Optical Communication Technologies and Networks, China. Asymmetrically clipped DC biased optical orthogonal frequency division multiplexing (AOD-OFDM) signals are experimentally transmitted in visible light communication system. We make an investigation of power allocation in ADO-OFDM and find the optimal power allocation ratio.

W3A.23

Compact Modeling of Laser Diode for Visible Laser Light Communication (VLLC) Systems, Can S. Wang¹, Bo Xu¹, Xianbo Li¹, Li Wang¹, Chik P. Yue¹; ¹Hong Kong Univ. of Sci & Tech, Hong Kong. A compact behavior model of a commercial TO-56 package 520-nm laser diode is presented for VLLC systems. The model exhibits good agreement with the measurement results for both NRZ and PAM4 modulation.

W3A.24

Security-Enhanced Chaos Communication with Optical Spectrum Expansion, Ning Jiang¹, Chao Wang¹, Anke Zhao¹, Jing Zhang¹, Hui Wang², Kun Qiu¹; ¹Univ of Electronic Science & Tech China, China; ²Westone Information Industry INC, 30th Inst. of CETC, China. We propose a chaos communication scheme by transforming the modulated chaotic carrier as an uncorrelated wideband signal with an optical-spectrum-expansion module. It is demonstrated that the message-security is greatly enhanced with respect to conventional cases.

Room S421

14:00–15:30

W3A • Poster Session

W3A.25

2 μm long period fiber grating fabricated by CO₂ laser, Le Liu¹, Meng Wang¹, Xiaoming Xi¹, Zefeng Wang¹; ¹National Univ of Defense Technology, China. Using a CO₂ laser, 2 μm long period fiber gratings (LPFG) are fabricated here for the first time. The transmission spectrum changing with the period, effective index modulation and grating length is investigated.

W3A.26

Withdrawn.

W3A.27

All-Optical Clock Recovery from 10 Gbps NRZ OOK and BPSK Data through Injection-Locking of Fiber Laser, Manas Srivastava¹, Balaji Srinivasan¹, Deepa Venkitesh¹; ¹Indian Inst. of Technology, Madras, India. We demonstrate all-optical clock recovery from 10 Gbps NRZ-OOK and NRZ-BPSK data through injection-locking of Erbium-doped fiber (EDF) laser after enhancement of clock tones using non-linearities in an SOA.

W3A.28

Adaptive fringe projection technique for phase error compensation, Han-Yen Tu¹, Ssu-Chia He²; ¹Dept. of Electrical Engineering, Chinese Culture Univ., Taiwan; ²Dept. of Electrical Engineering, Chinese Culture Univ., Taiwan. The non-sinusoidal problems of fringe projection lead to phase errors for three-dimensional shape measurement. For reducing phase measurement errors effectively and without time-consuming photometric calibration, the adaptive fringe projection technique is proposed in this work.

W3A.29

A new Pattern Recognition System Using Photoanisotropic Phenomena in Polarization-Sensitive Materials, Barbara N. Kilosani-dze¹, George Kakauridze¹, Irina Kobulashvili¹; ¹Georgian Technical Univ., Georgia. Objects recognition method is suggested based on determining parameters of the integral ellipse in the Fraunhofer diffraction region by the photoanisotropic copy of the object image while it is illuminated with nonactinic circularly polarized light

W3A.30

Supercontinuum Generation in an All-Normal Dispersion Tellurite Photonic Crystal Fiber, Feng Xu¹, Chao Mei¹, Jinhui Yuan^{1,2}, Feng Li^{2,3}, Zhe Kang³, Binbin Yan¹, Kuiru Wang¹, Xinzhu Sang¹, Xian Zhou³, Kangping Zhong³, Chongxiu Yu¹; ¹Beijing Univ of Posts & Telecom, China; ²The Hong Kong Polytechnic Univ. Shenzhen Research Inst., China; ³Photonics Research Centre, Dept. of Electronic and Information Engineering, The Hong Kong Polytechnic Univ., Hong Kong. We design a tellurite photonic crystal fiber with all-normal dispersion profile for generating supercontinuum (SC). The octave-spanning SC can be generated when the pump pulses with different widths, peak powers, and center wavelengths are used.

W3A.31

Chaotic pulse dynamics and synchronizations in Q-switched optical vortex pulses in an azimuthal symmetry breaking laser resonator, Jih-He Tu¹, Shang-Lin Yang¹, Chung-Po Tang¹, Yuan-Yao Lin¹; ¹National Sun Yat-Sen Univ., Taiwan. Chaotic dynamics and chaotic pulse synchronization are observed in optical vortex generated from a passive Q-switched laser resonator with broken an azimuthal symmetry when it was pumped by diode laser without critical beam shaping.

W3A.32

Passive mode-locking of a fiber optical parametric oscillator with optical time-stretch, Josephine Yi Qiu¹, Xiaoming Wei², Shuxing Du¹, Kenneth Kin-Yip Wong², Kevin K. Tsia², Yiqing Xu^{2,3}; ¹Huzhou Univ., China; ²Dept. of EEE, The Univ. of Hong Kong, China; ³College of ISEE, Zhejiang Univ., China. With the assistance of optical time-stretch using the lately developed free-space angular-chirp-enhanced delay cavity, we demonstrate the short pulse generation numerically by passively mode-locking a fiber optical parametric oscillator pumped by a quasi-CW pump.

W3A.33

Mid-Infrared Spectral Compression of Parabolic Pulses in a Chalcogenide Ridge Waveguide, Zeli Li¹, Jinhui Yuan^{1,2}, Feng Li^{2,3}, Zhe Kang², Banban Yan¹, Kuiru Wang¹, Xinzhu Sang¹, Chongxiu Yu¹; ¹Beijing Univ. of Posts and Telecommunications, China; ²The Hong Kong Polytechnic Univ., China; ³The Hong Kong Polytechnic Univ. Shenzhen Research Inst., China. We design a dispersion-engineered chalcogenide (As₂S₃) ridge waveguide to achieve the mid-infrared spectral compression of chirped parabolic pulses. Simulation results show that the compression factor can be up to 27 in a 6.6-mm long waveguide

W3A.34

Period-timing Bifurcation of the Pulse Train in an Actively Q-switched Fiber Laser, Chuang Ma¹, Ju Wang¹, Tianyuan Xie¹, Yang Yu¹, Tianyu Li¹, Shuaishuai Wang¹, Jinlong Yu¹, Yang Jiang²; ¹Tianjin Univ., China; ²GuiYang Univ., China. Period-doubling bifurcation, period-trebbling bifurcation and period-quadrupling bifurcation of the pulse train in an actively Q-switched fiber laser is experimentally observed in this paper.

W3A.35

Mid-infrared self-similar picosecond pulse compression in a suspended inversely tapered silicon strip waveguide, Yujun Cheng¹, Chao Mei¹, Jinhui Yuan^{1,2}, Feng Li², Zhe Kang², Xianting Zhang², Yin Xu², Binbin Yan¹, Kuiru Wang¹, Xinzhu Sang¹, Xian Zhou², Chongxiu Yu¹, Ping Kong A. Wai²; ¹Beijing Univ. of Posts and Telecommunications, China; ²Electronic and Information Engineering, The Hong Kong Polytechnic Univ., Hong Kong. We design a suspended inversely tapered silicon strip waveguide for high degree self-similar picosecond pulse compression. A 1.5-ps input pulse at wavelength 2250 nm is compressed to 46.73 fs in a 2.79-cm long waveguide taper.

W3A.36

Optical burst pulse generation from a gain-switched laser diode through CW laser light injection, Jui-Hung Hung¹, He-Jie Yan¹, Kazuo Sato¹, Hirohito Yamada¹, Lung-Han Peng², Hiroyuki Yokoyama¹; ¹Tohoku Univ., Japan; ²National Univ. of Taiwan, Taiwan. A novel method for producing optical burst pulses is demonstrated. Optical pulses having a several tens of picosecond duration, and a 100-200-ps period are generated from a gain-switched laser-diode under CW laser light injection.

W3A.37

Wavelength-Dependent Angular Distributions of Low-Energy Electrons in Mid-Infrared Strong Field Ionization, Zhiyang Lin¹; ¹Huaqiao Univ., China. The experimentally observed pronounced mid-infrared wavelength-dependent angular distributions (ADs) of low-energy electrons is attributed to the non-adiabatic effect by restoring to an improved semi-classical model.

W3A.38

Polarization coherence deterioration of conventional soliton in amplification, Yujia Li¹, Lei Gao¹, Tao Zhu¹, Yulong Cao¹; ¹Chongqing Univ., China. Nonlinear interactions during the amplification of conventional soliton are studied in terms of polarization change with statistical descriptions. Coherence degeneration of amplified lasers is manifested by an unordered polarization stability among different filtered wavelengths.

W3A.39

Ultrafast electron-phonon coupling and photo-induced strain in the morphotropic phase boundary of Bi₂By_{1-x}FeO₃ films, Zeyu Zhang¹, Juan Du¹; ¹Shanghai Inst of Optics and Fine Mech, China. Using ultrafast two-color pump-probe spectroscopy, the dysprosium doped-BiFeO₃ films on SrTiO₃ substrate have been investigated systematically. The doping induced structural transition and magnetic enhancement in BDFO is observed by ultrafast electron-phonon and spin-lattice interaction, respectively.

W3A.40

Inter-sublattice coupling dynamics in laser-induced ultrafast demagnetization processes of TbFeCo film, Zhifeng Chen¹, Xiaohui Fang¹, Chengyun Zhang¹, Rongbiao Deng¹, Bairu Xu¹; ¹Guangzhou Univ., China. Laser-induced ultrafast demagnetization of TbFeCo film is studied by employing a dual-color TR-MOKE measurement. Inter-sublattice exchange coupling is found to have significant contribution to the Tb demagnetization in ps time scale. The dynamics is discussed.

W3A.41

Enhanced nonlinearity in a tapered PCF with a central void core, Haihu Yu¹, Jian Ma¹, X Jiang¹, Yu Zheng¹; ¹National Engineering Laboratory for Fiber Optic Sensing Technology, Wuhan Univ. of Technology, China. We report the fabrication of a photonic crystal fiber with a central void, with enhanced nonlinearity via mode squeezing manipulation. Spectral broadening is observed by launching ultrafast pulses into an adiabatically tapered fiber piece.

W3A.42

Supercontinuum Generation in an Amorphous Silicon Strip-loaded Dielectric Waveguide, Yuhua Li¹, Jianguo Zhao², Roy Davidson², Brent E. Little^{2,3}, Sai Tak Chu¹; ¹Dept. of Physics, City Univ. of Hong Kong, China; ²QXP Technology Inc., China; ³State Key Laboratory of Transient Optics and Photonics, XIOPM, CAS, China. We demonstrate supercontinuum (SC) generation at 1550 nm in a high-index doped glass waveguide strip-loaded with a thin a-Si layer. The strip added 0.1 dB/cm to the propagation loss but it enhanced the SC generation.

W3A.43

Polarization Sensitive Femtosecond Mid-Infrared Spectrometer Using Chirped-Pulse Upconversion, Ryosuke Nakamura¹, Yoshizumi Inagaki^{1,2}, Nobuhiro Umemura³, Tomosumi Kamimura²; ¹Osaka Univ., Japan; ²Osaka Inst. of Technology, Japan; ³Chitose Inst. of Science and Technology, Japan. Polarization sensitive femtosecond mid-infrared spectrometer is developed based on chirped-pulse upconversion. A small signal from a Raman-active mode that couples to an infrared-active mode due to a slight decrease in the molecular symmetry is detected.

W3A.44

24 W Tm-doped silica-fiber laser at 2153 nm, Xiaoxi Jin¹, Xiong Wang², Jiabin Song¹, Xiaolin Wang¹, Hu Xiao¹, Pu Zhou¹; ¹National Uni of Defense Technology, China; ²China Satellite Maritime Tracking and Control Dept., China. We demonstrated a 24 W Tm-doped fiber laser at 2153 nm. A 1942 nm Tm-doped fiber laser was employed as pump laser. The temperature and fiber length were optimized to improve laser performance.

W3A.45

The realization of a topological insulator saturable absorber-based mode-locked solid state laser, Jia C. Lan¹, Yi-Ran Wang², Chao-Kuei Lee¹, Wei-Heng Song¹; ¹Photonics, National Sun Yat-sen Univ., Taiwan; ²State Key Laboratory of Crystal Materials, Inst. of Crystal Materials, China. In this paper, by using the prepared topological insulator saturable absorber mirror, a GHz, mode-locked Nd:YVO₄ bulk laser is realized for the first time with the output power of 180mW and pulse duration of 8ps

W3A.46

Gain-Switched and Passively Mode-Locked Thulium Fiber Laser at 2 μm , Pawel Grzes¹, Maria Michalska¹, Jacek Swiderski¹; ¹Inst. of Optoelectronics, Military Univ. of Technology, Poland. An all-fiber fast gain-switched and mode-locked (GS-ML) thulium-doped fiber laser (TDFL) is reported. The system delivers regular 2 μm mode-locked subpulses with duration < 100 ps recorded within one gain-switched pulse envelope

W3A.47

Modeling of soft X-ray Ar¹⁸-laser excited by capillary Z-pinch versus experiments, Anatolij A. Shapolov¹, Matyas Kiss¹, Balazs Fekete¹, Sandor Szatmari², Sergei V. Kukhlevsky¹; ¹Inst. of Physics, Univ. of Pecs, Hungary; ²Dept. of Experimental Physics, Univ. of Szeged, Hungary. The atomic kinetic description of lasing in the capillary Ar¹⁸-laser is connected to the 0-D or 1-D magneto-hydrodynamics models of capillary discharge Z-pinch. The models are in a good agreement with our experimental results.

W3A.48

Generation and Propagation of Anomalous Bessel Vortex Beam, Jun Zeng¹, Yuanjie Yang², Chengliang Zhao¹, Yangjian Cai¹; ¹College of Physics, Soochow Univ., China; ²School of Astronautics & Aeronautics, Univ. of Electronic Science and Technology of China, China. we propose and experimentally study an anomalous Bessel vortex beam. Unlike the traditional Bessel beams, the anomalous Bessel vortex beam carries decreasing orbital angular momentum (OAM) along the propagation axis in free space.

Room S421

14:00–15:30

W3A • Poster Session

W3A.49

Dynamics of Dual Frequency Mode-Locked Fiber Lasers, Xianting Zhang^{1,2}, Feng Li^{1,2}, Jinhui Yuan¹, Zhe Kang¹, Ping Kong A. Wai^{1,2}; ¹The Hong Kong Polytechnic Univ., Hong Kong; ²The Hong Kong Polytechnic Univ. Shenzhen Research Inst., Shenzhen, China. The nonlinear dynamics of a dual-frequency mode-locked fiber laser was investigated theoretically. Cross phase modulation between the two frequency channels induces a new gain loss dynamics which leads to unequal energy pulses in two channels.

W3A.50

288 km-long 2nd-order Raman fiber laser with resolvable mode structure, Han Wu¹, Zinan Wang¹, Yunjiang Rao¹; ¹Univ of Electronic Science & Tech China, China. A 288 km-long 2nd-order Raman fiber laser at 1550nm with mode separation of ~360 Hz is designed and experimentally demonstrated, which is the longest ever laser with resolvable mode structure, reported so far.

W3A.51

CW Tunable 3 μm Fiber Gas Laser Source, Zhiyue Zhou¹, Ni Tang¹, Zhixian Li¹, Wei Huang¹, Yulong Cui¹, Zefeng Wang¹; ¹National Univ of Defense Technology, China. We demonstrate a tunable 3 μm fiber laser source using acetylene-filled hollow-core fibers pumped with a tunable, narrowband and diode-seeded fiber amplifier. The maximum laser power is 766 mW, and the power efficiency is ~13%.

W3A.52

Difference-frequency Generation at 9.2 & 4.6 μm in LiGaS₂ Pumped by a 20-picosecond Nd:YAG/CaCO₃ Raman Laser, Sergei Smetanin², Michal Jelinek¹, Aleksey Kurus³, Lyudmila Isaenko^{3,4}, Vaclav Kubecek¹; ¹Czech Technical Univ. in Prague, Czechia; ²A.M. Prokhorov General Physics Inst., Russian Academy of Sciences, Russia; ³Siberian Branch Russian Academy of Sciences, Sobolev Inst. of Geology and Mineralogy, Russia; ⁴Novosibirsk State Univ., Russia. Single-pass frequency conversion of picosecond Nd:YAG/CaCO₃ Raman laser (1.064 / 1.203 & 1.384 μm) into the mid-infrared wavelengths of 9.2 and 4.6 μm by the difference-frequency generation in a LiGaS₂ crystal is presented.

W3A.53

Development of coherent pulse combining module, Jin Jang¹, Ki-Nam Joo¹; ¹Chosun Univ., Korea. In this investigation, we propose the practical compact divided pulse amplification (DPA) system, which consists of the pulse divider and combiner in the time domain (T-DPA) and space domain (S-DPA) by a multi-path interferometric structure.

W3A.54

Extra-cavity Pumped Parametric Raman Crystalline Anti-Stokes Laser at 954 nm with Collinear Orthogonally Polarized Beam Interaction at Tangential Phase Matching, Michal Jelinek¹, Sergei Smetanin^{2,3}, Dmitriy Tereshchenko³, Vaclav Kubecek¹; ¹Czech Technical Univ. in Prague, Czechia; ²Prokhorov General Physics Inst., Russian Academy of Sciences, Russia; ³National Univ. of Science and Technology MISIS, Russia. Tangentially phase-matched parametric Raman CaCO₃ anti-Stokes laser at 954 nm with the extra-cavity 1064-nm 6-ns laser pumping was investigated. The highest optical-to-optical efficiency into the anti-Stokes of ~4 % and 0.3-mJ output energy was achieved.

W3A.55

Compact Fe:ZnSe and Fe:ZnMnSe tunable lasers at 80 K pump with Er:YAG, Richard Svejkar¹, Jan Šulc¹, Helena Jelinková¹, Maxim E. Doroshenko², Nazar O. Kovalenko³, Andrey S. Gerasimenko³; ¹Czech Technical Univ. in Prague, Czechia; ²Laser Materials and Technology Research Center, AM Prokhorov General Physics Inst. of RAS, Russia; ³Inst. for Single Crystals, National Academy of Sciences of Ukraine, Ukraine. The influence of manganese concentration in compact Er:YAG pumped Fe:ZnMnSe tunable lasers at 80 K were investigated. Using a birefringent plate, the wavelength range of 3950 – 4830 nm (880 nm) was covered.

W3A.56

Fe:Zn_{0.8}Mn_{0.2}Se Spectroscopic Properties and Laser Generation at 5.0 – 5.8 μm in the Temperature Range of 78 – 300 K, Helena Jelinková¹, Maxim E. Doroshenko², Vjatcheslav Osiko², Michal Jelinek¹, Jan Šulc¹, David Vyhřidal¹, Nazar O. Kovalenko³, A. Gerasimenko³; ¹Czech Technical Univ. in Prague, Czechia; ²A.M. Prokhorov General Physics Inst., Russian Academy of Sciences, Russia; ³Inst. for Single Crystals, National Academy of Sciences of Ukraine, Ukraine. Temperature-dependent spectroscopic and laser properties of novel Fe:ZnMnSe crystal with high manganese concentration of 0.4 were investigated. Laser central wavelength varied from 5.0 μm at 78 K up to 5.8 μm at 300 K without any intracavity wavelength-selective element.

W3A.57

A 698 nm Hertz-Linewidth ultrastable diode laser, Linbo Zhang^{1,2}, Long Chen^{1,2}, Guanjun Xu¹, Jun Liu¹, Tao Liu¹, Shougang Zhang¹; ¹National Time Service Centre, Chinese Academy of Sciences, China; ²Univ. of Chinese Academy of Sciences, China. Two external cavity diode lasers are frequency-stabilized to two ultrahigh finesse optical resonant cavities with PDH method. The linewidth of each ECDL is measured to be about 1Hz by their beating and the frequency stability below 2.6×10^{-15} between 1s to 100s averaging time.

W3A.58

Wavelength tunable bidirectional Q-switched fiber laser based on carbon nanotube saturable absorber, Chuanhang Zou¹, Qianqian Huang¹, Tianxing Wang¹, mohammed AlArabi^{2,3}, Aleksey Rozhin^{2,4}, Chengbo Mou¹; ¹Key Laboratory of Specialty Fiber Optics and Optical Access Networks, Shanghai Univ., China; ²Aston Inst. of Photonic Technologies, Aston Univ., UK; ³Al Musanna College of Technology, Oman; ⁴Nanoscience Research Group, Aston Univ., UK. We demonstrate a wavelength tunable bidirectional Q-switched fiber laser based on carbon nanotube and a tunable bandpass filter with tuning range 51.43nm from 1515.43nm to 1566.86nm in clockwise and counter-clockwise direction for the first time.

W3A.59

Spectrally resolved shot-by-shot intensity noise characteristics of soliton spectrum broadening in normal dispersion single-mode fiber, Zijun Yao¹, Jie Chen¹, Ting Li¹, Yu Zhang¹, Xin Zhao¹, Zheng Zheng^{1,2}; ¹School of Electronic and Information Engineering, Beihang Univ., China; ²Beijing Advanced Innovation Center for Big Data-based Precision Medicine, China. Spectral intensity noise distribution of pulses after spectral broadening in single-mode fiber with normal dispersion is experimentally investigated, and vastly different noise magnitudes and some low-noise regions farther away from the pump wavelength are observed.

W3A.60

Generation of vector beams from wavelength-mismatched vortex plates, Teng-De Huang¹, Ting-Hua Lu¹; ¹Taiwan Normal Univ., Taiwan. The vector beam can be generated from wavelength-mismatched vortex plates, and it was mapped onto a small portion of the Poincaré sphere. All experimental results are consistent with the theoretical results.

W3A.61

Determination of the dioptric power of a thin-disk laser based on the translation of the stability zone, Deng Cao¹, Guangzhi Zhu¹, Jiaqi Gu¹, Xiao Zhu¹, Wenguang Zhao¹, Hailin Wang¹; ¹Huazhong Univ. of Science and Technology, China. The dioptric power of a thin-disk laser is determined by the method of equidistant translation of stability zone with constant shape. The experiments show that the method can determine the dioptric power effectively and precisely.

W3A.62

All polarization-maintaining ultra-broad and flat-topped spectrum Er-doped femtosecond fiber laser, Le Huang¹, Yu Chen¹, Shaozhen Liu¹, Jikun Yan¹, Xuanchao Qin¹, Tao Cao¹, Ziyue Guo¹, Kailin Hu¹, Jiahui Peng¹; ¹Huazhong Univ. of S&T, China. An all polarization-maintaining (PM) Erbium-doped fiber laser that produces ultrabroad and flat-topped spectrum with 3dB bandwidth of more than 60 nm is demonstrated. Hybrid mode-locking is employed to enable self-started mode-locking and spectral shaping.

W3A.63

Efficient suppression of high-order Stokes wave in high power linearly polarized Raman fiber laser using a novel flexible filter, Jiaxin Song¹, Haiyang Xu¹, Xiaoxi Jin¹, Hanwei Zhang¹, Jiangming Xu¹, Pu Zhou¹; ¹National Univ of Defense Technology, China. A novel all-fiber spectral-agile filter was designed and employed to suppress high order Stokes wave in high power linearly polarized Raman fiber laser. The maximum output power was increased by 24.2 %.

W3A.64

Transformation From Dissipative Solitons to Noise-Like Pulses in a Mode-Locked Yb-Doped Fiber Laser, Xingliang Li¹, Shumin Zhang¹, Mengmeng Han¹, Liangliang Chen¹, Zhenjun Yang¹; ¹Hebei Advanced Thin Films Laboratory, Hebei Normal Univ., China. We have demonstrated clearly the direct transition from dissipative soliton to noise-like pulses only by increasing the pump power in a nonlinear polarization rotation mode-locked Yb-doped fiber laser.

W3A.65

Compact THz Spectrometer Based on Varying Illumination on a Rough Semiconductor Surface, Tao Yang¹, Jia-cheng Ge², Ho-pui Ho³, Yong-yuan Zhu⁴, Wei Huang²; ¹Nanjing Univ. of Posts & Telecomm, China; ²Nanjing Univ. of Posts & Telecommunications, China; ³The Chinese Univ. of Hong Kong, Hong Kong; ⁴National Laboratory of Solid State Microstructures, Nanjing Univ., China. The terahertz spectrometer consists of three components, which are used for dispersion, modulation and detection respectively. With a calibration measurement process, one can reconstruct the terahertz spectra by solving a system of simultaneous linear equations.

W3A.66

Terahertz Antireflective Structures Fabricated via Femtosecond Laser Ablation, Xi Yu¹, Mahiro Takeuchi¹, Masaaki Sudo², Shingo Ono¹, Jongsuck Bae¹; ¹Nagoya Inst. of Technology, Japan; ²IMRA America, Inc., Japan. Terahertz antireflective structures on Si substrates are fabricated by femtosecond laser processing. The structure is constituted by periodic grooves at micro order. Evaluation results of reflectance by THz-TDS show that the surface reflectance is almost decreased to 0 and antireflection band was widened by improving aspect ratio of grooves.

W3A.67

Terahertz Wave Amplification in Stacked Graphene Layers, Montasir Qasymeh¹; ¹Abu Dhabi Univ., United Arab Emirates. We propose a novel technique for terahertz amplification in optically pumped stacked graphene layers. The terahertz amplification is achieved through a down conversion process, which is enabled by generating a backward terahertz wave.

W3A.68

Electric-Field Vector Imaging of Terahertz Surface Waves on an Indium tin Oxide Thin Film, Kenta Suzuki¹, Kenichi Oguchi¹, Makoto Okano¹, Shinichi Watanabe¹; ¹Keio Univ., Japan. We present a novel method for imaging terahertz electric-field vector using a rotating polarizer technique. We investigate the polarization-dependent propagation of terahertz surface waves on an indium tin oxide metal film.

W3A.69

Explanation for the discontinuous tunability of KTiPO₄ terahertz parametric oscillator, Dong Wu¹, Xingyu Zhang¹, Zhenhua Cong¹, Zengguang Qin¹, Zhaojun Liu¹, Xiaohan Chen¹, Jie Zang¹, Feilong Gao¹, Yuan Li¹, Chenyang Jia¹, Yue Jiao¹, Weitao Wang², Shaojun Zhang¹; ¹Shandong Univ., China; ²Laser Inst. of Shandong Academy of Sciences, China. By using the polariton dispersion relation in KTiPO₄ crystal and the coupled wave equations for stimulated polariton scattering, a semi-quantitative explanation for the discontinuous tunability of the KTiPO₄ terahertz parametric oscillator is given.

W3A.70

Multi-Position UV-Monitoring Sensor Based on FBG Coated with Photo-Responsive Polymer Material, GyeongSeo Seo¹, Hee-Taek Cho¹, Ok-Rak Lim¹, Tae-Jung Ahn¹; ¹Chosun Univ., Korea. We proposed an ultraviolet light sensor based on a fiber Bragg grating in combination with a photo-responsive polymer material. The sensor can be utilized to monitor UV lights in multiple positions.

Room S421

14:00–15:30

W3A • Poster Session

W3A.71

Helical Long-period Grating Inscription in Graded-index Few-mode Fiber for Temperature Sensing, Zuyao Liu¹, Yunqi Liu¹, Chengbo Mou¹, Songnian Fu²; ¹Shanghai Univ., China; ²Huazhong Univ. of Science and Technology, China. We experimentally demonstrate the fabrication of helical long-period grating (HLPG) in graded-index few-mode fiber by CO₂ laser. The fabricated HLPG is found to be sensitive to temperature with a high sensitivity up to 244 pm/°C.

W3A.72

A Long-Distance Fiber-Optic Arc-Flash Sensing System, Pu Wei¹, Lu Deng², Hui Huang³; ¹Nanjing Institute of Technology, China; ²Nari Group Corp., State Grid Electric Power Research Inst., China; ³Global Energy Interconnection Research Inst., State Grid Corporation of China, China. We propose and experimentally demonstrate a long-distance fiber-optic arc-flash sensing system. Using an optical energized VOA, the arc-flash signal can be transmitted by 4-km optical fiber, which meets the demand of the power industry.

W3A.73

Visualization of a periodic structure in arcjet plasma by laser absorption spectroscopy, Yoshiharu Yoshimura¹, Yutaro Sonoyama¹, Chihiro Suzuki², Leo Matsuoka³; ¹Graduate school of engineering, Hiroshima-Univ., Japan; ²National Inst. for Fusion Science, Japan. We performed spatially-resolved laser absorption spectroscopy of argon arcjet plasma with characteristic optical emission structures. We observed a periodic change of temperatures corresponding to the emission intensities along the jet axis.

W3A.74

Remote and real-time low dose rate gamma radiation measurement using NaI(Tl) based fiber optic sensor, Qiang Guo¹, Chengbo Mou¹; ¹Shanghai Univ., China. A low activity radiation fiber optic measurement system is investigated, NaI(Tl) scintillation crystal attached to a UV optical fiber act as the sensing probe. More than 200 counts can be obtained with the demonstrated sensor.

W3A.75

Laser tracking system for aquatic organisms, Yuki Kakushi¹, Yoshihiko Hibino¹, Cao Yang¹, Ryo Amano¹, Wataru Imajuku², Yasushi Mitsunaga³, Shinsuke Torisawa³, Yoshinobu Maeda³; ¹Kindai Univ., Japan; ²Kindai Univ., Japan; ³Kindai Univ., Japan. We released Chicken grunts (*Parapristipoma trilineatum*) equipped with capsule lens type retroreflective sheet at the experimental pond and estimated its position with Airborne Laser Bathymetry (ALB) from about 500 m above the sea.

W3A.76

A Fiber-Optic magnetometer Based on Graphene NEMS Using Superparamagnetic Nanoparticles, Zeng-Yong Liu¹, Shao-cheng Yan¹, Zhen-da Lu¹, Fei Xu¹; ¹Nanjing Univ., China. We demonstrate a fiber-optic magnetometer using superparamagnetic nanoparticles based on a graphene NEMS. The resonant frequency of the graphene NEMS shifts with the magnetic field. The sensor shows a sensitivity as high as ~ 104.5 kHz/T.

W3A.77

Metal corrosion measurement method based on optical reflection spectrum analysis, HeeTaek Cho¹, Ok-Rak Lim¹, GyeongSeo Seo¹, KyuHyuk Lee¹, TaeJun Park¹, SooYeon Cho¹, HeeJin Jang¹, Tae-Jung Ahn¹; ¹Chosun Univ., Korea. In this paper, we suggest a metal corrosion measurement method using optical reflection spectrum analysis. Herein, copper samples corroded at high temperatures, up to 900°C, were tested.

W3A.78

A sensor for saturated absorption spectroscopy measurement using a hollow waveguide, Dong T. Cai¹, Guangzhen Gao¹, Jow-Tsong Shy²; ¹Jiangsu Normal Univ., China; ²Dept. of Physics, National Tsing Hua Univ., Taiwan. A sensor for saturated absorption spectroscopy is built using a hollow waveguide with diameter of 300 μm. The performance of the sensor is demonstrated by observing the saturated absorption spectroscopy of acetylene around 1536 nm.

W3A.79

Silicone Optical Technology: Quasi Spatial Filter and Its Application for Multichannel Absorption Analysis, Chacriya Malasuk¹, Keisuke Nakakubo¹, Shota Tsuru¹, Hiroaki Yoshioka¹, Kinichi Morita^{1,2}, Yuta Nakashima³, Yuji Oki¹; ¹Dept. of I&E Visionaries, Kyushu Univ., Japan; ²New Business Development Office, USHIO INC., Japan; ³Advanced Science and Technology, Kumamoto Univ., Japan. Quasi spatial filter was purposed based on silicone optical technology (SOT). A simple structure as coaxial combination of a transparent polydimethylsiloxane (PDMS) core and carbon/PDMS clad was developed and then applied for multichannel absorption analysis.

W3A.80

D-shaped Photonic Crystal Fiber Sensing Probe for Biological Applications, Aruna Gandhi M S¹; ¹Shenzhen Graduate School, Peking Univ., China. Sensing performances of D-shaped photonic crystal fiber are investigated in this work. The highest sensitivity of 2000 nm/RIU in the refractive index ranges from 1.33 to 1.34 for the biological applications.

W3A.81

Evaporation rate sensor of liquids using a simple fiber optic configuration, Ok Rak Lim¹, HeeTaek Cho¹, GyeongSeo Seo¹, Min Ki Kwon¹, Tae-Jung Ahn¹; ¹Chosun Univ., Korea. The volatilization or evaporation rates of liquids were measured herein using the interference between the end surface of an optical fiber and the surface of the liquid on the fiber. We also measured these rates for deionized water and 99% ethanol solution. Our technique has a low cost and simple configuration.

W3A.82

Using Tapered Silicon Fibers to Detect High Refraction Index Liquid, Guan Hung Chen¹, Lon Wang¹, Nien Tsu Huang¹; ¹National Taiwan Univ., Taiwan. A tapered silicon fiber sensor embedded in a microfluidic channel is realized as an absorption sensor to detect liquid with high refractive index (RI), which is hardly obtainable by a traditional silica fiber.

W3A.83

A Surface Plasmon Resonance based Photonic Quasi-Crystal Fibre Biosensor with Fan-Shaped Analyte Channel for High Refractive Index Analytes, Suoda Chu¹, K. Nakkeeran¹, Abdosllam M. Abobaker², Sumeet S. Aphale¹, P. Ramesh Babu³, K. Senthilnathan³; ¹School of Engineering, Univ. of Aberdeen, UK; ²Dept. of Communications Engineering, College of Electronic Technology, Bani Walid, Libya; ³Dept. of Physics, School of Advanced Sciences, VIT Univ., India. We propose a surface plasmon resonance biosensor using a photonic quasi-crystal fibre with a fan-shaped channel for liquids of high refractive index (from 1.46 to 1.52) and it exhibits a maximum sensitivity of 6100 nm/RIU.

W3A.84

Nanoscale self-mixing interferometer based on multiple reflection and spectrum analysis algorithm, Yanting Zhang¹, Rui Wang¹, Zheng Wei¹, Xiulin Wang², Wencai Huang³; ¹Xiamen Univ., China; ²Jimei Univ., China. A high precision self-mixing interferometer was proposed by combining multiple reflection technique with spectrum analysis algorithm. The interferometer has the ability to measure nanoscale amplitude and the experiments show good agreement with the theory.

W3A.85

An oil-sealed thin-film silica microbubble based fiber-tip Fabry-Perot sensor for Enhancing temperature sensitivity, Guanjun Wang^{2,1}, Gao Wang¹; ¹North Univ. of China, China; ²Collage of Information Science&Technology, Hainan Univ., China. An improved pressure-assisted arc discharge technology was utilized to fabricate thin-film silica microbubble based fiber-tip temperature sensor. Then, it was coated with metal film before immersed with oil for ten times of sensitivity enhancement.

W3A.86

Phase detection autofocus pixels with plasmonic nanostructures, Seunghwan Choi¹, Yunkyung Kim¹; ¹Dept. of Electronic Engineering, dong-a Univ., Korea. A phase detection autofocus pixel having the plasmonic nanostructures formed by the subwavelength metal-insulator-metal stack arrays is reported. Using its wavelength selectivity by the incident angles, the autofocus performance is confirmed by the optical simulation.

W3A.87

A reflective optical phased array design based on elements with limited phase tuning range, Bo Yang^{1,2}, Minghua Chen^{1,2}, Hongwei Chen^{1,2}, SiGang Yang^{1,2}; ¹Electronic Engineering, Tsinghua Univ., China; ²National Research Center for Information Science and Technology, China. A reflective optical phased array model based on elements with small phase tuning range (~2 rad) is proposed. A steering range of ±8.9° with 5μm element spacing is achieved.

W3A.88

Reflective Differential Interference Contrast Microscopy for Retinal Cell Layer Imaging, Subeen Park^{1,2}, Juyeong Oh¹, Yu J. Kim³, Hyo-suk Kim¹, Chulki Kim¹, Hyung M. Kim², Kyoung M. Lee⁴, Dae Y. Kim⁵, Seok H. Kim⁴, Jae Hun Kim¹; ¹Korea Inst. of Science & Technology, Korea; ²Chemistry, Kookmin Univ., Korea; ³Ophthalmology, Seoul National Univ. Hospital, Korea; ⁴Ophthalmology, Seoul Metropolitan Government Seoul National Univ. Boramae Medical Center, Korea; ⁵Electrical Engineering, Inha Univ., Korea. We observed retinal cell layers using a reflective differential interference contrast (DIC) microscopy. This technique allows non-stained, transparent retinal cells to be possibly imaged in a three-dimensional view.

W3A.89

A Method of One-Exposure Coherent Diffraction Imaging Through the Turbid Media, Wusheng Tang¹, Wenjun Yi¹, Meicheng Fu¹, Lei Wang¹, Qianwen Nie¹, Mengjun Zhu¹, Xiujian Li¹, Ping Wang¹; ¹National Univ of Defense Technol, China. We use simple optical setup and algorithm of coherent diffraction imaging to reconstruct the object completely hidden behind an opaque diffuser. A linear model is deduced and we get the experimental results consistent with it.

W3A.90

Single-shot coded aperture structured illumination digital holographic microscopy for resolution enhancement, Han-Yen Tu², Xin-Ji Lai¹, Yu-Chih Lin¹, Chau-Jern Cheng¹; ¹National Taiwan Normal Univ., Taiwan; ²Chinese Culture Univ., Taiwan. This work proposes coded aperture structured illumination digital holographic microscopy for directional resolution enhancement. The Fresnel hologram at a single exposure with compressive sensing is applied to avoid temporal phase shifting process in structured illumination.

W3A.91

Joule level long pulse green laser and its application for the micro welding of copper and aluminum, Zhiqiang Fang¹, Baohua Zhu¹, Xiaoting Li¹, Jianqiang Liu¹, Jin Wang¹; ¹Institution of Laser Source for welding, Precision Welding Center for Information Science and Technology, Han's Laser Technology Co. Ltd., China; ²Precision Welding Division, Han's Laser Technology Co. Ltd., China. To solve the poor weldability of copper and aluminum, Hans Laser has developed a joule level long pulse green laser with high frequency doubling efficiency. The process experiment results showed that a greatly improved weld quality and splatter free micro welding of the dissimilar metals has been achieved.

W3A.92

Fabrication and Evaluation of Ce³⁺ Ion Doped CaF₂ Thin Film Phosphor, Masato Hishiki¹; ¹Nagoya Inst. of Technology, Japan. We fabricated Ce³⁺:CaF₂ thin films with different doping concentration in anticipation of use as a phosphor. We calculated practical doping concentration from lattice distortion and evaluated the optimized doping concentration for high efficiency light emission.

W3A.93

Patterning Oxidation via Femtosecond Laser Irradiation on Copper Substrate, Xi Yu¹, Masaaki Sudo², Fumihiro Itoigawa¹, Shingo Ono¹; ¹Nagoya Inst. of Technology, Japan; ²IMRA America, Inc., Japan. Patterning oxidation was performed by irradiating femtosecond laser pulses to surface of oxygen-free copper substrate. Conglomerates less than 1 μm were observed on irradiated area by SEM. Expansion (about 400 nm) and discoloration were observed by CLSM. Results of EDX, Raman spectroscopy and XRD suggested that the irradiated area was Oxidized.

W3A.94

Direct-bonding TC4 and PA plastics by a nanosecond laser lap joining technology, Zhihao Fang², Longfei Chen², Yingchun Guan^{1,3}; ¹School of Mechanical Engineering and Automation, Beihang Univ., China; ²School of Energy and Power Engineering, Beihang Univ., China; ³National Engineering Laboratory of Additive Manufacturing for Large Metallic Components, Beihang Univ., China. This study carried out the direct-bonding between titanium and polyamide using nanosecond laser, investigated the effect of the textured micro-groove depth on the strength of the joint and obtained the optimal joint strength.

Room S421

14:00–15:30

W3A • Poster Session

W3A.95

Modification of SiC surface transport properties via excimer laser irradiation in various atmosphere conditions, Zhenyuan Lin¹, Lingfei Ji¹, ¹Beijing Univ. of Technology, China. Excimer laser was employed for the surface modification of transport properties on n-type single-crystal 4H-SiC substrates. Corresponding electrical performance was measured and modified mechanism was analyzed.

W3A.96

Fabricating Fine Structures Induced by Femtosecond Laser on Molybdenum Surface, Masato Hishiki¹, ¹Nagoya Inst. of Technology, Japan. We fabricated nanostructures on molybdenum with a femtosecond laser, and pores and spikes that are smaller than LPSS were observed. Additionally, we controlled the wettability with micro and nanostructures as well as just nanostructures.

W3A.97

Research on the laser drilling property of glass fiber composite material by quasi-continuous-wave laser, Changyong Tian¹, ¹Key Laboratory of Functional Crystal and Laser Technology, Technical Inst. of Physics and Chemistry, Chinese Academic of Science, China. The laser drilling property of glass fiber composites irradiated by quasi-continuous wave laser (QCW) is researched under different subsonic tangential airflow velocities, based on a combination of online experimental system and off-line measuring system.

W3A.98

All-solid Microstructured Fiber for Coherent Supercontinuum Pumped by Sub-picosecond Pulse, Meisong Liao¹, ¹Shanghai Inst of Optics and Fine Mech, China. We proposed and fabricated an asterisk-shaped all-solid microstructured fiber, presenting a low, ultra-flat, and all-normal dispersions. An octave-spanning coherent SC pulse with a 0.5-ps pump pulse at 1.55 μm was numerically generated.

W3A.99

Quantum Noise Analysis of Gain Saturated Periodically Poled Lithium Niobate waveguides, Takuya Takemura¹, Shun Noguchi¹, Kunihiko Mori², Mitsunori Fukutoku², Wataru Imajuku¹, ¹Kindai Univ., Japan; ²NTT Network Innovation Labs., Japan. This paper analyses quantum noise in gain saturated Periodically Poled Lithium Niobate waveguides for optical repeater amplifier in fiber transmission systems. The feature of amplitude noise suppression can improve performance of signal-to-noise ratio in the systems.

W3A.100

Design of Logarithmic-Index Fiber for Orbital Angular Momentum (OAM) Transmission, Shuhui Li¹, Pei You¹, Zhe Xu¹, Ruixuan Zhao¹, Li Shen¹, Jian Wang¹, ¹Wuhan National Lab for Optoelectronics, China. We propose and design a fiber with logarithmic-index profile for orbital angular momentum (OAM) transmission. The designed fiber shows favorable performance of low mode crosstalk and tensile invariance property of mode field diameter (MFD).

W3A.101

Dual-core Photonic Crystal Fiber Multi-mode Selective Coupler Supporting up to Seven High Modes, Qihang Hu¹, Li Gao¹, Mingying Lan¹, Shanyong Cai¹, Song Yu¹, ¹State Key Laboratory of Information Photonics and Optical Communications, China. A multi-mode selective coupler based on asymmetric dual core photonic crystal fiber is proposed. Efficient mode conversion between LP₀₁ and high order modes is achieved, more than previous report. Minimum bandwidth can reach 2 nm.

W3A.102

Fabrication of chirped and tilted fiber Bragg gratings on LMA-DC fiber by phase mask technique, Meng Wang¹, Yulong Cui¹, Le Liu¹, Zefeng Wang¹, Xiaojun Xu¹, Xijia Gu², ¹National Univ of Defense Technology, China; ²Dept. of Electrical and Computer Engineering, Ryerson Univ., Canada. The inscription of chirped and tilted fiber Bragg gratings (CTFBGs) is demonstrated in hydrogen-loaded large-mode-area double-cladding (LMA-DC) fiber by a linearly chirped phase mask.

W3A.103

Design of Broadband Plasmonic Polarization Beam Splitter, Lanting Ji¹, Yang Gao¹, Yan Xu¹, Xiaoqiang Sun¹, Xibin Wang¹, Fei Wang¹, Daming Zhang¹, Zhiyong Li², ¹Jilin Univ., China; ²Inst. of Semiconductors, Chinese Academy of Sciences, China. A polarization beam splitter based on vertical coupling between plasmonic mode and optical mode is theoretically designed. A bandwidth of 250 nm at an extinction ratio of over 10 dB can be realized.

W3A.104

Transformation of the fiber based LP_{0n} modes into free-space LG_{0p} beams, Nitin Bhatia^{1,2}, Shailendra Varshney¹, ¹Indian Inst. of Technology Kharagpur, India; ²NIIT Univ., India. We show that the beam waist of the LG modes should be less than the fiber core diameter for transforming the LP_{0n} modes into free-space beams. The choice of beam waist does not alter the free-space propagation of the beam, given that the LG mode set is complete.

W3A.105

Design of polarization-maintaining rectangular core fiber supporting eight modes, Zihao Wang¹, Li Gao¹, Mingying Lan¹, Shanyong Cai¹, Song Yu¹, ¹State Key Laboratory of Information Photonics and Optical Communications, China. Polarization-maintaining rectangular core fiber is proposed. Eight modes are hold simultaneously under regular cladding, with extreme small dispersion over entire C and L bands. It's suitable for long-distance, high-capacity MIMO-free spatial division multiplexing.

W3A.106

Experimental Demonstration of Femtosecond-level Quantum Clock Synchronization, Quan Run ai^{1,2}, Ruifang Dong¹, Yiwei Zhai^{1,2}, Fei y. Hou^{1,2}, Tao Liu¹, Shougang Zhang¹, ¹Key Laboratory of Time and Frequency Primary Standards, National Time Service Center, CAS, China; ²Univ. of Chinese Academy of Sciences, China. Based on the second-order quantum interference between frequency entangled photons generated via parametric down conversion process, we have demonstrated a new experiment of synchronizing two clocks separated by 6-km fiber link. A synchronization accuracy of 13 ps has been achieved with a minimum timing stability of 60 fs.

W3A.107

Quantum secure ghost imaging, Xin Yao¹, Xu Liu¹, Wei Zhang¹, Yidong Huang¹, ¹Tsinghua Univ., China. We propose and experimentally demonstrate a scheme of quantum secure ghost imaging. It realizes information transmission over optical fibers by temporal ghost imaging, and performs the security test by monitoring the entanglement in photon pairs.

W3A.108

Enhanced coincidence between two independent heralded single-photons using a fiber-optic single-photon buffer, Akiko Tada¹, Naoto Namekata¹, Shuichiro Inoue¹, ¹Nihon Univ., Japan. We report on the all-fiber single-photon buffer for long-distance quantum communications. The coincidence between single photons generated by two independent heralded single-photon sources was successfully enhanced without degrading the polarization-entanglement.

W3A.109

Manipulating conditional photon statistics of lasers via second-order interference and post-selections, Kang-Hee Hong¹, Jisung Jung², Young-Wook Cho², Sang-Wook Han², Sung Moon², Kyunghwan Oh², Yong-Su Kim², Yoon-Ho Kim¹, ¹Pohang Univ of Sci & Tech (POSTECH), Korea; ²Korea Inst. of science and technology, Korea; ³physics, Yonsei Univ., Korea. Here we report theoretical analysis on the limits of manipulating conditional photon statistics of lasers via interference and post-selections. We demonstrate explicitly that photon anti-bunching cannot be obtained in such a scheme.

W3A.110

Compression of chirped biphotons by Fresnel-inspired binary phase shaping, Baihong Li^{1,2}, ¹Xi'an Univ. of Science & Technology, China; ²Key Laboratory of Time and Frequency Primary Standards, National Time Service Center, Chinese Academy of Sciences, China. We theoretically show that chirped biphotons can be compressed to Fourier-transform limited by shaping its spectrum using Fresnel-inspired binary phase shaping. This provides a way for the generation of single-cycle biphotons.

W3A.111

Homodyne detection of 1.57- μm squeezed vacuum pulse with degenerate optical parametric oscillator pumped by a common 785-nm laser, Akihito Omi¹, Aruto Hosaka¹, Masaya Tomita¹, Shintaro Niimura¹, Fumihiro Kannari¹, ¹Keio Univ., Japan. We generate 1.57- μm squeezed vacuum pulses by degenerate spontaneous parametric down conversion (DSPDC) and observe 3.5dB anti-squeezing and -0.48dB squeezing using local oscillator pulses generated from a degenerate synchronously pumped optical parametric oscillator.

W3A.112

Universal Model for Multi-mode NOON State Generation Using Fock State Filters, Lu Zhang¹, Kam Wai C. Chan¹, ¹Univ. of Oklahoma, USA. We present a universal model for generating multi-mode NOON states using Fock state filters. The generation efficiencies for different input scenarios such as coherent states and squeezed vacuum states are calculated for comparisons.

W3A.113

Measuring the topological charge of light beams generated by four-wave mixing in Rb vapours, Jack Muir¹, Nafia Rahaman¹, Alexander Akulshin¹, Russell McLean¹, ¹Swinburne Univ. of Technology, Australia. Collimated light generated via four wave mixing in atomic rubidium vapours excited by light carrying orbital angular momentum is analyzed, particularly the case of doughnut-shaped intensity profiles with zero topological charge.

W3A.114

Uncovering quantum interferences between photon numbers using the Fisher information of field quadrature estimates, Junyi Wu¹, Holger Hofmann¹, ¹Hiroshima Univ., Japan. We show that the reduction of the Fisher information of field quadrature displacements of squeezed states in lossy channels reveals characteristic patterns relating to quantum interferences between different photon numbers.

W3A.115

Wideband MZI based Thermo-Optic Switch with Slab Integrated Microheater in SOI, Ramesh K¹, Bijoy K. Das¹, ¹IIT MADRAS, India. Silicon waveguide slab integrated microheater is proposed in MZI configuration for efficient and broadband thermo-optic switch. Fabricated devices exhibit fast switching (~5 ms) and extinction of > 20-dB over a broad wavelength range (1520-1620 nm).

W3A.116

Robust Excitation of High-Q Nanocavities via a Super-Luminescent Diode, Risa Shiozaki¹, Kohei Ashida¹, Yasushi Takahashi¹, ¹Osaka Prefecture Univ., Japan. We employ a super-luminescent diode (SLD) as excitation light source for photonic crystal high-Q nanocavities. We demonstrate that the broad emission of the SLD enables robust and simultaneous excitation of eight high-Q L3-type nanocavities.

W3A.117

Successful fabrication of GaInAsP ridge waveguide laser diode using hydrophilic bonded InP/Si substrate, Hiromu Yada¹, Naoki Kamada¹, Yuya Onuki¹, Xu Han¹, Gandhi Kallarasani Periyanyagam¹, Kazuki Uchida¹, Hirokazu Sugiyama¹, Masaki Aikawa¹, Natsumi Hayasaka¹, Kazuhiko Shimomura¹, ¹Sophia Univ., Japan. We have successfully fabricated 1.5 μm GaInAsP ridge waveguide laser diode on InP/Si substrate and obtained laser emission. We have measured I-L-V characteristics and compared threshold current between InP/Si and InP substrate at several temperatures.

W3A.118

Robust TE0 + TE1 Waveguide Crossing, Pengfei Xu¹, Yanfeng Zhang¹, Yujie Chen¹, Siyuan Yu^{1,2}, ¹Sun Yat-sen Univ., China; ²Univ. of Bristol, UK. We proposed a silicon waveguide crossing device supporting both TE0 and TE1 modes, TE0 mode insertion loss about -1~ -1.2 dB and TE1 insertion loss about -0.5 ~ -1 dB, and the crosstalk is better than -30 dB.

W3A.119

Measurement of the Threshold of Stimulated Brillouin Scattering with Super-Gaussian-shaped Laser Pulses, Xuehua Zhu¹, Guanling Wang¹, Guangzhen Dai¹, Haojun Hu¹, ¹Anhui Polytechnic Univ., China. We present a novel method for measuring the threshold of stimulated Brillouin scattering (SBS) from the waveform of reflected light with large-aperture super-Gaussian-shaped laser pulses.

W3A.120

Suppression of SRS in a two-stage 1090 nm fiber amplifier using chirped and tilted fiber Bragg gratings, Meng Wang¹, Yulong Cui¹, Le Liu¹, Zefeng Wang¹, Xiaojun Xu¹, Xijia Gu¹, ¹National Univ of Defense Technology, China. We report here the suppression of stimulated Raman scattering in a 1090 nm two-stage fiber laser amplifier using chirped and tilted fiber Bragg gratings (CTFBGs).

Room S421

14:00–15:30

W3A • Poster Session

W3A.121

Modeling of TMI effect in high power multi-wavelength pumped Yb-doped fiber amplifier, Lingchao Kong¹, Jinyong Leng¹, Pu Zhou¹, Zongfu Jiang¹; ¹National Univ. of Defense Technology, China. We demonstrate a model to simulate the TMI effect in multi-wavelength pumped YDFA. The maximum output power is increased about 20% by optimizing the power ratio between the 915 nm and 976 nm pump laser

W3A.122

Graphene-incorporated sol-gel glass for saturable absorption of fiber lasers, Yusheng Zhang¹, Xueming Liu¹; ¹Zhejiang Univ., China. We successfully demonstrated all-fiber mode-locked laser with the graphene-incorporated sol-gel glass as the saturable absorber, and conventional soliton spectrum with Kelly sideband and spectral full width of 1.1 nm is obtained.

W3A.123

Experimental Study on the Mitigation of Photodarkening in Yb-doped Fibers by Li co-doping, Miao Li^{1,2}, Nan Zhao², Yehui Liu², Gui Chen², Jinyong Leng¹, Jinbao Chen¹, Jinyan Li²; ¹National Univ. of Defense Technology, China; ²Huazhong Univ. of Science and Technology, China. We experimentally demonstrated that Li⁺ ions doping into Yb-doped fiber is beneficial to mitigate the photodarkening-induced excess loss. The mechanism of alkali metal elements Li and Na co-doping to mitigate the PD effect is discussed.

W3A.124

High Power 1.5 μ m Fiber Gas Raman Laser Source, Zhixian Li¹, Wei Huang¹, Yulong Cui¹, Zefeng Wang¹; ¹National Univ. of Defense Technology, China. We report here a high-power 1.5 μ m gas Raman laser source using a methane-filled hollow-core fiber. The maximum average power is ~830 mW, which is about 20 times as much as the similar experiment reported.

W3A.125

A high-efficiency GaAs photodetector enhanced by a near-infrared dipole antenna, Yanni Tang¹; ¹Beijing Univ. of Posts and Telecomm, China. We present a plasmon-enhanced PN photodetector structure based on a GaAs nanowire decorated with a half-wave Hertz dipole antenna. An enhancement by a factor of 100 in the responsivity due to the antenna resonance.

W3A.126

Mode Converters Based on LPFGs at 1 μ m, Le Liu¹, Meng Wang¹, Xiaoming Xi¹, Zefeng Wang¹; ¹National Univ. of Defense Technology, China. Here we report a LP₀₁-LP₁₁ mode converter based on long-period fiber grating (LPFG) in a conventional two-mode fiber (TMF) operating at 1 μ m. The mode converter was fabricated with point-by-point technique using a CO₂ laser.

W3A.127

First-principles investigation of semiconductor-like MXenes, Qiran Chen^{1,2}, Weijun Fan^{1,2}, Dao Hua Zhang^{1,2}, Haibin Su³, Jisheng Pan⁴; ¹School of EEE, Nanyang Technological Univ., Singapore; ²OPTIMUS, Centre for OptoElectronics and Biophotonics, LUMINOUS! Centre of Excellence for Semiconductor Lighting and Displays, Nanyang Technological Univ., Singapore; ³School of Materials Science & Engineering, Nanyang Technological Univ., Singapore; ⁴Inst. of Materials Research and Engineering (IMRE), Agency for Science, Technology and Research (A*STAR), Singapore. MXenes are a large family of two-dimensional material composed of transition metal carbides or nitrides. This article gives theoretical investigation of a type of MXene that behave like semiconductors.

W3A.128

Frequency Noise Reduction of Injection-Locked Quantum Cascade Lasers, Xing-Guang Wang¹, Bin-bin Zhao¹, Cheng Wang¹; ¹ShanghaiTech Univ., China. This work theoretically shows that the optical injection significantly reduces the frequency noise of quantum cascade lasers in the low frequency range. Frequency detunings close to the positive locking boundary enhance the frequency noise peak.

W3A.129

Application of High-reflectivity Non-periodic Sub-wavelength Gratings with Small-angle Beam-steering Ability in Fabry-Perot Cavity, Shuai Zhang¹, Xiaofeng Duan¹, Gongqing Li¹, Kai Liu¹, Yongqing Huang¹, Xiaomin Ren¹; ¹Beijing Univ. of Posts and Telecomm, China. An axisymmetric high-reflectivity non-periodic sub-wavelength gratings (SWG) with small-angle beam-steering ability for reflected light is presented, and it brings a new characteristic of flexibly controlling the width of oscillation optical field for the improved Fabry-Perot (F-P) cavity which based on it.

W3A.130

Analysis of collagen fiber orientation using rapidly-polarization-modulated second-harmonic-generation microscopy, Takuya Sakaue¹, Eiji Hase^{1,2}, Takeo Minamikawa¹, Takeshi Yasui¹; ¹Tokushima Univ., Japan; ²Japan Synchrotron Radiation Research Inst., Japan. We constructed continuously-polarization-resolved SHG microscopy based on rapid polarization rotation every 15 degrees with electric-optic Pockells cell, and applied it for the quantitative analysis of collagen fiber orientation in biological tissues.

W3A.131

Imaging and Spectral Analysis of Ultra-weak Biophoton Emission and Delayed Luminescence from Human Skin, Torai Iwasa¹, Masaki Kobayashi¹; ¹Tohoku Inst. of Technology, Japan. Biophoton is spontaneous ultra-weak photon emission (UPE) from living body. Delayed luminescence is also UPE from living body but emission after visible light exposure. Both are associated with oxidative stress of the body. We have developed highly sensitive imaging and spectroscopic system for UPE and characterized them for diagnostic application.

W3A.132

A Study on the Sensitivity and Specificity of Tactile Sensation Induced by Pulse Laser, Hyung-Sik Kim¹, Jihun Jo¹, Mi-Hyun Choi¹, Soon-Cheol Chung¹; ¹Biomedical Eng., Konkuk Univ., Korea. Pulse laser of two energies was presented on the finger and the perceptual characteristic of the human response from the laser-based tactile sensation was observed.

W3A.134

Spectral Interferometry based SPR Phase Response on the Non-resonant Wavelengths, Meng-Syuan Jian¹, Ding-Zhang Tsai¹, Shih-Hsiang Hsu¹; ¹Electronic and Computer Engineering, National Taiwan Univ. of Science and Technology, Taiwan. A real-time, high sensitivity and label-free spectral interferometry-based surface plasma resonator biosensor is demonstrated. We prove that the Mycobacterium tuberculosis (MTB) DNA can be captured by the immobilized IS 6110 DNA probe successfully and the system sensitivity is showing -0.162 (rad/(\(\mug/mL)) from the non-resonant wavelengths.

W3A.135

Dual low coherence scanning interferometer for rapidly measuring large step height and thickness, Jun Woo Jeon¹, Hyo Mi Park¹, Ki-Nam Joo¹; ¹Chosun Univ., Korea. In this investigation, we propose a novel concept to measure large height steps on the topographic surface of a specimen and the thickness profile of a transparent optical plate using a low coherence scanning interferometry.

W3A.136

Mode Density Multiplication of an Optical Frequency Comb by N² with Phase Modulation, Taro Hasegawa^{1,2}, Hiroyuki Sasada^{1,2}; ¹Keio Univ., Japan; ²JST, ERATO, MINOSHIMA Intelligent Optical Synthesizer Project, Japan. We introduce a simple scheme for mode density multiplication of an optical frequency comb by square of an arbitrary integer with phase modulation. The mode density of an Er fiber comb is multiplied by 4².

W3A.137

Piezoelectric Resonance Laser Calorimetry for Optical Absorptance Testing of Crystal Boules, Georgii A. Aloian¹, Nikita Kovalenko¹, Irina Shebarshina¹, Aleksey Konyashkin²; ¹Moscow Inst. of Physics and Technol., Russia; ²Kotel'nikov Inst. of Radio-engineering and Electronics of RAS, Russia. Novel technique for measuring low optical absorption coefficients of massive crystal boules of arbitrary shape is proposed. The accuracy of the method was theoretically estimated.

W3A.138

A Simplified Distance Measurement Method Based on Optoelectronic Oscillator, Tianyuan Xie¹, Jinlong Yu¹, Ju Wang¹, Zixiong Wang¹, Chuang Ma¹, Yang Yu¹, Tianyu Li¹; ¹Tianjin Univ., China. We propose a long-range, high-precision distance measurement system with low complexity and cost based on optoelectronic oscillator. The relative measurement accuracy of 1.667 km is 3 \times 10⁻⁹.

W3A.139

Real-time spectroscopic ellipsometer using a depolarizer, Jin Sub Kim¹, Dae Hee Kim¹, Ki-Nam Joo¹; ¹Chosun Univ., Korea. In this investigation, spectroscopic ellipsometry using a LCP (Liquid crystal polymer) type of depolarizer, named as spatially phase-retarded spectroscopic ellipsometry (SPARSE), is proposed to significantly raise the measurement speed compared to the typical spectroscopic ellipsometry.

W3A.140

Development of a laser system for observation of light-induced drift of Cs atoms, Yuya Kusano¹, Noritaka Nishiya¹, Leo Matsuoaka¹; ¹Graduate School of Engineering, Hiroshima Univ., Japan. A laser system with a widely-tunable stabilized frequency suitable for observation of the light-induced drift was developed. The reference signal was obtained by dichroic atomic vapor spectroscopy over the range of 2 GHz.

W3A.141

Plasmon-assisted Random Lasing in Perovskite Quantum Dots, Si Q. Li¹, Jijun He¹, Yunfeng Wang¹, Decheng Yang¹, Siu Fung Yu¹, Dang Yuan Lei¹; ¹The Hong Kong Polytechnic Univ., Hong Kong. Here we report a plasmonic all-inorganic perovskite CsPbBr₃ quantum dots hybrid films for two photonics random laser. The gold nanorods with good optical confinement and strong plasmonic enhancement properties formed randomly closed-loop cavities for the green random laser which are applied for speckle-free imagine.

W3A.142

Thermal tuning of plasmon-bright-exciton coupling by redistribution of exciton density between bright and dark exciton, Tsz Wing Lo¹, Dang Yuan Lei¹; ¹The Hong Kong Polytechnic Univ., Hong Kong. We discover plasmon-exciton coupling strength in MoS₂ system and WS₂ system opposite to each other under thermal tuning. The variation comes from energy difference on bright and dark exciton due to redistribution of oscillator strength.

W3A.143

Complex-amplitude modulation of linear polarization via metasurface, Jangwoon Sung¹, Gun-Yeal Lee¹, Chulsoo Choi¹, Byounghee Lee¹; ¹Seoul National Univ., Korea. We present a novel complex amplitude modulation method for linear polarization from incident circular polarization. We achieved high efficiency up to 98% with fulfilling continuous and independent modulation of amplitude and phase.

W3A.144

Observation of a plasmon induced magnetic resonance in a gold sphere dimer-on-film nanocavity, Yongjun Meng^{1,2}, Qiang Zhang¹, Meng Qiu¹, Guang-Can Li¹, Chi Wah Leung¹, Xuewen Chen², Dang Yuan Lei¹; ¹Dept. of Applied Physics, Hong Kong Polytechnic Univ., Hong Kong; ²School of Physics, Huazhong Univ. of Science and Technology, China. We experimentally and theoretically reveal that a gold nanosphere-dimer-on-film nanocavity supports a strong in-plane magnetic dipolar resonance in a deep sub-wavelength region, induced by a current loop in the nanometer thick dimer-film gap.

W3A.145

Plasmonic Au/TiO₂-dumbbell-on-film nanocavities for high-efficiency hot-carrier generation and extraction, Aixue Shang¹, Dang Yuan Lei¹; ¹The Hong Kong Polytechnic Univ., Hong Kong. Au/TiO₂ dumbbell assembled on Au film optically establish plasmonic nanocavities, resulting in strong near-field enhancement and confinement and eventually contributing to the improved photocurrent, IPCE and decomposition rate.

W3A.146

Polarization conversion in toroidal metamaterial in optical spectral range, Sang-Eun Mun¹, Sun-Je Kim¹, Jongwoo Hong¹, Byounghee Lee¹; ¹Seoul National Univ., Korea. We propose a novel scheme to realize broadband polarization conversion using anisotropic metamaterial based on the fourfold symmetry breaking. The coupling of plasmon resonances generates orthogonal polarization component. Magnetic and toroidal resonances lead to bandwidth expansion of polarization conversion in optical spectral range.

Room S421

14:00–15:30

W3A • Poster Session

W3A.147

Tunable hybrid plasmonic split-ring resonator refractive index sensor for high FOM applications, Kishore K R¹; ¹Electronics And Communication Engineering, NIT TRICHY, India. We propose a hybrid plasmonic micro-ring resonator combining split-ring and photonic waveguide. The finite difference time domain analysis of the design exhibit strong field confinement and have a figure of merit of 216.67 /RIU which can be used for refractive index sensor application.

W3A.148

Coupling of a metasurface with two non-coplanar and inter-perpendicular graphene nanoribbon arrays, Feng Chao Ni¹, Ze T. Xie¹, Qi Chang Ma¹, Jin Tao², Jian Li¹, Hongyun Men¹, Xu Guang Huang¹; ¹South China Normal Univ., China; ²Wuhan Research Inst. of Posts Telecommunications, State Key Laboratory of Optical Communication Technologies and Networks, China. A graphene metasurface is proposed and investigated. Through the analysis of the light field, the formation mechanism of the spectral splitting is attributed to the coupling between localized and delocalized graphene surface plasmon polaritons.

W3A.149

Light-actuation of carbon nanotubes in liquids, Yujie Liu¹, Chunhui Zhu¹, Emmanuel Flahaut^{2,3}, Fengqiu Wang¹; ¹School of Electronic Science and Engineering, Nanjing Univ., China; ²CNRS, Institut Carnot Cirimat, France; ³Université de Toulouse; UPS, INP, Institut Carnot Cirimat; 118, route de Narbonne, F-31062 Toulouse cedex 9, France. We observed a novel phenomenon where single-wall carbon nanotube flocculations can be photo-actuated in liquids by either sunlight or laser irradiation. The light-actuation phenomenon is found highly repeatable.

W3A.150

Highly Efficient Multilayer Rhenium Disulfide-based Homo- and Hetero-junction Photovoltaic Devices, Kwan-Ho Kim¹, JeaWoo Shim¹, Jin-Hong Park¹; ¹Sungkyunkwan Univ., Korea. We demonstrated the photovoltaic devices based on ReS₂ homo- and hetero-junctions. First, ReS₂ based homo-junction photovoltaic device showed PCE of 2.4%. Furthermore, ReS₂/WSe₂ heterojunction exhibited high PCE of 12%.

W3A.151

Two-dimensional ReS₂ nanosheets based saturable absorbers for passively mode-locked fiber lasers, Mengyu Zhang¹, Jinde Yin¹, Peiguang Yan¹; ¹College of Optoelectronic Engineering, Shenzhen Univ., China. We prepared ReS₂ nanosheets by liquid-phase exfoliation and fabricated ReS₂ saturable absorbers with all-fiber integrated structure. Their nonlinear optical properties were investigated systematically. The results demonstrate that ReS₂ nanosheets own excellent nonlinear saturable absorption properties.

W3A.152

Polarization-independent and wide-incident-angle absorber with periodically patterned graphene-dielectric arrays, Gaige Zheng¹, Xiujuan Zou¹; ¹Nanjing Univ. of Information Sci. & Tech, China. A graphene optical absorber with periodically patterned grating is demonstrated. The proposed absorber exhibits polarization-insensitive behavior and maintains the high absorption above 90% within a wide range of incident angle (more than 80°).

W3A.153

Wearable Full-duplex Digital Transceiver for Underwater Optical Wireless Communications, Zixian Wei¹, Xin Mu¹, Hongyan Fu¹; ¹Tsinghua-Berkeley Shenzhen Inst., China. We demonstrate an UOWC system with up to 235 Mbps at BER of 1.0×10⁻³ over 11.5-meters in water, which is based on a compact full-duplex digital transceiver by integrating commercial available blue-LED and APD.

W3A.154

A Multichannel WDM-PON System with Port Agnostic Tunable SFP+ Transceiver Modules, Yang Liu¹, Da Li¹, Tiantian Zhang¹, Jian-Jun He¹; ¹Zhejiang Univ., China. We demonstrate a WDM-PON system with port agnostic tunable SFP+ transceiver modules. With low-frequency envelope-modulated message channel, error-free data transmission is achieved at 8.5 Gbps with a sensitivity better than -19 dBm.

W3A.155

Visible Light Communication based on Orbital Angular Momentum Multiplexing, Youpeng Xie¹, Lei Ting¹, Zhang Shan¹, Xiaocong L. Yuan¹; ¹Shenzhen Univ., China. We propose and demonstrate a visible light communication based on orbital angular momentum multiplexing. The coaxial two signal channels achieve the transmission of the audio and video, which improve the capacity of the system.

W3A.156

Visible Frequency Comb in a Silica Microbubble Resonator, Sho Kasumie¹, Jonathan Ward¹, Sile Nic Chormaic¹, Yong Yang²; ¹OIST Graduate Univ., Japan; ²Aston Inst. of Photonic Technologies, UK. Kerr frequency comb generation in a microbubble resonator have its advantage in its manipulatability of the total dispersion of the cavity. Here we try to improve the comb so it include more comb lines and extend to shorter wavelength.

W3A.157

Photonic multiple microwave frequency measurement based on a swept frequency silicon microring resonator, Feng Zhou¹, Hao Chen¹, Xu Wang¹, Linjie Zhou², Jianji Dong¹, Xinliang Zhang¹; ¹Wuhan National Lab for Optoelectronics, China; ²State Key Laboratory of Advanced Optical Communication Systems and Networks, Dept. of Electronic Engineering, Shanghai Jiao Tong Univ., China. A photonic multiple microwave frequency measurement system is presented based on a swept frequency silicon microring resonator. The measurement bandwidth, accuracy and multi-frequency resolution are 25 GHz, ±510 MHz and 5 GHz, respectively.

W3A.158

A Tunable Narrowband Microwave Photonic Bandpass Filter with An Ultra-high-Q Silicon Microring Resonator, Huaqing Qiu¹, Feng Zhou¹, Yuhao Yao¹, Jianji Dong¹, Yuan Yu¹, Xi Xiao², Xinliang Zhang¹; ¹Wuhan National Lab for Optoelectronics, China; ²State Key Laboratory of Optical Communication Technologies and Networks, Wuhan Research Inst. of Posts & Telecommunications, China. A 170-MHz 3-dB bandwidth microwave photonic bandpass filter is achieved owing to utilize an ultra-high-Q as 1.14×10⁶ of the silicon microring resonator. The central frequency could be tuned from 2.0 GHz to 18.4 GHz.

15:30–16:00 Coffee Break

Room S223

Room S224

Room S225

Room S226

Room S227

Room S228

These concurrent sessions are grouped across two pages. Please review both pages for complete session information.

16:00–18:00

W4A • Advanced Light Sources II

Presider: Anting Wang; Univ. of Sci & Tech of China, China

W4A.1 • 16:00

Multi-GHz mode-locked Yb:YAG channel waveguide laser using SESAM and carbon nanotube saturable absorbers, Sun Young Choi¹, Thomas Calmano², Fabian Rotermund¹, Clara Saraceno³, Christian Kränkel⁴, ¹Dept. of Physics, KAIST, Korea; ²Institut für Laser-Physik, Universität Hamburg, Germany; ³Photonics and Ultrafast Laser Science, Ruhr-Universität Bochum, Germany; ⁴Zentrum für Lasermaterialien, Leibniz-Institut für Kristallzüchtung, Germany. We demonstrated GHz modelocking of femtosecond-laser inscribed Yb:YAG channel waveguide lasers using SESAM and single-walled carbon nanotube saturable absorber. Sub-2-ps pulses at multi-GHz repetition rates are generated from a dispersion-managed compact laser cavity with watt-level output powers.

W4A.2 • 16:15

Growth, Characterization and Laser Operation of Tm³⁺, Na⁺ codoped CNGG (Tm:CNNGG) Disordered Garnet, Zhongben Pan^{2,1}, Hualei Yuan², Xiaojun Dai², Huaqiang Cai², Josep Serres³, Xavier Mateos³, Magdalena Aguilo³, Francesc Diaz³, Yicheng Wang¹, Yongguang Zhao^{1,4}, Pavel Loiko⁵, Uwe Griebner¹, Valentin Petrov¹; ¹Max Born Inst., Germany; ²Inst. of Chemical Materials, China; ³Universitat Rovira i Virgili, Spain; ⁴Jiangsu Normal Univ., China; ⁵TMO Univ., Russia. A Tm,Na-codoped calcium niobium garnet (Tm:CNNGG) crystal was grown and its structure and spectroscopic properties characterized. A diode-pumped Tm:CNNGG laser generated 0.63 W with 24.2% slope efficiency. Tunability from 1885 to 2053 nm was achieved.

16:00–18:00

W4B • Nonlinear Nanophotonics and Waveguides

Presider: Cornelia Denz; Westfaelische Wilhelms Univ Munster, Germany

W4B.1 • 16:00 Invited

High Nonlinear Figure of Merit Nonlinear Optics Leveraging Ultra-Silicon-Rich Nitride Devices, Dawn T. Tan¹; ¹Singapore Univ. of Technology & Design, Singapore. Nonlinear optics leveraging CMOS-compatible, ultra-silicon-rich nitride devices is presented. Films are engineered to possess high Kerr nonlinearity and negligible two-photon absorption at telecommunications wavelengths. We demonstrate high-gain optical parametric amplifiers, wavelength conversion, slow light and supercontinuum devices.

16:00–18:00

W4C • Infrared and Terahertz Materials and Light Sources for High Performance Applications

Presider: Fabien Sorin; Ecole Polytechnique Federale de Lausanne, Switzerland

W4C.1 • 16:00 Invited

Chalcogenide Planar Waveguides for Infrared Applications, Duk-Yong Choi^{1,2}; ¹Laser Physics Centre, Australian National Univ., Australia; ²College of Information Science and Technology, Jinan Univ., China. I review recent research activities of my group on chalcogenide planar waveguides for near- and mid-infrared applications. Also, new research directions including the hybrid integration of chalcogenides with silicon and silica platforms are covered.

16:00–18:00

W4D • Integrated Nanophotonic Devices

Presider: Xinlun Cai; Sun Yat-Sen Univ., China

W4D.1 • 16:00 Invited

Flat Subwavelength Grating Achromatic Lens over Whole Visible Bandwidths, Yasha Yi¹; ¹Univ. of Michigan, USA. The achromatic micro grating lens covering the whole visible wavelength is demonstrated by utilizing relatively low index contrast gratings. Our works are promising for compact integrated nanophotonic devices on chip.

16:00–18:00

W4E • Fiber Devices I

Presider: John Canning; Univ. of Technology Sydney, Australia

W4E.1 • 16:00 Invited

Fiber Integrated Silicon Photonics, Anna C. Peacock¹; ¹Univ. of Southampton, UK. This paper reviews the recent advancements in the fabrication and application of silicon core optical fibers. Particular focus is placed on novel materials and device designs for use in optical signal processing systems.

16:00–18:00

W4F • Dual-comb Spectroscopy and its Applications

Presider: Xiaoguang Zhang; Beijing Univ. of Posts and Telecom, China

W4F.1 • 16:00 Invited

Electro-Optic Dual Optical Frequency Combs Outside of the Metrology Lab: Opportunities in and Beyond Spectroscopy, Pedro Martin-Mateos¹, Pablo Acedo¹; ¹Universidad Carlos III de Madrid, Spain. The rapid evolution of Electro Optic Dual Comb spectrometer design during the last years have opened new opportunities for such powerful optical technique beyond the research/metrology lab that are reviewed in this work.

These concurrent sessions are grouped across two pages. Please review both pages for complete session information.

16:00–18:00
W4G • Holographic Technologies
 Presider: Limin Xiao; Fudan Univ., China

16:00–18:00
W4H • Integrated Photonics
 Presider: Andrew Poon; Hong Kong Univ of Science & Technology, Hong Kong

16:00–18:00
W4I • Optical Signal Characterization
 Presider: Leslie Rusch; Universite Laval, Canada

16:00–18:00
W4J • Integrated Devices for Communications
 Presider: Duncan MacFarlane; Southern Methodist Univ., USA

16:00–18:00
W4K • Biophotonics and Applications V
 Presider: Daniele Tosi; Nazarbayev Univ., Kazakhstan

16:00–18:00
W4L • Fiber Devices & Sensing II
 Presider: Zinan Wang; Univ. Electronic Sci. & Tech. of China, China

W4G.1 • 16:00 **Tutorial**
Displaying Digital Holograms on Phase-only Devices, Peter Tsang¹; ¹City Univ. of Hong Kong, Hong Kong. A number of methods for generating phase-only hologram (POH) are reviewed in this tutorial. These works share the common advantage that the POHs generated can be displayed directly on a single phase-only spatial light modulator.

W4H.1 • 16:00 **Invited**
Quantum Communication using Integrated Silicon Photonics, Shayan Mookherjee¹; ¹Univ. of California San Diego, USA. Silicon microring resonators have made major recent improvements in high-quality entangled photon pair generation, with CAR > 19,000 and g2(0) < 0.006. They are now being used in prototypical quantum optical communication links.

W4I.1 • 16:00 **Invited**
Image Processing Techniques for Signal Processing in Optical Communication Systems, Tianwai Bo¹, Calvin C. K. Chan², Hoon Kim¹; ¹School of Electrical Engineering, Korea Advanced Inst. of Science and Technology (KAIST), Korea; ²Dept. of Information Engineering, The Chinese Univ. of Hong Kong, Hong Kong. We review the image processing techniques for signal processing in optical communication systems. Their applications in optical performance monitoring and compensation of common phase error are discussed in terms of implementation complexity and system performance.

W4J.1 • 16:00 **Invited**
Hybrid Photonic Integration and Plasmonic Devices - New Perspectives for High-Speed Communications and Signal Processing, Christian Koos¹, Sebastian Randel¹, Wolfgang Freude¹, Larry R. Dalton², Stefan Wolf¹, Clemens Kieninger¹, Yasar Kutuvantavida¹, Matthias Lauermann¹, Delwin Elder², Sascha Muehlbrandt¹, Heiner Zwickel¹, Argishti Melikyan¹, Tobias Harter¹, Sandeep Ummethala¹, Muhammad R. Billah¹, Matthias Blaicher¹, Philipp I. Dietrich¹, Tobias Hoese¹; ¹Karlsruhe Inst. of Technology (KIT), Germany; ²Univ. of Washington, USA. Hybrid photonic integration allows to combine the advantages of different material platforms while maintaining the scalability advantages of monolithically integrated systems. Here we give an overview on our research in the field of hybrid integration, combining multi-chip approaches on a package level with hybrid on-chip integration.

W4K.1 • 16:00 **Invited**
New Progress of Photoacoustic Imaging Technology in Biomedical Applications, Da Xing¹, Sihua Yang¹; ¹South China Normal Univ., China. This report presented the new progresses in photoacoustic dermoscopy, all-optical photoacoustic microscopy, intravascular photoacoustic tomography, photoacoustic elasticity and viscosity imaging toward biomedical and clinical applications.

W4L.1 • 16:00 **Invited**
Specialty Few Mode Fiber and Its Application, Songnian Fu¹; ¹Huazhong Univ of Science & Technology, China. We review the design, fabrication and characterization of several specialty few mode fibers (FMFs) including elliptical-core FMF(e-FMF), panda type FMF(P-FMF), and panda type e-FMF(PE-FMF). Those specialty FMFs and its corresponding applications have lots of potentials to be further exploited.

These concurrent sessions are grouped across two pages. Please review both pages for complete session information.

W4A • Advanced Light Sources II—Continued

W4A.3 • 16:30

High-power femtosecond pulse generation seeded by planar waveguide Yb:YAG ceramic laser, Daping Luo¹, Yang Liu¹, Chao Yang¹, Chao Wang¹, Wenchao Zhang¹, Wenxue Li¹; ¹East China Normal Univ., China. We demonstrate high-power femtosecond pulse generations in chirped-pulse and self-similar amplifiers both seeded by a Yb:YAG ceramic laser. After amplification, the CPA can emit 100-W, 250-fs pulses while the SSA can output 60-W, 60-fs pulses.

W4A.4 • 16:45

Passively mode-locked Thulium-doped nanoengineered Yttrium-Alumina Silica fiber laser, Yin-Wen Lee¹, Jen-Yen Chuang¹, J. T. Lin², Y. W. Jhang², Shyamal Das³, Anirban Dhar³, M. C. Paul³; ¹National Taipei Univ. of Technology, Taiwan; ²Industrial Technology Research Inst., Taiwan; ³CSIR-Central Glass and Ceramic Research Inst., India. We have successfully developed a mode-locked fiber laser utilizing a nano-engineered Tm³⁺-doped yttrium-alumina-silica (YAS) glass fiber. Such kind of new material fiber exhibits the better capability of cluster elimination than commercial Tm³⁺-doped silica fibers.

W4B • Nonlinear Nanophotonics and Waveguides—Continued

W4B.2 • 16:30

Optical Pulse Generation Using Fast Graphene Saturable Absorbers on Silicon Waveguides, Guoqin Liu¹, Shaodong Hou¹, Hong Wang¹, Ning Yang¹, Chi Zhang¹, Nengli Dai¹, Yi Wang¹; ¹Wuhan National Laboratory for Optoelectronics, Huazhong Univ. Of Science And Technology, China. The graphene/silicon hybrid waveguide is applied into a ring cavity laser system working as fast saturable absorber with a recovery time of ~48 ps. Q-switched mode-locking pulses are achieved with a threshold of 11 mW.

W4B.3 • 16:45

Sub-surface Layer of Silicon Single Crystal Periodically Nanostructured by Near-infrared Femtosecond Laser Pulses, Iaroslav Gnilitzkyi^{1,2}, Vitaly Gruzdev³, Xiaoqing He³, Olga Sergaeva³, Pengfei Ji⁴, Tommi White³, Yuwen Zhang³; ¹UNIMORE, Italy; ²NoviNano Inc., Ukraine; ³Univ. of Missouri, USA; ⁴Southern Univ. of Science and Technology, China. Structure of subsurface layer beneath silicon single-crystal surface periodically nanostructured by femtosecond laser suggests significant contribution of laser-driven defect generation to formation of periodic surface ripples by few laser pulses in a broad fluence range.

W4C • Infrared and Terahertz Materials and Light Sources for High Performance Applications—Continued

W4C.2 • 16:30 Invited

Lithium Niobate Nanophotonics for Ultra-fast Optoelectronics, Cheng Wang^{1,2}; ¹City Univ. of Hong Kong, Hong Kong; ²Harvard Univ., USA. We demonstrate a nanophotonic lithium niobate platform that simultaneously features sub-wavelength optical confinement, ultralow optical propagation loss and ultra-fast electro-optic control capability (> 100 GHz). These devices are promising for future chip-scale ultra-fast optoelectronic interface.

W4D • Integrated Nanophotonic Devices—Continued

W4D.2 • 16:30

Genetic-algorithm-optimized wideband on-chip polarization rotator with an ultrasmall footprint, Zejie Yu¹, Haoran Cui¹, Xiankai Sun¹; ¹The Chinese Univ. of Hong Kong, Hong Kong. With a genetic algorithm, we designed an onchip TE0-TM0 polarization rotator with a footprint of 0.96µm×4.2µm and experimentally demonstrated its conversion loss of ~2.5dB and extinction ratio of ~10dB in the wavelength range of 1440–1580nm.

W4D.3 • 16:45

Nondetrimental Surface Modification of Ultrahigh-Q Photonic Crystal Silicon Nanocavities, Takahiro Ito¹, Kohei Ashida¹, Kei Kinoshita², Rai Moriya², Tomoki Machida^{2,3}, Kenichi Maeno⁴, Tatsuro Endo⁴, Koji Yamada⁵, Makoto Okano⁵, Yasushi Takahashi¹; ¹Dept. of Physics and Electronics, Osaka Prefecture Univ., Japan; ²Inst. of Industrial Science, Univ. of Tokyo, Japan; ³CREST, Japan Science and Technology Agency (JST), Japan; ⁴Dept. of Applied Chemistry, Osaka Prefecture Univ., Japan; ⁵National Inst. of Advanced Industrial Science and Technology, Japan. We investigated the influence of surface preparation procedures on the resonance characteristics of silicon nanocavities. We demonstrate that ultrahigh-Q factors larger than one million can be maintained when applying preparation procedures that support attaching nanomaterials.

W4E • Fiber Devices I—Continued

W4E.2 • 16:30 Invited

Optical Nanofibers for Fiber-in-line Quantum Photonics, Kohzo Hakuta¹, Ramachandrarao Yalla¹, K. Muhammad Shafi¹; ¹Univ. of Electro-Communications, Japan. Recent progress in quantum photonics with optical nanofibers (ONFs) is reported. Emphasis is on the photon channeling into the fiber guided modes for a hybrid system of an ONF cavity and a single quantum emitter.

W4F • Dual-comb Spectroscopy and its Applications—Continued

W4F.2 • 16:30

Real-time corrections of air refractive index fluctuation using two-color interferometry with optical frequency combs, Yoshihisa Iki-sawa¹, Tomohiro Makino^{1,2}, Yoshiaki Nakajima^{1,2}, Guan hao Wu³, Kaoru Minoshima^{1,2}; ¹The Univ. of Electro-Communications, Japan; ²Japan Science and Technology Agency (JST), ERATO MINOSHIMA Intelligent Optical Synthesizer (IOS) Project, Japan; ³Tsinghua Univ., China. We developed a technique to correct large and fast variation of air refractive index using two-color interferometry with optical frequency combs. This technique will enhance the applicability of high-accuracy optical distance measurements under air turbulence.

W4F.3 • 16:45

Fourier transform spectroscopic optical microscopy using dual-comb spectroscopic technique, Takeo Minamikawa^{1,2}, Shota Nakano¹, Eiji Hase^{3,1}, Takahiko Mizuno^{1,2}, Hirotsugu Yamamoto^{4,2}, Takeshi Yasui^{1,2}; ¹Tokushima Univ., Japan; ²JST-ERATO Minoshima Intelligent Optical Synthesizer Project, Japan; ³Japan Synchrotron Radiation Research Inst. (JASRI), Japan; ⁴Utsunomiya Univ., Japan. We developed a Fourier transform spectroscopic optical microscope employing dual-comb spectroscopy. We realized the observation with two different contrasting mechanisms, i.e., amplitude and phase, with tightly focused light without mechanical step-scan in time domain.

These concurrent sessions are grouped across two pages. Please review both pages for complete session information.

W4G • Holographic Technologies—Continued

W4H • Integrated Photonics—Continued

W4H.2 • 16:30

An ultra-compact multimode waveguide crossing based on subwavelength asymmetric Y-junction, Weijie Chang¹, Lulu Lu¹, Deming Liu¹, Minming Zhang¹; ¹Huazhong Univ. of Science and Technology, China. An ultra-compact multimode waveguide crossing composed of a pair of asymmetric Y-junctions based on subwavelength structures is proposed and demonstrated with a footprint of $34 \times 34 \mu\text{m}^2$, low insertion loss < 1.5 dB.

W4H.3 • 16:45

Improved CMOS compatible photonic crystal demultiplexer, Shengji Jin¹, Yuta Ooka¹, Tomohiro Tetsumoto¹, Nurul A. Daud¹, Naotaka Kamioka¹, Taku Okamura¹, Takasumi Tanabe¹; ¹Keio Univ., Japan. We optimized a compact photolithographically fabricated photonic crystal DeMUX and obtained flat and high transmittance between channels. A thermal analysis showed that a footprint of $110 \mu\text{m}^2/\text{ch}$ is possible with PhC technology.

W4I • Optical Signal Characterization—Continued

W4I.2 • 16:30

OSNR Monitoring and Modulation Format Recognition Based on Neural Networks and Normalized Autocorrelation Function, Zhuili Huang¹, Jifang Qiu¹, Honghang Zhou¹, Xue Ji¹, Jian Wu¹; ¹Beijing Univ. of Posts and Telecom., China. We experimentally demonstrate the use of neural networks in combination with normalized autocorrelation function (NACF) of noisy signal for simultaneous optical signal to noise ratio (OSNR) monitoring and modulation format recognition (MFR).

W4I.3 • 16:45

Joint Modulation Format, Bit-Rate and OSNR Identification Using Cascaded Deep Neural Networks, Yuanxiang Chen¹, Yongtao Huang¹, Kaile Li¹, Yitong Li¹, Jianguo Yu¹; ¹Beijing Univ. of Posts and Telecommunications, China. Cascaded deep neural networks model trained with signal amplitude histograms is developed for joint optical modulation format, bit-rate and OSNR identification. The averaged joint identification accuracy is 98.78% for four modulation formats.

W4J • Integrated Devices for Communications—Continued

W4J.2 • 16:30

O-L band bias-free high-speed UTC-PD for advanced optical fiber communications, Toshimasa Umezawa¹, Atsushi Kanno¹, Kouichi Akahane¹, Atsushi Matsumoto¹, Naokatsu Yamamoto¹; ¹National Inst of Information & Comm Tech, Japan. We present an O-L band high-baud-rate UTC-PD excluding a bias circuit, which can be operated at zero bias. The 100 Gbaud (NRZ) good eye diagram performances were confirmed for 1320 nm and 1550 nm.

W4J.3 • 16:45

A Horn-Waveguide Asymmetric RSOA as Colorless Transmitter in WDM-PON with Reduced Crosstalk, Chengliang Zuo¹, Xun Li²; ¹Huazhong Univ. of Science and Techn, China; ²McMaster Univ., Canada. A horn-waveguide reflective semiconductor optical amplifier was studied. Experimental results reveal that it can reduce downstream extinction ratio from 5 dB to 1.2 dB, and a 5 Gbps upstream signal was reloaded with clear eye-opening.

W4K • Biophotonics and Applications V—Continued

W4K.2 • 16:30 **Invited**

Super-resolution Dipole Orientation Microscopy, Peng Xi¹, Karl Zhanghao¹, Long Chen², Juntao Gao²; ¹Dept. of Biomedical Engineering, Peking Univ., China; ²Dept. of Automation, Tsinghua Univ., China. With the modulation of fluorescent excitation polarization, here we report a novel super-resolution microscopy technique in which the orientation of the fluorophores can be mapped in addition to super-resolution imaging.

W4L • Fiber Devices & Sensing II—Continued

W4L.2 • 16:30 **Invited**

Multicore Optical Fiber Sensors, Rodrigo Amezcua Correa¹, E. Antonio-Lopez¹, O. Arrizabalaga², J. Zubia², A. Schülzgen¹, J. Villatoro^{2,3}; ¹Univ. of Central Florida, CREOL, USA; ²Dept. of Communications Engineering, Escuela de Ingeniería de Bilbao, Univ. of the Basque Country (UPV/EHU), Spain; ³IKERBASQUE—Basque Foundation for Science, Spain. We review recent multicore optical fiber-based interferometric sensors for vibration, strain and temperature monitoring. Simple, highly sensitive sensors operating in reflection and transmission mode have been fabricated using short segments of strongly coupled core MCFs.

These concurrent sessions are grouped across two pages. Please review both pages for complete session information.

W4A • Advanced Light Sources II—Continued

W4A.5 • 17:00

1GHz harmonic mode-locked fiber laser by using carbon nanotubes film saturable absorber, Qianqian Huang¹, Chuanhang Zou¹, Tianxing Wang¹, Mohammed AlAraini^{2,3}, Aleksey Rozhin^{2,4}, Chengbo Mou¹; ¹Key Laboratory of Specialty Fiber Optics and Optical Access Networks, Shanghai Univ., China; ²Aston Inst. of Photonic Technologies, Aston Univ., UK; ³Al Musanna College of Technology, Oman; ⁴Nanoscience Research Group, Aston Univ., UK. Passively harmonic mode locking in a fiber laser based on single wall carbon nanotubes polyvinyl alcohol film is experimentally implemented. 916MHz pulses at the 34th harmonic with 41dB super-mode suppression ratio can be generated.

W4A.6 • 17:15

LD pumped Q-switched Nd:YAG slab laser with stable output within temperature range of -30 - 50 degrees centigrade, Wei Xie^{1,2}, Xiao Chen^{1,2}, Xiuhua Ma¹, Xiaolei Zhu¹, Zhengyang Jiang^{1,2}, Junxuan Zhang¹, Shiguang Li¹, Weibiao Chen¹; ¹Shanghai Inst. of Optics and Fine Mechanics, Chinese Academy of Sciences, China; ²University of Chinese Academy of Science, China. A temperature insensitive all solid state laser functioning from -30 to 50 degrees centigrade without cooling facility is realized. Maximum output pulse energy about 95mJ is obtained over above temperature range.

W4B • Nonlinear Nanophotonics and Waveguides—Continued

W4B.4 • 17:00

320Gbps physical random bit generation from chaotic optoelectronic oscillator with silicon modulator, Wenjing Tian^{1,2}, Lei Zhang^{1,2}, Jianfeng Ding¹, Xin Fu¹, Lin Yang^{1,2}; ¹State Key Laboratory on Integrated Optoelectronics, Inst. of Semiconductors, Chinese Academy of Sciences, China; ²College of Materials Science and Opto-Electronic Technology, Univ. of Chinese Academy of Sciences, China. We demonstrate a physical random bit generation scheme based on a chaotic optoelectronic oscillator with silicon Mach-Zehnder modulator. The randomness of the 320Gbps sequence after two self-delay XOR operations is verified with NIST statistical tests.

W4B.5 • 17:15

Characterization of Acoustic Phonons in InGaAsP MQW by Asynchronous Optical Sampling, Kenichi Hitachi¹, Mayu Someya^{1,2}, Atsushi Ishizawa¹, Tadashi Nishikawa², Hideki Gotoh¹; ¹NTT Basic Research Laboratories, Japan; ²Tokyo Denki Univ., Japan. We measured transient reflectivity in an InGaAsP multi-quantum well by asynchronous optical sampling with an Er-doped fiber laser. The oscillation in longitudinal acoustic phonons induced by resonant Raman scattering lasts more than 1 ns.

W4C • Infrared and Terahertz Materials and Light Sources for High Performance Applications—Continued

W4C.3 • 17:00

Terahertz Signal Generation Based on a Dual-Mode 1.5 μ m DFB Semiconductor Laser, Song Tang¹, Bin Hou¹, Song Liang², Dejun Chen³, Lianping Hou¹, John Marsh¹; ¹School of Engineering, Univ. of Glasgow, UK; ²School of Optoelectronic Information, Univ. of Electronic Science and Technology of China, China; ³Inst. of Semiconductors, Chinese Academy of Sciences, China. A novel dual-mode DFB semiconductor diode laser has been demonstrated. Using photomixing techniques, a terahertz signal at ~560 GHz has been generated. The THz signal shows power fluctuations related to mode competition in the laser.

W4C.4 • 17:15

Generation of THz Radiation by Sampled Grating DBR Mode Locked Laser Diodes, Lianping Hou¹, Bin Hou¹, Song Liang², Dejun Chen², John Marsh¹; ¹Univ. of Glasgow, UK; ²Univ. of Electronic Science and Technology of China, China; ³Inst. of Semiconductors, Chinese Academy of Sciences, China. 640 GHz THz signals were generated based on 1.55 μ m operating wavelength sampled grating distributed-Bragg-reflector mode locked laser diodes and photomixing techniques which will pave a way to provide compact low-cost, robust THz sources.

W4D • Integrated Nanophotonic Devices—Continued

W4D.4 • 17:00

Experimental demonstration of single Fabry-Perot resonator based optical add-drop filters in silicon, Qingzhong Huang¹, Qiang Liu¹, Jinsong Xia¹; ¹Huazhong Univ. of Sci. and Tech., China. We have demonstrated highly efficient add-drop filters based on a single travelling-wave like Fabry-Perot resonator in silicon. A dropping efficiency of 68% is realized, and only 8% of light is left at the through port.

W4D.5 • 17:15

High Quality Factor Deuterated Silicon Nitride (SiN:D) Microring Resonators, Zeru Wu¹, Zengkai Shao¹, Zihan Xu¹, Yanfeng Zhang¹, Lin Liu¹, Chunchuan Yang¹, Yujie Chen¹, Siyuan Yu^{1,2}; ¹Sun Yat-sen Univ., China; ²Univ. of Bristol, UK. We demonstrate low-loss deuterated SiN microring resonators fabricated by low-temperature plasma-deposition technique with a high intrinsic quality factor of up to 1.2×10^8 at 1547.6 nm, and $>0.8 \times 10^8$ throughout 1500 - 1600 nm.

W4E • Fiber Devices I—Continued

W4E.3 • 17:00

Diameter Measurement of Optical Nanofibers by Using a Commercial and Standardized Ruled Grating, Ming Zhu¹, Yaoting Wang¹, Yizhi Sun¹, Wei Ding¹; ¹CAS Inst. of Physics, China. A precise and in-situ measurement of diameter of optical nanofibers (ONFs) is presented. Mounting a commercial micron-scale-period ruled grating on ONF forms a high-order Bragg reflector, making possible convenient diagnosis of the ONF diameter.

W4E.4 • 17:15

Design of an Elliptical-Core Few-Mode Fiber for Mode-Independent Wavelength Conversion, Joseph C. Slim¹, Mathilde Gay¹, Christophe Peucheret¹; ¹Institut Foton, France. An elliptical-core graded-index fiber that allows simultaneous intramodal wavelength conversion of mode-multiplexed signals is proposed. The fiber breaks the degeneracy between the LP_{11a} and LP_{11b} modes and prevents detrimental intermodal processes.

W4F • Dual-comb Spectroscopy and its Applications—Continued

W4F.4 • 17:00

Dual-comb spectroscopy using a hybrid mode-locked fiber laser, Ting Li¹, Xin Zhao¹, Zijun Yao¹, Yuehan Wu¹, Jie Chen¹, Zheng Zheng^{1,2}; ¹School of Electronic and Information Engineering, Beihang Univ., China; ²Beijing Advanced Innovation Center for Big Data-based Precision Medicine, China. Dual-comb absorption spectroscopy is realized by using a dispersion-managed, hybrid mode-locked fiber laser, which emits two pulse trains with different bandwidths due to hybrid pulse formation mechanisms.

W4F.5 • 17:15

Dual-comb based Angle Measurement Method Using a Grating and a Corner Cube Combined sensor, Siyu Zhou¹, Zebin Zhu¹, Shilin Xiong¹, Kai Ni², Qian Zhou², Guanhao Wu^{1,2}; ¹State Key Laboratory of Precision Measurement Technology and Instruments, Dept. of Precision Instrument, Tsinghua Univ., Beijing 100084, China, China; ²Division of Advanced Manufacturing, Graduate School at Shenzhen, Tsinghua Univ., Shenzhen 518055, China, China. We present an angle measurement method of dual-comb interferometry which uses a grating and a corner cube combined sensor. The precision is better than 10 arc-seconds within 3000 arc-seconds and 30 arc-seconds within 7800 arc-seconds.

These concurrent sessions are grouped across two pages. Please review both pages for complete session information.

W4G • Holographic Technologies—Continued

W4G.2 • 17:00 **Invited**
Polarization Holography and its Application to Optical Data Storage, Toyohiko Yatagai¹; ¹Utsunomiya Univ., Japan. To increase data capacity for holographic mass-data storage, some techniques are presented, including dual-channel polarization lography and angular multiplication techniques. Theoretical and experimental results are described.

W4H • Integrated Photonics—Continued

W4H.4 • 17:00
Valley-controlled light flow in a photonic crystal waveguide, Xiaodong Chen¹, Fulong Shi¹, Weimin Deng¹, Jianwen Dong¹; ¹Sun Yat-Sen Univ., China. With the valley degree of freedom, we demonstrate the unidirectional propagation of bulk states and topological transport of edge states in a photonic crystal waveguide.

W4H.5 • 17:15
Demonstration of CdTe microwires as mid-infrared optical waveguides, Chenguang Xin¹, Xin Guo¹, Limin Tong¹; ¹Zhejiang Univ., China. CdTe microwires (MWs) with diameters of several micrometers were fabricated. Excellent MIR optical waveguiding properties were obtained experimentally with waveguiding losses of several dB/cm, which demonstrated these MWs as promising waveguides for MIR microphotronics.

W4I • Optical Signal Characterization—Continued

W4I.4 • 17:00
A Frequency-domain Kalman Scheme for Large PMD and Ultra-fast RSOP in PDM-QPSK System, Zibo Zheng¹, Nan Cui¹, Lixia Xi¹, Xiaoguang Zhang¹, Wenbo Zhang¹, Yuanyuan Fang², Liangchuan Li²; ¹Beijing Univ of Posts & Telecom, China; ²Network Research Dept., Huawei Technologies Co., Ltd., China. With reasonable simplified polarization modelling for fiber channel, we propose a window-split frequency domain Kalman scheme to equalize the signal distortion induced by combined large DGD (more than 200ps) and fast RSOP (up to 2Mrad/s).

W4I.5 • 17:15
Time Domain Measurement of MPI caused by Double Rayleigh Scattering in Distributed Raman Amplifiers, Toshihiko Sugie¹, Hiroji Masuda², Kazuo Aida³; ¹NTT Electronics Corporation, Japan; ²Shimane Univ., Japan; ³Ex-Professor of Shizuoka University, Japan. An MPI-based time-domain method for evaluating DRS in transmission fiber with distributed Raman amplifiers is proposed; it combines self-heterodyne detection and OSW. We characterize the MPI with/without distributed Raman amplifiers at 1.5 μ m.

W4J • Integrated Devices for Communications—Continued

W4J.4 • 17:00
Front-rear LI linearity correlation of uncooled (-40 to +90°C) InGaAlAs DML for robust tracking error in 10G-EPON ONU, Jack Jia-Sheng Huang^{1,2}; ¹Optoelectronics R&D, Source Photonics, USA; ²Optoelectronics R&D, Source Photonics Taiwan, Taiwan. Uncooled directly modulated lasers are key components for optical transmission in 10G-EPON. In this paper, we study the front to rear LI characteristics of DML and demonstrate robust tracking error performance over a wide temperature range (-40 to +90°C). Design factors for optimal uncooled tracking error are discussed.

W4J.5 • 17:15
16x16 AWG Router Based on Silicon Oxynitride Waveguide Platform, Shuxin Wang¹, Tingting Lang², Yue Wu¹, Jian-Jun He¹; ¹Zhejiang Univ., China; ²China Jiliang Univ., China. We experimentally demonstrate a 16x16, 200 GHz cyclic AWG router using silicon oxynitride waveguides. Insertion losses vary from -1.34 dB to -5.27 dB and crosstalks vary from -19 dB to -20.5 dB for all channels.

W4K • Biophotonics and Applications V—Continued

W4K.3 • 17:00
Live Visualization of Granule Release from Cells with Simultaneous Cellular Observation by Laser Speckle, Munenori Yamamura¹, Saki Tsukijima¹, Keisuke Ohta², Yasuyuki Hirakawa¹, Kei-ichiro Nakamura²; ¹NIT, Kurume College, Japan; ²School of Medicine, Kurume Univ., Japan. Live monitoring of granule release from living cells was performed when the cells were observed by a laser speckle microscope estimating the LS fluctuation.

W4K.4 • 17:15
Label-free Diagnosis of Cervical Cancer based on Ultrahigh Resolution Optical Coherence Microscopy and Machine Learning, Xianxu Zeng², Xiaolan Zhang², Tao Xu³, Canyu Li², Xiaofang Wang², Jason Jerwick¹, Yuan Ning¹, Yihong Wang⁴, Linlin Zhang², Zhan Zhang², Yutao Ma³, Chao Zhou¹; ¹Lehigh Univ., USA; ²The Third Affiliated Hospital of Zhengzhou Univ., China; ³Wuhan Univ., China; ⁴Warren Alpert Medical School of Brown Univ., USA. Current tools for cervical cancer screening cannot provide real-time results or localize suspicious regions. Label-free optical coherence microscopy combined with a machine learning algorithm shows great potential to provide real-time diagnosis of human cervical diseases.

W4L • Fiber Devices & Sensing II—Continued

W4L.3 • 17:00
Temperature Sensor by Using Highly Germanium-doped Fiber, Lifeng Bao^{1,2}, Xinyong Dong¹, Perry P. Shum², Changyu Shen¹; ¹China Jiliang Univ., China; ²Nanyang Technological Univ., Singapore. We demonstrate a temperature sensor by splicing a short highly germanium-doped fiber to a single mode fiber with a bowknot-type taper. The sensor possesses miniature size of 1.4 mm and high sensitivity of 100 pm/°C.

W4L.4 • 17:15
Ultrahigh sensitivity low-cost optical fiber temperature sensors, Yi Liu¹, Xin Cheng¹, Changyuan Yu¹, Hwa-yaw Tam¹; ¹The Hong Kong Polytechnic Univ., Hong Kong. A high sensitivity, low-cost optical fiber temperature sensor is proposed. Its sensitivity and resolution are 11.66nm/°C and 8.3x10⁻³ °C over the interval of 28-41°C. It is larger 1000 times than that of FBG sensors.

Room S223

Room S224

Room S225

Room S226

Room S227

Room S228

These concurrent sessions are grouped across two pages. Please review both pages for complete session information.

W4A • Advanced Light Sources II—Continued

W4A.7 • 17:30

Simulation Model of Multiple Oxide-Aperture VCSEL, Shun-Chieh Hsu¹, Yu-Ming Huang¹, Yu-Yun Cho¹, Chun-Yen Peng², Chao-Hsin Wu², Gong-Ru Lin², Hao-Chung Kuo¹, Chien-Chung Lin¹; ¹National Chiao Tung University, Taiwan; ²National Taiwan Univ., Taiwan. An oxide VCSEL model was built based on measured results. We then design a new multiple oxide-apertured VCSEL based on this model. The simulation result shows that the bandwidth can be improved and reaches 24GHz.

W4A.8 • 17:45

Anomalous Spectral Broadening in High Quality-Factor, 1-GHz Mode-locked Oscillator using Yb:CALGO crystal, Shota Kimura¹, Takuma Nakamura¹, Shuntaro Tani¹, Yohei Kobayashi¹; ¹The Inst. for Solid State Physics, The Univ. of Tokyo, Japan. An Yb:CALGO Kerr-lens mode-locked oscillator at 1-GHz repetition rate was developed. We found an anomalous spectral broadening at a high pumping-power condition, which lead to a pulse duration of 22 fs.

W4B • Nonlinear Nanophotonics and Waveguides—Continued

W4B.6 • 17:30

Kilohertz PPLN Optical Parametric Oscillator with Intracavity Difference-Frequency Generation in OPGaAs, Andrey Boyko^{1,2}, Dmitry Kolker², Li Wang¹, Peter Schunemann³, Nadezhda Kostyukova^{2,4}, Shekhar Guha⁵, Vladimir Panyutin¹, Georgi Marchev¹, Andre Schirrmacher⁴, Valentin Petrov¹; ¹Max Born Inst., Germany; ²Novosibirsk State Univ., Russia; ³BAE Systems, USA; ⁴Special Technologies, Russia; ⁵Air Force Research Laboratory, USA; ⁶Canlas Laser Processing, Germany. Intracavity difference-frequency generation (DFG) in orientation-patterned GaAs (OPGaAs) produces an average power of 24 mW at 6.74 μ m using a Nd:YAG laser pumped Mg-doped periodically-poled LiNbO₃ (Mg:PPLN) nanosecond optical parametric oscillator (OPO) at 1.5 kHz.

W4B.7 • 17:45

Mid-infrared difference frequency generation of Er and Yb fiber lasers radiation in periodically poled crystals, Igor Larionov^{1,2}, Alexander Gulyashko², Valentin Tyrtshynny²; ¹Dept. of Physical and Quantum Electronics, Moscow Inst. of Physics and Technology, Russia; ²NTO «IRE-Polus», Russia. The parametric generation of mid-infrared radiation in the periodically poled lithium niobate and lithium tantalate nonlinear-optical crystals was investigated. Up to 10 W of output radiation near 3 μ m wavelength was obtained with 20% efficiency

W4C • Infrared and Terahertz Materials and Light Sources for High Performance Applications—Continued

W4C.5 • 17:30

Widely tunable (2-6THz) Terahertz vortex source, Katsuhiko Miyamoto^{1,2}, Kazuki Sano¹, Tomohito Yamaski¹, Takahiro Miyakawa¹, Takashige Omatsu^{1,2}; ¹Chiba Univ., Japan; ²Molecular chirality research center, Chiba Univ., Japan. We have developed a widely tunable terahertz (THz) vortex source with an average power of ~3 μ W and a frequency tuning range of 2-6 THz. The handedness of the THz vortex output in this system is also controlled.

W4C.6 • 17:45

Enhancement of Nonlinearity by Terahertz Vortex Beam, Bong Joo Kang¹, Katsuhiko Miyamoto², Won Tae Kim¹, Kwang Jun Ahn³, Takashige Omatsu², Fabian Rotermund¹; ¹KAIST, Korea; ²Chiba Univ., Japan; ³Ajou Univ., Korea. High-power THz vortex beam was generated based on optical rectification in nonlinear crystal and mode conversion by employing spiral phase plate. Subsequent application of vortex beam for nonlinear spectroscopy in graphene shows enhanced nonlinear characteristics.

W4D • Integrated Nanophotonic Devices—Continued

W4D.6 • 17:30 Invited

Miniature Silicon Nanobeam Resonator Tuned by GST Phase Change Material, Linjie Zhou¹, Hanyu Zhang¹, Hao Hu¹, Liangjun Lu¹, Jianping Chen¹, Aziz, B. M. Rahman²; ¹Shanghai Jiao Tong Univ., China; ²City, Univ. of London, UK. We report a silicon optical nanobeam resonator with central hole infiltrated with a thin layer of Ge₂Sb₂Te₃ (GST) material. The resonances can be tuned when the GST changes its phases between the amorphous and crystalline states.

W4E • Fiber Devices I—Continued

W4E.5 • 17:30

Optimization Design of Fiber Optical Parametric Amplifier with Multi-Stage High Nonlinear Fiber, Kai Wang¹, Rahat Ullah¹, Yiyang Wang², Lei Shu³, Jianzhao Yin⁵; ¹State Key Laboratory of Information Photonics and Optical Communications, Beijing Univ Posts & Telecommunications, China; ²School of Information and Communication, Guilin Univ. of Electronic Technology, China; ³School of Astronautics, Harbin Inst. of Technology, China; ⁴Inst. of Optoelectronics, Nanjing Univ. of Information Science & Technology, China; ⁵State Grid Rushan Power Supply Company, China. We propose one optimization algorithm of longitudinal zero dispersion wavelength management. Optimized high nonlinear fiber enables a single pump fiber optical parametric amplifier with a gain of 20 \pm 1.6 dB over 35 nm bandwidth.

W4E.6 • 17:45

Resonant State Expansion in Fiber Geometries, Swaathi H. Upendar¹, Izzatjon Allayarov¹, Guangrui Li², Markus Schmidt^{2,3}, Thomas Weiss¹; ¹4th Physics Inst., Univ. of Stuttgart, Germany; ²Leibniz Inst. of Photonic Technology e.V., Germany; ³Otto Schott Inst. of Material Research, Friedrich Schiller Univ., Germany. We extend the resonant state expansion to guiding geometries such as step-index and photonic crystal fibers. By correctly normalizing all modes, this approach allows for predicting the guiding properties in perturbed and disordered fibers.

W4F • Dual-comb Spectroscopy and its Applications—Continued

W4F.6 • 17:30

Frequency Domain 2D Incoherent Comb Interferometry for Single-shot Tomographic Imaging, Futoshi Kokubun¹, Tatsutoshi Shioda¹; ¹Saitama Univ., Japan. Frequency-domain VIPA installed comb interferometry has been developed for 2D single-shot tomography. An etalon co-installed with VIPA to generate 2.2 THz incoherent comb brings multiple and periodic higher-order interference fringes, which expands the measurement range.

W4F.7 • 17:45

Spatially scanning dual-comb spectroscopy for precise measurement of refractive index and thickness profiles of solids, Yue Wang^{1,2}, Akifumi Asahara^{1,2}, Ken-ichi Kondo^{1,2}, Kaoru Minoshima^{1,2}; ¹Univ. of Electro-Communications, Japan; ²Japan Science and Technology Agency (JST), ERATO MINOSHIMA Intelligent Optical Synthesizer (IOS) Project, Japan. Raster-scanning dual-comb spectroscopy is used to simultaneously evaluate the refractive index and thickness profiles of solid samples. Refractive index and step structure profiles of glass plates are evaluated successfully with 10⁻⁴ uncertainty.

18:00–22:00 Conference Reception and Banquet, Convention Hall

These concurrent sessions are grouped across two pages. Please review both pages for complete session information.

W4G • Holographic Technologies—Continued

W4G.3 • 17:30

Incoherent Digital Holography Adaptive Imaging by Phase Diversity, Yuhong Wan¹, hongqiang Zhou¹, Tianlong Man¹; ¹Beijing Univ. of Technology, China. We developed an adaptive imaging technique by Fresnel incoherent digital holography combined with phase diversity (PD-FINCH). The experimental results demonstrated the improvement of reconstructed image quality after adaptive wavefront aberration compensation.

W4G.4 • 17:45

Applying the principle of orthogonality of high dimensional random vectors to obtain high-density, large-volume 3D holographic display, Ghaith Makey¹, Özgün Yavuz¹, Denizhan K. Kesim¹, Ahmet Turali¹, Parviz Elahi¹, Johnny Toumi², Moustafa Sayem El-Daher², Serim Ilday¹, Onur Tokel¹, F. Ömer Ilday¹; ¹Bilkent Univ., Turkey; ²Damascus Univ., Syrian Arab Republic. The efforts toward truly 3D displays are far from exploiting the full potential of holography. Here, we apply the principle of orthogonality of high dimensional random vectors to obtain unprecedented dense, large volume holograms.

W4H • Integrated Photonics—Continued

W4H.6 • 17:30

Transient Analysis of Photonic-Crystal Surface-Emitting Lasers via Time-Dependent 3D Coupled-Wave Theory, Takuya Inoue¹, Ryohei Morita¹, Masahiro Yoshida¹, Menaka D. Zoysa¹, Yoshinori Tanaka¹, Susumu Noda¹; ¹Kyoto Univ., Japan. We develop time-dependent three-dimensional coupled-wave theory for photonic-crystal surface-emitting lasers (PCSELS), which enables comprehensive analyses of lasing characteristics of high-power PCSELS under high current injection including relaxation oscillation, spatial hole-burning, and lasing spectra.

W4H.7 • 17:45

Resistive Switching and Electrochromic Characteristics of DNA Biopolymer Devices, Li Yang¹, Yu-Chueh Hung¹; ¹Inst. of Photonics Technologies, National Tsing Hua Univ., Taiwan. We present both resistive switching and electrochromic characteristics of a transparent DNA biopolymer-based device. The device exhibits an on/off ratio of ~100 at 0.4V and more than 20% change in transmittance under applied voltages.

W4I • Optical Signal Characterization—Continued

W4I.6 • 17:30

Maximum-Likelihood Mth Power Carrier Phase Estimation for Coherent Optical Communication, Yan Li^{1,2}, Ming-Wei Wu³, Xin-Wei Du¹, Gurusamy Mohan¹, Changyuan Yu⁴, Pooi-Yuen Kam^{1,2}; ¹National Univ. of Singapore, Singapore; ²National Univ. of Singapore (Suzhou) Research Inst., China; ³School of Information and Electronic Engineering, Zhejiang Univ. of Science and Technology, China; ⁴Dept. of Electronic and Information Engineering, The Hong Kong Polytechnic Univ., Hong Kong. We propose a maximum-likelihood (ML) Mth power carrier phase estimator which is optimized considering the amplitude of received signal. Significant improvement can be achieved compared to conventional Mth power which relies on intuitive nonlinear operations.

W4I.7 • 17:45

Novel FM-Noise Spectrum Measurement Based on Three-Wave Interference, Shuhei Yamaoka¹, Yojiro Mori¹, Hiroshi Hasegawa¹, Ken-ichi Sato¹; ¹Nagoya Univ., Japan. This paper proposes a novel FM-noise spectrum measurement scheme for future ultra-dense digital coherent systems that is based on three-wave interference and DSP. The effectiveness of the proposed scheme is confirmed through simulations and experiments.

W4J • Integrated Devices for Communications—Continued

W4J.6 • 17:30

Integrated optoelectronic transceiving chips, Kai Liu¹, Yongqing Huang¹, Xiaofeng Duan¹, Qi Wang¹, Qi Wei¹, Xiaomin Ren¹, Shiwei Cai¹; ¹Beijing Univ. of Posts and Telecomm., China. A pair of integrated optoelectronic chips is proposed for short WDM transceiver. One is emitting at 848.1nm and receiving at 805.3nm, while the other is emitting at 805.3nm and receiving at 848.1nm.

W4J.7 • 17:45

Proposal of Integrated-Optical Circuit for Recognition of 8PSK-Coded Label for Photonic Label Router, Nyam-Erdene Ocbayar¹, Munkhbayar Adiya¹, Hiroki Kishikawa¹, Nobuo Goto¹; ¹Tokushima Univ., Japan. Label recognition is a key function in photonic label routing. We propose an 8-ary PSK (8PSK) recognition circuit based on a basic waveguide-type circuit for recognition of optical label encoded in quadrature-PSK format.

W4K • Biophotonics and Applications V—Continued

W4K.5 • 17:30

Fiber-optic Activity Monitoring With Machine Learning, Qihang Zeng^{1,2}, Wei Xu³, Changyuan Yu^{2,4}, Na Zhang³, Cheungchuen Yu²; ¹School of Electronic Engineering, Xidian Univ., China; ²Centre of Advanced Microelectronic Devices, National Univ. of Singapore (Suzhou) Research Inst., China; ³Anlight Optoelectronic Technology Inc., China; ⁴Dept. of Electronic and Information Engineering, The Hong Kong Polytechnic Univ., Hong Kong. Unobtrusive activity monitoring based on fiber-optic Mach-Zehnder interferometer is proposed, employing deep bi-directional long short-term memory network, realizing three activities recognition with accuracy of 99.2% and resolution of 0.5s.

W4K.6 • 17:45

Autofluorescence Spectroscopy for Cell Monitoring, Derrick Yong¹, Ahmad Amirul Abdul Rahim², Jesslyn Ong², May Win Naing²; ¹Precision Measurements Group, Singapore Inst. of Mfg Tech, Singapore; ²Bio-Manufacturing Programme, Singapore Inst. of Mfg Tech, Singapore. We used autofluorescence spectroscopy to determine the metabolic activity of cells. Results show noticeable differences in activity at different cell confluencies. The non-contact and non-destructive nature of the method makes it suitable for cell monitoring.

W4L • Fiber Devices & Sensing II—Continued

W4L.5 • 17:30

Application of Fibre-optical Mechanical & Thermal Multi-parameter Instrument in hydraulic structure, Chao Wang^{1,2}, Kun Liu^{1,2}, Junfeng Jiang^{1,2}, Shuang Wang^{1,2}, Xuezhi Zhang^{1,2}, Yuanyao Li³, Xiaojun Fan^{1,2}, Xin Li^{1,2}, Rundong Wang^{1,2}, Mengdi Li^{1,2}, Yi Huang^{1,2}, Yong Du^{1,2}, Tiegeng Liu^{1,2}; ¹School of Precision Instrument and Opto-Electronics Engineering, Tianjin Univ., China; ²Key Laboratory of Opto-electronics Information Technology (Tianjin Univ.), China; ³Tianjin Inst. of Metrological Supervision Testing, China. Fibre-optical Mechanical & Thermal Multi-parameter Instrument is based on the principle of discrete optical fiber sensing. In this research it is applied to monitor underflow of hydraulic structure model. The result indicates that the velocity and turbulent frequency can be detected by the instrument.

W4L.6 • 17:45

High-birefringence two-core fiber vector bending sensor, Chang-He Cheng¹, Zhengyong Liu², Chuang Wu¹, Li-Peng Sun¹, Jie Li¹, Bai-Ou Guan¹, hwa-yaw Tam²; ¹Jinan Univ., China; ²Hong Kong Polytechnic University, Hong Kong. We propose and demonstrate a simple vector bending sensor based on polarization dependent supermodes interference in a high birefringence two-core photonic crystal fiber. The bending responses of both two polarizations depend on the bending direction.

18:00–22:00 Conference Reception and Banquet, Convention Hall

These concurrent sessions are grouped across two pages. Please review both pages for complete session information.

08:00–18:00 Registration, S221 Foyer of HKCEC

08:30–10:00

Th1A • Novel Laser Sources I

Presider: Zhichao Luo; South China Normal Univ., China

Th1A.1 • 08:30 **Invited**

Practical Tabletop-Scale Femtosecond X-Ray Laser Light Sources for Science and Technology, Henry C. Kapteyn^{1,2}, Margaret M. Murnane^{2,1}; ¹Kapteyn-Murnane Laboratories Inc., USA; ²JILA and Dept. of Physics, Univ. of Colorado, USA. Recent advances in ultrafast solid-state and fiber lasers make possible robust and practical tabletop-scale light sources in the vacuum-ultraviolet, extreme-ultraviolet, and soft x-ray spectral regions. These sources are being applied for a wide variety of applications.

08:30–10:00

Th1B • Nonlinear Spectroscopy and Imaging

Presider: Xinhuan Feng; Jinan Univ., China

Th1B.1 • 08:30 **Invited**

Nonlinear 3D Photonic Structures by Femtosecond Laser Lithography, Cornelia Denz¹, Joerg Imbrock¹, Mousa Ayoub¹, Haissam Hanafi¹; ¹Westfaelische Wilhelms Univ Munster, Germany. We explore a novel ferroelectric domain engineering approach based on infrared femtosecond laser lithography and thermal control. Various nonlinear photonic structures are created without any external electric field in the volume of lithium niobate.

08:30–10:00

Th1C • Frequency Control and Measurement for Optical Metrology

Presider: Bowen Li; Univ. of Hong Kong, Hong Kong

Th1C.1 • 08:30 **Invited**

Self-action Mitigation for High Repetition Rate Ultrashort Pulses Using Fractional Temporal Self-imaging, Mohamed Seghilani¹, Reza Maram¹, Luis Romero Cortes¹, Jose . Azana¹; ¹INRS-Energie Materiaux et Telecom, Canada. We review recent work on mitigation of nonlinear propagation impairments of optical pulses through reversible pulse division using fractional temporal self-imaging, overcoming limitations of previous methods for application at high repetition rates (> GHz).

08:30–10:00

Th1D • Quantum Information Processing II

Presider: Guofeng Zhang; The Hong Kong Polytechnic Univ., Hong Kong

Th1D.1 • 08:30 **Invited**

Time-domain Multiplexed Measurement-based Quantum Computing for Large-scale Optical Quantum Computing, Akira Furusawa¹; ¹Univ. of Tokyo, Japan. I will explain the methodology of time-domain multiplexing measurement-based quantum computing. With this methodology the size of the quantum computer is independent of the number of qubits for quantum computing, which means it has real scalability.

08:30–10:00

Th1E • Fiber Devices II

Presider: Peter Dragic; Univ of Illinois at Urbana-Champaign, USA

Th1E.1 • 08:30 **Invited**

Fibers with Liquid Cores: A New Way to Control Supercontinuum Generation and Soliton Dynamics, Markus Schmidt¹, Kay Schaarschmidt¹, Ramona Scheibinger¹, Mario Chemnitz¹; ¹Leibniz Inst. of Photonic Technology, Germany. Liquid core fibers offer unique features such as hybrid nonlinear responses, wide transmission windows and real-time tuning capabilities. Here I will report on hybrid temporal solitons, coherent supercontinuum generation and real-time dispersive wave tuning.

08:30–10:00

Th1F • Metamaterials and Meta-devices

Presider: Xifeng Ren; Key laboratory of quantum information, China

Th1F.1 • 08:30 **Invited**

Experimental Realization of Unidirectional Zero Reflection from Bianisotropic Microwave to Elastic Metamaterials, Jensen Li¹; ¹Dept. of Physics, Hong Kong Univ. of Science and Technology, Hong Kong. We introduce the concept of passive Parity-time symmetry to bianisotropic metamaterials, which can possess exceptional points. We experimentally demonstrate the associated unidirectional zero reflection in both microwave and elastic metamaterials.

These concurrent sessions are grouped across two pages. Please review both pages for complete session information.

08:00–18:00 Registration, S221 Foyer of HKCEC

08:30–10:00

Th1G • 2D Nonlinear Materials
Presider: Han Zhang, Shenzhen Univ., China

Th1G.1 • 08:30 **Invited**

2D Nonlinear Optical Materials, Jun Wang¹; ¹Shanghai Inst of Optics and Fine Mech, China. The saturation of two-photon absorption (TPA) in four types of layered transition metal dichalcogenides (TMDCs) (MoS₂, WS₂, MoSe₂, WSe₂) was systemically studied both experimentally and theoretically.

08:30–10:00

Th1H • Nanostructures for Optoelectronic Applications
Presider: Xuming Zhang; The Hong Kong Polytechnic Univ., Hong Kong

Th1H.1 • 08:30

Tunable Amplified Spontaneous Emission and Lasing from All-inorganic Perovskite Nanocube, Zhengzheng Liu¹, Zhiping Hu², Tongchao Shi¹, Zeyu Zhang¹, Xin Xing¹, Xiaosheng Tang², Juan Du¹, Yuxin Leng¹; ¹Shanghai Inst of Optics and Fine Mech, China; ²Chongqing Univ., China. We report high-quality and low-threshold lasing, enhanced stability, and excellent wavelength tunability from a facile solution-processed sub-wavelength size of cesium lead halide perovskite CsPbX₃ (X= I/Br/Cl) nanocubes under both one- and two-photon excitation

Th1H.2 • 08:45

High-Q Nanocavity-Based Raman Laser Fabricated on a (100) SOI Substrate with a 45-Degree-Rotated Top Silicon Layer, Yukiko Yamauchi¹, Makoto Okano², Susumu Noda³, Yasushi Takahashi¹; ¹Osaka prefecture Univ., Japan; ²National Inst. of Advanced Industrial Science and Technology, Japan; ³Kyoto Univ., Japan. We report a low-threshold Raman laser based on nanocavities fabricated on an improved (100) SOI substrate with a 45-degree-rotated top silicon layer. We consider that this SOI substrate enables mass production of silicon Raman lasers.

08:30–10:00

Th1I • Probabilistic Signal Shaping
Presider: Fan Zhang; Peking Univ. China

Th1I.1 • 08:30

Simultaneous RSOP and Carrier Phase Noise Equalization for Probabilistic Shaping QAM Signals Based on Extended Kalman Filter, Nannan Zhang¹, Qisong Shang¹, Zibo Zheng¹, Nan Cui¹, Wenbo Zhang¹, Hengying Xu¹, Xianfeng Tang¹, Lixia Xi¹, Xiaoguang Zhang¹; ¹Beijing Univ of Posts & Telecom, China. We propose a joint equalization method for rotation station of polarization (RSOP) and carrier phase noise (CPN) utilizing EKF for probabilistic shaping QAM(PS-QAM). The influences of RSOP and CPN are analyzed by numerical simulation.

Th1I.2 • 08:45

A Flexible Overhead Probabilistic Shaping Scheme for QC-LDPC Coded PM-64QAM Optical System, Shanyong Sun¹, LiQian Wang¹, Dongdong Wang¹, Xue Chen¹, Qijia Xu¹; ¹Beijing Univ. of Posts and Telecommunications, China. We propose a flexible overhead probabilistic shaping QC-LDPC coded modulation scheme, which is easy to implement and it can all exceed the traditional QC-LDPC coded modulation scheme in the case of 16.7%, 8.3% and 5.5% overhead.

08:30–10:00

Th1J • Silicon Photonics Devices
Presider: Liang Wang; Univ. of Sci and Tech of China, China

Th1J.1 • 08:30 **Tutorial**

Monolithically Integrated 3D Silicon Photonics, Joyce K. Poon¹; ¹Electrical and Computer Engineering, Univ. of Toronto, Canada. I will review multilayer silicon nitride-on-silicon (SiN-on-Si) photonic platforms that incorporate several SiN waveguide layers on top of an active Si waveguide layer. These 3D photonic platforms enable very large-scale photonic circuits.

08:30–10:00

Th1K • Display Technologies
Presider: Toyohiko Yatagai; Utsunomiya Univ., Japan

Th1K.1 • 08:30 **Invited**

Volumetric Bubble Display, Yoshio Hayasaki¹, Kota Kumagai¹; ¹Utsunomiya Univ., Japan. Volumetric bubble display using high viscosity liquid is presented. The bubbles are produced by the holographic parallel femtosecond laser pulse excitations.

08:30–10:00

Th1L • Waveguides and Sensors
Presider: Songnian Fu; Huazhong Univ of Science & Technology, China

Th1L.1 • 08:30

Resonant tunneling diode photodetectors for mid-infrared gas-sensing based on GaSb substrate, Florian Rothmayr¹, Andreas Pfenning², Caroline Kistner¹, Johannes Koeth¹, Georg Knebl², Anne Schade², Sebastian Krueger², Lukas Worschech², Fabian Hartmann², Sven Höfling^{2,3}; ¹nanoplus Nanosystems and Technologies GmbH, Germany; ²Physikalisches Institut and Röntgen Center for Complex Material Systems (RCCM), Universität Würzburg, Germany; ³SUPA, School of Physics and Astronomy, Univ. of St. Andrews, UK. We fabricated resonant tunneling diode photodetectors with a GaInAsSb absorption layer and a GaAsSb/AlAsSb double barrier. The detector cut-off wavelength is 3.5 μ m and reaches a peak sensitivity of 0.85 A/W at 2004 nm.

Th1L.2 • 08:45

All-Optical Ammonia Gas Sensor Using Silicon Microring Resonator Covered with Graphene, Masayasu Sato¹, Hiroki Kishikawa¹, Nobuo Goto¹, Shin-ichiro Yanagiya¹, Shien-Kuei Liaw²; ¹Tokushima Univ., Japan; ²National Taiwan Univ. of Science and Technology, Taiwan. All-optical gas sensor consisting of graphene covered silicon microring resonator is proposed. Ammonia gas increases the Fermi level of graphene. The gas concentration can be detected by the resonant-wavelength shift by microring resonator.

These concurrent sessions are grouped across two pages. Please review both pages for complete session information.

Th1A • Novel Laser Sources —Continued

Th1A.2 • 09:00

Miniaturized Mid-infrared All-fiber Laser at 2.9 μm , Weiwei Li¹, Tuanjie Du¹, Kaijie Wang¹, Hongjian Wang¹, Zhengqian Luo¹; ¹Xiamen Univ., China. We report the first demonstration of a miniaturized mid-infrared all-fiber laser operating at 2.9 μm . The linear laser cavity consists of a 55 cm Ho³⁺:ZBLAN fiber, a 1154 nm Raman fiber laser as pump source, and a fiber end-faced mirror. Stable lasing at 2865 nm was achieved with the maximum output power of 67 mW and a slope efficiency of ~48.9%.

Th1A.3 • 09:15

Harmonic mode-locking generation from a Cr:ZnSe laser synchronously pumped by a picosecond thulium doped fiber laser, Xiangbao Bu¹, Fangzhou Tan¹, Ying Liu¹, Shuxian Qi¹, Pu Wang¹; ¹Beijing Univ. of Technology, China. We report 209 MHz harmonic mode-locking of a 2420 nm Cr:ZnSe laser synchronously pumped by a 1935 nm, 104.5 MHz, 112 ps thulium doped fiber laser. Self-starting behavior was investigated by a chopper wheel.

Th1B • Nonlinear Spectroscopy and Imaging—Continued

Th1B.2 • 09:00

Coherent Raman Microspectroscopy for Non-Contact and Non-Destructive Measurements of Carrier Concentrations in Wide-Bandgap Semiconductors, Yu Okano¹, Ken Goto^{3,2}, Akito Kuramata^{3,2}, Shigenobu Yamakoshi^{3,2}, Hisashi Murakami^{5,4}, Bo Monemar^{4,6}, Yuki Obara¹, Yoshinao Kumagai^{5,6}, Kazuhiko Misawa^{1,4}; ¹Applied Physics, Tokyo Univ. of Agriculture and Tech, Japan; ²Tamura Corporation, Japan; ³Novel Crystal Technology, Japan; ⁴Inst. of Global Innovation Reserach, Tokyo Univ. of Agriculture and Technology, Japan; ⁵Applied Chemistry, Tokyo Univ. of Agriculture and Technology, Japan; ⁶Physics, Chemistry and Biology (IFM), Linkoping Univ., Sweden. We developed a coherent Raman microspectroscopy that realizes a three-dimensional visualization of the spatial distribution of optical phonon modes in wide-bandgap semiconductors. This microspectroscopy will be a powerful tool for measuring the carrier concentration in semiconductors.

Th1B.3 • 09:15

Single-shot Ultrafast Burst Imaging by Spectrally Sweeping Pulse Train with 100-ps Interval, Hirofumi Nemoto¹, Takakazu Suzuki¹, Yuki Yamaguchi¹, Fumihiko Kannari¹; ¹Keio Univ., Japan. We generate a spectrally sweeping 100-ps-interval pulse train for ultrafast burst imaging. Adopting those pulses to sequentially timed all-optical mapping photography utilizing spectral filtering (SF-STAMP), we realize single-shot burst imaging with a sub-nanosecond time window.

Th1C • Frequency Control and Measurement for Optical Metrology—Continued

Th1C.2 • 09:00

Offset Frequency Measurement of a Broad-band Optical Comb Generated in a Waveguide-Type Periodically Poled Lithium Niobate Crystal, Junia Nomura^{1,2}, Kaho Taguchi¹, Yusuke Hisai^{1,2}, Kazumichi Yoshii^{1,2}, Feng-Lei Hong^{1,2}; ¹Dept. of Physics, Yokohama National Univ., Japan; ²JST, ERATO, MINOSHIMA Intelligent Optical Synthesizer Project, Japan. We developed an ultra-broadband frequency comb in a WG-PPLN and measured the offset frequency of the comb by using an iodine-stabilized laser at 532 nm. The visible comb is generated through the $\chi^{(2)}$ process.

Th1C.3 • 09:15

Repetition rate multiplication of fiber-based frequency comb with high side-mode suppression ratio, Yoshiaki Nakajima^{1,2}, Akiko Nishiyama^{1,2}, Takuya Hariki^{1,2}, Kaoru Minoshima^{1,2}; ¹Univ. of Electro-Communications, Japan; ²JST ERATO MINOSHIMA IOS Project, Japan. All-fiber-based mode-filtering has been developed for repetition multiplication of fiber-based frequency comb with multiplication factor of 11. We achieved high side-mode suppression ratio of approximately 40 dB with 536.0-MHz repetition-rate fiber-based mode-filtered comb.

Th1D • Quantum Information Processing II—Continued

Th1D.2 • 09:00

Extending gradient echo memory using machine learning and single photons, Anthony C. Leung^{1,2}, Aaron Tranter^{1,2}, Karun Paul^{1,2}, Jesse Everett^{1,2}, Pierre Vernaz-Gris^{1,2}, Daniel Higginbottom^{1,2}, Geoff Campbell^{1,2}, Ping Koy Lam^{1,2}, Ben Buchler^{1,2}; ¹Centre for Quantum Computation and Communication Technology, Dept. of Quantum Science, The Australian National Univ., Australia; ²Dept. of Quantum Science, The Australian National Univ., Australia. Gradient echo memory is the most efficient quantum memory protocol to date. Recent additions of machine learning and compatible single photons can raise its performance and the possibility of using it as a quantum gate.

Th1D.3 • 09:15

Design of a Multistage Quantum Pulse Gate in the Frequency Domain, Shintaro Niimura¹, Aruto Hosaka¹, Masaya Tomita¹, Akihito Omi¹, Fumihiko Kannari¹; ¹Keio Univ., Japan. We propose a multistage quantum pulse gate which efficiently mix multimode quantum states in the frequency domain. Furthermore we introduce a practicable quantum simulator for calculating Frank Condon factors.

Th1E • Fiber Devices II—Continued

Th1E.2 • 09:00

Converting between CVB and OAM beams, Hongwei Zhang¹, Yange Liu¹, Zhi Wang¹, Ya Han¹, Kang Yang¹; ¹Nankai Univ., China. We have proposed a method to generate cylindrical vector beams (CVBs) based on a mode selective coupler (MSC) and convert it to orbital angular momentum (OAM) beams using a quarter-wave plate (QWP) at wavelength of 1550 nm.

Th1E.3 • 09:15

Ultra-broadband mode converter based on an apodized long-period grating in two-mode fiber, Yunhe Zhao¹, Yunqi Liu¹, Chen Jiang¹, Chengbo Mou¹, Tingyun Wang¹; ¹Shanghai Univ., China. We demonstrate an ultra-broadband LP₀₁-LP₁₁ mode converter based on an apodized long-period grating in two-mode fiber via CO₂-laser inscription. The proposed device provides mode conversion efficiency higher than 90% over a bandwidth of ~180 nm.

Th1F • Metamaterials and Meta-devices—Continued

Th1F.2 • 09:00

Tunable Hyperbolic Metamaterials for Novel Photonic Devices, Marcin R. Kieliszczyk¹, Bartosz Janaszek¹, Anna Tysza-Zawadzka¹, Robert Mroczynski¹, Pawel Szczepanski^{1,2}; ¹Inst. of Microelectronics and Optoelectronics, Warsaw Univ. of Technology, Poland; ²National Inst. of Telecommunications, Poland. Hyperbolic metamaterials (HMMs) are proven suitable for tunable filters, controlled gain/absorption and mode propagation in waveguides, including mode coupling. We present opportunities which HMMs bring to the design of novel passive and active photonic devices.

Th1F.3 • 09:15

Control of mode propagation in tunable hyperbolic metamaterial waveguides, Bartosz Janaszek¹, Marcin R. Kieliszczyk¹, Anna Tysza-Zawadzka¹, Pawel Szczepanski^{1,2}; ¹Inst. of Microelectronics and Optoelectronics, Warsaw Univ. of Technology, Poland; ²National Inst. of Telecommunications, Poland. We demonstrate waveguides based on hyperbolic metamaterials providing means for controlled propagation in near-infrared, including slow light effects and controlled mode propagation, including power flow direction.

These concurrent sessions are grouped across two pages. Please review both pages for complete session information.

Th1G • 2D Nonlinear Materials—Continued

Th1G.2 • 09:00 Invited
2D carbon allotrope with incorporated Au-Ag nanoclusters – laser-induced synthesis and optical characterization, Alina A. Manshina¹, Yuriy Petrov¹, Iliya Kolesnikov¹, Nikolai Mitetelo², Tatiana Murzina², Muhammad Butt³, Martin Neugebauer³, Peter Banzer³, Gerd Leuchs³; ¹*Saint Petersburg State Univ., Russia*; ²*Moscow state Univ., Russia*; ³*Max-Planck Inst. for the Science of Light, Germany*. We discuss the laser-induced fabrication and detailed structural and optical characterization of a novel carbon allotrope intercalated with bimetallic nanoclusters.

Th1H • Nanostructures for Optoelectronic Applications—Continued

Th1H.3 • 09:00
Controlling the lasing and hybrid plasmonic laser actions based on lead halide perovskite nanosheets at the bottom, Qinghai Song¹; ¹*Harbin Inst. of Technology, China*. We report here a simple approach to precisely control the lasing and hybrid plasmonic laser (spaser) actions based on MAPbX₃ perovskite nanosheets by tailoring the substrate.

Th1H.4 • 09:15
Demonstration of Self-pulsating Photonic-Crystal Surface-Emitting Lasers, Ryohei Morita¹, Takuya Inoue¹, Menaka D. Zoysa¹, Kenji Ishizaki¹, Yoshinori Tanaka¹, Susumu Noda¹; ¹*Kyoto Univ., Japan*. We demonstrate self-pulsation with a pulse width of 100 ps and a beam divergence angle of 0.35° in a photonic-crystal surface-emitting laser by introducing a saturable absorber section and employing a new double-hole photonic crystal.

Th1I • Probabilistic Signal Shaping—Continued

Th1I.3 • 09:00
On the optimum decision threshold for probabilistically shaped PAM constellation, Wenjing Zhang², Shaohua Hu², Xingwen Yi^{1,2}, Jing Zhang², Wenjing Zhou², Xiang Gao²; ¹*Sun Yat-sen Univ., China*; ²*Univ. of Electronics and Technology of China, China*. We investigate and derive the optimum decision threshold for probabilistically shaped PAM constellation. Both in simulation and experiment, we verify our analysis and show a lower BER performance compared with the conventional median threshold.

Th1I.4 • 09:15
Probabilistic Shaping QC-LDPC Coded Modulation Scheme for Optical Fiber Systems, Qijia Xu¹, LiQian Wang¹, Dongdong Wang¹, Xue Chen¹, shanyong sun¹; ¹*Beijing Univ of Posts & Telecom, China*. We proposed a probabilistic shaping QC-LDPC coded modulation scheme, which can achieve 0.33dB OSNR improvement at the BER of 10⁻⁵ compared with the traditional QC-LDPC coded modulation scheme with the same total overhead.

Th1J • Silicon Photonics Devices—Continued

Th1K • Display Technologies—Continued

Th1K.2 • 09:00
Laser Splashed Three-dimensional Nanostructures for Crypto-Display, Dejiao Hu¹, Yudong Lu¹, Yaoyu Cao¹, Xiangping Li¹; ¹*Jinan Univ., China*. We report a crypto-display metasurface fabricated by laser splashed 3D nanostructures. Splashing morphologies that scatter angle-sensitive colors are realized through irradiation of a single femtosecond pulse onto titanium film. Angularly-anisotropic color image encryption are demonstrated.

Th1K.3 • 09:15
Optical Crosstalk Reduction in Quantum-Dot-Based Full-Color micro-LED Display by Lithographic-Fabricated Photoresist Mold, Yung-Min Pai¹, chih-hao Lin¹, Huang-Yu Lin¹, Chun-Fu Lee¹, cheng-huan CHEN¹, Hao-Chung Kuo¹; ¹*National Chiao Tung Univ., Taiwan*. The full-color emission RGB quantum dot (QD)-based micro-LED array with reduced optical crosstalk effect by photoresist mold. The crosstalk effect of the well-confined QDs in the window by the fluorescence microscope.

Th1L • Waveguides and Sensors—Continued

Th1L.3 • 09:00
Compact spectrometer based on a multimode silicon waveguide device, Yuhang Wan¹, Yitong Shi¹, Mengxuan Cheng¹, Yu Zhang¹, Zijun Yao¹, Zheng Zheng^{1,2}; ¹*School of Electronic and Information Engineering, Beihang Univ., China*; ²*Beijing Advanced Innovation Center for Big Data-based Precision Medicine, China*. A highly compact spectroscopic measurement scheme is proposed based on a fabricated on-chip silicon device that consists of a multimode interference waveguide containing randomly distributed disturbances with an anomalous wavelength dependent spectral-to-spatial map.

Th1L.4 • 09:15
Temperature-insensitive Waveguide Sensor Based on Vernier-effect, Yang Zhang¹, Jun Zou², Jian-Jun He¹; ¹*Zhejiang Univ., China*; ²*Zhejiang Univ. of Technology, China*. We proposed a temperature-insensitive sensor using cascaded microring resonator and Mach-Zehnder Interferometer (MZI) filter. Temperature sensitivity of the sensor was less than 29 pm/K in a temperature range from 20 °C to 40 °C.

These concurrent sessions are grouped across two pages. Please review both pages for complete session information.

Th1A • Novel Laser Sources I—Continued

Th1A.4 • 09:30

Wavelength tunable carbon nanotube mode-locked fiber laser based on an all-fiber birefringent filter, Bingbing Lu¹, Chuanhang Zou¹, Qianqian Huang¹, Zhijun Yan², mohammed AlAraini^{3,4}, Aleksey Rozhin^{3,5}, Chengbo Mou¹; ¹Key Lab of Specialty Fiber Optics and Optical Access Networks, Shanghai Univ., China; ²School of Optical and Electronic Information, Huazhong Univ. of Science and Technology, China; ³Aston Inst. of Photonic Technologies, Aston Univ., UK; ⁴Al Musanna College of Technology, Oman; ⁵Nanoscience Research Group, Aston Univ., UK. A wavelength tunable carbon nanotube mode-locked fiber laser based on an all-fiber birefringent filter consisting of 45° tiled fiber grating and polarization maintaining fiber is demonstrated with a tuning range of 30 nm.

Th1A.5 • 09:45

Fourier domain mode-locked lasers with an optical intensity modulator, Xiaolong Yuan¹, Feng Li^{2,3}, Qian Li¹, P K A Wai^{2,3}; ¹School of Electronic and Computer Engineering, Peking Univ., China; ²The Hong Kong Polytechnic Univ. Shenzhen Research Inst., China; ³Dept. of Electronic and Information Engineering, The Hong Kong Polytechnic Univ., Hong Kong. We propose and study an FDML laser with an intracavity intensity modulator. Numerical simulations show that the pulse quality can be significantly improved if a short pulse modulation is applied to the intracavity signal.

Th1B • Nonlinear Spectroscopy and Imaging—Continued

Th1B.4 • 09:30

Magnetic sub-Wavelength Imaging using High-Harmonic Radiation, Sergey Zayko¹, Ofer Kfir¹, Michael Heigl², Murat Sivis¹, Manfred Albrecht², Claus Ropers³; ¹IV. Physical Inst. – Solids and Nanostructures, Univ. of Göttingen, Germany; ²Inst. of Physics, Univ. of Augsburg, Germany. We demonstrate nanoscale magnetic imaging with sub-20 nm spatial resolution using high-harmonic radiation. This first demonstration will allow for comprehensive studies of ultrafast spin dynamics with nanometer spatial and femtosecond temporal resolution using a lab-scale source.

Th1B.5 • 09:45

Ultrafast dynamics and coherent vibrations in zinc chlorin aggregates, Tongchao Shi¹, Juan Du¹, Zhengzheng Liu^{1,2}, Zeyu Zhang¹, Yuxin Leng^{1,2}, Tomohiro Makino³, Hitoshi Tamiaki⁴, Masaki Kobayashi⁵; ¹Shanghai Inst of Optics and Fine Mech, China; ²ShanghaiTech Univ., China; ³Ryukoku Univ., Japan; ⁴Ritsumeikan Univ., Japan; ⁵The Univ. of Electro-Communications, Japan. The ultrafast dynamics of zinc chlorin aggregates were studied by 7.1fs transient absorption spectroscopy. And interaction of the Frenkel exciton with the coherent molecular vibrations were obtained by 7.1fs real-time vibrational spectroscopy.

Th1C • Frequency Control and Measurement for Optical Metrology—Continued

Th1C.4 • 09:30

Frequency-Stabilized Pump Laser for Wavelength Conversion in Long-Distance Quantum Communication, Kohei Ikeda¹, Yusuke Hisai¹, Tomoyuki Horikiri¹, Kazumichi Yoshii¹, Hideo Kosaka¹, Feng-Lei Hong¹; ¹Yokohama National Univ., Japan. We develop a compact frequency-stabilized laser at 1064 nm for wavelength conversion in long-distance quantum communication. Linewidth and frequency stability are demonstrated to be sufficient to connect nitrogen-vacancy centers in diamond in remote nodes.

Th1C.5 • 09:45

High-Resolution No-Scanning 3D Image Detection Using Sum-Frequency Generation of Chirped Optical Frequency Combs, Yurina Tanaka^{1,2}, Takashi Kato^{1,2}, Megumi Uchida^{1,2}, Akifumi Asahara^{1,2}, Kaoru Minoshima^{1,2}; ¹The Univ. of Electro-Communications, Japan; ²Japan Science and Technology Agency (JST), ERATO MINOSHIMA Intelligent Optical Synthesizer (IOS) Project, Japan. No-scanning 3D imaging with 3- μ m depth accuracy was demonstrated with optical frequency combs using a 2D color-image detection method with a spectral filter pair. No significant image degradation due to nonlinear optical detection was observed.

Th1D • Quantum Information Processing II—Continued

Th1D.4 • 09:30

Witness assisted eigenspectra solver on a silicon quantum photonic simulator, Antonio Gentile¹, Raffaele Santagati¹, Jianwei Wang¹, Stefano Paesani¹, Nathan Wiebe², Jarrod McClean^{3,7}, Damien Bonneau¹, Joshua Silverstone¹, Sam Morley-Short¹, Peter Shadbolt⁴, David Tew^{1,4}, Xiaoqi Zhou⁵, Jeremy O'Brien¹, Mark Thompson¹; ¹Univ. of Bristol, UK; ²Quantum Architectures and Computation Group, Microsoft Research, USA; ³Quantum AI Lab, Google Inc., USA; ⁴Imperial College London, UK; ⁵State Key Laboratory of Optoelectronic Materials and Technologies and School of Physics, Sun Yat-sen Univ., China; ⁶Max Planck Inst. for Solid State Research, Germany; ⁷Lawrence Berkeley National Laboratory, USA. We demonstrate a new protocol capable of finding ground and excited states of physical Hamiltonians via an eigenstate witness. The experimental test employs a silicon quantum photonic device, embedding arbitrary controlled unitary operations.

Th1D.5 • 09:45

Characterizing the Temporal Mode of Single-Photon State Generated from Cold Atoms, Zhenjie Gu¹, Ce Yang¹, Peng Chen¹, Jiefei Chen¹; ¹East China Normal Univ., China. Single photons with pure temporal state are able to be generated and manipulated in cold atoms. We demonstrate the amplitude and phase of their temporal-mode function are both revealed in homodyne detection of photon currents.

Th1E • Fiber Devices II—Continued

Th1E.4 • 09:30

A High-Index Ring Core Layer for Highly Sensitive Micro Fiber Mach-Zehnder Temperature Sensors, Xuan Li¹, Yu-Jian Hu², Nan-Kuang Chen^{3,4}, Xiaoguang Zhang¹, Lixia Xi¹, Hu Zhang¹; ¹State Key Laboratory of Information Photonics and Optical Communications, Beijing Univ. of Posts and Telecoms, China; ²National United Univ., Taiwan; ³Shandong Provincial Key Laboratory of Optical Communication Science and Technology, Liaocheng Univ., China; ⁴School of Physics Sciences and Information Technology, Liaocheng Univ., China. We demonstrate micro fiber Mach-Zehnder interferometric temperature sensors based on tapered ring core fiber with a thinned high-index ring structure to separate core and cladding modes to improve the temperature sensitivity up to 60 pm/°C.

Th1E.5 • 09:45

Volatile organic gas recognition with an in-line fiber Mach-Zehnder interferometer coated with ZIF-8, Wanying Zhang¹, JieYun Wu¹, Ting Hao², Yang Liu¹, Kaixin Chen¹, Kin S. Chiang^{1,2}; ¹Univ of Electronic Science and Technology of China, China; ²Electronic Engineering, City Univ. of Hong Kong, Hong Kong. We demonstrate an in-line fiber Mach-Zehnder interferometer coated with the metal-organic framework ZIF-8 for volatile organic gas recognition. The ZIF-8 coating can absorb different gases and cause significant shifts of the interference fringes of the MZI.

Th1F • Metamaterials and Meta-devices—Continued

Th1F.4 • 09:30 **Invited**

Tunable Conducting Oxide Epsilon-Near-Zero Meta-Devices, Aleksei Anopchenko¹, Long Tao¹, Sudip Gurung¹, Jingyi Yang¹, Subhajit Bej¹, Catherine Arndt¹, Ho Wai H. Lee^{1,2}; ¹Dept. of Physics, Baylor Univ., USA; ²The Inst. for Quantum Science and Engineering, TexasA&M, USA. This talk will review our recent development on an electrically tunable conducting oxide metasurface that can tune the optical phase and amplitude and a broadband, tunable, and ultrathin conducting oxide epsilon-near-zero perfect absorber.

10:00–10:30 Coffee Break

These concurrent sessions are grouped across two pages. Please review both pages for complete session information.

Th1G • 2D Nonlinear Materials—Continued

Th1G.3 • 09:30

Multi-Photon Absorption in Monolayer Transition-Metal Di-Chalcogenides and its Applications for Sub-band Multi-Photon Detection, Wei Ji^{1,2}, ¹National Univ. of Singapore, Singapore; ²Shenzhen Univ., China. Multi-photon absorption spectra in monolayer transition-metal di-chalcogenides have been calculated by quantum mechanical perturbation theories for the first time. Their applications have been demonstrated for sub-band multi-photon detections.

Th1G.4 • 09:45

Determination of the optical constants of atomically thin MoS₂ by spectroscopic ellipsometry, Michele Merano¹; ¹Universita degli Studi di Padova, Italy. In literature, the optical constants of monolayer MoS₂ are extracted from experimental data modelling the crystal as a three dimensional slab. We use the surface current model, and compare the two procedures with surprising results.

Th1H • Nanostructures for Optoelectronic Applications—Continued

Th1H.5 • 09:30 **Invited**

Semiconductor Nanowires for Optoelectronics Applications, Chennupati Jagadish¹; ¹Australian National Univ., Australia. In this talk, I will present our results on nanowire growth and characterization. I will discuss our work on Nanowire lasers, THz detectors, solar cells and engineered neuronal growth and their function.

Th1I • Probabilistic Signal Shaping—Continued

Th1I.5 • 09:30

Submarine Cable Ageing and Repair Management Using Adaptable Probabilistic Constellation Shaping, Omar Ait Sab¹, Philippe Plantady¹, Alain Calsat¹, Suwimol Dubost¹, Pascal Pecci¹, Vincent Letellier¹; ¹Alcatel Submarine Networks, France. We experimentally demonstrate that an OSNR distortion of 5.5dB can be compensated for by using two PCS formats without any in-line gain flatness management over 7445km submarine transmission link at the expense of only 3% capacity loss.

Th1I.6 • 09:45

A Novel Scheme to Increase Receiver Sensitivity of PAM-4 Signal in Optical Amplified Network, Hanlin Feng¹; ¹Shanghai Jiao Tong Univ., China. We propose and demonstrate a novel scheme to increase receiver sensitivity of PAM-4 signal in optical amplified network. Non-uniform PAM-4 signal is generated to suppress signal-spontaneous beating noise from optical amplifier and reduce power penalty.

Th1J • Silicon Photonics Devices—Continued

Th1J.2 • 09:30 **Invited**

Silicon-based III-V Quantum Dot Materials and Devices, Huiyun Liu¹; ¹Univ. College London, UK. III-V Quantum-dot (QD) materials and lasers directly grown on Si platform are the most prospective candidate to realize on-chip optical sources for Si photonics. The recent progress made in this field are discussed.

Th1K • Display Technologies—Continued

Th1K.4 • 09:30

Dynamic 3D holographic display with enhanced viewing angle by using a nonperiodic pinhole array, Jongchan Park¹, KyeoReh Lee¹, YongKeun Park¹; ¹KAIST, Korea. We demonstrate a flat-panel wavefront modulator for generating dynamic holographic images. A nonperiodic photon sieve is combined with a liquid crystal display panel to generate holographic images with a large area and wide viewing angle.

Th1K.5 • 09:45

Optical illusion by scattering light manipulated with a spatial light modulator, Hexiang He^{2,1}, Kam Sing Wong¹; ¹Hong Kong Univ of Science & Technology, Hong Kong; ²Foshan Univ., China. We introduce an optical illusion method by transforming the object light into a designed illusion image with a spatial light modulator and a scattering medium. Both theoretical and experimental results show the method to be robust and easy-to-use.

Th1L • Waveguides and Sensors—Continued

Th1L.5 • 09:30

Highly Sensitive Temperature Sensor based on a Long Period Waveguide Grating with Polymer Upper Cladding and Metal Under Cladding, Nabarun Saha¹, Arun Kumar¹; ¹Indian Inst. of Technology, Delhi, India. We propose a temperature sensor based on a long period grating inscribed metal clad ridge waveguide with polymer upper cladding, which shows a very high sensitivity and does not require any polarization control.

Th1L.6 • 09:45

Nanoscale strain gauges composed of micro-disk lasers embedded in a flexible substrate, TaoJie Zhou², Jie Zhou¹, Yuzhou Cui², Xiu Liu², Zhaoyu Zhang²; ¹Peking Univ., Shenzhen Graduate School, School of Electronic and Computer Engineering, China; ²School of Science and Engineering, The Chinese Univ. of Hong Kong, Shenzhen, China. Compact visible microdisk lasers were fabricated and embedded in a deformable polydimethylsiloxane (PDMS) polymer substrate. A smooth wavelength tuning of 1.5 nm and 2.6 nm for microdisk lasers with the diameter of 1.2 μm and 1.5 μm are demonstrated under 36% strain, respectively.

10:00–10:30 Coffee Break

These concurrent sessions are grouped across two pages. Please review both pages for complete session information.

10:30–12:30

Th2A • Novel Laser Sources II

Presider: Meng Zhang; Beihang Univ., China

Th2A.1 • 10:30 **Invited**

New Schemes of Raman Fiber Lasers with Random Distributed Feedback, Sergey A. Babin¹; ¹Inst. of Automation and Electrometry, Russia. We review recent results on cascaded Raman fiber lasers (RFLs) with broadband random distributed feedback (RDFB) enabling tuning in 1–2 micron range, and directly diode-pumped RFL with RDFB in multimode GRIN fiber at <1 micron.

Th2A.2 • 11:00

Switchable dual-mode pulsed fiber laser with few-mode fiber grating, Yu Cai¹, Zhiqiang Wang¹, Xuxing Zhang¹; ¹Nanjing Univ of Posts & Telecomm, China. A switchable dual-mode pulsed fiber laser by using a two-mode fiber Bragg grating for mode discrimination and SESAM for mode-locking has been demonstrated. Stable pulsed operation on separate or simultaneous fundamental mode and inter-coupling mode can be obtained, respectively.

10:30–12:30

Th2B • Solitons and Temporal Wave Guiding, and Frequency Comb

Presider: Stephane Coen; Univ. of Auckland, New Zealand

Th2B.1 • 10:30 **Invited**

Pulse-driven Microresonator Solitons, Ewelina Obrzud^{1,2}, Steve Lecomte¹, Tobias Herr¹; ¹Swiss Cent for Electronics and Microtech, Switzerland; ²Observatoire de Genève, Université de Genève, Switzerland. Nonlinear optical microresonator driven by picosecond laser pulses can generate temporal dissipative solitons. These femtosecond soliton pulses can be all-optically controlled and are generated at a fraction of the power required in continuous-wave driven systems.

Th2B.2 • 11:00

Soliton Bursts in Nonlinear Microcavity, Wenwen Cui¹, Heng Zhou¹, Yong Geng¹, Baojian Wu¹, Kun Qiu¹; ¹Univ of Electronic Science & Tech China, China. We demonstrate new dissipative Kerr soliton formation route with red-detuned pump entrance and observe soliton bursts in microcavity. We show that ignition of soliton burst requires much less pump tuning than conventional blue-pump-entry soliton generation.

10:30–12:30

Th2C • Integrated Optical Devices for Switching Multiplexing and Signal Processing

Presider: Daoxin Dai; Zhejiang Univ., China

Th2C.1 • 10:30 **Tutorial**

Silicon Photonic Devices for Optical Signal Processing in Wavelength, Polarization and Mode Domains, Yikai Su¹; ¹Shanghai Jiao Tong Univ., China. We review recent progress on silicon photonic devices for optical signal processing, including nanobeam devices for wavelength filtering and switching, directional couplers for polarization/mode processing, and subwavelength grating devices for multi-dimensional processing.

10:30–12:30

Th2D • High Energy Laser

Presider: Deepak Jain; DTU Fotonik, Denmark

Th2D.1 • 10:30 **Invited**

High Energy and Broad Bandwidth Ti:Sapphire Chirped Pulse Amplifier in 10 PW Laser, Xiaoyan Liang¹, Zebiao Gang¹, Lianghong Yu¹, Wenqi Li¹, Zhen Guo¹, Yanqi Liu¹, Cheng Wang¹, Shuai Li¹, Yuxin Leng¹, Ruxin Li¹, Zhizhan Xu¹; ¹Shanghai Inst of Optics & Fine Mechanics, China. The amplified energy of 339 J from the SULF laser was achieved with 235 mm diameter Ti:sapphire in final amplifier. After compressor, the measured pulse duration of 21.0 fs supported the peak power of 10.3PW.

Th2D.2 • 11:00 **Invited**

Recent Performance of the Fusion Laser Facility SG-III, Qihua Zhu¹; ¹China Academy Of Engineering Physics (CAEP), China. Abstract not available.

10:30–12:30

Th2E • Special Fibers II

Presider: Markus Schmidt; Leibniz Inst. of Photonic Technology, Germany

Th2E.1 • 10:30 **Invited**

World-Beating Performance from Hollow Core Fibers, Jonathan C. Knight¹, Fei Yu^{1,2}; ¹Univ. of Bath, UK; ²Shanghai Inst. of Optics and Fine Mechanics, China. Hollow core optical fibers have the potential to outperform conventional optical fibers in numerous ways. We report on ultra-low loss fibers for the mid-infrared and the ultraviolet, the absence of solarization, mid-IR gas lasers and prospects for the lowest optical fiber loss ever.

Th2E.2 • 11:00 **Invited**

Tailored Glasses Optimized for Optical Fiber-Based Photonic Applications, Peter D. Dragic¹, Maxime Cavillon², Matthew Tuggle², Nanjie Yu¹, Courtney Kucera², Joshua Parsons², Thomas Hawkins², John Ballato²; ¹Univ of Illinois at Urbana-Champaign, USA; ²Clemson Univ., USA. Silica glass, arguably the most ubiquitous of all optical materials, is a pillar of modern fiber optics. However, careful compositional tuning can render fibers with far more remarkable properties for a wide range of applications.

10:30–13:30

Th2F • Plasmonics Metasurfaces

Presider: Jensen Li, Hong Kong Univ. of Science & Tech, Hong Kong

Th2F.1 • 10:30 **Invited**

Sieving Photons for Wavefront Manipulation, Jinghua Teng¹; ¹A*STAR, Singapore. This talk will introduce our work on using photon sieves to manipulate optical wavefront for high tolerance hologram generation, orbital angular momentum control and sub-diffraction limit focusing.

Th2F.2 • 11:00

Using Metasurfaces to Control Random Light Emission, Zhengtong Liu¹, Egor Khaidarov^{2,3}, Ramón Paniagua-Dominguez², Song Sun^{1,4}, Ping Bai¹, Ching Eng Png¹, Hilmi Volkan Demir², Arseniy I. Kuznetsov²; ¹Inst. of High Performance Computing, Singapore; ²Data Storage Inst., Singapore; ³Nanyang Technological Univ., Singapore; ⁴Microsystem & Terahertz Research Center, China Academy of Engineering Physics, China. Metasurfaces have been designed for plane waves or point emitters with precise positions, but generally fail to control emission from random light emitters such as LEDs. We demonstrate a method that resolves this problem.

These concurrent sessions are grouped across two pages. Please review both pages for complete session information.

10:30–12:15

Th2G • 2D Materials for Mode Locking and Nonlinear Photonics

Presider: Han Zhang; Shenzhen Univ., China

Th2G.1 • 10:30 **Invited**

2D Materials for Mode-locking of Bulk 2 Micron Lasers: Alternatives to SESAMs, Yicheng Wang¹, Zhongben Pan¹, Yongguang Zhao^{1,2}, Weidong Chen¹, Mark Mero³, Fabian Rotermund³, Pavel Loiko⁴, Xavier Mateos⁵, Xiaodong Xu², Jun Xu⁶, Haoai Yu⁷, Huaijin Zhang⁷, Uwe Griebner¹, Valentin Petrov¹; ¹Max Born Inst., Germany; ²Jiangsu Normal Univ., China; ³KAIST, Korea; ⁴ITMO Univ., Russia; ⁵URV, Spain; ⁶Tongji Univ., China; ⁷Shandong Univ., China. We review the recent progress in passively mode-locked Tm- and Ho-lasers operating near 2 μm , comparing saturable absorbers based on carbon nanostructures (SWCNTs and graphene) with SESAMs, employed in lasers based on different active media.

Th2G.2 • 11:00 **Invited**

Mid-infrared Ultrafast Lasers Based on Two-dimension Materials, Guoqiang Xie¹, Zhipeng Qin¹; ¹Shanghai Jiao Tong Univ., China. In this talk, mid-infrared ultrafast lasers from 2 μm to 3.5 μm based on two-dimension materials will be introduced. The two-dimension materials provide opportunity for generating ultrashort pulses in long mid-infrared wavelength.

10:30–12:30

Th2H • Light-matter Interactions in Micro/nano-structures

Presider: Xuming Zhang; The Hong Kong Polytechnic Univ., Hong Kong

Th2H.1 • 10:30 **Invited**

Light-Matter Interactions Within Extreme Dimensions: Strategies to Surpassing Conventional Nanophotonics, Qiaoqiang Gan¹; ¹State Univ. of New York at Buffalo, USA. We will present an overview of new strategies to boost the light-matter interaction within extremely small dimensions.

Th2H.2 • 11:00

Ultrahigh-Efficiency Nonlinear Mechanical Intermodal Coupling in High-Q Square Nano-membrane, Da In Song¹, Dae Seok Han¹, Myeongsoo Kang¹; ¹Dept. of Physics, KAIST, Korea. We experimentally demonstrate optomechanically driven nonlinear mechanical intermodal coupling by using high-Q square nano-membranes. Pumping via radiation forces as low as 34 pN, we achieve ultrahigh-efficiency coupling of the first-order mode into the higher-order ones.

10:30–12:30

Th2I • Polarization Effects and Optical Networking

Presider: Changjian Guo; The Hong Kong Polytechnic Univ., Hong Kong

Th2I.1 • 10:30

A Low-Complexity and Fast Adaptive Stokes-Space-Based Polarization Demultiplexing Technique for Optical Fiber Transmissions with Low Polarization Mode Dispersion, Xiong Wu¹, Jie Liu¹, Junwei Zhang¹, Siyuan Yu^{1,2}; ¹Sun Yat-Sen Univ., China; ²Univ. of Bristol, UK. We propose a low-complexity fast adaptive polarization demultiplexing technique in Stokes-Space for optical fiber transmissions with low polarization mode dispersion. Experimental results of a polarization-multiplexed QPSK system confirm the feasibility of the proposed technique.

Th2I.2 • 10:45

2-Parameter-SOP and 3-Parameter-RSOP Fiber Channel: Trouble and Solution for Polarization Demultiplexing using Stokes Space, Nan Cui¹, ZiBo Zheng¹, Wenbo Zhang¹, Lixia Xi¹, Xianfeng Tang¹, Xiaoguang Zhang¹; ¹Beijing Univ. of Posts and Telecomm, China. We present a 3-parameter representation for RSOP model, and based on it propose a PolDemux method using extended Kalman filter. The method is independent on RSOP models, and performs well in time-varying RSOP scenarios.

Th2I.3 • 11:00

Performance improvement on polarization state and phase tracking based on pilot-aided adaptive Kalman filter, Qian Xiang¹, Juntao Cao¹, Yanfu Yang¹, Qun Zhang¹, Yong Yao¹; ¹Dept. of Electronic Information Engineering, Harbin Inst. of Technology (Shenzhen), China. A novel polarization and phase tracking scheme based on adaptive Kalman filter is proposed. Compared with extended Kalman filter, the proposed scheme shows fast polarization tracking capability, high linewidth tolerance and quick convergence speed.

10:30–12:30

Th2J • Advanced Modulators

Presider: Christian Koos; Karlsruhe Inst. of Technology KIT, Germany

Th2J.1 • 10:30 **Invited**

Advanced Architectures for QAM Modulators, Unaiza Tariq¹, Duncan L. MacFarlane¹; ¹Electrical Engineering, Southern Methodist Univ., USA. Deviations to the input parameters of QAM can cause errors in the output, causing the output to deviate from its ideal position on the constellation diagram. This paper suggests adding feedback to the modulator branches to reduce the error in the output signal.

Th2J.2 • 11:00 **Invited**

III-V/Si Integration Platform for Laser Diodes and Mach-Zehnder Modulators, Tatsuro Hiraki¹, Takuma Aihara¹, Koichi Hasebe¹, Koji Takeda¹, Takuro Fujii¹, Takaaki Kakitsuka¹, Tai Tsuchizawa¹, Hiroshii Fukuda¹, Shinji Matsuo¹; ¹NTT Device Technology Labs, Japan. We demonstrate membrane III-V/Si integrated devices. An InGaAsP/Si metal-oxide-semiconductor capacitor Mach-Zehnder modulator shows small V_{mL} (0.09 Vcm), and a laser diode coupled to a 0.2- μm -thick Si waveguide shows a fiber coupled power of 4.6 mW.

10:30–12:30

Th2K • Imaging Technologies

Presider: Jung-Hoon Park; Ulsan National Inst of Science & Tech, Korea

Th2K.1 • 10:30 **Invited**

Micro Fourier Transform Profilometry (μFTP): 3D imaging at 10,000 fps, Chao Zuo¹; ¹Nanjing Univ of Science and Technology, China. We present a new 3D dynamic imaging technique, Micro Fourier Transform Profilometry (μFTP), which can capture 3D surfaces of transient, time evolving events at up to 10,000 fps. We demonstrate μFTP 's broad utility by imaging several transient scenes, for example, balloon's explosion triggered by a flying dart.

Th2K.2 • 11:00 **Invited**

Ultrahigh-Speed Optical Coherence Tomography and its Applications, Chao Zhou¹; ¹Lehigh Univ., USA. Optical coherence tomography (OCT) enables 3D imaging of biological tissue with micron-scale resolutions in vivo. Recent technical advances to achieve ultrahigh-speed OCT and its novel applications will be discussed.

10:30–12:30

Th2L • Distributed Fiber Sensing

Presider: Xuping Zhang; Nanjing Univ., China

Th2L.1 • 10:30 **Invited**

A Review on Advances in Fiber-optic Distributed Acoustic Sensors (DAS), Zuyuan He¹, Qingwen Liu¹, Xinyu Fan¹, Dian Chen¹, Shuai Wang¹, Guangyao Yang¹; ¹Shanghai Jiao Tong Univ., China. Latest advances in fiber-optic distributed acoustic sensors (DAS) are reviewed. Field demonstrations of DAS based on Φ -OTDR with fading-suppression are shown, and newly developed DAS based on time-gated digital optical frequency domain reflectometry introduced.

Th2L.2 • 11:00 **Invited**

Phase-Sensitive OTDR Based on Coherent Detection, Zinan Wang¹, Ji Xiong¹, Yun Fu¹, Yunjiang Rao¹; ¹Univ. Electronic Sci. & Tech. of China, China. Phase-sensitive optical time domain reflectometry (Φ -OTDR) as a versatile tool for distributed sensing has drawn great attention in both academic and industrial sectors. Recent progress at UESTC in Φ -OTDR is presented with emphasis on coherent detection scheme, and future prospects are discussed.

These concurrent sessions are grouped across two pages. Please review both pages for complete session information.

Th2A • Novel Laser Sources II—Continued

Th2A.3 • 11:15

Sub-70fs generation from passively mode locked Erbium doped fiber laser using 45° tilted fiber grating, Tianxing Wang¹, Zhijun Yan², Qianqian Huang¹, Chuanhang Zou¹, Chengbo Mou¹, Kaiming Zhou³, Lin Zhang³; ¹Key Laboratory of Specialty Fiber Optics and Optical Access Networks, Shanghai Univ., China; ²School of Optical and Electronic Information, Huazhong Univ. of Science and Technology, China; ³Aston Inst. of Photonic Technologies, Aston Univ., UK. We have demonstrated an all-fiber Erbium doped ultrafast laser by inserting a 45° tilted fiber grating. After optimizing the balance between intra-cavity nonlinearity and dispersion, an ultrashort pulse with sub-70 fs pulse duration can be achieved.

Th2A.4 • 11:30

Elegant modes of confocal laser resonators with OAM and its intracavity self-healing properties, Alfonso I. Jaimes-Nájera¹, Songjie Luo², Jixiong Pu², Sabino Chávez-Cerda¹; ¹INAOE, Mexico; ²Fujian Provincial Key Laboratory of Light Propagation and Transformation, College of Information Science and Engineering, Huaqiao Univ., China. Elegant beams were introduced as a variant to standard Gaussian beams that are not eigenmodes of confocal cavities. We remove this asymmetry by superposing a finite number of elegant Laguerre-Gauss beams, rendering a new family of single pass cavity eigenmodes.

Th2B • Solitons and Temporal Wave Guiding, and Frequency Comb—Continued

Th2B.3 • 11:15

Strong resonant radiation limits Kerr cavity soliton existence in longitudinally modulated resonators, Alexander U. Nielsen¹, Bruno Garbin¹, Stephane Coen¹, Stuart G. Murdoch¹, Miro J. Erkintalo¹; ¹The Dodd-Walls Centre for Photonic and Quantum Technologies, Dept. of Physics, The Univ. of Auckland, New Zealand. We have experimentally and numerically studied the effects of dispersion management on temporal Kerr cavity solitons. We find that the solitons can parametrically excite strong resonant sidebands that affect their range of existence.

Th2B.4 • 11:30

Fiber-Optic Solitons with Gain and Loss, Alexander Hause¹, Christoph Mahnke¹, Fedor Mitschke¹; ¹Univ. of Rostock, Germany. Propagation of solitons in fibers with gain or loss beyond the perturbative regime is considered. Analytical results, corroborated with soliton eigenvalues from numerical studies, predict generation and decay of solitons, and the energy budget.

Th2C • Integrated Optical Devices for Switching Multiplexing and Signal Processing—Continued

Th2C.2 • 11:30

Integrated Multi-Functional Photonic Filters Based on Mode-Split Cascaded Sagnac Loop Reflectors, Jiayang Wu¹, Tania Moein¹, Xingyuan Xu¹, David Moss¹; ¹Swinburne Univ. of Technology, Australia. We propose and demonstrate integrated multi-functional photonic filters implemented by mode-split cascaded Sagnac loop reflectors (SLRs). A wide range of filter shapes for diverse applications are experimentally achieved and show good agreement with theory.

Th2D • High Energy Laser—Continued

Th2D.3 • 11:30

1 TW-Class OPCPA Pumped with Fiber Laser Seeded Two-Cascaded Yb:YAG Rod Amplifier-Compressor, Aleksej Rodin^{1,2}, Paulius Mackonis¹; ¹Center for Physical Sciences and Technology, Lithuania; ²Ekspla Ltd, Lithuania. Fiber laser seeded two-stage double-pass chirped pulse amplifier-compressor based on Yb:YAG rods with scalable output energy from 20 mJ to 60 mJ at a repetition rate of 100 Hz, a pulsewidth of 1.2 ps and excellent beam quality is used to pump 1 TW-class OPCPA

Th2E • Special Fibers II—Continued

Th2E.3 • 11:30

Optimized design of 125- μ m 6-core fiber with large effective area for wideband optical transmission, Shoulin Jiang^{1,2}, Lin Ma², Martin Miguel¹, Zuyuan He², Jayanta K. Sahu¹; ¹Optoelectronics Research Centre, Univ. of Southampton, UK; ²Shanghai Jiao Tong Univ., China. We propose an optimized design of heterogeneous trench-assisted 125- μ m 6-core fiber with A_{eff} about 90 μ m², λ_c about 1300 nm, and XT<-30 dB/100 km for wideband transmission. Relative core multiplicity factor of 6.75 was achieved.

Th2F • Plasmonics Metasurfaces—Continued

Th2F.3 • 11:15

Optical Superchirality in a Perfect Lattice of Three-dimensional Nano-holes with High Q-factor and large area, Meng Qiu⁴, Yidong Hou², Ho M. Leung¹, Che T. Chan¹, Jinglei Du², Wei Jin⁴, Dang Yuan Lei³; ¹Dept. of Physics, The Hong Kong Univ. of Science and Technology, Hong Kong; ²College of Physical Science and Technology, Sichuan Univ., China; ³Dept. of Applied Physics, The Hong Kong Polytechnic Univ., Hong Kong; ⁴Dept. of Electrical Engineering, The Hong Kong Polytechnic Univ., Hong Kong. We demonstrate a lattice of 3D chiral plasmonic nano-holes, with strong relative optical circular dichroism ~0.5, high Q-factor up to 45, and a perfect lattice of 1cm². This CD enhancement is due to the interaction between the chiral response of the chiral holes and the scattering modes of the lattice.

Th2F.4 • 11:30

The radiation-reaction force in two-dimensional atomic crystals and metasurfaces, Michele Merano¹; ¹Universita degli Studi di Padova, Italy. Retardation effects are very relevant in the expression of local electromagnetic fields in two-dimensional systems. How do we go from the microscopic description to the macroscopic one? The radiative-reaction electric field connects micro to macro.

These concurrent sessions are grouped across two pages. Please review both pages for complete session information.

Th2G • 2D Materials for Mode Locking and Nonlinear Photonics—Continued

Th2G.3 • 11:30 **Invited**
On-chip Chalcogenide-glass Nonlinear Photonics Using 2D-Material Mode-locked Fiber Lasers, Zhengqian Luo¹; ¹Xiamen Univ., China. In this talk, we will present our recent research progress on on-chip CHGs-based nonlinear photonic devices using 2D-material mode-locked fiber lasers, mainly including 1) supercontinuum source integrated on-chip spectroscopic sensor, 2) on-chip optical frequency combs based on cascaded four-wave mixing, and 3) on-chip Raman soliton generation.

Th2H • Light-matter Interactions in Micro/nanostructures—Continued

Th2H.3 • 11:15
Resonant Third Harmonic Generation Microscopy of amorphous-silicon sub-wavelength nanostructures, Jayanta Deka¹, Keshav Kumar Jha¹, Sruti Menon¹, Lal Krishna¹, Varun Raghunathan¹; ¹Indian Inst. of Science, India. We demonstrate multispectral third harmonic generation microscopy of amorphous silicon two-dimensional nanostructure arrays. Sub-wavelength structures designed with resonance at the fundamental wavelength result in enhancement of third-harmonic by a factor of ~ 370.

Th2H.4 • 11:30
Plasmonic-Dielectric Mushroom Nanoantenna for Fluorescence Enhancement, Song Sun^{1,4}, Ru Li^{1,4}, Mo Li^{1,4}, Qingguo Du^{2,5}, Ping Bai³; ¹CAEP Microsystem and Terahertz Center, China; ²School of Information Engineering, Wuhan Univ. of Technology, China; ³Electronics and Photonics, A*STAR Inst. of High Performance Computing, Singapore; ⁴CAEP Institute of Electronic Engineering, China; ⁵Key Laboratory of Fiber Optic Sensing Technology and Information Processing, Wuhan Univ. of Technology, China. A plasmonic-dielectric mushroom nanoantenna is proposed to achieve an enhancement-factor (far-field intensity) twice (20-times) as high as that from a pure metallic antenna by matching the Stokes-shift of the emitter, accompanied with an improved directivity.

Th2I • Polarization Effects and Optical Networking—Continued

Th2I.4 • 11:15
Three-dimensional Stokes-vector based Polarization Recovery for Polarization Diversity Coherent Optical Detection, Soo-Min Kang¹, Dong-Yoon Han¹, Kyoung-Hak Mun¹, Sang-kook Han¹; ¹Yonsei Univ., Korea. State of polarization variation of ONUs is critical in CO-OFDMA-PON uplink detection due to different fiber-birefringence and polarization-sensitive components. Stokes-Vector of pilot-tone based polarization recovery is proposed and its performance is verified experimentally.

Th2I.5 • 11:30
Dynamic Virtual Network Embedding with Distance Adaptive RSA over SDM-Based Elastic Optical Networks, Lijie Cheng¹, Xiaosong Yu¹, Zhu Liu², Xiao Liao², Ping Jia³, Wei Li³, Wenjing Li², Ruijie Zhu⁴, Yajie Li¹, Yongli Zhao¹, Jie Zhang¹; ¹Beijing Univ. of Posts and Telecommunications, China; ²State Grid Information & Telecommunication Group CO., LTD, China; ³State Grid Jiangsu Electric Power Company Information & Telecommunication Branch, China; ⁴Zhengzhou University, China. A virtual network embedding strategy is proposed with distance-adaptive RSA over space-division-multiplexing based elastic optical networks. It not only improves network flexibility and spectrum utilization but also reduces the failure rate of virtual network embedding.

Th2J • Advanced Modulators—Continued

Th2J.3 • 11:30
Intensity and Phase Modulators at 1.55 μm with InAs/InGaAs Quantum Dots Epitaxially Grown on Silicon, Prashanth Bhasker¹, Justin Norman¹, John Bowers¹, Nadir Dagli¹; ¹Univ. of California Santa Barbara, USA. InAs quantum dot core electro-optic modulators are fabricated on (100) silicon substrates opening up large-scale III-V photonic integration. Mach-Zehnder modulator with 8 mm long electrode has 2.2V Vpi and less than 3 dB/cm propagation loss.

Th2K • Imaging Technologies—Continued

Th2K.3 • 11:30 **Invited**
Time-stretch Imaging and Beyond, Cheng Lei¹, Yasuyuki Ozeki¹, Keisuke Goda¹; ¹Univ. of Tokyo, Japan. Optofluidic time-stretch imaging has been widely studied and applied for its capability to acquire high-quality images at high speed. Here, we present recent advances and trends in its applications to biomedical research and treatment.

Th2L • Distributed Fiber Sensing—Continued

Th2L.3 • 11:30
Improvement of Brillouin Frequency Shift Estimation Accuracy in BOTDR Using Cross Correlation with Reference Spectrum Tracking, Wei Yang^{1,2}, Yuanhong Yang³; ¹China Academy of Electronics and Information Technology, China; ²CETC Research Center for Development and Strategy, China; ³School of Instrumentation Science and Opto-electronics Engineering, Beihang Univ., China. We propose an approach using cross correlation with reference spectrum tracking to improve Brillouin frequency shift estimation accuracy in BOTDR by studying the influence factor on cross-correlated spectrum symmetry. Simulations and experiments verify its advantage.

These concurrent sessions are grouped across two pages. Please review both pages for complete session information.

Th2A • Novel Laser Sources II—Continued

Th2A.5 • 11:45

Generation and manipulation of polarization dependent sidebands in a fiber parametric oscillator, Kangwen Yang¹, Peng Zhao¹, Pengbo Ye¹, Qiang Hao¹, Kun Huang¹, Heping Zeng¹; ¹Univ of Shanghai Science & Technology, China. A tunable fiber optical parametric oscillator was demonstrated to generate and control of scalar and cross-phase modulation instabilities at 779-793 nm and 864-978 nm respectively, which could be used in coherent anti-Stokes Raman spectroscopy.

Th2A.6 • 12:00

A compact and robust polarization-maintain fiber laser with a locked repetition rate, Zhiwei Zhu¹, Zejiang Deng¹, Chao Wang¹, Chenglin Gu¹, Yang Liu¹, Daping Luo¹, Wenxue Li¹; ¹East China Normal Univ., China. A compact and robust mode-locked fiber laser with a locked repetition rate is demonstrated in a polarization-maintain fiber ring cavity. The repetition rate is locked at 108 MHz and the standard deviation of the controlled signal is 0.997 mHz in a 10-hours test.

Th2A.7 • 12:15

Designs of Nanostructured Materials made by Glancing Angle Deposition for Improved Spectral Brightness of Solid-State Lasers, Koffi Amouzou¹, Jean-Francois Bisson¹, Gabriel Gallant¹, Kris Bulmer¹, Georges Bader¹; ¹Universite de Moncton, Canada. We present two types of nanostructured laser mirrors designed for suppressing spatial hole burning. They were made with Glancing Angle Physical vapor deposition. First, helically-nanostructured materials. Second, thick anisotropic coatings behaving as halfwave plates.

Th2B • Solitons and Temporal Wave Guiding, and Frequency Comb—Continued

Th2B.5 • 11:45

Dispersion and nonlinearity jointly engineered silicon waveguide taper for self-similar parabolic pulse propagation, Chao Mei^{1,2}, Feng Li², Jinhui Yuan^{1,2}, Zhe Kang², Xianting Zhang², Yin Xu², Binbin Yan¹, xinzhuan Wang¹, Kuiru Wang¹, Chongxiu Yu¹, Ping Kong A. Wa²; ¹Beijing Univ of Posts & Telecom, China; ²The Hong Kong Polytechnic Univ., Hong Kong. We analytically investigate the condition of passive self-similar propagation for parabolic pulse. Based on the derived condition, a dispersion and nonlinearity jointly engineered silicon waveguide taper for the parabolic similariton propagation is designed and analyzed.

Th2B.6 • 12:00

Mid-infrared Optical Frequency Comb via Coherent Supercontinuum Processes in Nano-photonic Waveguides, Hairun Guo¹, Wenle Weng¹, Martin H. Pfeiffer¹, Tobias J. Kippenberg¹; ¹École polytechnique fédérale de Lausanne, Switzerland. We demonstrated mid-infrared optical frequency comb generation via coherent supercontinuum generation process, in a large-cross-section silicon nitride nano-photonic waveguide. We experimentally assessed the coherence of the mid-infrared dispersive wave that serves as the frequency comb.

Th2B.7 • 12:15

Investigation of semiconductor optical amplifier gain recovery through dual-comb asynchronous optical sampling, Ningning Yang¹, Liao Chen¹, Haidong Zhou¹, Xi Zhou¹, Xin Dong¹, Chi Zhang¹, Xinliang Zhang¹; ¹Wuhan National Lab for Optoelectronics, China. We perform a novel pump-probe scheme based on dual-comb asynchronous optical sampling (ASOPS) with 10.86-ns observation range, 2-ps temporal resolution and 1-kHz frame rate, and investigate the semiconductor optical amplifier (SOA) gain recovery process.

Th2C • Integrated Optical Devices for Switching Multiplexing and Signal Processing—Continued

Th2C.3 • 11:45

A Silicon Photonic Optical Add-Drop Multiplexer based on Mode-Selective Device and Bragg Grating, Zifei Wang¹, Bruno Taglietti¹, Ming Ma¹, Lawrence R. Chen¹; ¹McGill Univ., Canada. We demonstrate a compact add-drop multiplexer using Bragg grating in a mode-selective device for the silicon-on-insulator (SOI) platform. The proposed design has crosstalk lower than -42 dB within the 3 dB bandwidth of 1.6 nm.

Th2C.4 • 12:00 **Invited**

Silicon Integrated Devices for On-chip Mode Multiplexing, Yaocheng Shi¹, Hongnan Xu¹; ¹Zhejiang Univ., China. On-chip multi-mode communication has attracted much attention for its potential to greatly expand the bandwidth of data transmission. In this paper, we will introduce some silicon integrated devices for on-chip mode multiplexing, including the multiplexers, multimode crossing and the multimode bending.

Th2D • High Energy Laser—Continued

Th2D.4 • 11:45

Impact of disk laser geometry on excess nonlinear heat release, Mikhail R. Volkov¹, Ivan Kuznetsov¹, Ivan Mukhin¹; ¹Inst. of Applied Physics of the RAS, Russia. Disk active elements of various doping and geometry are investigated for heat sources and lasing. Yb:YAG of 10% doping has strong overheating under high excitation level. The phenomenon is most severe for thin disk, while composite disk shows much less overheating. The latter case shows less lasing efficiency but better small-signal gain.

Th2D.5 • 12:00

Mode Instability in Yb:YAG Crystalline Fiber Amplifiers, Shicheng Zhu^{1,2}, Jinyan Li², Xiuquan Ma¹; ¹School of Mechanical Science and Engineering, Huazhong Univ. of Science and Technology, China; ²Wuhan National Laboratory for Optoelectronics, Huazhong Univ. of Science and Technology, China. Mode instability (MI) in Yb:YAG crystal fiber amplifiers is investigated through full numerical simulations. The MI threshold in a 50/250 Yb:YAG crystalline fiber is found to be greater than 10kW.

Th2E • Special Fibers II—Continued

Th2E.4 • 11:45

High resolution imaging microstructured optical fibres, Stephen C. Warren-Smith¹, Alastair Dowler¹, Hoa Huynh¹, Heike Ebendorff-Heidepriem¹; ¹Univ. of Adelaide, Australia. We show that an imaging fibre with a pixel pitch of 2 µm is theoretically achievable using silica-based microstructured fibres. Preliminary fabrication results are presented using extrusion of glass through 3D printed titanium dies.

Th2E.5 • 12:00

Single-polarization single-mode double-layer hollow-core antiresonant fiber, Shibo Yan¹, Shuqin Lou¹, Xin Wang¹, Zhen Xing¹; ¹Beijing Jiaotong Univ., China. A single-polarization single-mode double-layer hollow-core antiresonant fiber with two single-polarization regions (1545-1552 and 1591-1596 nm) is proposed. The polarization extinction ratio is 14155 while the loss of x-polarized is 0.036 dB/m at 1550 nm.

Th2F • Plasmonics Metasurfaces—Continued

Th2F.5 • 11:45 **Invited**

High-efficiency, Multifunctional and Tunable Metasurfaces, Lei Zhou¹; ¹Fudan Univ., China. Metasurfaces, ultrathin metamaterials composed by array of planar "meta-atoms" with pre-designed electromagnetic (EM) properties, have attracted extensive attention recently. In this talk, I will summarize our recent efforts in this field, focusing on the tunability, efficiency, and multifunctionality issues of them.

Th2F.6 • 12:15 **Tutorial**

Soft Metamaterials: Self-Gauged Assembly, Non-Equilibrium Matters, and 3D Super-Resolution Imaging; Xiang Zhang¹; ¹Univ. of Hong Kong, Hong Kong. We explore "soft metamaterials" with building blocks that have a strong propensity for self-assembly/re-assembly. In this regards, the structure units can be artificially evolving during the formation of soft metamaterials. Particularly, we explore the self-feedback mechanism between structures and properties for self-selective assembly of complex metamaterial nanoarchitectures with tailored symmetries. We expand structural design using soft metamaterial approach to achieve isotropic negative index metamaterials and Brownian optical imaging. We also explore approach for realizing bandgap materials that reside far from equilibrium and emerge enslaved to an external drive. Experimental results are providing supports as well as new insights into such new type of soft metamaterials that facilitate self-responsive material applications.

12:30–14:00 Lunch

These concurrent sessions are grouped across two pages. Please review both pages for complete session information.

Th2G • 2D Materials for Mode Locking and Nonlinear Photonics—Continued

Th2G.4 • 12:00

Enhanced third-order optical nonlinearity of flexibly synthesized h-BN film via localized laser oxidation, Ren Jun^{1,2}, Xiaorui Zheng², Weiwei Lei³, Dan Liu³, Pu Wang¹, Baohua Jia²; ¹Beijing Univ. of Technology, China; ²Swinburne Univ. of Technology, Australia; ³Deakin Univ., Australia. Hexagonal boron nitride film was achieved using ball-milled exfoliation and functionalization method for high concentration solution. Enhanced third-order nonlinearity was investigated during interaction with high intensity laser source owing to the formation of oxidation group.

Th2H • Light-matter Interactions in Micro/nano-structures—Continued

Th2H.5 • 11:45

Enhancing the Stability and Emission of CsPbBr₃ Quantum Dots by Embedding in Silica Spheres, Zhengzheng Liu¹, Zhiping Hu², Xiaosheng Tang², Juan Du¹, Yuxin Leng¹; ¹Shanghai Inst of Optics and Fine Mech, China; ²Chongqing Univ., China. Enhanced amplified spontaneous emission has been obtained from perovskite CsPbBr₃ quantum dots embedded in waterless silica spheres. The blinking characteristic of CsPbBr₃/SiO₂ has been suppressed and photostability has been improved significantly.

Th2H.6 • 12:00

Flexible Dielectric Microsphere-Embedded Film for Enhanced-Raman Spectroscopy, Cheng Xing¹, Yinzhou Yan¹, Yijian Jiang¹; ¹Beijing Univ. of Technology, China. A dielectric microsphere-embedded film was developed as a flexible Raman enhancer, which provides a >10-fold enhancement ratio and can be coupled with traditional SERS active substrates for ultrasensitive Raman trace-detection.

Th2H.7 • 12:15

Narrow-linewidth Lasing and Kerr Soliton Comb with a Regular Laser Diode, Nikolay G. Pavlov^{3,2}, Grigory Lihachev^{1,2}, Andrey Voloshin², Sergey Koptyaev⁴, Michael L. Gorodetsky^{1,2}; ¹Lomonosov Moscow State Univ., Russia; ²Russian Quantum Center, Russia; ³Moscow Inst. of Physics and Technology, Russia; ⁴Samsung R&D Inst. Russia, Russia. We demonstrate single-frequency lasing with ultra-narrow linewidth and coherent soliton comb generation from a regular multi-frequency Fabry-Perot laser diode to self-injection locked to an optical crystalline high-Q microresonator.

Th2I • Polarization Effects and Optical Networking—Continued

Th2I.6 • 11:45

Non-Equal Granularity Light-Tree based Multicast Flow Aggregation Scheme in Elastic Optical Datacenter Networks, Xin Li¹, Ying Tang¹, Tao Gao¹, Lu Zhang¹, Shanguo Huang¹; ¹State Key Laboratory of Information Photonics and Optical Communications, Beijing Univ of Posts & Telecom, China. A non-equal granularity light-tree (NeGLt) which supports the user-desired spectrum allocation is designed for multicast flow aggregation (MFA) scheme. Simulations show that NeGLt-MFA can greatly reduce spectrum consumption and has an extensive application scope.

Th2I.7 • 12:00

Routing Algorithm Based on DTN Protocols for Free-Space Optical MANET, Yufei Luo¹, Zhan Gao¹, Anhong Dang¹; ¹Peking Univ., China. Optical mobile ad-hoc networks suffer from the atmospheric turbulence. A new kind of routing algorithm based on disruption-tolerant network protocols is proposed. The proposed scheme improves the delivery ratio by 40% in severe network environment.

Th2I.8 • 12:15

Using Multi-Layer Perceptron to Estimate the OSNR of Unestablished Lightpaths, Dong Fu¹, Min Zhang¹, Bo Xu¹, Baojian Wu¹, Kun Qiu¹; ¹Univ of Electronic Science & Tech China, China. We investigate a multi-layer perceptron framework to predict the OSNR of unestablished lightpaths considering interference effects and optical monitoring uncertainties. It achieves more than 99% accuracies when the errors are less than 0.5 dB.

Th2J • Advanced Modulators—Continued

Th2J.4 • 11:45

Mach-Zehnder Modulators Based on Hybrid Silicon and Lithium Niobate Platform, mingbo he¹, Xinlun Cai¹; ¹Sun Yat-Sen Univ., China. We design and demonstrate a silicon and LN hybridly integrated Mach-Zehnder interferometer modulators. The fabricated devices show a half-wave electro-optic modulation efficiency of 2.25V.cm and data rates up to 5Gbps.

Th2J.5 • 12:00

Analysis of Ultra-High Speed Mach-Zehnder Hybrid Polymer/Sol-Gel Waveguide Modulators, Yasufumi Enami^{1,2}, Atsushi Seki³, Shin Masuda⁴, Jingdong Luo⁴, Alex Jen^{4,5}; ¹Kochi Univ. of Technology, Japan; ²College of Optical Sciences, Univ. of Arizona, USA; ³Advantest Laboratory, Japan; ⁴Chemistry, City Univ. of Hong Kong, Hong Kong; ⁵Material Science and Engineering, Univ. of Washington, USA. The bandwidth of >130 GHz for the hybrid modulators is calculated numerically and analytically based on experimentally obtained device parameters. The measured reduction of electro-optic response is 1.5 dB at a frequency of 67 GHz for the modulator with the electrode length of 5 mm.

Th2J.6 • 12:15

Unified Design Scenarios on Broadband Modulators and Polarizers with Graphene-Hybrid Silicon Waveguides, Yuan Meng¹, Shengwei Ye², Yijie Shen¹, Futai Hu¹, Rongguo Lu², Yong Liu², Mali Gong¹; ¹State Key Laboratory of Precision Measurement Technology and Instruments, Dept. of Precision Instrument, Tsinghua Univ., China; ²State Key Laboratory of Electronic Thin Films and Integrated Devices, School of Optoelectronic Information, Univ. of Electronic Science and Technology of China, China. A comprehensive analysis with unified design scenarios upon graphene-laminated silicon waveguides is presented. By judiciously designing effective mode index, versatile device functionalities can be achieved. A broadband polarization-independent amplitude modulator is also demonstrated.

Th2K • Imaging Technologies—Continued

Th2K.4 • 12:00 **Invited**

Multispectral Imaging Based on Random Dispersion Structures and Conversion Materials, Tao Yang¹, Qing-feng Geng¹, Xiao Shen¹, Xing-ao Li¹, Wei Huang¹, Ho-pui Ho²; ¹Nanjing Univ of Posts & Telecomm, China; ²Dept. of Biomedical Engineering, The Chinese Univ. of Hong Kong, Hong Kong. Spatiospectral response of random dispersion structures is used for the retrieval of 400 wavelengths over an infrared spectral range 1530-1570 nm. Transmission spectra of 4 FBGs are reconstructed with a monochromatic CCD.

Th2L • Distributed Fiber Sensing—Continued

Th2L.4 • 11:45

Processing Differential Brillouin Gain Spectrum by Support Vector Machine in DPP-BOTDA, Huan Wu¹, Liang Wang¹, zhiyong zhao², Nan Guo², Chester C.T. Shu¹, Chao Lu²; ¹The Chinese Univ. of Hong Kong, Hong Kong; ²The Hong Kong Polytechnic Univ., Hong Kong. SVM has been applied to successfully extract temperature from differential BGSs in DPP-BOTDA of different spatial resolution. Compared with LCF, SVM has better performance under high spatial resolution and low SNR with shorter processing time.

Th2L.5 • 12:00

Distributed Stress Measurement in Polarization-Maintaining Fiber Based on Polarization-OTDR, Zejia Huang¹, Chongqing Wu¹, Zhi Wang¹, Jian Wang¹, Lanlan Liu¹; ¹Beijing Jiaotong Univ., China. A novel scheme based on polarization-sensitive optical time-domain reflectometry (P-OTDR) for distributed stress measurement in polarization-maintaining fiber (PMF) is proposed with spatial resolution of 1 meter and positioning accuracy of 0.5 meter.

Th2L.6 • 12:15

Measuring Very Low Frequency with Phase-OTDR assisted by an Auxiliary Interferometer, Feng Wang¹, Quan Yuan¹, Tao Liu¹, Xuping Zhang¹; ¹College of Engineering and Applied Sciences, Nanjing Univ., China. A phase-OTDR assisted by an auxiliary interferometer is proposed. The minimum detectable frequency can reach to 0.1 Hz on a 5 km sensing fiber with 10 m spatial resolution.

12:30–14:00 Lunch

These concurrent sessions are grouped across two pages. Please review both pages for complete session information.

14:00–15:30

Th3A • Vectorial Light Sources

President: Jiajing Tu; Univ. of Science & Technology Beijing, China

Th3A.1 • 14:00 **Invited**

Square-wave Dynamics in the Er:Yb-doped Double-clad Fiber Laser, yichang meng^{1,2}, Georges Semaan¹, Fatma Benbrahim^{1,4}, Meriem Kemel¹, Mohamed Salhi¹, Andrey Komarov³, Francois . Sanchez¹; ¹Universite d'Angers, France; ²School of Sciences, Hebei Univ. of Science and Technology, China; ³Russian Academy of Sciences, Russia; ⁴Université de Carthage, Tunisia. We have experimentally demonstrated dissipative soliton resonance (DSR) in double-clad Er:Yb-doped fiber lasers with dual amplifier figure-of-eight and ring cavity. In anomalous dispersion regime, different features of DSR are demonstrated.

Th3A.2 • 14:30

Low threshold tunable 2 μm optical vortex laser source, Roukuya Mamuti¹, Shungo Araki¹, Katsuhiko Miyamoto^{1,2}, Takashige Omatsu^{1,2}; ¹Chiba Univ., Japan; ²Molecular chirality research center, Chiba Univ., Japan. We report on a tunable 2 μm optical vortex laser source formed of a periodically poled stoichiometric lithium tantalate (PPSLT) optical parametric oscillator with a singly-resonant cavity configuration. A milli-joule level vortex output was generated at a low lasing threshold (1.2 mJ), with its wavelength being tuned within a range of 1.85-2.03 μm.

14:00–15:30

Th3B • High-field Technologies

President: Dangyuan Lei; The Hong Kong Polytechnic Univ., Hong Kong

Th3B.1 • 14:00 **Invited**

Short-scale Photon-phonon Interactions, Birgit Stiller¹, Moritz Merklein¹, Benjamin Eggleton¹; ¹Univ. of Sydney, Australia. Using photon-phonon interactions, we experimentally demonstrate the storage of 200ps-long optical pulses for over 70 pulse widths. We moreover show that this concept is suitable for the non-reciprocal storage at multiple optical wavelengths.

Th3B.2 • 14:30

Relativistic high-order harmonic generation from laser plasmas using few-cycle laser pulses, Guangjin Ma^{1,2}, Dmitrii Kormin³, Chunlai Li², Zhiping Zhou¹, Jin He^{1,2}, Laszlo Veisz^{3,4}; ¹School of Electronics Engineering and Computer Science, Peking Univ., China; ²Shenzhen SoC Key Laboratory, PKU-HKUST Shenzhen-Hong Kong Institution, China; ³Max-Planck-Institut fuer Quantenoptik, Germany; ⁴Dept. of Physics, Umea Univ., Sweden. We investigate relativistic high-order harmonic generation from intense few-cycle laser and plasma interactions via particle-in-cell simulations. Differences of spectral and temporal structures in XUV beam resulted from few-cycle and non-few-cycle driver pulses are compared.

14:00–15:30

Th3C • Germanium Modulators and Ge Photonics

President: Linjie Zhou; Shanghai Jiao Tong Univ., China

Th3C.1 • 14:00

High-contrast quantum-confined Stark effect in Ge/SiGe quantum well stacks on Si with ultra-thin buffer layers, Srinivasan Ashwyn Srinivasan^{1,2}, Clement Porret¹, Ewoud Vissers¹, Pieter Geiregat², Dries VanThourhout^{1,2}, Roger Loo¹, Marianna Pantouvaki¹, Joris Van Campenhout¹; ¹imec, Belgium; ²Univ. of Ghent, Belgium. Quantum-confined Stark effect with a record absorption contrast of 2.5 for 1V swing is demonstrated in Ge/GeSi quantum well stacks grown on Si using ultra-thin buffer layers, targeting future integration in a silicon photonics platform.

Th3C.2 • 14:15

56 Gb/s Si/GeSi Optical Modulator, Lorenzo Mastronardi¹, Mehdi Banakar¹, Ali Khokhar¹, Nannicha Hattasan¹, Teerapat Rutirawut¹, Thalia Dominguez Bucio¹, Kasia Grabska¹, Callum Littlejohns^{1,2}, Alexandre Bazin¹, Goran Mashanovich¹, Frederic Gardes¹; ¹Univ. of Southampton, UK; ²Silicon Technologies Centre of Excellence, NTU, Singapore. We present experimental measurements of an EAM modulator developed on an 800 nm SOI platform. Measurements show a dynamic ER of 5.2 dB at 56 Gb/s at 1566 nm and power consumption of 44 fJ/bit.

Th3C.3 • 14:30

Optical Waveguides by Germanium Ion Implantation on Silicon-on-Insulator Platform, Xia Chen¹, Milan M. Milosevic¹, Ali Khokhar¹, David Thomson¹, Graham Reed¹; ¹Univ. of Southampton, UK. We demonstrated a new type of integrated photonic waveguides formed by Ge ion implantation in the silicon slab on silicon-on-insulator platform. They were successfully fabricated and characterised, and can be potentially erased by laser annealing.

14:00–15:30

Th3D • Power Scaling and Plasmonics

President: Sui Zhan; China Academy of Engineering Physics, China

Th3D.1 • 14:00

Detection of histamine using molecular imprinted hydrogel coated SPR based fiber optic probe, Vivek Semwal¹, Banshi D. Gupta¹; ¹Indian Inst. of Technology, Delhi, India. In the present study, we report a surface plasmon resonance based fiber optic sensor for histamine detection utilizing molecular imprinted hydrogel as a sensing layer. The sensor works in the range 1-10 μM histamine concentration.

Th3D.2 • 14:15

Potassium ion-selective SPR sensor based on GO-chitosan nanocomposite for agriculture application, Banshi D. Gupta¹, Anisha Pathak¹, Vivek Semwal¹; ¹Indian Inst. of Technology, Delhi, India. Fabrication and characterization of a fiber optic potassium ion sensor based on surface plasmon resonance using 18-crown-6 doped GO-chitosan nanocomposite have been carried out for soil nutrients. The sensor operates in the range 0-200 μM.

Th3D.3 • 14:30

Preparation Progress of Low-NA Yb Doped Large Mode Area Silica Fiber Origin From Sol-Gel Method, Chunlei Yu¹; ¹Shanghai Inst of Optics & Fine Mechanics, China. The progress of Low refractive index Yb doped silica core glass origin from sol-gel method and the application on LMA PCF fiber is introduced.

14:00–15:30

Th3E • Waveguide Devices II

President: Xin Gai; City Univ. of Hong Kong, Hong Kong SAR

Th3E.1 • 14:00 **Invited**

UWB Signal Processing Based on Silicon Photonic Integrated Circuits, Ke Xu¹; ¹College of Chemistry, Univ. of California Berkeley, USA. Abstract not available.

Th3E.2 • 14:30 **Invited**

Detailed characterization of free-carrier generation and recombination in silicon nano-waveguides, Paulo C. Dainese¹; ¹Univ. of Campinas, Brazil. We review recent results on free-carrier dynamics in silicon nano-waveguides. Linear and nonlinear generation rates are accurately characterized, while the recombination dynamics is observed to be dominated by a trap-assisted mechanism.

14:00–15:30

Th3F • Integrated Microwave Photonics II

President: Guillermo Carpintero; Universidad Carlos III de Madrid, Spain

Th3F.1 • 14:00 **Invited**

An Integrated Optoelectronic Oscillator, Ming Li¹; ¹Inst. of Semiconductor, CAS, China. In this paper, we proposed and experimentally demonstrate a novel integrated OEO, in which the optical parts are manufactured using a monolithically integrated InP technology platform and the electrical part assembles on a single PCB.

Th3F.2 • 14:30 **Invited**

Chip-based Reconfigurable Microwave Photonic Filter and Time Delay Line, Simin Li¹, Jing Feng¹, Shilong Pan¹; ¹Nanjing Univ. Aeronaut. Astronaut., China. We propose an approach to realize a reconfigurable microwave photonic filter and time delay line using a single optical micro-ring resonator (MMR). Based on the multi-wavelength single sideband modulation, the MMR responses are mapping to microwave frequency with tunable center frequency and magnitude.

These concurrent sessions are grouped across two pages. Please review both pages for complete session information.

14:00–15:30

Th3G • Structured 2D Surfaces

Presider: Arno Rauschenbeutel, Humboldt-Universität zu Berlin, Germany

Th3G.1 • 14:00 **Tutorial**

Ultrathin Structured 2D Surfaces: Hybridizing 2D Materials & Metasurfaces, Chengwei Qiu¹; ¹National Univ. of Singapore, Singapore. Interfacial engineering via artificially constructed nanostructures hold great potentials for advanced light-matter interactions. I will discuss the fundamental and emerging results for meta-photonic devices by hybridizing metasurfaces and 2D materials.

14:00–15:30

Th3H • Entanglement and Squeezed States I

Presider: Jin-Shi Xu; Univ of Science and Technology of China, China

Th3H.1 • 14:00 **Invited**

Engineering Narrowband Biphotons, Shengwang Du¹; ¹Hong Kong Univ of Science & Technology, Hong Kong. We describe quantum state engineering of narrowband biphotons in diverse degrees of freedom, including time frequency, polarization, and position momentum. These biphotons are produced from spontaneous four-wave mixing in atomic ensembles.

Th3H.2 • 14:30

Periodic suppression and enhancement of spontaneous two-photon emission via interference, Dong-Gil Im¹, Yosep Kim¹, Yoon-Ho Kim¹; ¹Dept. of physics, POSTECH, Korea. We demonstrate that an effective boundary condition can be introduced to spontaneous two-photon emission by making use of a continuous-wave multi-mode pump. This effect results in periodic suppression and enhancement of spontaneous two-photon emission via interference over the pump coherence length.

14:00–15:30

Th3I • Signal Processing for Optical Transmsison

Presider: Jian Zhao; South China Univ. of Technology, China

Th3I.1 • 14:00

Performance improvement of ACO-OFDM system using OCT precoding combined with digital peak-clipping, Siyi Dong¹, J He¹, Ming Chen², Qinghui Chen¹, Rui Deng¹, Jie Ma¹, Lin Chen¹; ¹Hunan Univ., China; ²Hunan Normal Univ., China. Orthogonal circulant matrix transform precoding (OCT) combined with peak-clipping based PAPR reduction technique is firstly proposed for ACO-OFDM system and experimentally demonstrated in an IM/DD system with a cost-efficient directly modulated laser.

Th3I.2 • 14:15

Enhanced LDPC based differential iteration decoding Scheme for PDM 16-QAM Coherent Optical Communication Systems, Wenxiang Cao¹, J He¹, Zhihua Zhou¹; ¹Hunan Univ., China. An enhanced LDPC based differential iteration decoding scheme is applied in 400-Gb/s PDM 16-QAM coherent optical communication systems. The simulation results show that, the system performance can be greatly improved by using the proposed method.

Th3I.3 • 14:30

Performance of Opto-Electronic Phase Conjugation in Intensity-Modulated Signal Transmission Systems, Masayuki Matsumoto¹, Shinogu Takeda¹; ¹Wakayama Univ., Japan. Spectral inversion of intensity-modulated signals by an opto-electronic phase conjugator is demonstrated. It is shown that broad-linewidth (30MHz) DFB laser can be used as the local oscillator (LO) and frequency difference between the signal and LO as large as 14GHz is tolerated.

14:00–15:30

Th3J • 2D and Metamaterial

Presider: Howard Lee; Baylor Univ., USA

Th3J.1 • 14:00 **Invited**

Mid-infrared Optoelectronics in 2D Materials, Qijie Wang¹, Xuechao Yu¹, Alexander Dubrovkin¹; ¹Nanyang Technological Univ., Singapore. In this talk, I am going to present our recent research in applying 2D materials for applications in the mid-infrared regime, such as room temperature broadband 2D material based photodetectors and ultraconfined phonon polariton devices.

Th3J.2 • 14:30 **Invited**

Integration and Nonlinearity of 2D Materials with Silica Microfibers, Fei Xu¹; ¹Nanjing Univ., China. We will show several kinds of two-dimensional-material-microfiber-integrated devices and the optoelectronic and nonlinear applications (e.g., second harmonic generation and detector) will also be discussed.

14:00–15:30

Th3K • Microscopy

Presider: Chao Zuo; Nanjing Univ of Science and Technology, China

Th3K.1 • 14:00 **Invited**

Recent Technology Development in Optical Diffraction Tomography for 3D Cell Imaging, Renjie Zhou¹; ¹The Chinese Univ. of Hong Kong, Hong Kong. Optical diffraction tomography (ODT) is becoming an important cell imaging tool. To enable more biomedical imaging applications, we are recently developing more advanced ODT systems that have high imaging speed as well as depth selectivity.

Th3K.2 • 14:30

Probing and Imaging Vectorial Optical Field by Heterodyne Near-field Microscopy and Nanopolarimetry, Benfeng Bai¹, Lin Sun¹, Tong Cui¹, Jia Wang¹; ¹Tsinghua Univ., China. We report near-field microscopic theory and methods that employ heterodyne technique and nanopolarimetry for probing and imaging vectorial features of optical field in nanostructures, including the spin-orbit interaction and magnetic field component of optical field.

14:00–15:30

Th3L • Novel Fiber Structures

Presider: Guiyao Zhou; South China Normal Univ., China

Th3L.1 • 14:00 **Invited**

A Novel Structure of Microfiber-based Sensor for Onsite/in-situ Detection of Heavy Metal Ions, Xuping Zhang¹, Wenbin Ji¹, Stephanie H. Yap², Guanghui Wang¹, Yi Xin Zhang¹, Ken Tye Yong², Sweechuan tjin²; ¹Nanjing Univ., China; ²Nanyang Technological Univ., Singapore. We propose a novel sensing structure for onsite/in-situ detection of heavy metal ions based on a non-adiabatic microfiber sandwiched by two fiber Bragg gratings (FBG). The surface of the microfiber is functionalized with chelating agent.

Th3L.2 • 14:30

Relative Humidity Measurement Based On Micro Fiber with Quantum Dot gel coating, Siqi Hu¹, Guofeng Yan², Chunzhou Wu¹, Sailing He¹; ¹Zhejiang Univ., China; ²Zhejiang Lab, China. A optical fiber relative humidity sensor based on a microfiber with quantum dot gel coating was proposed and experimentally demonstrated. The RH Sensitivity of 37.7 %/RH was obtained with good repeatability.

These concurrent sessions are grouped across two pages. Please review both pages for complete session information.

Th3A • Vectorial Light Sources—Continued

Th3A.3 • 14:45

Tunable repetition rate mode-locked all-fiber laser with cylindrical-vector beams output, Ruishan Chen¹, Junna Yao¹, Fangling Sun¹, Jinghao Wang¹, Anting Wang¹, Hai Ming¹; ¹Dept. of Optics and Optical Engineering, Univ of Sci & Tech of China, China. We propose and demonstrate a mode-locked all-fiber cylindrical-vector beam (CVB) laser with high efficiency and tunable repetition rate. By controlling the intra-cavity polarization states, both azimuthally polarized and radially polarized beams are selectively obtained under harmonic mode-locking (HML) states.

Th3A.4 • 15:00

All-fiber actively Q-switched cylindrical vector beam laser based on a mode selective coupler, Tiantian Ruan¹, Hongdan Wan¹, Jie Wang¹, Zuxing Zhang¹, Lin Zhang¹; ¹Nanjing Univ. of Posts&telecomm, China. High purity, pulsed cylindrical vector beams (CVBs) can be generated by using a mode selective coupler (MSC) as the transverse mode converter and mode splitter in an all-fiber actively Q-switched fiber laser

Th3A.5 • 15:15

Power- and Frequency-Scalable Modulation of the Optical Orbital Angular Momentum, Jean-Francois Bisson¹, Katsuhiko Miyamoto², Takashige Omatsu²; ¹Universite de Moncton, Canada; ²Graduate school of Engineering, Chiba Univ., Japan. We present a device that can modulate the orbital angular momentum (AOM) of a laser beam. The proposed design can be scaled up to several GHz using existing commercial devices.

Th3B • High-field Technologies—Continued

Th3B.3 • 14:45

Spatiotemporal analysis of XUV pulse generation in gas HHG, Lifeng Wang¹, Hao Li¹, Ying Zhang¹; ¹SIMTech, Singapore. We numerically analyze spatiotemporal profile of HHG. A detailed physical picture of HHG over four-dimensional spatiotemporal spaces is studied for the first time, which may benefit potential applications like super-resolution XUV imaging, XUV tweezer.

Th3B.4 • 15:00

Phase-matched soft x-ray high-order harmonics driven by loosely focused TW femtosecond infrared pulses, Kotaro Nishimura^{1,2}, Yuxi Fu¹, Akira Suda², Katsumi Midorikawa¹, Eiji J. Takahashi¹; ¹Attosecond Science Research Team, RIKEN Center for Advanced Photonics, Japan; ²Dept. of Physics, Tokyo Univ. of Science, Japan. We generate high-flux soft x-ray phase-matched high-order harmonics driven by loosely focused 80-mJ, 45-fs, 1.55- μ m infrared pulses. The maximum harmonic photon energies attained are 270 and 350 eV in Ne and He, respectively.

Th3B.5 • 15:15

Controlled HHG with a Sub-Cycle mJ-Level Parametric Waveform Synthesizer, Roland E. Mainz^{1,2}, Yudong Yang^{1,2}, Giulio Maria Rossi^{1,2}, Fabian Scheiba^{1,2}, Giovanni Cirmi^{1,2}, Franz Kaertner^{1,2}; ¹Center for Free-Electron Laser Science, Germany; ²Physics Dept. and CUI, The Hamburg Centre for Ultrafast Imaging, Germany. We present high-harmonic generation (HHG) driven with a sub-cycle mJ-level parametric waveform synthesizer. The HHG yield and spectral shape can be controlled by varying the carrier-envelope phase and the relative phase in the synthesizer channels.

Th3C • Germanium Modulators and Ge Photonics—Continued

Th3C.4 • 14:45

Invited

Mid-infrared Germanium Photonic Integrated Circuits for on-chip Biochemical Sensing, Zhenzhou Cheng¹, Ting-Hui Xiao¹, Ziqiang Zhao¹, Wen Zhou², Mitsuru Takenaka¹, Hon K. Tsang², Keisuke Goda¹; ¹The Univ. of Tokyo, Japan; ²The Chinese Univ. of Hong Kong, Hong Kong. We report our recent progress on mid-infrared germanium photonic integrated circuits. Specifically, a suspended-membrane waveguide, focusing subwavelength grating coupler, microring resonator, and photonic crystal nanocavities are demonstrated based on a germanium-on-insulator wafer.

Th3C.5 • 15:15

Mid-Infrared Photonic Technology on Silicon-on-Insulator (SOI) Platform, Hong Wang¹; ¹Nanyang Technological Univ., Singapore. Development of Si-photonics devices covering the MIR range based on SOI platform is reported. A new Ge-on-silicon nitride platform for the applications beyond the wavelength of 3.8 μ m will also be discussed.

Th3D • Power Scaling and Plasmonics—Continued

Th3D.4 • 14:45

High power all-fiberized oscillator based on tapered fiber, Hanwei Zhang¹, Baolai Yang¹, Xiaolin Wang¹, Chen Shi¹, Pu Zhou¹, Xiaojun Xu¹; ¹National Univ. of Defense Technology, China. In this letter, we demonstrate a high power all-fiberized, tapered Yb-doped fiber based oscillator for the first time. The output laser is more than 260 W with fundamental mode operation and further power increasing is possible.

Th3D.5 • 15:00

Invited

High Power Mid-infrared Supercontinuum Sources: Current Status and Future Perspectives, Deepak Jain¹, Ole Bang^{1,2}; ¹DTU Fotonik, Denmark; ²NKT Photonics, Denmark. Mid-infrared fiber based supercontinuum sources have great potential for several applications. This paper reviews their current status of power scaling and discusses the challenges and future development in power scaling.

Th3E • Waveguide Devices II—Continued

Th3E.3 • 15:00

Multi-Photon Fabrication of Ultra-compact Optical Waveguides in Polydimethylsiloxane, Ye Pu¹, Giulia Panusa¹, Jieping Wang¹, Christophe Moser¹, Demetri Psaltis¹; ¹Ecole Polytechnique Federale de Lausanne, Switzerland. We demonstrate the fabrication of ultra-compact, low-loss optical waveguides in polydimethylsiloxane through multiphoton polymerization, without a photoinitiator, using laser direct writing. The transmission loss was measured 0.03 dB/cm in the 650-700 nm band.

Th3E.4 • 15:15

Depressed circular cladding waveguide lasers in Nd:YAG crystal inscribed by femtosecond laser, Shi-Ling Li¹; ¹Qufu Normal Univ., China. Depressed cladding waveguides were fabricated in Nd:YAG crystals with a loss of 0.40 dB/cm. They showed laser operation at 1064 nm. Multi- and single-modes waveguide lasers were realized. A slope efficiency of 32.6% was obtained.

Th3F • Integrated Microwave Photonics II—Continued

Th3F.3 • 15:00

Integrated Kerr optical frequency comb-based broadband RF channelizer, Xingyuan Xu¹, Jiayang Wu¹, Thach Nguyen², Sai Tak Chu³, Brent E. Little⁴, Roberto Morandotti⁵, Arnan Mitchell², David Moss¹; ¹Swinburne Univ. of Technology, Australia; ²RMIT Univ., Australia; ³City Univ. of Hong Kong, Hong Kong; ⁴Chinese Academy of Science, China; ⁵INRS, Canada. A broadband RF channelizer based on an integrated micro-comb source is demonstrated, with 19GHz RF bandwidth and spectral slice resolution of 1.04 GHz. This approach offers reduced complexity and potential cost for microwave signal detection.

Th3F.4 • 15:15

A Tunable Microwave Frequency Multiplication System Based on Injection Locking without Photodetector, Shuaishuai Wang¹, Ju Wang¹, Tianyu Li¹, Chuang Ma¹, Tianyuan Xie¹, Yang Yu¹, Jinlong Yu¹; ¹Tianjin Univ., China. Using a directly modulated laser to injection locking the high-order sideband of modulated light, multiplication frequency is detected at its radio frequency port. Instead of employing photodetector, the proposed tunable frequency multiplication system costs low obviously.

15:30–16:00 Coffee Break

These concurrent sessions are grouped across two pages. Please review both pages for complete session information.

Th3G • Structured 2D Surfaces—Continued

Th3G.2 • 15:00 **Invited**
2D Materials for Inkjet Printing of Optoelectronics and Photonics, Meng Zhang¹, Tawfique Hasan²; ¹Beihang Univ., China; ²Univ. of Cambridge, UK. We present printable and uniform optical saturable absorber devices fabricated using inkjet-printing technique for high performance ultrafast laser sources. Such fabrications technique significant expand the scope for achieving mass-production, low-cost photonic and optoelectronic devices.

Th3H • Entanglement and Squeezed States I—Continued

Th3H.3 • 14:45
Experimental observation of quantum correlations between measurement errors using entangled photon pairs as a probe, Masataka Iinuma¹, Yutaro Suzuki², Masayuki Nakano¹, Holger Hofmann¹; ¹Hiroshima Univ., Japan; ²Kyoto Univ., Japan. We experimentally observed a quantum correlation between two measurement errors in a joint measurement by using entangled photon pairs as a probe. The results obtained exceed the limits of classical statistics.

Th3H.4 • 15:00
Quantum interferometric spectroscopy, Rui-Bo Jin¹, Ryosuke Shimizu²; ¹Wuhan Inst. of Technology, China; ²The Univ. of Electro-Communications, Japan. The difference- and sum-frequency distribution of the biphoton wavefunctions were extracted by applying a Fourier transform on the time-domain Hong-Ou-Mandel interference (HOMI) and the NOON state interference (NOONI) patterns.

Th3H.5 • 15:15
Closed-Loop Operation of Optical Lattice Clock at National Time Service Center, Qinfang Xu¹, Mojuan Yin¹, Yebing Wang¹, Jie Ren¹, Yang Guo¹, Hong Chang¹; ¹National Time Service Center, China. The Hz-level spectroscopy of ⁸⁷Sr clock transition in an optical lattice is demonstrated. The fractional frequency difference averages of ⁸⁷Sr optical lattice clock is achieved to 6×10^{-17} at an average time of 3000 s.

Th3I • Signal Processing for Optical Transmissions—Continued

Th3I.4 • 14:45
DFT-spread Combined with Pre-compensation scheme for UWB-over-fiber System, Changqing Xiang¹, J He¹, Kaiquan Wu¹, Yaoqiang Xiao¹; ¹Hunan Univ., China. A DFT-spread combined with pre-compensation scheme is proposed in 64QAM MB-OFDM UWBoF system. By using it, the simulation results show that transmission performance of system improves by 3.3dB compared to that without DFT-spread and pre-compensation.

Th3I.5 • 15:00
High Stability Frequency Transfer over a 35 km Fiber Link Based on Injection-Locked OEO, Yang Yu¹, Jinlong Yu¹, Zixiong Wang¹, Ju Wang¹, Tianyuan Xie¹, Chuang Ma¹; ¹Tianjin Univ., China. A 10 GHz frequency transfer experiment was realized over a 35 km fiber link. An injection-locked optoelectronic oscillator was used in the remote site for stabilization of the phase noise.

Th3I.6 • 15:15
Multiple-User SC-FDMA System with Sub-Nyquist Receiver and PAPR Reduction, Hao-Hsiang Chang¹, Wen-Huang Chen¹, Chao-Wei Chen¹; ¹National Chiao Tung Univ., Taiwan. We demonstrate 43.63-Gbps SC-FDMA with 0.5-GSample/s sampling-rate receiver for each 32-user. Meanwhile, PAPR reduction is included in the proposed SCFDMA system. We also compare results with L-FDMA, LFDMA, and OFDM utilizing high sampling-rate ADC.

Th3J • 2D and Metamaterial—Continued

Th3J.3 • 15:00
Spectral Line Shape and Modulation Response of Asymmetric Non-Hermitian Photonic Meta-Molecules, Anastasios Bountis¹; ¹Nazarbayev Univ., Kazakhstan. A photonic dimer of two optically coupled lasers is analyzed as an optical meta-molecule for non-Hermitian photonic applications. Spectral signatures of exceptional points and Hopf bifurcations are shown for generic asymmetric configurations. A significant enhancement in the small signal modulation response under differential pumping is observed.

Th3J.4 • 15:15
The Comparative Aging Study for Different Co-precipitation Methods of Quantum Dots in NaCl Solids, Yu-Ming Huang¹, Chung-Ping Yu¹, Li-Ann Ke¹, Chung-Ping Huang³, Shu-Hsiu Chang², Chien-Chung Lin¹; ¹Inst. of Photonic System, National Chiao-Tung Univ., Tainan, Taiwan.; ²Inst. of Imaging and Biomedical Photonics, National Chiao-Tung Univ., Taiwan; ³Inst. of Lighting and Energy Photonics, National Chiao-Tung Univ., Taiwan. A comparative study about colloidal quantum dot and NaCl co-precipitation methods was set up. After the 300-hour aging tests, the samples made by saturated-salt method is better in terms of degradation and spectral characteristics.

Th3K • Microscopy—Continued

Th3K.3 • 14:45
A programmable time-stretch microscopy based on dispersion-tuned swept laser, Xin Dong¹, Xi Zhou¹, Chi Zhang¹, Xinliang Zhang¹; ¹Wuhan National Lab for Optoelectronics, China. Dispersion-tuned swept laser (DTSL) is applied to the ultrafast time-stretch microscopy for the first time, and achieves large and programmable time-stretch ratio with minimum dispersion and suitable modulation frequency within the laser cavity.

Th3K.4 • 15:00
Imaging biological specimens and advanced materials with correlative far-field near-field microscopy, Stefan G. Stanciu¹, Denis E. Tranca¹, Catalin Stoichita¹, Radu Hristu¹, George A. Stanciu¹; ¹Universitatea Politehnica din Bucuresti, Romania. We discuss an imaging approach that allows a better understanding of nanoscale datasets collected with Apertureless Scanning Near-Field Optical Microscopy, based on a multimodal system that incorporates multiple ASOM and far-field Laser Scanning Microscopy variants.

Th3K.5 • 15:15
Spurious Transmission in Liquid Crystal Tunable Filter Operation in Microscopy, Wynn Dunn Gil Improso¹, Paul Leonard Atchong C. Hilario², Giovanni A. Tapang¹; ¹National Inst. of Physics, Philippines; ²Electrical and Electronics Engineering Inst., Univ. of the Philippines Diliman, Philippines. We investigate the effect of incidence angle to the transmitted power of a liquid crystal tunable filter (LCTF) with a 632nm laser source. Spurious transmission in other wavelengths was observed in non-normal incidence angles

Th3L • Novel Fiber Structures—Continued

Th3L.3 • 14:45
Enhanced Nanoparticle Detection with Quasi-droplet Modes, Jonathan Ward¹, Fuchuan Lei¹, Sile Nic Chormaic¹; ¹Okinawa Inst of Science & Technology, Japan. We demonstrate nanoparticle sensing with quasi-droplet modes in an ultrathin-walled hollow whispering gallery resonator. Experimental results show 400 MHz mode shifts for interaction with 100 nm particles and a corresponding linewidth broadening of 75 MHz.

Th3L.4 • 15:00
Ultra-Low-Loss Spliceless Fiber Ring Resonators for Resonant Micro-Optic Gyroscopes, Yi Lin¹, Huihan Ma¹, Zhonghe Jin¹; ¹School of Aeronautics and Astronautics, Zhejiang Univ., China. A new record for ultra-low-loss spliceless fiber ring resonators, to the best of our knowledge, is demonstrated experimentally. The measured finesse and Q-factor of the 60-cm long fiber ring resonator are 1324 and 3.7×10^5 , respectively.

Th3L.5 • 15:15
Sub-nano-Tesla, Shield-less, Field Compensation-Free Inelastic Wave Mixing Magnetometry for Bio-magnetism, Lu Deng¹, Yvonne Y. Li², Feng Zhou¹, Eric Y. Zhu³, Edward W. Hagley¹; ¹National Inst of Standards & Technology, USA; ²Harvard Medical School, Dana-Farber Cancer Inst., USA; ³Electrical Engineering, Univ. of Toronto, Canada. We report an inelastic-wave-mixing-enhanced Zeeman-coherence atomic magnetometry scheme that results in sub-nT magnetic field detection at human-body temperatures without employing magnetic field shielding, field compensation, and RF-modulation spectroscopy.

15:30–16:00 Coffee Break

These concurrent sessions are grouped across two pages. Please review both pages for complete session information.

16:00–18:00

Th4A • Characteristics of Shortpulse Lasers

Presider: Zhi-Chao Luo; South China Normal Univ, China

Th4A.1 • 16:00

Ultra-Compact Frequency-Stabilized Lasers at Visible Wavelengths, Kazumichi Yoshi^{1,2}, Yusuke Hisai^{1,2}, Junia Nomura^{1,2}, Feng-Lei Hong^{1,2}; ¹Yokohama National Univ., Japan; ²JST, ERATO, MINOSHIMA Intelligent Optical Synthesizer Project, Japan. We have developed iodine-stabilized lasers using ultra-compact diode laser modules at 531, 561 and 594 nm. The achieved frequency stabilities were typically 4×10^{-13} at an averaging time of 1000 s.

Th4A.2 • 16:15

256 MHz, 1 W femtosecond fiber laser at 780 nm for two-photon microscopy, Wan Yang¹, Danlei Wu^{1,2}, Guanyu Liu¹, Bingying Chen¹, Lishuang Feng², Zhigang Zhang¹, Aimin Wang¹; ¹Peking Univ, China; ²Beihang Univ., China. A robust 780 nm femtosecond fiber laser was demonstrated with 191 fs pulse width, 256 MHz repetition rate and 1 W average power. It is ideal for two-photon microscopic imaging.

Th4A.3 • 16:30

Stable and Synchronized Time-lens Source for Real-Time Characterization of Noise-Like Pulses, Bowen Li¹, Jiqiang Kang¹, Ying Yu¹, Pingping Feng¹, Kenneth Kin-Yip Wong¹; ¹Univ. of Hong Kong, Hong Kong. Stable and synchronized reference pulses are generated from a time-lens source, triggered by noise-like pulses in a mode-locked fiber laser. This represents an essential step towards single-shot measurement of temporal details inside the noise-like pulses.

16:00–18:00

Th4B • Nonlinear Optical Technologies

Presider: Birgit Stiller; Univ. of Sydney, Australia

Th4B.1 • 16:00 **Invited**

Dissipative polarization domain walls as persisting topological defects, Stephane Coen^{1,2}, Bruno Garbin^{1,2}, Julien Fatome¹, Yandong Wang^{1,2}, François Leo⁴, Gian-Luca Oppo⁵, Stuart G. Murdoch^{1,2}, Miro J. Erkintalo^{1,2}; ¹Physics, The Univ. of Auckland, New Zealand; ²The Dodd-Walls Centre, New Zealand; ³Université de Bourgogne Franche-Comté, France; ⁴Université Libre de Bruxelles, Belgium; ⁵Univ. of Strathclyde, UK. We experimentally demonstrate the existence of dissipative polarization domain walls in a normally dispersive Kerr resonator. We excite and trap them with appropriate external signals thus realizing an all-optical buffer for topological data.

Th4B.2 • 16:30

Self-Focusing Suppression in Ultrahigh-Intensity Lasers, Efim A. Khazanov¹, Vald Ginzburg¹, Anton Kochetkov¹; ¹Inst. of Applied Physics, Russia. We experimentally confirmed that free space run acts as a spatial filter and drastically suppresses small-scale self-focusing in laser beam with intensity order of TW/cm^2 . The measurements were done by two independent techniques.

16:00–18:00

Th4C • Novel Laser System and its Applications

Presider: DongSheng Ding; Univ. of Science and Technology of China, China

Th4C.1 • 16:00 **Invited**

High Power 2 μm Fiber Laser and its Applications, Xia Yu¹; ¹Precision Measurements Group, Singapore Inst. of Manufacturing Technology, Singapore. We report our work on high power thulium-doped fiber lasers at 2 μm , including high repetition rate high average power laser based on resonant pumping, high-energy laser based on CPA and medium power CW lasers.

Th4C.2 • 16:30

High Temperature Operation of Integrated Optical Fiber, Christopher Holmes¹, Paul Gow¹, Alex Jantzen¹, Alan Gray¹, Senta Scholl¹, James gates¹, Peter Smith¹; ¹Univ. of Southampton, UK. Integrated optical fiber is a planarized format, enabling ruggedized integrated functionality for silica optical fiber. This work is the first demonstration showing the platform's operation at temperatures exceeding 1000°C.

16:00–18:00

Th4D • High Power CW Lasers and Coherent Combining

Presider: Wenn Jing Lai; Nanyang Tech Univ., China

Th4D.1 • 16:00 **Invited**

Advances in High Power Beam Combinable Fiber Lasers, Pu Zhou¹; ¹National Univ of Defense Technology, China. We will review the research progress on high power beam combinable fiber lasers, then we will demonstrate our recent progress in our group: a 4 kW level narrow-linewidth fiber laser based on tandem pumping scheme.

Th4D.2 • 16:30

Quantum Limits of Coherent Beam Combining, Gerd Leuchs^{2,3}, Christian R. Mueller¹, Florian Sedlmeir¹, Sourav Chatterjee¹, Nicoletta Haarlammert⁴, Cesar Jauregui⁵, Thomas Schreiber⁴, Jens Limpert⁵, Andreas Tünnermann^{4,5}, Christoph Marquardt^{1,2}; ¹Max Planck Inst. for the Science of Light, Germany; ²Physics, Univ. Erlangen-Nürnberg, Germany; ³Inst. of Applied Physics, Russian Academy of Sciences, Russia; ⁴Fraunhofer Inst. for Applied Optics and Precision Engineering, Germany; ⁵Inst. of Applied Physics, Univ. of Jena, Germany. We report the first quantum mechanical noise limit calculations for coherent beam combining and compare our results to quantum-limited amplification. We highlight a favourable noise scaling for both pure and noisy input states.

16:00–18:00

Th4E • Plasmon-enhanced Spectroscopies and Imaging

Presider: Dangyuan Lei; The Hong Kong Polytechnical Univ., Hong Kong

Th4E.1 • 16:00 **Invited**

Harnessing Surface Plasmons with Structured-surface and Structured-light, Xiaocong L. Yuan¹; ¹Shenzhen Univ., China. In this presentation, structured surfaces and structured light are introduced to manipulate SPPs with more degrees of freedom, yielding many attractive techniques such as super-resolved imaging, ultra-high sensitive bio-sensing, surface-enhanced Raman spectroscopy.

Th4E.2 • 16:30

Plasmono-Atomic Interactions at the Fiber Tip, Eng Aik Chan¹, Giorgio Adamo¹, Syed Abdullah Aljunid¹, Martial Ducloy^{1,3}, David Wilkowski¹, Nikolay Zheludev^{1,2}; ¹Nanyang Technological Univ, Singapore; ²Univ. of Southampton, UK; ³Univ. Paris13, France. Plasmono-atomic interaction affecting hyperfine structure of atomic lines can be detected at the end of optical fiber bearing metamaterial nanostructure which paves the way for a new type of ultra-compact fiberized atoms-metamaterial devices.

16:00–18:00

Th4F • Radio Over Fiber and Optical Wireless Communication

Presider: Kun Zhu; The Hong Kong Polytechnical Univ., Hong Kong

Th4F.1 • 16:00 **Invited**

Highly stable dissemination of microwave and millimeter wave signals over fiber-optic links, Yi Dong¹, Weilin Xie¹, Wei Wei¹, Zhanguwei Li¹, Xiaocheng Wang¹, Nan Deng¹; ¹Beijing Institute of Technology, China. Highly stable microwave and millimeter wave signal dissemination over fiber-optic links is realized based on the transfer of high frequency optically-carried signals relying on the microwave photonics assisted precise phase and frequency discrimination and control.

Th4F.2 • 16:30 **Invited**

Power-over-Fiber for Radio-over-Fiber-Based Distributed Antenna Systems, Motoharu Matsuura¹; ¹Graduate School of Informatics and Engineering, Univ. of Electro-Communications, Japan. Power-over-fiber is one of the essential technologies for simultaneously transmitting data and power in a same optical fiber. This paper introduces power-over-fiber towards practical applications of radio-over-fiber-based distributed antenna systems for future mobile networks.

These concurrent sessions are grouped across two pages. Please review both pages for complete session information.

16:00–18:00

Th4G • 2D Photonics Devices

Presider: Han Zhang, Shenzhen Univ., China

Th4G.1 • 16:00 **Invited**

Two-Dimensional Layered Materials/Silicon Heterojunctions for Energy and Optoelectronic Applications, Jiansheng Jie¹; ¹*Inst. of Functional Nano and Soft Materials Laboratory (FUNSOM), Soochow Univ., China*. We report investigation on 2D layered material/silicon heterojunction based photovoltaic and optoelectronic devices to solve the problem of low light absorption of monolayer materials as well as difficulties in controllable doping and p-n junction fabrications.

Th4G.2 • 16:30 **Invited**

On-Chip Nanowire Photonic Devices, Limin Tong¹; ¹*Zhejiang Univ., China*. By integrating free-standing optical nanofibers and nanowires with microfluidic channels or silicon photonic chips, we show on-chip nanowire photonic devices including optical sensors, interferometers, modulators and light emitting devices with small footprints and high flexibility.

16:00–18:00

Th4H • Novel Photonic Structures

Presider: Xuming Zhang; The Hong Kong Polytechnic Univ., Hong Kong

Th4H.1 • 16:00 **Invited**

Optofluidic Lattice and Single Bacteria and Nanoparticle Manipulation, Ai-Qun Liu¹; ¹*Nanyang Technological Univ., Singapore*. Three different types of optical hopping mechanisms are studied in the optofluidic chip and also trap different bacteria in the optofluidic lattice. The particle enabled bacteria hopping can be used for the antibody screening and direct binding efficiency measurement.

Th4H.2 • 16:30 **Invited**

Plasmonic Enhancement for Optoelectronic Devices, Dao Hua Zhang¹; ¹*Nanyang Technological Univ., Singapore*. We present split ring resonators (SRRs) and their applications, two-dimensional metallic square hole array enhanced mid-wave infrared photodetectors with room temperature detectivity of 8×10^9 Jones and new type of two-terminal millimetre wave photodetectors with a room temperature noise equivalent power of 1.5×10^{-13} W Hz^{-1/2}.

16:00–18:00

Th4I • Optical Access Technologies

Presider: Songnian Fu; Huazhong Univ. of Science and Technology, China

Th4I.1 • 16:00 **Invited**

Simplified signal processing for high-speed PON, Lilin Yi¹, Lei Xue¹, Weisheng Hu¹; ¹*Shanghai Jiao Tong Univ., China*. We have experimentally demonstrated symmetric 4*25 Gb/s TWDM-PON and 50 Gb/s TDM-PON based on 10G class devices. Low-cost DMLs are used as transmitter and simple optical signal process is used for bandwidth equalization and DSP simplification.

Th4I.2 • 16:30

Digital Orthogonal Filtering-Multiplexed Access over IMDD PON systems utilizing EML, Xiao I. Zhang¹, Chongfu Zhang¹, Chen Chen², Mingyue Zhu¹, Wei Jin¹, Kun Qiu¹; ¹*Univ. Electron. Sci. & Technol. China, China*; ²*School of Electrical and Electronic Engineering, Nanyang Technological Univ., Singapore*. We investigate the power budget performance of implementing a digital orthogonal filtering-multiplexed access (DFMA) technology for the passive optical network (PON) systems by using electro-absorption modulated lasers (EMLs)

16:00–18:00

Th4J • Entanglement and Squeezed States II

Presider: Li You; Tsinghua Univ. China

Th4J.1 • 16:00 **Invited**

Unconditional Shot-noise-limit Violation in Photonic Quantum Metrology, Geoffrey Pryde¹, Sergei Slussarenko¹, Morgan Weston¹, Helen Chrzanowski², Lynden Shalm³, Varun Verma³, Sae Woo Nam³; ¹*Griffith Univ., Australia*; ²*Univ. of Oxford, UK*; ³*National Inst. of Standards and Technology, USA*. We demonstrate the first unconditional violation of the shot noise limit in photonic NOON-state interferometry. Using ultrahigh-efficiency source and detectors we outperform ideal classical measurement without employing postselection, or correction for loss and imperfections.

Th4J.2 • 16:30

Multipartite Quantum Entanglement and Quantum Correlation from cascaded Four-wave Mixing Processes with spatial multiplexing, Jietai Jing¹; ¹*East China Normal Univ., China*. Four-wave mixing (FWM) process with spatial multiplexing is a promising candidate for building quantum network. We experimentally investigate multipartite quantum correlation and theoretically study multipartite quantum entanglement from cascaded FWM processes.

16:00–18:00

Th4K • Imaging and Applications

Presider: Wen Chen; The Hong Kong Polytechnic Univ., Hong Kong

Th4K.1 • 16:00 **Invited**

High-temperature Optical Techniques Development and Its Application in Thermal Barrier Coatings, W. He¹, Huimin Xie¹, Q. Zhang¹, Y.J. Yin¹, Z.W. Liu², L.F. Wu¹, X.L. Dai¹; ¹*AML, Dept. of Engineering Mechanics, Tsinghua Univ., China*; ²*School of Aerospace Engineering, Beijing Inst. of Technology, China*. Owing to demanding operating environment and multilayered structure, the experimental characterization of thermal barrier coatings is challenging. Herein, our ongoing work on the high-temperature optical techniques for their deformation and residual stress measurements are reviewed.

Th4K.2 • 16:30 **Invited**

Seeing the Unseen Using Micro-Optical Coherence Tomography, Si Chen¹, Xinyu Liu¹, Nanshuo Wang¹, Xianghong Wang¹, Linbo Liu¹; ¹*Nanyang Technological Univ., Singapore*. Micro-optical coherence tomography technologies improve the spatial resolution of OCT by an order of magnitude. These technical advances, including interferometric spectral combination and multiple aperture synthesis enable subcellular level spatial resolution of intact biological tissues in vivo and ex vivo for the first time.

16:00–18:00

Th4L • Optical Fiber Gratings, Sensors & Technology

Presider: Xinyong Dong; China Jiliang Univ., China

Th4L.1 • 16:00 **Invited**

Long-Period Fiber Grating Sensors Based on High Order Mode Coupling, Yunqi Liu¹; ¹*Shanghai Univ., China*. We demonstrate the fabrication of long-period fiber gratings and helical long-period gratings in specialty fibers using focused carbon dioxide laser. The mode coupling and sensing characteristics of the gratings were investigated experimentally and theoretically.

Th4L.2 • 16:30

Spectral modulation and refractive index sensing characteristics of Ex-TFG coated with gold nanoshell, Huafeng Lu¹, Jiao Lu¹, Bin-bin Luo¹, Shenghui Shi¹, Mingfu Zhao¹; ¹*Chongqing Key Laboratory of Optical Fiber Sensor and Photoelectric Detection, Chongqing Univ. of Technology, China*. Excessively tilted fiber grating (Ex-TFG) sensor coated by gold nanoshell is reported, showing that both of the increase of refractive index sensitivity and intensity change of TM mode are greater than those of TE mode.

These concurrent sessions are grouped across two pages. Please review both pages for complete session information.

Th4A • Characteristics of Shortpulse Lasers—Continued

Th4A.4 • 16:45

Timing Jitter of High Repetition Rate Mode-locked Fiber Lasers, Yan Wang¹, Haochen Tian², Yuxuan Ma¹, Youjian Song², Zhigang Zhang¹; ¹Peking Univ., China; ²Tianjin Univ., China. We characterized the timing jitter of two 880 MHz Yb-doped mode-locked fiber lasers using the optical cross-correlation technique. The lowest residual timing jitter is 3.5 fs rms (integrated from 5MHz to 100 kHz).

Th4A.5 • 17:00

Chromium and cobalt doped saturable absorbers for passively Q-switched visible lasers, Hiroki Tanaka^{1,2}, Elena Castellano-Hernández², Christian Kränkel^{2,3}, Shogo Fujita¹, Fumihiko Kannari¹; ¹Keio Univ., Japan; ²Center for Laser Materials, Leibniz Inst. for Crystal Growth, Germany; ³Inst. of Laser-Physics, Universität Hamburg, Germany. We present a detailed characterization of Cr³⁺ and Co²⁺-doped oxides as saturable absorbers for the visible spectral region. The first visibly emitting Q-switched laser utilizing a Co²⁺:Gd₃Ga₅O₁₂ saturable absorber is demonstrated.

Th4A.6 • 17:15

Intensity Noise Comparison of Mode-Locked Fiber Lasers Based on Nonlinear Amplifying Loop Mirror and Nonlinear Polarization Rotation, Sijia Wang¹, Peng Qin¹; ¹Qian Xuesen Laboratory of Space Technology, Chinese Academy of Space Technology, China. We demonstrate ~82% reduction in the rms relative intensity noise (10 Hz–100 kHz) of mode-locked fiber lasers by the nonlinear amplifying loop mirror compared with nonlinear polarization rotation, under similar 30-nm output spectral bandwidth.

Th4B • Nonlinear Optical Technologies—Continued

Th4B.3 • 16:45

Single shot measurement of the femtosecond laser pulse, Qingwei Yang¹, Jun Kang¹, Ziruo Cui¹, Ailin Guo¹, Haidong Zhu¹, Meizhi Sun¹, Ping Zhu¹, Qi Gao¹, Xinglong Xie¹, Jianqiang Zhu¹; ¹Shanghai Inst. of Optics and Fine Mechanics, China. To meet the requirements of single shot femtosecond laser pulse diagnostic, some methods have been taken. Through carefully design and experiment, a single shot autocorrelator suit for the SGII SPW laser facility is achieved.

Th4B.4 • 17:00

Time-resolved circular-dichroism spectrometer for coherent control experiments, Yuma Saito¹, Hironori Ito¹, Kazuhiko Misawa^{1,2}; ¹Dept. of Applied Physics, Tokyo Univ. of Agriculture and Tech., Japan; ²Inst. of Global Innovation Reserach, Tokyo Univ. of Agriculture and Tech., Japan. We developed a time-resolved circular-dichroism spectrometer to conduct coherent control experiments of chiral materials. The spectrometer yielded satisfactory results for two reference samples, chiral camphor sulfonic acid and [Ru(bpy)₃]²⁺

Th4B.5 • 17:15

Spectral dynamics measurement using a free-space angular-chirp-enhanced delay cavity, Ying Yu¹, Xiaoming Wei^{1,2}, Jianglai Wu¹, Jingjiang Xu¹, Kenneth Kin-Yip Wong¹, Kevin K. Tsia¹, Yiqing Xu^{1,3}; ¹Univ. of Hong Kong, Hong Kong; ²California Inst. of Technology, USA; ³Zhejiang Univ., China. We present a study of spectral dynamics measurement using the lately invented apparatus named free-space angular-chirp enhanced delay (FACED) cavity. The shot-to-shot spectra are observed and the corresponding spectral correlation maps are analyzed.

Th4C • Novel Laser System and its Applications—Continued

Th4C.3 • 16:45 **Invited**

Nonlinear Plasmonics with Extremely High-Q Resonances, Harald W. Giessen¹; ¹Universiteit Stuttgart, Germany. Abstract not available.

Th4C.4 • 17:15

Thermal Regimes of Laser Reduction of Graphene Oxide, Sergey E. Svyakhovskiy¹, Nikita Minaev², Stanislav Evlashin²; ¹M. V. Lomonosov Moscow State Univ., Russia; ²Inst. of Laser and Information Technology of Russian Academy of Sciences, Russia; ³Skolkovo Inst. of Science and Technology, Russia. The far-reaching method of the graphene oxide photoreduction has been developed for the robust production of graphene nanoflakes. We study the influence of photoreduction spectra on optical and electrical properties and the material surface wettability.

Th4D • High Power CW Lasers and Coherent Combining—Continued

Th4D.3 • 16:45

Coherent Beam Combining for Ultrashort Intensity Laser Systems, Yan-Qi Gao¹; ¹Shanghai Inst. of Laser Plasma, China. Three kinds of factors, including phase distribution, spectral dispersion and longitudinal chromatism, are investigated for ultra-short beam combining. General control requirements are given. High-quality combining is realized, and time jitter is less than 150 attosecond.

Th4D.4 • 17:00 **Invited** Withdrawn.

Th4E • Plasmon-enhanced Spectroscopies and Imaging—Continued

Th4E.3 • 16:45

Plasmon hybridization in plasmonic dimer-on-film nanocavity for photoluminescence enhancement, Guangcan Li¹, Meng Qiu¹, Dang Yuan Lei¹; ¹The Hong Kong Polytechnic Univ., Hong Kong. We demonstrate a plasmonic nanoparticle-dimer-on-film nanocavity with plasmon hybridization-induced quality factor improvement, which exhibits ~200 times photoluminescence intensity enhancement and ~4.6 times linewidth reduction.

Th4E.4 • 17:00

Surface enhanced infrared absorption spectroscopy using super absorbing metasurface with sub-5-nm gaps, Dengxin Ji¹, Qiaoqiang Gan¹; ¹State Univ. of New York at Buffalo, USA. We developed a super absorbing metamaterial surface with sub-5-nm gaps and demonstrated its application for boosted surface enhanced infrared absorption spectroscopy using its extremely enhanced localized field.

Th4E.5 • 17:15

Plasmonic Narrow Bandpass Filters Based on Metal-Dielectric-Metal for Multispectral Imaging, Xin He¹, Nicholas O'Keefe¹, Dechuan Sun¹, Yajing Liu¹, Hemayet Uddin², Ampalavanapillai Nirmalathas¹, Ranjith R. Unnithan¹; ¹the Univ. of Melbourne, Australia; ²Melbourne Centre for Nanofabrication, Australia. This paper presents a novel plasmonic filter design to reduce the full width half maximum (FWHM) of transmission spectrum based on hexagonal array of holes with Metal-Dielectric-Metal structure for multispectral imaging applications.

Th4F • Radio Over Fiber and Optical Wireless Communication—Continued

Th4F.3 • 17:00

Nonlinearity mitigation in multi-band OFDM IF over Fiber system using signal spectral power shaping, InHo Ha¹, Hyoung-Joon Park¹, Sang-kook Han¹; ¹Yonsei Univ., Korea. A nonlinear mitigation technique with spectral shaping of signal power is proposed in analog multi-IF over Fiber link using OFDM signal. Its feasibility was experimentally verified through EVM performance and channel linearity.

Th4F.4 • 17:15 **Invited**

RoF links in the front-haul network for the future 5G communications, Diego Perez-Galacho¹, Victor Nacher-Castellet¹, Salvador Sales¹; ¹PRL, ITEAM, Universitat Politècnica València, Spain. Radio over Fiber together with Spatial Division Multiplexing appears as the best suitable solution to implement next generation 5G fronthaul. This approach has been used to demonstrate RF optical links of 10km distance with up to 1000Mbps data rate for a BER below 10⁻³.

These concurrent sessions are grouped across two pages. Please review both pages for complete session information.

Th4G • 2D Photonics Devices—Continued

Th4G.3 • 17:00

High Speed Single-Layer Graphene-Si Electro-Absorption Modulator, Chiara Alessandrini¹, Inge Asselberghs¹, Steven Brems¹, Cedric Huyghebaert¹, Joris Van Campenhout¹, Dries VanThourhout², Marianna Pantouvaki¹; ¹imec, Belgium; ²Ghent Univ., Belgium. We demonstrate a single-layer graphene electro-absorption modulator on Si waveguides with modulation depth of 0.026 dB/um for 6.5 Vpp and 17 GHz 3dB bandwidth.

Th4G.4 • 17:15

Anomalous Photoresponse Based on 2D Material Gated Transistors, Nan Guo¹, Huicong Chang¹, Junku Liu¹, Yi Jia¹, Lin Xiao¹; ¹Qian Xuesen Lab of Space Technology, China. We report on a WSe₂ gated transistor. The photocarriers excited in WSe₂ enhance the conductivity of WSe₂. Negative gate voltages are applied to the ZnO channel through WSe₂. Remarkable negative photocurrents are obtained.

Th4H • Novel Photonic Structures—Continued

Th4H.3 • 17:00

Demonstration of Pseudospin-dependent topological charge transformation in photonic graphene, Daohong Song¹, Xiuying Liu¹, Shiqi Xia¹, Zhixuan Dai¹, Liqin Tang¹, Jingjun Xu¹, Zhigang Chen^{1,2}; ¹The MOE Key Laboratory of Weak-Light Nonlinear Photonics, TEDA Applied Physics Inst. and School of Physics, Nankai Univ., China; ²Dept. of Physics and Astronomy, San Francisco State Univ., USA. Momentum-matched selective excitation of two sublattices with vortex beams leads to direct observation of pseudospin-dependent conical diffraction and topological charge transformation, including spin-orbital angular momentum conversion arising from inherent degree-of-freedom in photonic graphene.

Th4H.4 • 17:15

Switchable Topological Edge States in Next-Nearest-Neighbour Coupled Resonator Lattices, Daniel Leykam¹, Sunil Mittal^{2,3}, Mohammad Hafezi^{2,3}, Yidong Chong⁴; ¹Inst. for Basic Science, Korea; ²Joint Quantum Inst., USA; ³University of Maryland, USA; ⁴Nanyang Technological Univ., Singapore. We find that next-nearest-neighbour coupling in ring resonator lattices induces topological transitions and one-way edge modes. We design topological waveguides that are easily switchable using thermal, electro-optic, or nonlinear effects, enabling robust on-chip photon routing.

Th4I • Optical Access Technologies—Continued

Th4I.3 • 16:45

Experimental Demonstration of Optical MIMO NOMA Passive Optical Network, Bangjiang Lin¹, Xuan Tang¹, Chun Lin¹, Zhenlei Zhou¹, Haiguang Zhang¹, Zabih Ghassemloo¹; ¹Chinese Academy of Sciences, Quanzhou Inst. of Equipment Manufacturing, China. We experimentally demonstrate an optical MIMO NOMA-PON system, which offers a higher system capacity. The MIMO demultiplexing and the inter-user interference mitigation are realized with efficient channel equalization.

Th4I.4 • 17:00

Wavelength Control Techniques for Tunable LD-based Colorless ONUs in WDM PON, Bingchang Hua¹, Zhiguo Zhang¹, Yanxu Chen¹, Qi Guo¹, Cheng Ju¹, Xue Chen¹, Rengzhong Guo², Chenying Jiang²; ¹State Key Laboratory of Information Photonics and Optical Communications (Beijing Univ. of Posts and Telecommunications), China; ²Information and Telecommunication branch, Jiujiang Electric Power Supply Company, China. A colorless light source is indispensable for low-cost and plug-and-play ONUs in WDM PON. Four kinds of wavelength control methods for tunable LD-based colorless light source used in colorless ONU are designed and experimentally measured.

Th4I.5 • 17:15 Invited

A High-Speed and Long-Reach UWOC Link, Chung-Yi Li¹, You-Ruei Wu¹, Zhen-Han Wang¹, Yong-Nian Chen¹, Hai-Han Lu¹, Wen-Shing Tsai²; ¹National Taipei Univ. of Technology, Taiwan; ²Dept. of Electrical Engineering, Ming Chi Univ. of Technology, Taiwan. A high-speed (5 Gbps) and long-reach (52.5 m) underwater wireless optical communication link is demonstrated. Competent bit error rate and constellation map are acquired over a 50-m GI-POF transport with a 2.5-m underwater link.

Th4J • Entanglement and Squeezed States II—Continued

Th4J.3 • 16:45

First Demonstration of nonlocal two-way quantum clock synchronization on fiber link, Fei Y. Hou^{1,2}, Ruifang Dong¹, Runai Quan^{1,2}, Xiao Xiang¹, Tao Liu¹, Shougang Zhang¹; ¹National Time Service Center, China; ²Univ. of Chinese Academy of Sciences, China. We have demonstrated a two-way quantum clock synchronization by using frequency entangled pulses. For two clocks separated by 20km fiber, a timing stability of 0.85ps was achieved at averaging time of 5120s with a synchronization accuracy of 10ps.

Th4J.4 • 17:00

Binary Homodyne Detection for Observing Quadrature Squeezing in Satellite Links, Christian R. Mueller^{1,2}, Kaushik P. Seshadreesan^{1,2}, Christian Peuntinger^{1,2}, Christoph Marquardt^{1,2}; ¹Quantum Information Processing, MPI for the Science of Light, Germany; ²Dept. of Physics, Univ. of Erlangen-Nuremberg (FAU), Germany. We demonstrate the efficiency of homodyne detection with merely one bit of detector resolution and we analyze the feasibility of quadrature squeezing detection in satellite links using optical communication technology already in orbit.

Th4J.5 • 17:15

Second-order temporal interference with thermal light: Interference beyond the coherence time, Yong Sup Ihn¹, Yosep Kim¹, Vincenzo Tamma², Yoon-Ho Kim¹; ¹Pohang Univ. of Sci. and Tech., Korea; ²Faculty of Science, Univ. of Portsmouth, UK. We report an experimental demonstration for a counter-intuitive phenomenon in multi-path interferometer with thermal light. The second-order interference between two pairs of correlated optical paths emerges even for the much longer time delay in each pair than the source coherence time.

Th4K • Imaging and Applications—Continued

Th4K.3 • 17:00 Invited

Overcoming the Multiple Scattering Limit for Bio-Imaging, Jung-Hoon Park¹; ¹Ulsan National Inst of Science & Tech, Korea. Multiple scattering still remains as the ultimate barrier for in-vivo deep tissue imaging. Here, we will discuss our efforts to overcome multiple scattering and enable diffraction limited, or even sub-wavelength resolution imaging through highly scattering media and living biological tissue.

Th4L • Optical Fiber Gratings, Sensors & Technology—Continued

Th4L.3 • 16:45

Humidity Sensor Based on Long Period Grating Coated with Polyethylene Glycol/Polyvinyl Alcohol, Yunlong Wang¹, Yunqi Liu¹, Fang Zou¹, Chen Jiang¹, Lu Huang¹, Tingyun Wang¹; ¹Shanghai Univ., China. A novel relative humidity sensor based on long period grating coated with polyethylene glycol /polyvinyl alcohol film is reported. The sensor has a high sensitivity (1.2902 nm/RH) in RH range of 60% to 95% RH.

Th4L.4 • 17:00

Simultaneous Measurement of Tilt Angle and Temperature Based on a Taper-Shaped Polymer Incorporating a Fiber Bragg Grating, Jhe-Yong Guo¹, Meng-Shan Wu¹, Cheng-Ling Lee¹, Chi-Feng Lin¹, Wen-Fung Liu²; ¹National United Univ., Taiwan; ²Dept. of Electrical Engineering, Feng Chia Univ., Taiwan. We propose a novel taper-shaped polymer incorporating a fiber Bragg grating (FBG) for simultaneously measuring tilt angle (θ) and temperature (T). Experimental results show that both parameters can be simultaneously measured with good discrimination.

Th4L.5 • 17:15

Sensing characteristics of sampled Bragg gratings produced in helical fibers, Peng Ma^{2,1}, Gaoyang Chen², Jie Li², Li-Peng Sun², Chuang Wu², Bai-Ou Guan²; ¹Jinan Univ., China; ²Inst. of Photonics Technology, Jinan Univ., China. We investigate the sensing characteristics for a sampled Bragg grating formed in a helical single-mode fiber. This sensor features structural simplicity, high integration, flexibility, and low cost, and thus has prospects in practical applications.

These concurrent sessions are grouped across two pages. Please review both pages for complete session information.

Th4A • Characteristics of Shortpulse Lasers—Continued

Th4A.7 • 17:30

Influence of Intra-Cavity Loss on Mode-Locking of Fiber Lasers, Goran Kovacevic¹, Takuma Shirahata¹, Pengtao Yuan¹, Sze Y. Set¹, Shinji Yamashita¹; ¹RCAST, Univ. of Tokyo, Japan. We experimentally characterize the influence of intra-cavity loss on mode-locking of fiber lasers using a variable attenuator and NPR. We back-up our results numerically and hope they will open a path to high loss components in fiber lasers, like optical chips or high percentage output couplers.

Th4A.8 • 17:45

1/1.5 μm dual-band high-energy square-wave mode-locked fiber laser based on Er/Yb-codoped double cladding fiber, Songlin Zhang¹, Weiqi Liu¹, Chunyu Guo¹, Shuangchen Ruan¹, Peiguang Yan¹, Jinzhang Wang¹, Ping Hua¹, Xiaogang Ge¹; ¹Shenzhen Univ., China. A 1 μm /1.5 μm dual-band simultaneously mode-locked fiber laser with high-energy square-wave pulses has been demonstrated based on a common Erbium/ Ytterbium-codoped double cladding fiber.

Th4B • Nonlinear Optical Technologies—Continued

Th4B.6 • 17:30

Compression of optical pulses using a free-space angular-chirp-enhanced delay cavity, Ying Yu¹, Xiaoming Wei^{1,2}, Jianglai Wu¹, Jingjiang Xu¹, Kenneth Kin-Yip Wong¹, Kevin K. Tsia¹, Yiqing Xu^{1,3}; ¹Univ. of Hong Kong, Hong Kong; ²California Inst. of Technology, USA; ³Zhejiang Univ., China. We present a study of compression of optical pulses using a free-space angular-chirp enhanced delay (FACED) cavity. The amount of induced dispersion can be adjusted by simply modifying the geometry of the FACED cavity.

Th4B.7 • 17:45

Time-domain Ptychographic Retrieval of Over-octave-spanning IR Pulses from XFROG Measurement, Y. C. Lin¹, Yasuo Nabekawa¹, Katsumi Midorikawa¹; ¹RIKEN, Japan. We present the application of time-domain ptychographic algorithm for reconstructing both the over-octave-spanning IR spectrum and gate pulses recorded by an XFROG setup. The two pulses are reliably characterized from a single XFROG spectrogram.

Th4C • Novel Laser System and its Applications—Continued

Th4C.5 • 17:30 Invited

High power femtosecond FCPA laser and its application in VUV sources generations, Zhigang Zhao¹, Yohei Kobayashi¹; ¹Univ. of Tokyo, Japan. 10.7-eV source with improved beam profile and stability was prepared by employing a specially designed Lens-Window-Prism (LWP) device, driven by a homemade fiber chirped pulse amplifier (FCPA) laser system at 1 MHz.

Th4D • High Power CW Lasers and Coherent Combining—Continued

Th4D.5 • 17:30

1.5kW All-Fiber Continuous-Wave Laser, Kui Y. Song¹, Yuanhong Yang¹, Xuexia Zhang²; ¹Beihang Univ., China; ²Inst. of Laser Engineering, Beijing Univ. of Technology, China. A prototype of 1.5kW fiber laser with the center wavelength 1080 nm has been demonstrated and developed, and the corresponding optical-to-optical conversion efficiency is 73.3%. The Stimulated Raman Scattering (SRS) is well suppressed.

Th4D.6 • 17:45

A 900-Watt quasi-CW diamond Raman laser, Sergei Antipov¹, Alexander Sabella², Soumya Sarang¹, Robert J. Williams¹, David J. Spence¹, Richard P. Mildren¹; ¹Macquarie Univ., Australia; ²Defence Science and Technology Group, Australia. A high beam quality diamond Raman laser operating in the quasi-CW regime with 900 W output power in 100 μs pulses was demonstrated above the modelled cavity stability limit. A 40 \times brightness enhancement was measured.

Th4E • Plasmon-enhanced Spectroscopies and Imaging—Continued

Th4E.6 • 17:30

Au-Nanoparticles Fabricated Using femtosecond pulse for Surface-Enhanced Raman Spectroscopy, Wending Zhang¹, Cheng Li¹, Kun Gao¹, Fanfan Lu¹, Feng Gao², Ting Mei¹; ¹Northwestern Polytechnical Univ., China; ²Nankai Univ., China. Au-nanoparticles (Au-NPs) substrates for surface-enhanced Raman spectroscopy (SERS) are fabricated by scanning an Au-film using femtosecond pulse. The Au-NPs SERS substrates exhibit high activity and excellent reproducibility.

Th4E.7 • 17:45

Label-free Imaging to Single Nanoparticle by Surface Plasmon Polariton In-plane Scattering, Xuqing Sun¹, Hongyao Liu¹, Liwen Jiang^{1,2}, Wei Xiong¹, Yaqin Chen¹, Xinchao Lu¹; ¹Inst. of Microelectronics of Chinese Academy of Sciences, China; ²Univ. of Chinese Academy of Sciences, China. We study the physical mechanism of surface plasmon polariton in-plane scattering with single nanoparticle, which is vital to understand the electromagnetic interaction with nanoparticle. Also, the polarized bright spot is linear with the nanoparticle's size.

Th4F • Radio Over Fiber and Optical Wireless Communication—Continued

Th4F.5 • 17:45

Experimental Characterization of Variable Background Light to APD-Based OWC System Performance, Daomin Chen¹, Chao Li¹, Zhengyuan Xu¹; ¹Univ. of Science and Technology of China, China. Characterization of variable background light from a blue LED to an LD/APD-based optical wireless communication (OWC) link performance was experimentally investigated. The results reveal both APD's gain and bandwidth degrade the performance, ignoring shot noise.

18:30–20:30 Post Deadline Papers

These concurrent sessions are grouped across two pages. Please review both pages for complete session information.

Th4G • 2D Photonics Devices—Continued

Th4G.5 • 17:30

Enhanced Self-Phase Modulation in Graphene-integrated Silicon Waveguides, Qi Feng¹, Hui Cong¹, Wenqi Wei^{1,2}, Bin Zhang¹, Jianhuan Wang¹, Jieyin Zhang¹, Ting Wang¹, Jianjun Zhang¹; ¹*Inst. of Physics, CAS, China*; ²*School of Physics and Technology, Wuhan University, China*. Silicon-on-insulator waveguides covered with graphene in different lengths have been fabricated. We demonstrated the enhanced self phase modulation and Kerr nonlinearity in graphene-integrated silicon waveguides.

Th4G.6 • 17:45

The substrate influence on the optoelectronic properties of 2D materials, Linjun Li¹, Bo Liu², Weijie Zhao², Goki Eda², Kianping Loh²; ¹*Zhejiang Univ., China*; ²*National Univ. of Singapore, Singapore*. 2D materials are known for their highly susceptible to environmental influence. Here we show the influence of different substrates to the exciton/trion related bandgap engineering of two typical materials, MoS₂ and WS₂ nanosheets.

Th4H • Novel Photonic Structures—Continued

Th4H.5 • 17:30

Chiral Light-matter Interaction in Dielectric Photonic Topological Insulators, Sang Soon Oh¹, Ben Lang², Daryl M. Beggs¹, Diana L. Huffaker¹, Matthias Saba³, Ortwin Hess³; ¹*Cardiff Univ., UK*; ²*Univ. of Bristol, UK*; ³*Imperial College London, UK*. A unidirectional chiral edge mode in photonic topological insulators can be selectively excited by a circularly-polarized dipole source. We show that the directionality is also determined by the position of the dipole source.

Th4H.6 • 17:45

Fabrication Of Dual-focus Microlens Array By Using Dynamic Optical Projection Stereolithography, Ouyang Xia¹, Zhengkun Yin^{1,2}, Jushuai Wu¹, A. Ping Zhang¹, Changhe Zhou²; ¹*Dept. of Electrical Engineering, The Hong Kong Polytechnic Univ., Hong Kong*; ²*Shanghai Inst. of Optics and Fine Mechanics, Chinese Academy of Sciences, China*. A new optical fabrication technology for fabrication of dual-focus microlens array is presented. We experimentally demonstrated that the surface of microlens can be precisely tailored by the technology to engineer the focal structure of microlens.

Th4I • Optical Access Technologies—Continued

Th4I.6 • 17:45

High Speed Geometrically Shaped 8-QAM modulation based Underwater Visible Light Communication System, Xingbang Wu¹, Fangchen Hu¹, Shangyu Liang¹, Nan Chi¹; ¹*Fudan Univ., China*. We demonstrate an underwater VLC system at 1.2m transmission distance with geometrically shaped 8-QAM modulation. The best performance can be achieved by utilizing circle 8QAM modulation and the highest data rate is 1.4 Gb/s.

Th4J • Entanglement and Squeezed States II—Continued

Th4J.6 • 17:30

1.5- μ m Narrow-band Two-photon Source for Long-distance Quantum Communication, Kazuya Niizeki¹, Kohei Ikeda¹, Mingyang Zheng², Xiuping Xie², Kotaro Okamura³, Nobuyuki Takei^{4,5}, Naoto Namekata⁶, Shuichiro Inoue⁶, Hideo Kosaka¹, Tomoyuki Horikiri^{1,7}; ¹*Dept. of physics, Yokohama National Univ., Japan*; ²*Jinan Inst. of Quantum Technology, China*; ³*Kanagawa Univ., Japan*; ⁴*Inst. for Molecular Science, Japan*; ⁵*SOKENDAI (The Graduate Univ. for Advanced Studies), Japan*; ⁶*Nihon Univ., Japan*; ⁷*JST, PRESTO, Japan*. We demonstrate a narrow-band telecom two-photon source for long-distance quantum communication. The second-order cross-correlation function reveals narrow linewidth of 2.4 MHz and the highest spectral brightness of 3.94×10^5 pairs/(s•MHz•mW).

Th4J.7 • 17:45

Spatially resolved control of ac-Stark shifts in cold atomic ensemble, Mateusz Mazelanik¹, Adam Leszczynski¹, Michal Lipka¹, Michal Parniak¹, Michal Dabrowski¹, Wojciech Wasilewski¹; ¹*Univ. of Warsaw, Poland*. We demonstrate spatially resolved control of fictitious magnetic fields generated by an optically induced ac-Stark shift as a versatile tool to efficiently prepare complex spin patterns in cold atomic ensemble.

Th4K • Imaging and Applications—Continued

Th4K.4 • 17:30

Internal Strain Imaging of Visibly-Opaque Black Rubbers by Terahertz Polarization Spectroscopy, Atsuto Moriwaki¹, Makoto Okano¹, Shinichi Watanabe¹; ¹*Keio Univ., Japan*. We succeed to develop the internal strain imaging technique for visibly-opaque black rubbers using terahertz polarization spectroscopy. Our novel method allows the nondestructive and contactless evaluation of the internal triaxial strain without any preprocesses.

Th4K.5 • 17:45

Fast and high-quality object reconstruction based on Fourier spectrum acquisition in single-pixel imaging, Yin Xiao^{2,1}, Wen Chen^{2,1}; ¹*Dept. of Electronic and Information Engineering, The Hong Kong Polytechnic Univ., China*; ²*The Hong Kong Polytechnic Univ. Shenzhen Research Inst., China*. In single-pixel imaging, Fourier spectrum acquisition method is applied to generate an initial guess in Gerchberg-Saxton-like algorithm to reduce measurement number, improve convergence rate and recover high-quality object at the same time.

Th4L • Optical Fiber Gratings, Sensors & Technology—Continued

Th4L.6 • 17:30

Characteristics of CO₂-laser Inscribed Polarization-maintaining Fiber Helical Long Period Gratings, Chen Jiang¹, Yunqi Liu¹, Yunhe Zhao¹, Tingyun Wang¹; ¹*Shanghai Univ., China*. **Abstract:** We demonstrate the fabrication of helical long period gratings inscribed in polarization-maintaining fiber using CO₂-laser, the effects of writing parameters on the gratings characteristics to the surrounding refractive index was investigated experimentally.

Th4L.7 • 17:45

Advanced Fiber Bragg Grating Hydrogen Sensor by UV-Irradiation, Shiwen Yang^{1,2}, Xuexiang Zhong^{1,2}, Minghong Yang^{1,2}; ¹*Wuhan Univ. of Technology, China*; ²*National Engineering Laboratory for Fiber Optics Sensing Technology, China*. Ultraviolet light was induced into the FBG hydrogen sensing system to improve the repeatability of the sensor, experiment results show that the relative error in 40 tests under UV irradiation has been reduced by 54.2%.

18:30–20:30 Post Deadline Papers

08:30–10:00
F1A • Mid infrared
Lightsource

Presider: Jinhui Yuan; Beijing Univ. of Posts and Telecommunications, China

F1A.1 • 08:30

High-Efficiency Watt-Level Mid-Infrared Fiber Lasers Beyond 3 μm using Dy:ZBLAN, Robert I. Woodward¹, Matthew Majewski¹, Gayathri Bharathan¹, Darren D. Hudson¹, Alex Fuerbach¹, Stuart D. Jackson¹; ¹Macquarie Univ., Australia. We demonstrate an optimized in-band-pumped dysprosium fiber laser with 73% slope efficiency and 1.1 W output at 3.15 μm : the first watt-level fiber source in the 3.0–3.4 μm region and highest ever efficiency mid-IR fiber laser.

F1A.2 • 08:45

Handedness control of a mid-infrared 3.5 μm optical vortex MgO:PPLN parametric oscillator, Yusufu Taximaiti¹, Ranziguli Fulati¹, Sujian Niu¹, Katsuhiko Miyamoto², Takashige Omatsumi²; ¹Xinjiang Normal Univ., China; ²Chiba Univ., Japan. We generate the first millijoule-level tunable mid-infrared (3.362–3.677 μm) optical vortex output with a topological charge l of ± 1 by a 1 μm vortex pumped quasi-phase matching MgO-doped periodically poled lithium niobate (MgO:PPLN) optical parametric oscillator.

F1A.3 • 09:00

Low-threshold dual-waveband 3 μm and 2 μm pulse generation based on hybrid pumping, Yiwen Shi¹, Jianfeng Li¹, Hongyu Luo¹, Yao Xu¹, Fei Liu¹, Ying Gao¹, Yong Liu¹; ¹Univ. of Electronic Science & Tech China, China. Using hybrid pumping of CW laser diode at 1150 nm and Tm³⁺-doped pulsed fiber laser at 1950 nm, we demonstrate a dual-waveband Ho³⁺-doped ZBLAN pulsed fiber laser at ~ 2 and ~ 3 μm with low threshold of 1.7 W at 2 μm . Maximum output power of 136.6 and 26 mW at 2971.9 and 2062.3 nm were obtained with the repetition rate of 50 and 25 kHz, respectively.

08:30–10:00

F1B • Fiber Devices III

Presider: Liang Wang; The Chinese Univ. of Hong Kong, Hong Kong

F1B.1 • 08:30 **Invited**

3D printing, photonics and the IoT, John Canning^{1,2}, Kevin Cook¹; ¹Univ. of Technology Sydney, Australia; ²Univ. of Sydney, Australia. 3D-print prototyping and custom packaging is easier, rapid and increasingly low cost, circumventing traditional approaches, disrupting manufacture and greatly accelerating the IoT.

F1B.2 • 09:00

Laser performances of Yb-doped aluminophosphosilicate fiber under γ -radiation, Ying Y. Wang¹, Cong Gao¹, Kun Peng¹, Li Ni¹, Xiaolong Wang¹, Huan Zhan¹, Yuwei Li¹, Lei Jiang¹, Aoxiang Lin¹, Jianjun Wang¹, Feng Jing¹; ¹China Academy of Engineering Physics, China. Laser performances of Yb-doped aluminophosphosilicate fiber were investigated under γ -radiation. The slope-efficiency and insert loss were sensitive to γ -radiation and exhibited obvious degradation. Effects of Al/P-codoping on radiation-induced photodarkening and dopant-chosen for radiation-hardening were discussed.

08:30–10:00

F1C • Emerging Technologies in Microwave Photonics

Presider: Simin Li; Nanjing Univ. Aeronaut. Astronaut., China

F1C.1 • 08:30 **Invited**

Key Techniques of Orbital Angular Momentum based Wireless Communication, Shilie Zheng¹; ¹Zhejiang Univ., China. OAM based wireless communications have drawn much attention, however the inherent characteristics of OAM waves pose several challenges. In this paper some key techniques are proposed to solve such problems of OAM based communications.

F1C.2 • 09:00

Nonlinear Dynamics of Microwave State Switching in a Semiconductor Laser with Feedback, Jia Xin Dong¹, Sze-Chun Chan^{1,2}; ¹Dept. of Electronic Engineering, City Univ. of Hong Kong, China; ²State Key Laboratory of Millimeter Waves, City Univ. of Hong Kong, China. State switching in a semiconductor laser with feedback is investigated both experimentally and numerically. Toggled between stable and oscillatory states, the laser dynamics generates a microwave signal with a transient time below 0.7 ns.

08:30–10:00

F1D • Entanglement and Squeezed States III

Presider: Guofeng Zhang; The Hong Kong Polytechnic Univ., Hong Kong

F1D.1 • 08:30 **Invited**

Productions of Many Atom Entangled States and Their Interferometric Applications, Li You¹; ¹Tsinghua Univ., China. Interferometric precision with N uncorrelated particles is bounded by the standard quantum limit (SQL). We report deterministic generations of entangled atomic states as well as their sensing precisions more than 8dB beyond the SQL.

F1D.2 • 09:00

Generation of ultra-short wavelength two-photon NOON state for high precision quantum metrology, Bao-Sen Shi¹, Zhi-Yuan Zhou¹, Shi-Long Liu¹; ¹Key Lab. of Quantum Information, China. 525-nm two-photon NOON-state is generated by quantum frequency up-conversion of 1547-nm photon pairs. The up-converted two photons are highly indistinguishable with nearly perfect Hong-Ou-Mandel-interference and two-photon visibility high enough to beat the standard quantum limit.

08:30–10:00

F1E • Optical Fiber Sensing and Microfluidics

Presider: Zhiyong Zhao; The Hong Kong Polytechnic Univ., Hong Kong

F1E.1 • 08:30 **Tutorial**

New Approaches to Optical Fiber Sensing, Ali Masoudi¹, Angeliki Zafeiropoulou¹, Andrei L. Donko¹, Wanvisa Talataisong¹, Rand M. Ismaeel¹, Martynas Beresna¹, Gilberto Brambilla¹; ¹Univ. of Southampton, UK. Optical fibre sensors can be classified in point, quasi-distributed and distributed sensors. This tutorial will review the different types of optical fibre sensors, with a focus on recent developments that can improve sensitivity, dynamic range and resolution.

08:30–10:00

F1F • Related Technologies and Applications for Imaging, Display and Storage

Presider: Tao Yang; Nanjing Univ. of Posts & Telecom, China

F1F.1 • 08:30

Fabrication of Flexible White Light Emitting Diodes from Photoluminescent Polymer Materials with Excellent Color Quality, Yung-Min Pai¹, Chih-Hao Lin¹, Cheng-huan Chen¹, Hao Chung Kuo¹; ¹National Chiao Tung Univ., Taiwan. This study flexible light-emitting diodes. Ultra-violet flip-chip for the pumping source and combined with polymer and quantum dot films achieved excellent CRI values ($R_a = 96$ and $R_9 = 96$), with high reliability, demonstrating high suitability

F1F.2 • 08:45

A Laser Beam Homogenization Technology Based on Diffractive Optical Component and Corresponding Experimental Research, Xin Cai Zhao¹, Peng Gao¹, Maojie Ran¹, Ningwen Liu¹, Lihua Chang¹, Jian Li¹, Weifeng Wen¹, Qixian Peng¹; ¹Inst. of fluid physics, CAEP, China. We proposed a method of laser beam homogenization based on diffractive optical components. Experiments show that the homogenization system and the image processing reduce the focal spot non-uniformity from 37.02% to 8.6%.

F1F.3 • 09:00

A Real-time, Precise Artery Pulse Monitor System Based on Graphene-Coated Fiber, Shengyao Xu¹, Zhang Y. An¹, Yuan X. Guang¹, Zhengyang Li¹, Siyao Zang¹, Yongqing Huang¹; ¹Beijing Univ. of Posts and Telecom, China. A precise radial artery pulse monitor system integrated the graphene-coated fiber was designed and fabricated. The device is low-powered and wearable while ensuring the accuracy of the pulse signals by means of real-time signal processing.

F1A • Mid infrared Lightsources—Continued**F1A.4 • 09:15**

High tunable bandwidth 2 μ m single-frequency fiber laser for next-generation gravitational wave detection, Shuxian Qi¹, Yubin Hou¹, Qian Zhang¹, Pu Wang¹; ¹Beijing Univ. of Technology, China. We demonstrate a low noise, GHz sweeping bandwidth all silica fiber single-frequency distributed Bragg reflection laser and a 160W power fiber amplifier at 1992.6 nm for next-generation gravitational wave detection.

F1A.5 • 09:30

Flat-gain Wide-band Thulium-based Fiber Laser, Elizabeth M. Lee^{2,1}, Jiaqi Luo^{2,1}, Biao Sun², Junhua Ji², Vincent Larry Ramalingam^{2,1}, Xia Yu², Qijie Wang¹; ¹School of Electrical & Electronic Engineering, Nanyang Technological Univ., Singapore; ²Precision Measurements Group, Singapore Inst. of Manufacturing Technology, Singapore. We report a design method for flat-gain wide-band all-fiber laser using cascaded bidirectional pumping of multi-segment thulium-doped fibers. Experimental demonstration of two-fiber setup achieved the widest reported 3-dB bandwidth of 178nm centered at 1944nm.

F1A.6 • 09:45

High-repetition-rate gain-switching at 2.103 μ m pumped by h-shaped pulses, Hongyu Luo¹, Jianfeng Li¹, Fei Liu¹, Yiwen Shi¹, Yong Liu¹; ¹Univ Electronic Sci & Tech China (UESTC), China. We demonstrate h-shaped pulse generation in a NPR mode-locked thulium-doped fiber laser at 1.98 μ m. Its potential as a pump for a high-repetition-rate (1.435 MHz) gain-switched holmium-doped fiber laser at 2.103 μ m is presented.

F1B • Fiber Devices III—Continued**F1B.3 • 09:15**

Employing Tricyclic Fusion Method to Splice a Silicon Cored Fiber with a Single Mode Fiber, Yung-Lin H. Hsu², Lon Wang², Nian Jia-Ruei¹, Tsai Yao-Yang¹; ¹Mechanical Engineering, Taiwan; ²Electrical Engineering, Photonics and Optoelectronics, Taiwan. A silicon cored fiber (SCF) spliced with a single mode fiber (SMF) by employing a novel method called Tricyclic Fusion is shown to have lower splicing loss as compared with the use of a conventional fusion splicer.

F1B.4 • 09:30

Analyzing the mode distribution of few-mode fiber by mode-frequency mapping, Hailong Zhou¹, Jianji Dong¹, Su Chen², Lei Shen², Xinliang Zhang¹; ¹Huazhong Univ of Science & Technology, China; ²State key laboratory of optical fiber and cable manufacture technology, Yangtze optical fiber and cable joint stock limited company, China. The fiber modes are mapped to different frequencies by using dynamic phase masks. The complex amplitudes at these frequencies indicate the amplitudes and phases of the fiber modes.

F1B.5 • 09:45

Characterizing the Single mode - Multimode - Multimode (SMm) device for exciting a single radial mode in a multimode fiber, Nitin Bhatia^{1,2}, Partha Mondal¹, Shailendra Varshney¹; ¹Indian Inst. of Technology Kharagpur, India; ²IIIT Univ., India. We demonstrate an all-fiber method to determine the wavelengths at which a fabricated SMm device provides a single mode output. This method is quick and does not require measurement of the modal weights.

F1C • Emerging Technologies in Microwave Photonics—Continued**F1C.3 • 09:15**

Demonstration of spectral holes in homogenous Brillouin gain profile in microwave domain, Siva Shakthi A¹, Arjali B. Yelkar¹, Ravi Pant¹; ¹ISER Thiruvananthapuram, India. We report demonstration of room temperature artificial spectral hole burning in microwave domain. Narrow spectral hole with 3 dB linewidth ~6 MHz and depth > 35 dB are burned in homogeneously broadened Brillouin gain spectra.

F1C.4 • 09:30

Tunable Suppression Ratio and SFDR Enhanced Single Sideband Generation on an Integrated Platform, Awanish Pandey¹, Shankar K. Selvaraja¹; ¹Indian Inst. of Science, India. On-chip side-band suppression with enhanced SFDR and tunable suppression ratio (5dB-44dB) is demonstrated over 42Km SMF. 100 dBHz^{2/3} SFDR is achieved by suppressing the 3IMD with back drop port of a self-coupled micro ring resonator.

F1C.5 • 09:45

Generating Multiple Chirped Microwave Waveforms Using an Integrated Arrayed Waveguide Sagnac Interferometer, Parisa Moslemi¹, Martin Rochette¹, Lawrence R. Chen¹; ¹McGill U., Canada. We demonstrate an integrated multi-channel spectral shaper in silicon photonics for generating two chirped microwave waveforms simultaneously with a central frequency of ~ 45 GHz and RF chirps of -273.3 GHz/ns and +233.1 GHz/ns and time bandwidth products of 17.8 and 26.9.

F1D • Entanglement and Squeezed States III—Continued**F1D.3 • 09:15**

Enhanced Fluorescence Collection from Color Centers via Channeling Through a Diamond Pyramid, Victor Leong¹, Sumin Choi¹, Gandhi Alagappan², Leonid Krivitsky¹; ¹Data Storage Inst., A*STAR, Singapore; ²Inst. of High Performance Computing, A*STAR, Singapore. We study silicon-vacancy centers in commercial diamond AFM tips. Fluorescence collection is enhanced by ~15 \times when collected at the base due a channeling effect given by the tapered geometry.

F1D.4 • 09:30

Experimental two-way communication with one photon, Francesco Massa¹, Amir Moqanaki¹, Joshua A. Kettlewell^{1,2}, Flavio Del Santo¹, Borivoje Dakic^{1,2}, Philip Walther¹; ¹Univ. of Vienna, Austria; ²Inst. for quantum optics and quantum information (IQOQI), Austrian Academy of Science, Austria; ³Singapore Univ. of Technology and Design, Singapore; ⁴Centre for Quantum Technologies, National Univ. of Singapore, Singapore. We experimentally demonstrate that quantum superposition permits two-way communication between two distant parties that can exchange only one photon and show that the transmitted bits and the direction of communication remain private

F1D.5 • 09:45

Generation of near IR correlated photon pairs in optical nano-fibers, Jin-Hun Kim¹, Yong Sup Ihn¹, Heedeuk Shin¹, Yoon-Ho Kim¹; ¹Pohang Univ of Science & Technology, Korea. We report the generation of near-IR nondegenerate correlated photon pairs in a 13-cm-long optical nano-fiber. The coincidence-to-accidental ratio (CAR), 400 has been achieved at average pump power of 70 μ W.

F1E • Optical Fiber Sensing and Microfluidics—Continued**F1E.2 • 09:30**

Unprocessed whole blood sensing using micropost-embedded microfluidics with guided-mode resonance, Chan Te Hsiung¹, Meng-Zhe Tsai¹, Yang Chen¹, Cheng-Sheng Huang¹, Hsin-Yun Hsu², Pei-Ying Hsieh²; ¹Mechanical Engineering, National Chiao Tung Univ., Taiwan; ²Applied Chemistry, National Chiao Tung Univ., Taiwan. We demonstrate a Lab-on-a-chip (LOC) system for whole blood sensing. The LOC consists of a microfluidic chip including an array of microposts for cell filtration and a label-free guided-mode resonance biosensor for real-time quantification.

F1E.3 • 09:45

Optical fiber-tip microfluidic refractive-index sensor, Mian Yao^{1,2}, Ouyang Xia², A. Ping Zhang¹, Hwa-Yaw Tam², Ping Kong A. Wai¹; ¹Dept. of Electronic and Information Engineering, The Hong Kong Polytechnic Univ., Hong Kong; ²Dept. of Electrical Engineering, The Hong Kong Polytechnic Univ., Hong Kong. We present a miniature refractive-index sensor based on a fiber-top suspended mirror device. An optical 3D μ -printing technology was demonstrated to fabricate ultrathin suspended diaphragms on the end face of optical fiber for microfluidic sensing.

F1F • Related Technologies and Applications for Imaging, Display and Storage—Continued**F1F.4 • 09:15**

Computational Analysis of Optically Pumped Quantum Dots Array on the Glass for Micro-LED Applications, Chung Ping Guang¹, Chien-Chung Lin³, Shu-Hsiu Chang², Yu-Ming Huang³, Chung-Ping Yu³, Hao-Chung Kuo⁴; ¹Inst. of Lighting and Energy Photonics, National Chiao-Tung Univ., Taiwan; ²Inst. of Imaging and Biomedical Photonics, National Chiao-Tung Univ., Taiwan; ³Inst. of Photonic System, National Chiao-Tung Univ., Taiwan; ⁴Inst. of Electro-Optical Engineering, National Chiao-Tung Univ., Taiwan. An optical simulation of tri-pixel structure quantum dot display was evaluated numerically. The light cross-talk phenomenon is obtained by analyzing optical field distribution from various lens design and glass thicknesses.

F1F.5 • 09:30

A Hole-filling Method for DIBR Based on Convolutional Neural Network, Yongrui Li¹, Xinzhu Sang¹, Duo Chen¹, Peng Wang¹, Huachun Wang¹, Jinhui Yuan^{1,2}, Kuiru Wang¹, Binbin Yan¹; ¹State Key Laboratory of Information Photonics and Optical Communications, Beijing Univ. of Posts and Telecommunications, China; ²Photonics Research Centre, Dept. of Electronic and Information Engineering, The Hong Kong Polytechnic Univ., Hong Kong. There are holes for images generated by Depth-Image-Based Rendering (DIBR) method due to occlusion of foreground. An algorithm to fill holes based on convolutional neural networks is presented. PSNR of the image after filling holes is 32.65dB.

F1F.6 • 09:45

Broadband Achromatic Aplanatic Flat Doublet in Mid-infrared, Hao Chenglong^{1,2}, Changyuan Yu^{1,3}, Cheng-Wei Qiu¹; ¹National Univ. of Singapore, Singapore; ²National Univ. of Singapore (Suzhou) Research Inst., China; ³The Hong Kong Polytechnic Univ., Hong Kong. We propose a broadband achromatic aplanatic flat doublet, which works at 3.8 μ m to 4.4 μ m. The combination of sapphire flat lens and fused silica flat lens suppress the chromatic aberration and off-axial aberrations simultaneously.

Room S223

10:30–12:30
F2A • Laser Comb Technologies

Presider: Guoqing Chang;
Center for Free Electron Laser Science, USA

F2A.1 • 10:30

Half-cycle mJ-level CEP-stable Pulses from Parametric Waveform Synthesis, Giulio Maria Rossi^{1,2}, Roland E. Mainz^{1,2}, Fabian Scheiba^{1,2}, Yudong Yang^{1,2}, Giovanni Cirmi^{1,2}, Franz Kaertner^{1,2}; ¹DESY - CFEL, Germany; ²Physics Dept. and The Hamburg Centre for Ultrafast Imaging, Univ. of Hamburg, Germany. Nearly transform-limited, carrier-envelope phase stable, 3.4 fs pulses with central wavelength of 1.8 μm are generated via parametric waveform synthesis. The mJ-level energy, at 1 kHz repetition rate, allows for waveform-controlled bright high-harmonic generation.

F2A.2 • 10:45

Nonlinear amplification for a 10 W, 750-MHz Yb: fiber frequency comb, Hirotsuka Ishii¹, Bo Xu^{1,2}, Yuxuan Ma^{1,3}, Isao Matsushima^{1,2}, Yoshiaki Nakajima^{1,2}, Thomas Schibli⁴, Zhigang Zhang³, Kaoru Minoshima^{1,2}; ¹The Univ. of Electro-Communications, Japan; ²Japan Science and Technology Agency, ERATO MINOSHIMA Intelligent Optical Synthesizer Project, Japan; ³Peking Univ., China; ⁴Univ. of Colorado, USA. In this study, a self-referenced 750-MHz Yb: fiber frequency comb was amplified to achieve an average power of 10 W with nonlinear amplification. Pulse duration of 107 fs and a clear comb structure was obtained.

F2A.3 • 11:00

Brillouin Lasing and Frequency Comb Generation in Bulk CVD Diamond, Robert J. Williams¹, Zhenxu Bai^{1,2}, Soumya Sarang¹, David J. Spence¹, Richard P. Mildren¹; ¹Macquarie Univ., Australia; ²Harbin Inst. of Technology, China. We report a Brillouin laser in diamond bulk pumped by a Raman-generated intracavity field at 1.24 μm . Configurations for single-Stokes and frequency comb operation are demonstrated, foreshadowing new opportunities for extremely-bright lasers and on-chip diamond devices.

Room S224

10:30–12:30
F2B • Novel Plasmonics Nanostructures and Phenomena

Presider: Wending Zhang,
Northwestern Polytechnical Univ., China

F2B.1 • 10:30 **Invited**

Anisotropic Plasmonic Light Scattering, Jianfang Wang¹; ¹Dept. of Physics, The Chinese Univ. of Hong Kong, Hong Kong. Control of light propagation in space is important in optical and optoelectronic devices, photonic circuits and solar energy harvesting. Plasmonic nanostructures are demonstrated to scatter light in specific directions in space.

F2B.2 • 11:00

Designed conversion of spin and orbital angular momentum, Gun-Yeal Lee¹, Jang-woon Sung¹, Byounggho Lee¹; ¹Seoul National Univ., Korea. A novel metasurface providing arbitrarily designed spin-orbit interactions of light has been proposed. Our theoretical and experimental demonstrations show the great potential of the phenomenon for various applications including optical communications and quantum optical process.

Room S225

10:30–12:30
F2C • Photonic Microwave Generation, Processing and Measurement

Presider: Motoharu Matsuura;
Univ. of Electro-Communications, Japan

F2C.1 • 10:30 **Invited**

Microwave Nanophotonic Technologies for Instantaneous Frequency Measurement Systems, Maurizio Burla¹, Xu Wang², Ming Li³, Lukas Chrostowski², Jose Azana⁴; ¹ETH Zurich, Switzerland; ²Univ. of British Columbia, Canada; ³Inst. of Semiconductors, China; ⁴Institut National de la Recherche Scientifique, Canada. This paper describes recent solutions for microwave instantaneous frequency measurement (IFM) systems based on integrated microwave photonics, with particular emphasis on the use of waveguide Bragg gratings (WBG) as a possible approach for the creation of a monolithic photonic IFM system.

F2C.2 • 11:00

Wideband Microwave Frequency Down-Conversion with Optical Harmonics Intensifier and Low-Frequency Local Oscillator, Xinhai Zou¹, Shang Jian Zhang¹, Heng Wang¹, Mengke Wang¹, Zhiyao Zhang¹, Yali Zhang¹, Yong Liu¹; ¹Univ. of Electron. Sci&Tech of China, China. A photonic-based method for wideband microwave frequency down-conversion is proposed and demonstrated by using a low-frequency electrical local oscillator and an optical harmonics intensifier through cascaded four-wave mixing in a semiconductor optical amplifier.

Room S226

10:30–12:30
F2D • Optical Technologies for Communications

Presider: Hai Han Lu;
National Taipei Univ. of Technology, Taiwan

F2D.1 • 10:30 **Invited**

Silicon Photonics Transceiver, Jinyu Mo¹; ¹MACOM, China. In this talk, we discuss recent advance on integrated silicon photonics transceiver for data center applications, including optical passive alignment, 100G CWDM4 SiPh transmitter and PAM-4 transmission system based on silicon photonics.

F2D.2 • 11:00

High-Security Stream-Cipher Generation Employing Synchronized Random Bit Generation and RC4 Algorithm, Chenpeng Xue¹, Ning Jiang¹, Xiaoyan Zhao¹, Anke Zhao¹, Yanhua Hong², Kun Qiu¹; ¹Univ of Electronic Science & Tech China, China; ²Bangor Univ., UK. We propose a new stream-cipher generation scheme based on the correlated physical random bit generation with synchronized chaotic lasers and pseudo-random bit extension RC4 algorithm. The proposed scheme shows high-security, extensible rate and strong robustness.

Room S227

10:30–12:30
F2E • Laser Dynamics

Presider: Feng Li;
The Hong Kong Polytechnic Univ., Hong Kong

F2E.1 • 10:30 **Invited**

Soliton Transient Dynamics in Ultrafast Fiber Lasers, Zhi-Chao Luo¹, Meng Liu¹, Aiping Luo¹, Wen-Cheng Xu¹, Qi Guo¹; ¹South China Normal Univ, China. We review our recent results on the investigations of soliton transient dynamics in ultrafast fiber lasers, i.e., the buildup dynamics of dissipative soliton and conventional soliton, soliton explosions, rogue wave generation, real-time spectral features of vector soliton. Our findings may be useful for better understanding the soliton dynamics.

F2E.2 • 11:00

Generation of scalar and vector solitons in a bidirectional mode-locked fiber laser, Yang Xiang¹, Yiyang Luo¹, Bowen Liu¹, tao liu¹, Zhijun Yan¹, Deming Liu¹, Qizhen Sun¹; ¹Huazhong Univ of Science and Technology, China. We report on a bidirectional fiber laser mode-locked by the nonlinear polarization rotation technique. Experimentally, the scalar and vector solitons are observed in the opposite directions of a fiber laser for the first time.

Room S228

10:30–12:30
F2F • Technologies and Approaches for Optical Transmission and Processing

Presider: Gabriella Cincotti;
Univ. Roma Tre, Italy

F2F.1 • 10:30 **Invited**

Polarization Maintaining Few Mode Fibers for Space Division Multiplexing, Sophie La-Rochelle¹, Alessandro Corsi¹, Jun Ho Chang¹, Leslie Rusch¹, Younes Messaddeq¹; ¹Universite Laval, Canada. We review proposals of polarization maintaining fibers for short reach MIMO-less space division multiplexing. We summarize transmission experiments with an elliptical ring core fiber and propose hole-assisted elliptical core designs to scale the capacity.

F2F.2 • 11:00 **Invited**

Distributed Raman Amplification for Combating Optical Nonlinearities in Fibre Transmission, Mingming Tan¹, Mohammad A. Al-Khateeb¹, Md A. Iqbal¹, Andrew Ellis¹; ¹Aston Univ., UK. The paper reviews distributed Raman amplification technologies which can provide near symmetric signal power profiles, in order to maximize the efficiency of optical nonlinearity compensation in long-haul optical transmission systems using mid-link optical phase conjugation.

Room S223

F2A • Laser Comb Technologies—Continued

F2A.4 • 11:15

Continuous-Wave Brillouin Laser Using Bulk Diamond, Zhenxu Bai^{1,2}, Robert J. Williams¹, Ondrej Kitzler¹, Soumya Sarang¹, David J. Spence¹, Richard P. Mildren¹, ¹MQ Photonics Research Centre, Macquarie Univ., Australia; ²National Key Laboratory of Science and Technology on Tunable Laser, Harbin Inst. of Technology, China. We report a novel platform for Brillouin lasers in bulk, based on diamond. Continuous-wave lasing at 532.16-nm is demonstrated in a doubly-resonant ring cavity, from which we deduce a gain coefficient $g_p = 60$ cm/GW.

F2A.5 • 11:30

Mode-resolved dual-comb spectroscopy with a free-running polarization-maintain fiber laser cavity, Zejiang Deng¹, Chao Wang¹, Yangcheng Ou¹, Zhiwei Zhu¹, Chenglin Gu¹, Yang Liu¹, Daping Luo¹, Wenxue Li¹; ¹East China Normal Univ., China. A simple and robust dual-comb scheme with different repetition rates is demonstrated from a passively mode-locked polarization-maintain fiber cavity. With mutual coherent properties in a single cavity, mode-resolved spectroscopy is obtained with free-running state.

F2A.6 • 11:45

All-polarization-maintaining Er-fiber-based dual optical frequency combs with nonlinear amplifying loop mirror, Yoshiaki Nakajima^{1,2}, Yuya Hata¹, Kaoru Minoshima^{1,2}; ¹Univ. of Electro-Communications, Japan; ²JST ERATO MINOSHIMA IOS Project, Japan. An all-polarization-maintaining Er-fiber-based dual-comb fiber laser with nonlinear-amplifying-loop-mirror is demonstrated for realizing simple and robust dual-comb spectroscopy using two mutually coherent combs with slightly different repetition rates emitted from the laser cavity.

Room S224

F2B • Novel Plasmonics Nanostructures and Phenomena—Continued

F2B.3 • 11:15

Ultra-narrow Nanoslit Cavities for High-Q Resonances in the Visible Range, Kai Chen¹, Gary Razinkas², Henning Vieker³, Heiko Gross², Xiaofei Wu², André Beyer³, Armin Gölzhäuser³, Bert Hecht²; ¹Jinan Univ., China; ²Universität Würzburg, Germany; ³Universität Bielefeld, Germany. We fabricated asymmetric nanoslit cavities by milling with helium ion microscope on the edge of single-crystal gold stripes with one end open to the air. The cavities exhibit high-Q multiple resonances in the visible range.

F2B.4 • 11:30

Asymmetric spin splitting of Gaussian beam reflected from an air-chiral interface, Chen Qi¹; ¹Jinan Univ., China. We investigate systematically the chirality induced asymmetric spin splitting when Gaussian beams reflected from an air-chiral interface. We find that one spin component of the reflected beam can undergo large displacement near points of $|r_{pp}|=|r_{sp}|$.

F2B.5 • 11:45

Angle-insensitive Broadband Absorption in Tapered Patch Antennas, Lu Liu¹, Hao Peng¹, Xiangxiao Ying¹, Zhe Li¹, Yadong Jiang¹, Jimmy Xu^{1,2}, Zhijun Liu¹; ¹Univ. of Electronic Science & Tech China, China; ²Brown Univ., School of Engineering, USA. Near-perfect broadband absorption is demonstrated in a tapered-strip patch antenna array for large angles up to 75°. The angle-insensitive absorption is attributed to an angle-independent coupling mechanism between multiple magnetic resonances and free-space incident light.

Room S225

F2C • Photonic Microwave Generation, Processing and Measurement—Continued

F2C.3 • 11:15

Microwave Generation by an Optoelectronic Oscillator with 1.55 μ m AlGaInAs/InP Microcavity Laser, Yue-De Yang¹; ¹Inst. of Semiconductors, CAS, China. We demonstrate the optoelectronic oscillator based on a 1.55 μ m direct-modulated AlGaInAs/InP microcavity laser for microwave generation. Single sideband phase noise of -116 dBc/Hz at 10 kHz frequency offset is obtained for the generated signal.

F2C.4 • 11:30

Photonics based Microwave Frequency Shifter for Doppler Shift Compensation in High-Speed Railways, Ruiqi Zheng¹, Youxue Kong¹, Erwin Chan², Yuan Cao¹, Xudong Wang¹, Xinhuan Feng¹, Bai-Ou Guan¹; ¹Inst. of Photonics Technology, Jinan Univ., China; ²School of Engineering and Information Technology, Charles Darwin Univ., Australia. A photonic signal processor for removing the Doppler effect in high-speed railway mobile communication is simulated with results agree with theory. It is based on a time stretch/compress system to shift a microwave signal frequency.

F2C.5 • 11:45

Wideband Jamming Signal Generator Based on Dual Coherent Optical Frequency Combs, Hui Gao¹, Wenjuan Chen², Zhenzhou Tang², Dan Zhu²; ¹Science and Technology on Antenna and Microwave Laboratory, China; ²Nanjing Univ. of Aeronautics and Astronautics, China. Jamming signal covering 11~15GHz generated from an intermediate frequency covering 3~4GHz based on dual coherent optical frequency combs was demonstrated. The SNR and the LO suppression of the generated signal were both greater than 50dB.

Room S226

F2D • Optical Technologies for Communications—Continued

F2D.3 • 11:15

Chaos communication using chaos synchronization of monolithic silicon micro-cavities, Yongjiao Niu¹, Jia-Gui Wu^{1,2}, Shaojie Wang¹, Ciwei Luo¹, Shukai Duan¹, Chee Wei Wong²; ¹Southwest Univ., College of Electronic and Information Engineering, China; ²Univ. of California, Fang Lu Mesoscopic Optics and Quantum Electronics Laboratory, USA. We propose a long distance optics encryption system using silicon optomechanical (OM) micro-chips. Based on chaos synchronization between two slave OM micro-cavities, two 50Mb/s messages oppositely transmitted and effectively decrypted over 500 km.

F2D.4 • 11:30

Wideband Complexity-Enhanced Optical Chaos Generation and its Application for Fast Random Bit Generation, Anke Zhao¹, Ning Jiang¹, Chao Wang¹, Jing Zhang¹, Kun Qiu¹; ¹Univ. of Electronic Science & Tech China, China. A flat-spectrum optical chaos generation scheme which affords significant bandwidth enhancement and perfect time-delay-signature suppression is proposed and demonstrated. Based on this, true random bit generation can up to 800 Gb/s can be directly achieved.

F2D.5 • 11:45

Joint-Switching Characteristics of LCoS-Based Wavelength Selective Switches, Kosuke Yamashita¹, Masahiko Jinno¹; ¹Kagawa Univ., Japan. We show that inter-subchannel crosstalk of a joint-switching wavelength-selective-switch based on a liquid-crystal-on-silicon spatial-light modulator significantly degrades while the applied optical attenuation increases even in an interleaved fiber arrangement.

Room S227

F2E • Laser Dynamics—Continued

F2E.3 • 11:15

Bidirectional mode-locked Er-fiber laser with symmetrical cavity configuration, Yuya Hata², Yoshiaki Nakajima^{2,1}, Kaoru Minoshima^{2,1}; ¹JST, ERATO MINOSHIMA Intelligent Optical Synthesizer Project, Japan; ²The Univ. of Electro-Communications, Japan. Bidirectional mode-locked Er-fiber laser with two saturable absorber mirrors and nonlinear polarization rotation is developed. Remarkable broad optical spectra in both directions with high relative stability is performed owing to symmetrical cavity configuration.

F2E.4 • 11:30

Picosecond and Femtosecond Operation of a Diode-pumped Nd:Gd:SrF₂ Laser, Václav Kubeček¹, Michal Jelinek¹, Miroslav Cech¹, David Vyhřal¹, Fengkai Ma², Dapeng Jiang², Liangbi Su²; ¹Czech Technical Univ. in Prague, Czechia; ²CAS Key Laboratory of Transparent and Opto-functional Inorganic Materials, Shanghai Inst. of Ceramics, Chinese Academy of Sciences, China. Passively mode-locked operation of diode-pumped Nd:Gd:SrF₂ laser is reported. Trains of 1.9 ps pulses at 1051 nm, 1.2 ps at 1059 nm, or 321 fs at 1053.5 nm were obtained for pump power lower than 1.3 W.

F2E.5 • 11:45

Observation of Soliton Molecules in a Fiber Laser Based on WS₂ Saturable Absorber, Bowen Liu¹, Yang Xiang¹, Yiyang Luo¹, Zhijun Yan¹, Yingxiang Qin¹, Qizhen Sun¹, Xiahui Tang¹; ¹Huazhong Univ. of Science and Technology, China. We report the observation of soliton molecules in a WS₂ fiber laser. Experimentally, tightly bound soliton molecules and bunch of soliton molecules are respectively obtained which unveils the dynamics of soliton complexes in fiber lasers.

Room S228

F2F • Technologies and Approaches for Optical Transmission and Processing—Continued

F2F.3 • 11:30

Frequency Spacing and Offset Tunable Multiple-Frequency-Spaced Optical Comb Generation Using Multiple-Parallel Phase Modulator, Takahide Sakamoto¹, Akito Chiba²; ¹National Inst of Information & Comm Tech, Japan; ²Gunma Univ., Japan. We propose reconfigurable optical comb generation using multiple-parallel phase modulator. Frequency spacing and offset of the generated combs are flexibly multiplied in several times against the driving frequency. Design criteria is clarified and numerically verified.

F2F.4 • 11:45

Rapid and accurate generation of Laguerre-Gaussian vortex beams using digital micro-mirror device, Lei Liu¹, Yesheng Gao¹, Xingzhao Liu¹; ¹Shanghai Jiao Tong Univ., China. We propose a novel method for fast switchable, reconfigurable optical vortex beams generation with significantly high precision using a DMD. For Laguerre-Gaussian mode, the fidelity under the proposed method can reach 0.9969 and the corresponding RMSE can be as low as 0.0146.

Room S223**F2A • Laser Comb Technologies—Continued****F2A.7 • 12:00**

An hybrid er:fiber femtosecond Laser for optical frequency comb applications, Yanyan Zhang^{1,2}, Lulu Yan^{1,2}, Pan Zhang¹, Bingjie Rao^{1,2}, Shougang Zhang^{1,2}, Haifeng Jiang^{1,2}; ¹National Time Center Service, China; ²Univ. of Chinese Academy of Science, China. An Er:fiber-based femtosecond laser employing nonlinear amplifier loop mirror (NALM) and nonlinear polarization evolution (NPE) mode-locking mechanisms is demonstrate. The hybrid laser combines advantages of good robustness of NALM and low noise feature of NPE.

F2A.8 • 12:15

Numerical analysis on double frequency-spacing optical comb for optimization of RF signals driving I-Q MZM, Akito Chiba¹, Yuta Moteki¹, Nobuhiro Kobayashi¹, Takahide Sakamoto^{2,3}, Kazumasa Takada¹; ¹Gunma Univ., Japan; ²NICT, Japan; ³Japan Science and Technology agency, Japan. A numerical simulation is conducted for generating double-frequency-spacing optical frequency comb by an in-phase and quadrature optical modulator. RF-signal condition driving the comb has been optimized for generating the comb with low spectral-roughness.

Room S224**F2B • Novel Plasmonics Nanostructures and Phenomena—Continued****F2B.6 • 12:00**

Plasmonic analogue of strong coupling in gold nanorods, Yixiao Gao¹, Limin Tong¹; ¹Zhejiang Univ., China. We numerically analyze the plasmonic interaction between dipole mode in a gold nanorod and dark mode in a nanorod dimer. Spectral splitting satisfies the strong coupling criterion. Electromagnetic energy Rabi oscillation is also observed.

F2B.7 • 12:15

Point-like surface plasmon polariton source from complementary split-ring resonators, Jin-Kyu Yang¹; ¹Optical Engineering, Kongju National Univ., Korea. We numerically studied about the point-like surface plasmon polariton source from the complementary split-ring resonator (CSRR). When the normal incident light was lineally polarized parallel to the symmetric axis of the CSRR, monopole-like point SPP source was excited.

Room S225**F2C • Photonic Microwave Generation, Processing and Measurement—Continued****F2C.6 • 12:00**

Experimental Analysis of Multiple Beam Injection in SMFP-LD for Multi-RF Generation, Bikash Nakarmi¹, Hao Chen¹, Shilong Pan¹; ¹Nanjing Univ Aeronautics & Astronautics, China. In this paper, we use injection locking with negative wavelength detuning in a single SMFP-LD to demonstrate multi-RF generation of same and different bands. Further, we analyzed different parameters required for multi-RF generation using SMFP-LD.

F2C.7 • 12:15

Microwave Photonic Upconverter With Frequency Doubling Based on Dual-Polarization Dual-Parallel Mach-Zehnder Modulator, Dayong Wang^{1,2}, Jingnan Li^{1,2}, Yunxin Wang^{1,2}, Jiahao Xu^{1,2}, Tao Zhou³, Xin Zhong³, Dengcai Yang^{1,2}, Feng Yang^{1,2}; ¹College of Applied Sciences, Beijing Univ. of Technology, China; ²Beijing Engineering Research Center of Precision Measurement Technology and Instruments, Beijing Univ. of Technology, China; ³Science and Technology on Electronic Information Control Laboratory, China. A microwave photonic frequency upconverter based on dual-polarization dual-parallel Mach-Zehnder modulator is proposed. The frequency doubled upconversion signal is obtained by beat frequency between the +1st-order intermediate frequency sideband and the -2nd-order local oscillator sideband.

Room S226**F2D • Optical Technologies for Communications—Continued****F2D.6 • 12:00**

Capacity of FSO systems over lognormal fading channels with generalized pointing errors, Ruben Boluda-Ruiz², Antonio Garcia-Zambrana¹, Beatriz Castillo-Vazquez¹, Carmen Castillo-Vazquez², Khalid Qaraqe²; ¹Communications Engineering, Univ. of Málaga, Spain; ²Electrical and Computer Engineering, Texas A&M Univ. at Qatar, Qatar; ³Mathematical Analysis, Statistics and Operations Research and Applied Mathematics, Univ. of Malaga, Spain. A novel approximate closed-form expression for the ergodic capacity of FSO communication systems over log-normal atmospheric turbulence channels with generalized pointing errors is obtained which is valid from low to high SNR.

F2D.7 • 12:15

Improvement of positioning accuracy in visible light positioning system using orthogonal frequency division multiple access, Yitong Xu¹, Zixiong Wang¹, Jiahui Sun¹, Jian Chen², Shiyong Han³, Changyuan Yu⁴, Jinlong Yu¹; ¹Tianjin Univ., China; ²Nanjing Univ. of Posts and Telecommunications, China; ³Nankai Univ., China; ⁴The Hong Kong Polytechnic Univ., Hong Kong. We proposed a novel power allocation scheme to improve the positioning accuracy in VLP system using OFDMA. The signal's power is allocated to minimize the differences among errors of square of estimated transmission distances.

Room S228**F2F • Technologies and Approaches for Optical Transmission and Processing—Continued****F2F.5 • 12:00**

High resolution photonic RF switching based on coherent Brillouin interactions, Anjali B. Yelikal¹, Siva Shakthi A¹, Ravi Pant¹; ¹IISER Thiruvananthapuram, India. We report the demonstration of an electrically controlled two-channel microwave photonic switch of 40 dB extinction exploiting coherent interaction of Stokes and anti-Stokes fields associated with the stimulated Brillouin scattering in polarization maintaining fiber.

F2F.6 • 12:15

Joint Fine Time Synchronization and Channel Estimation for PDM-CO-OFDM System, Yuanxiang Chen¹, Yongtao Huang¹, Kaile Li¹, Yitong Li¹, Jianguo Yu¹; ¹Beijing Univ. of Posts and Telecommunications, China. We propose a joint fine time synchronization and channel estimation method for PDM-CO-OFDM system. The method can effectively correct synchronous error of CHU sequence caused by CD and PMD and improve channel estimation accuracy. A signal Q-value improvement of 0.8 dB is achieved after 2400 km SSMF transmission.

12:30–14:00 Lunch**Afternoon Tours**

Key to Authors and Presiders

A

A, Siva Shakthi - F1C.3, F2F.5
Abbasirad, Najmeh - W2H.2
Abdelsalam, Dahi - Tu2F.2
Abdul Rahim, Ahmad Amirul
- W4K.6
Abobaker, Abdosllam M. - W3A.83
Abshire, James B. - Tu3A.2
Acedo, Pablo - W4F.1
Adamo, Giorgio - Th4E.2
Adiya, Munkhbayar - W4J.7
Afshar V, Shahraam - W1L.2
Aguilo, Magdalena - W4A.2
Ahmed, Zeeshan - W3A.2
Ahn, Kwang Jun - W4C.6
Ahn, Tae-Jung - W3A.70, W3A.77,
W3A.81
Aida, Kazuo - W4I.5
Aihara, Takuma - Th2J.2
Aikawa, Masaki - W3A.117
Ait Sab, Omar - Th1I.5
Akahane, Kouichi - W4J.2
Akiwa, Yuki - Tu3C.6
Akosman, Ahmet E. - Tu2B.1
Akulshin, Alexander - W3A.113
Alagappan, Gandhi - F1D.3
Alam, Shaiful - Tu3A.5
Alaraimi, Mohammed - Th1A.4,
W3A.58, W4A.5
Alaskar, Yazeed - W2J.5
Albadri, Abdulrahman - W2J.5
Albrecht, Manfred - Th1B.4
Alessandri, Chiara - Th4G.3
Ali, Muhsin - W1L.2
Alias, Mohd Sharizal - W2J.5
Aljunid, Syed Abdullah - Th4E.2
Al-Khateeb, Mohammad A. - F2F.2
Allan, Graham R. - Tu3A.2
Allayarov, Izzatjon - W4E.6
Allcock, David T. - W1A.3
Aloian, Georgii A. - W3A.137
Alyamani, Ahmed - W2J.5
Amano, Ryo - W3A.75
Ambrosio, Antonio - W1H.2, W2H.1
Amemiya, Tomohiro - Tu2H.5
Amezcuca Correa, Rodrigo - W4L.2
Amouzou, Koffi - Th2A.7
An, Chengwu - Tu3F.7
An, Zhang Y. - F1F.3

Anderson, Miles - W2F.1
Andreoli, Louis - W1D.4
Anopchenko, Aleksei - Th1F.4
Anthur, Aravind P. - Tu3D.3
Antipov, Sergei - Th4D.6
Antonio-Lopez, E. - W4L.2
Anyi, Caroline - Tu3F.4
Aphale, Sumeet S. - W3A.83
Arai, Shigehisa - Tu2H.5
Araki, Shungo - Th3A.2
Araneda, Gabriel - W2G.1
Arnold, Catherine - Th1F.4
Arrizabalaga, O. - W4L.2
Arslan, Dennis - W2H.2
Asahara, Akifumi - Th1C.5, W4F.7
Asahina, Yu - W2F.3
Asaka, Toru - W2E.5
Ashida, Kohei - W3A.116, W4D.3
Asselberghs, Inge - Th4G.3
Ataie, Vahid - Tu2D.6
Atature, Mete - Tu3G.3
Atta, Muhammad Asim - W3A.21
Ayoub, Mousa - Th1B.1
Azana, Jose - F2C.1, Th1C.1

B

B. Yelikar, Anjali - F1C.3, F2F.5
Babin, Sergey A. - Th2A.1
Bader, Georges - Th2A.7
Bae, Ji - Tu2B.5
Bae, Jongsuck - W3A.66
Bahir, Gad - Tu2C.2
Bai, Benfeng - Th3K.2, W3A.10
Bai, Ping - Th2F.2, Th2H.4
Bai, Yingxing - Tu3L.8
Bai, Zhenxu - F2A.3, F2A.4
Baker, Christopher - Tu3F.3
Ballato, John - Th2E.2
Ban, Guoxun - W2B.5
Banakar, Mehdi - Th3C.2
Bang, Li - W3A.5
Bang, Ole - Th3D.5
Banzer, Peter - Th1G.2
Bao, Lifeng - W4L.3
Barbone, Matteo - Tu3G.3
Barner-Kowollik, Christopher -
W1E.3, W2E
Barry, Liam P. - Tu3D.3
Bartolini, Saverio - W2C.4

Barua, Pranabesh - Tu3A.5
Bazin, Alexandre - Th3C.2
Bean, Brian R. - Tu3A.2
Beggs, Daryl M. - Th4H.5
Bej, Subhajit - Th1F.4
Belli, Federico - W2A.1
Benbraham, Fatma - Th3A.1
Beresna, Martynas - F1E.1
Bermak, Amine - W3A.21
Beyer, André - F2B.3
Bharathan, Gayathri - F1A.1
Bhasker, Prashanth - Th2J.3
Bhatia, Nitin - F1B.5, W3A.104
Bhattacharjee, Sayan - Tu3H.2
Bian, Shihang - W3A.22
Billah, Muhammad R. - W4J.1
Bisson, Jean-Francois - Th2A.7,
Th3A.5
Biswas, Abhijit - Tu3H.2
Blaicher, Matthias - W4J.1
Blatt, Rainer - W2G.1
Bo, Tianwai - Tu2I.2, W2I, W4I.1
Bodnar, Nathan - W1C.1
Boluda-Ruiz, Ruben - F2D.6
Bonneau, Damien - Th1D.4
Bouchand, Romain - W2F.1
Bountis, Anastasios - Th3J.3
Bowen, Warwick P. - Tu2G.1, Tu3F.3
Bowers, John - Th2J.3
Boyko, Andrey - W4B.6
Bradford, Joshua - W1C.1
Brambilla, Gilberto - F1E.1
Brems, Steven - Th4G.3
Brox, Olaf - W2J.2
Brunner, Daniel - W1D.4
Bu, Xiangbao - Th1A.3
Buchler, Ben - Th1D.2
Bucio, Thalia Dominguez - W2D.1
Bulmer, Kris - Th2A.7
Burd, Shaun C. - W1A.3
Burla, Maurizio - F2C.1
Butt, Muhammad - Th1G.2

C

C. Warren-Smith, Stephen - Th2E.4
Cai, Dong T. - W3A.78
Cai, Huaqiang - W4A.2
Cai, Qianhang - Tu3G.4
Cai, Shanyong - W3A.101, W3A.105

Cai, Shiwei - W4J.6
Cai, Xinlun - Th2J.4, Tu2H.2, W4D
Cai, Yangjian - W3A.48
Cai, Yong-Jing - Tu3J.6
Cai, Yu - Th2A.2
Calmano, Thomas - W4A.1
Calsat, Alain - Th1I.5
Camp, Jordan B. - W2L.3
Campbell, Geoff - Th1D.2
Campo, Giulio - W2C.4
Cancio, Pablo - W2C.4
Canning, John - F1B.1, W4E
Cao, Chun-Fang - Tu2H.4
Cao, Deng - W3A.61
Cao, Honglong - W3A.22
Cao, Juncheng - Tu2C.4
Cao, Juntao - Th2I.3, W3A.19
Cao, Ling - Tu3B.4
Cao, Tao - W3A.62
Cao, Victoria - W1F.2
Cao, Wenxiang - Th3I.2
Cao, Yaoyu - Th1K.2
Cao, Yu Long - Tu2B.4
Cao, Yuan - F2C.4, W2L.4
Cao, Yulong - W3A.38
Capasso, Federico - W1H.2, W2H.1
Cappelli, Francesco - W2C.4
Carpintero, Guillermo - Th3F,
W1L.2, W2J.4
Castellano-Hernández, Elena
- Th4A.5
Castillo-Vazquez, Beatriz - F2D.6
Castillo-Vazquez, Carmen - F2D.6
Cavillon, Maxime - Th2E.2
Cech, Miroslav - F2E.4
Cen, Qizhuang - W3A.18
Cha, Myoungsik - Tu3F.6, W2B.6
Chan, Calvin C.K. - Tu2I, Tu3I, W4I.1
Chan, Che T. - Th2F.3
Chan, Eng Aik - Th4E.2
Chan, Erwin - F2C.4
Chan, Kam Wai C. - W3A.112
Chan, Sze-Chun - F1C.2, Tu3G
Chan, Terence - W1I.2
Chang, Chin-Lun - W2E.1
Chang, Guoqing - F2A, Tu3B.2,
W1G.3
Chang, Hao-Hsiang - Th3I.6, W2I.4

Chang, Hong - Th3H.5, Tu3G.6
Chang, Huicong - Th4G.4
Chang, Jun Ho - F2F.1
Chang, Lihua - F1F.2
Chang, Shu-Hsiu - F1F.4, Th3J.4
Chang, Weijie - W4H.2
Chang, Yin-Jung - W3A.11
Chang, Zeshan - Tu3E.4
Charlton, Martin - W3A.2, W3A.8
Chatterjee, Sourav - Th4D.2
Chaudhary, Kundan - W2H.1
Chávez-Cerda, Sabino - Th2A.4
Che, Di - Tu2I.1
Chemnitz, Mario - Th1E.1
Chen, Bingying - Th4A.2
Chen, Chao-Wei - Th3I.6, W2I.4
Chen, Chen - Th4I.2
Chen, Cheng-Huan - F1F.1, Th1K.3
Chen, Cuiguang - W3A.14
Chen, Daomin - Th4F.5
Chen, Dejun - W4C.3, W4C.4
Chen, Dian - Th2L.1
Chen, Duo - F1F.5
Chen, Feiliang - W1J.3
Chen, Gaoyang - Th4L.5
Chen, Guan Hung - W3A.82
Chen, Gui - W3A.123
Chen, Hao - F2C.6, W3A.157
Chen, Haozhe - W3A.22
Chen, Hongda - W2A.6
Chen, Hongwei - W3A.87
Chen, Huan - W2I.5
Chen, Jeffrey R. - Tu3A.2
Chen, Jian - F2D.7
Chen, Jianping - W4D.6
Chen, Jie - W3A.59, W4F.4
Chen, Jiefei - Th1D.5
Chen, Jinbao - W3A.123
Chen, Jinn-Kuen - W2E.1
Chen, Kai - F2B.3
Chen, Kaixin - Th1E.5
Chen, Lawrence R. - F1C.5, Th2C.3
Chen, Liangliang - W3A.64
Chen, Liao - Th2B.7, Tu2D.2, Tu2D.3
Chen, Lin - Th3I.1
Chen, Long - W3A.57, W4K.2
Chen, Longfei - W3A.94
Chen, Ming - Th3I.1
Chen, Minghua - W3A.87

Chen, Nan-Kuang - Th1E.4
Chen, Peng - Th1D.5
Chen, Qiao - W2K.6
Chen, Qinghui - Th3I.1
Chen, Qiran - W3A.127
Chen, Quanan - W1J.2
Chen, Rong - Tu3K.6
Chen, Ruishan - Th3A.3
Chen, Shufan - W2G.6
Chen, Si - Th4K.2
Chen, Siming - W1F.2
Chen, Su - F1B.4
Chen, Weibiao - W4A.6
Chen, Weicheng - W3A.14
Chen, Weidong - Th2G.1, Tu3L.5
Chen, Wen - Th4K, Th4K.5
Chen, Wen-Huang - Th3I.6, W2I.4
Chen, Wenjuan - F2C.5
Chen, Xia - Th3C.3
Chen, Xianfeng - W3A.3
Chen, Xiao - W4A.6
Chen, Xiaodong - W4H.4
Chen, Xiaohan - W3A.69
Chen, Xin - W2E.4, W2J.7
Chen, Xue - Th1I.2, Th1I.4, Th4I.4,
W2I.5
Chen, Xuewen - W3A.144
Chen, Yang - F1E.2, Tu3J.6, Tu3K.5
Chen, Yanxu - Th4I.4
Chen, Yaqin - Th4E.7
Chen, Yi-Yuan - W2J.6
Chen, Yong-Nian - Th4I.5, W2I.3
Chen, Yu - W3A.62
Chen, Yuanxiang - F2F.6, W4I.3
Chen, Yu-Huan - W3A.11
Chen, Yu-Hui - Tu2G.2
Chen, Yujie - W3A.118, W4D.5
Chen, Yun - Tu3I.4
Chen, Yuping - W3A.3
Chen, Zhifeng - W3A.40
Chen, Zhigang - Th4H.3
Cheng, Chang-He - W4L.6
Cheng, Chau-Jern - W3A.90
Cheng, Chung-Wei - W2E.1
Cheng, Lijie - Th2I.5
Cheng, Mengxuan - Th1L.3
Cheng, Xin - W4L.4
Cheng, Xinyu - Tu3H.3
Cheng, Yuhao - W2G.6

Cheng, Yujun - W3A.35
 Cheng, Zhenzhou - Th3C.4, Tu2L
 Chenglong, Hao - F1F.6
 Chi, Nan - Th4I.6
 Chi, Xiaoming - W2G.6
 Chiang, Kin S. - Th1E.5, Tu2E,
 Tu3E.4, Tu3E.5
 Chiba, Akito - F2A.8, F2F.3
 Cho, Heetaek - W3A.70, W3A.77,
 W3A.81
 Cho, Sooyeon - W3A.77
 Cho, Young-Wook - W2G.4,
 W3A.109
 Cho, Yu-Yun - W4A.7
 Choi, Chulsoo - W3A.143
 Choi, Duk-Yong - W4C.1
 Choi, Heejoo - Tu3F.6, W2B.6
 Choi, Inho - Tu2F.2
 Choi, Ju Won - W2B.4
 Choi, Mi-Hyun - W3A.132
 Choi, Seunghwan - W3A.86
 Choi, Sukhyun - Tu2F.2
 Choi, Sumin - F1D.3
 Choi, Sun - Tu2B.5
 Choi, Sun Young - W4A.1
 Chong, Harold M. - W1F.1
 Chong, Yidong - Th4H.4
 Chrostowski, Lukas - F2C.1
 Chrzanowski, Helen - Th4J.1
 Chu, Chu Q. - W1A.4
 Chu, Sai Tak - Th3F.3, Tu3H.5,
 W3A.42
 Chu, Suoda - W3A.83
 Chu, Tao - Tu3L.7
 Chu, Tingting - Tu3K.4
 Chuang, Jen-Yen - W4A.4
 Chung, Hwan Seok - W2I.2
 Chung, Soon-Cheol - W3A.132
 Cincotti, Gabriella - F2F, W1K.1
 Cirmi, Giovanni - F2A.1, Th3B.5
 Cirmi, Giovanni - Tu3B.5
 Coen, Stephane - Th2B, Th2B.3,
 Th4B.1
 Colombe, Yves - W2G.1
 Cong, Hui - Th4G.5
 Cong, Zhenhua - W3A.69
 Consolino, Luigi - W2C.4
 Cook, Justin - W1C.1
 Cook, Kevin - F1B.1
 Corsi, Alessandro - F2F.1
 Cui, Haoran - W4D.2
 Cui, Jiahua - W1G.2
 Cui, Nan - Th1I.1, Th2I.2, W4I.4

Cui, Tong - Th3K.2, W3A.10
 Cui, Wenwen - Th2B.2
 Cui, Xiaojuan - Tu3L.5
 Cui, Yulong - W3A.102, W3A.120,
 W3A.124, W3A.51
 Cui, Yuzhou - Th1L.6
 Cui, Ziruo - Th4B.3

D

Dabrowski, Michal - Th4J.7, W2G.2
 Dagli, Nadir - Th2J.3
 Dai, Daoxin - Th2C, Tu2H.1
 Dai, Guangzhen - W3A.119
 Dai, Nengli - W4B.2
 Dai, X.L. - Th4K.1
 Dai, Xiaojun - W4A.2
 Dai, Xiaoxiao - W1I.4
 Dai, Yitang - W3A.18
 Dai, Zhixuan - Th4H.3
 Dainese, Paulo - Tu3E
 Dainese, Paulo C. - Th3E.2
 Dakic, Borivoje - F1D.4
 Dalton, Larry R. - W4J.1
 Dang, Anhong - Th2I.7
 Das Gupta, Tapajyoti - W1C.2
 Das, Bijoy K. - W3A.115
 Das, Shyamal - W4A.4
 Daud, Nurul A. - W4H.3
 Davidson, Roy - W3A.42
 De Felipe, David - W1L.2
 De Natale, Paolo - W2C.4
 De Sterke, C. Martijn - Tu3J.3
 De, Suvrano - W1K.2
 Decker, Manuel - W2H.2
 Deka, Jayanta - Th2H.3
 Del Santo, Flavio - F1D.4
 Della Casa, Pietro - W2J.2
 Dembele, Vamara - Tu2F.2
 Deminsky, Petro - W1E.2
 Demir, Hilmi Volkan - Th2F.2
 Deng, Junhong - W2H.4
 Deng, Li - Tu2I.5
 Deng, Lu - Th3L.5, Tu3F.5, W3A.72
 Deng, Nan - Th4F.1
 Deng, Ning - W2I.1
 Deng, Rongbiao - W3A.40
 Deng, Rui - Th3I.1, Tu2I.2
 Deng, Weimin - W4H.4
 Deng, Yunchao - W1K.4
 Deng, Zejiang - F2A.5, Th2A.6
 Deng, Zilan - W2H.5
 Deng, Zi-Lan - W2H.4

Denz, Cornelia - Th1B.1, W4B
 Devlin, Robert C. - W1H.2
 Dhar, Anirban - W4A.4
 Diaz, Francesc - W4A.2
 Dietrich, Philipp I. - W4J.1
 Ding, Dongsheng - Th4C
 Ding, Jianfeng - W4B.4
 Ding, Junjie - W3A.22
 Ding, Qianshan - W1K.4
 Ding, Wei - W4E.3

Dominguez Bucio, Thalia - Th3C.2
 Dong, Bo - Tu3L, W2L.1
 Dong, Fengzhong - Tu3L.5
 Dong, Jia Xin - F1C.2
 Dong, Jianji - F1B.4, W3A.157,
 W3A.158
 Dong, Jianwen - W4H.4
 Dong, Ruifang - Th4J.3, W3A.106
 Dong, Siyi - Th3I.1
 Dong, Xin - Th2B.7, Th3K.3, Tu2D.2
 Dong, Xinyong - Th4L, W4L.3
 Dong, Yi - Th4F.1
 Dong, Yibo - W2A.6
 Donko, Andrei L. - F1E.1
 Doo, Kyeonghwan - W2I.2
 Doroshenko, Maxim E. - W3A.55,
 W3A.56
 Dowler, Alastair - Th2E.4
 Dragic, Peter D. - Th1E, Th2E.2
 Du, Jinglei - Th2F.3
 Du, Jinjin - Tu3G.5
 Du, Juan - Th1B.5, Th1H.1, Th2H.5,
 W3A.39
 Du, Minling - W2A.7
 Du, Qingguo - Th2H.4
 Du, Shengwang - Th3H.1, W2G
 Du, Shuxing - W3A.32
 Du, Tuanjie - Th1A.2
 Du, Xin-Wei - W4I.6
 Du, Yong - W4L.5
 Duan, Shukai - F2D.3
 Duan, Xiaofeng - W3A.129, W4J.6
 Dubost, Suwimol - Th1I.5
 Dubrovkin, Alexander - Th3J.1
 Ducloy, Martial - Th4E.2

E

Eason, Robert W. - W1E.4
 Eboroff-Heidepriem, Heike
 - Th2E.4
 Eda, Goki - Th4G.6
 Eggleton, Benjamin J. - Th3B.1,
 Tu3E.1

Elafandy, Rami - W2J.5
 Elahi, Parviz - W4G.4
 Elder, Delwin - W4J.1
 Ellis, Andrew - F2F.2
 Enami, Yasufumi - Th2J.5
 Endo, Takashi - W1J.4
 Endo, Tatsuro - W4D.3
 Erkintalo, Miro J. - Th2B.3, Th4B.1
 Everett, Jesse - Th1D.2
 Evlashin, Stanislav - Th4C.4

F

Faerman, Arkady - W1H.1
 Fahey, Molly E. - Tu3A.2, Tu3L.8,
 W2L.3
 Faist, Jerome - W2C.4
 Falkner, Matthias - W2H.2
 Fallahi, Arya - W2C.3
 Fan, Haixia - Tu2E.3, Tu3I.4
 Fan, Jintao - W1G.2
 Fan, Shanhui - Tu2J.2
 Fan, Weijun - W3A.127
 Fan, Xiaojun - W4L.5
 Fan, Xinyu - Th2L.1
 Fang, Chunyu - Tu3K.4
 Fang, Juncheng - Tu3I.2
 Fang, Shaobo - Tu3B.5
 Fang, Xiaohui - W3A.40
 Fang, Yuanyuan - W4I.4
 Fang, Zhihao - W3A.94
 Fang, Zhiqiang - W3A.91
 Fasold, Stefan - W2H.2
 Fatome, Julien - Th4B.1
 Fei, Peng - Tu3K.4, Tu3K.6, W1K.3
 Fekete, Balazs - W3A.47
 Feng, Hanlin - Th1I.6, W1I.3
 Feng, Jing - Th3F.2
 Feng, Lishuang - Th4A.2
 Feng, Pingping - Th4A.3, Tu2D.4
 Feng, Qi - Th4G.5
 Feng, Tianhua - W3A.6
 Feng, Xian - Tu3B.3
 Feng, Xinhuan - F2C.4, W2L.4,
 Th1B
 Fernandez-Gonzalvo, Xavier
 - Tu2G.2
 Ferrari, Andrea - Tu3G.3
 Fischer, Marc - W2F.6
 Flahaut, Emmanuel - W3A.149
 Forstner, Stefan - Tu3F.3
 Freude, Wolfgang - W4J.1
 Fu, Ching-Shu - Tu3K.5
 Fu, Dong - Th2I.8

Fu, Hongyan - W3A.153
 Fu, Meicheng - W3A.89
 Fu, Songnian - Th1L, Th4I, W3A.71,
 W4L.1
 Fu, Xin - W4B.4
 Fu, Yun - Th2L.2
 Fu, Yuxi - Th3B.4
 Fu, Zhanglong - Tu2C.4
 Fuerbach, Alex - F1A.1
 Fujii, Daichi - Tu3A.6, Tu3F.2
 Fujii, Shun - Tu3H.4, W1B.3
 Fujii, Takuro - Th2J.2
 Fujita, Shogo - Th4A.5, W1A.5
 Fujiwara, Kentaro - Tu3C.6
 Fukano, Hideki - Tu2L.4
 Fukuchi, Yutaka - W2D.5
 Fukuda, Hiroshi - Th2J.2
 Fukutoku, Mitsunori - W3A.16,
 W3A.17, W3A.99
 Fulati, Ranziguli - F1A.2
 Furukawa, Hideaki - Tu3I.3
 Furusawa, Akira - Th1D.1

G

Gai, Xin - Th3E, Tu3E.2
 Gallant, Gabriel - Th2A.7
 Galli, Iacopo - W2C.4
 Galvanauskas, Almantas - Tu3A.1
 Gan, Qiaoqiang - Th2H.1, Th4E.4
 Gang, Zebiao - Th2D.1
 Gao, Cong - F1B.2
 Gao, Feilong - W3A.69
 Gao, Feng - Th4E.6
 Gao, Guangzhen - W3A.78
 Gao, Hui - F2C.5
 Gao, Jing - W2A.5
 Gao, Juntao - W4K.2
 Gao, Kun - Th4E.6
 Gao, Lei - Tu2B.4, W3A.38
 Gao, Li - W3A.101, W3A.105
 Gao, Peng - F1F.2
 Gao, Qi - Th4B.3
 Gao, Shoufei - Tu2E.2, Tu3B.4
 Gao, Tao - Th2I.6
 Gao, Xiang - Th1I.3
 Gao, Yang - W3A.103
 Gao, Yan-Qi - Th4D.3
 Gao, Yesheng - F2F.4
 Gao, Ying - F1A.3
 Gao, Yixiao - F2B.6
 Gao, Zhan - Th2I.7
 Garbin, Bruno - Th2B.3, Th4B.1

García-Muñoz, Luis Enrique - W1L.2
 Garcia-Zambrana, Antonio - F2D.6
 Gardes, Frederic - Th3C.2, W2D.1
 Gates, James - Th4C.2
 Gay, Mathilde - W4E.4
 Ge, Jia-Cheng - W3A.65
 Ge, Renyou - Tu2H.2
 Ge, Xiaogang - Th4A.8
 Geiregat, Pieter - Th3C.1
 Geiselmann, Michael - W2F.1
 Geng, Qing-Feng - Th2K.4
 Geng, Yong - Th2B.2, W2F.2
 Gentile, Antonio - Th1D.4
 Gerasimenko, Andrey S. - W3A.55,
 W3A.56
 Ghadiani, Bahareh - W2F.1
 Ghassemloo, Zabih - Th4I.3
 Ghosh, Somnath - Tu3H.2
 Giessen, Harald W. - Th4C.3
 Ginzburg, Vald - Th4B.2
 Giunta, Michele - W2F.6
 Gnilitzky, Iaroslav - W4B.3
 Goda, Keisuke - Th2K.3, Th3C.4,
 Tu2F.1
 Götzhäuser, Armin - F2B.3
 Gong, Mali - Th2J.6
 Gong, Qian - Tu2H.4
 Gong, Qihuang - Tu1A.2
 Gonzalez, Brayler - Tu3A.2
 Gorodetsky, Michael L. - Th2H.7
 Goto, Ken - Th1B.2
 Goto, Nobuo - Th1L.2, W1D.2,
 W4J.7
 Gotoh, Hideki - W2F.5, W4B.5
 Gow, Paul - Th4C.2
 Grabska, Kasia - Th3C.2
 Gray, Alan - Th4C.2
 Griebner, Uwe - Th2G.1, Tu2B.5,
 W4A.2
 Grigorova, Teodora - W2A.1
 Gross, Heiko - F2B.3
 Gruzdev, Vitaly - W4B.3
 Grzes, Pawel - W3A.46
 Gu, Bobo - W2K.1
 Gu, Chao - W2G.6
 Gu, Chenglin - F2A.5, Th2A.6
 Gu, Jiaqi - W3A.61
 Gu, Jiabin - Tu3H.3
 Gu, Xijia - W3A.102, W3A.120
 Gu, Zhenjie - Th1D.5
 Gu, Zhichen - Tu2H.5
 Guan, Bai-Ou - F2C.4, Th4L.5,
 W2L.4, W4L.6

- Guan, Shanhong - W3A.18
Guan, Yingchun - W3A.94
Guang, Yuan X. - F1F.3
Guha, Shekhar - W4B.6
Gui, Tony - W11.2
Guina, Mircea - W1A.3
Gulyashko, Alexander - W4B.7
Gunji, Shohei - Tu2F.4
Guo, Ailin - Th4B.3
Guo, Changjian - W21.6, Th21
Guo, Chunyu - Th4A.8
Guo, Guang-Can - Th3J.6
Guo, Hairun - Th2B.6, W1B.2, W2F.1
Guo, Jhe-Yong - Th4L.4
Guo, Jia - W1J.5
Guo, L. Jay - Tu3K.1, Tu2K
Guo, Nan - Th2L.4, Th4G.4
Guo, Qi - F2E.1, Th4I.4
Guo, Qiang - W3A.74
Guo, Rengzhong - Th4I.4
Guo, Tuan - Tu3K
Guo, Weihua - W1J.2
Guo, Xin - W4H.5
Guo, Yang - Th3H.5
Guo, Zhen - Th2D.1
Guo, Ziyue - W3A.62
Gupta, Banshi D. - Th3D.1, Th3D.2, Tu2L.3
Gupta, Ratnesh K. - Tu3G.5
Gurung, Sudip - Th1F.4
Guzmán, Robinson - W1L.2, W2J.4
- H**
- Ha, Inho - Th4F.3
Haarlammer, Nicoletta - Th4D.2
Hafezi, Mohammad - Th4H.4
Hagley, Edward W. - Th3L.5, Tu3F.5
Hajjiyev, Elnur - Tu3G.4
Hakuta, Kohzo - W4E.2
Halder, Arindam - Tu3A.5
Han, Dae Seok - Th2H.2
Han, Dong-Yoon - Th2I.4
Han, Feng - Tu3B.3
Han, Jiaguang - Tu2C.3
Han, Lawrence I. - Tu3A.2
Han, Luo - Tu3L.5
Han, Mengmeng - W3A.64
Han, Sang-Kook - Th2I.4, Th4F.3
Han, Sang-Wook - W2G.4, W3A.109
Han, Shiyong - F2D.7
Han, Xu - W3A.117
- Han, Ya - Th1E.2
Han, Young-Geun - W2L.2
Hanafi, Haissam - Th1B.1
Hanawa, Masanori - W3A.20
Hänsel, Wolfgang - W2F.6
Hao, Qiang - Th2A.5
Hao, Ting - Th1E.5
Hara, Kazutaka - W2F.5
Harada, Yukiko - Tu3A.6
Hariharan, Anand - Tu3A.2
Hariki, Takuya - Th1C.3
Harter, Tobias - W4J.1
Hartmann, Fabian - Th1L.1
Hasan, Tawfique - Th3G.2
Hase, Eiji - W3A.130, W4F.3
Hasebe, Koichi - Th2J.2
Hasegawa, Hiroshi - W4I.7
Hasegawa, Minoru - Tu3H.4
Hasegawa, Taro - W3A.136
Hasman, Erez - W1H.1
Hata, Yuya - F2A.6, F2E.3, Tu3A.3
Hattasan, Nannicha - Th3C.2
Hause, Alexander - Th2B.4
Hawkins, Thomas - Th2E.2
Hayasaka, Natsuki - W3A.117
Hayasaki, Yoshio - Th1K.1
He, Chengdong - Tu3G.4
He, Hexiang - Th1K.5
He, J. - Th3I.1, Th3I.2, Th3I.4
He, Jian-Jun - Th1L.4, W1J.5, W2J.7, W3A.154, W4J.5
He, Jijun - W3A.141
He, Jin - Th3B.2
He, Jing - Tu2I.2
He, Mingbo - Th2J.4
He, Peijun - W1E.4
He, Sailing - Th3L.2
He, Ssu-Chia - W3A.28
He, W. - Th4K.1
He, Xiaoqing - W4B.3
He, Xin - Th4E.5, Tu3F.3
He, Yuan - W3A.6
He, Zuyuan - Th2E.3, Th2L.1
Hecht, Bert - F2B.3
Hegmann, Frank A. - Tu3C.1
Heigl, Michael - Th1B.4
Hemalaxmi R. - Tu3L.3
Herr, Tobias - Th2B.1
Hess, Ortwin - Th4H.5
Hibino, Yoshihiko - W3A.75
Higginbottom, Daniel - Th1D.2, W2G.1
- Hilario, Paul Leonard Atchong C. - Th3K.5
Hirakawa, Yasuyuki - W4K.3
Hiraki, Tatsuro - Th2J.2
Hisai, Yusuke - Th1C.2, Th1C.4, Th4A.1, W2F.3
Hishiki, Masato - W3A.92, W3A.96
Hitachi, Kenichi - W2F.5, W4B.5
Hitomi, Kenya - W2F.5
Ho, Ho-Pui - Th2K.4, W3A.65
Ho, Jia-Jung - W2F.1
Höfling, Sven - Th1L.1
Hofmann, Holger - Th3H.3, W3A.114
Holmes, Christopher - Th4C.2
Holzwarth, Ronald - W2F.6
Hong, Feng-Lei - Th1C.2, Th1C.4, Th4A.1, W2F.3, W2G.3
Hong, Jongwoo - W3A.146
Hong, Kang-Hee - W3A.109
Hong, Lingsong - Tu3H.5
Hong, Yanhua - F2D.2
Honjo, Toshimori - W2G.5
Hoose, Tobias - W4J.1
Hori, Atsuhiko - W1B.3
Horikiri, Tomoyuki - Th1C.4, Th4J.6, W2G.3
Horvath, Sebastian P. - Tu2G.2
Hosaka, Aruto - Th1D.3, W3A.111
Hou, Bin - W4C.3, W4C.4
Hou, Fei Y. - Th4J.3, W3A.106
Hou, Lianping - W4C.3, W4C.4
Hou, Shaodong - W4B.2
Hou, Yidong - Th2F.3
Hou, Yubin - F1A.4
Hou, Yu-Shuang - W1D.3
Hou, Zhiyun - Tu2E.3, Tu3I.4
Hristu, Radu - Th3K.4
Hsieh, Pei-Ying - F1E.2
Hsiung, Chan Te - F1E.2
Hsu, Hsin-Yun - F1E.2
Hsu, Hsu-Cheng - W3A.7
Hsu, Shih-Hsiang - W3A.134
Hsu, Shun-Chieh - W4A.7
Hsu, Wensyang - Tu3K.5
Hsu, Yung-Lin H. - F1B.3
Hu, Chi - W1K.4
Hu, Dejiao - Th1K.2, W2H.5
Hu, Fangchen - Th4I.6
Hu, Futai - Th2J.6
Hu, Guijun - W3A.14
Hu, Hao - W4D.6
Hu, Haojuan - W3A.119
- Hu, Huan - Tu2D.6
Hu, Jianling - W3A.22
Hu, Jonathan - Tu3B.3
Hu, Kailin - W3A.62
Hu, Ming-Lie - W1G.2
Hu, Qianggao - Tu2I.5
Hu, Qihang - W3A.101
Hu, Shaohua - Th1I.3
Hu, Siqi - Th3L.2
Hu, Weisheng - Th4I.1
Hu, Xiaolong - W2G.6
Hu, Yu-Jian - Th1E.4
Hu, Zhiping - Th1H.1, Th2H.5
Hua, Bingchang - Th4I.4
Hua, Ping - Th4A.8
Hua, Yi - Tu3B.2
Huang Chen, Sung-Wen - W2J.6
Huang, Cheng-Sheng - F1E.2, Tu3K.5
Huang, Cheng-Yeh - Tu3K.5
Huang, Cheng-Yi - W3A.12
Huang, Chung Ping - F1F.4, Th3J.4
Huang, Chun-Hui - Tu2B.2
Huang, Feng - W1J.3
Huang, Hui - W3A.72
Huang, Jack Jia-Sheng - W4J.4
Huang, Jih-Kai - W3A.2
Huang, Kun - Th2A.5
Huang, Le - W3A.62
Huang, Liyan - Tu2I.5, W3A.15
Huang, Lu - Th4L.3
Huang, Nien-Tsu - W3A.82
Huang, Pin-Han - F2E.6
Huang, Qianqian - Th1A.4, Th2A.3, Tu3A.7, W2A.3, W3A.58, W4A.5
Huang, Qing - Tu2L.2
Huang, Qingzhong - W4D.4
Huang, Quandong - Tu3E.5
Huang, Shanguo - Th2I.6
Huang, Teng-De - W3A.60
Huang, Wei - Th2K.4, W3A.124, W3A.51, W3A.65
Huang, Wencai - W3A.84
Huang, Xu Guang - W3A.148
Huang, Yao-Wei - W1H.2
Huang, Yi - W4L.5
Huang, Yidong - W3A.107
Huang, Yongqing - F1F.3, W3A.129, W4J.6
Huang, Yongtao - F2F.6, W4I.3
Huang, Yong-Zhen - W1J.1, W2J
Huang, Yu-Ming - F1F.4, Th3J.4, W4A.7
- Huang, Zejia - Th2L.5
Huang, Zhuili - W4I.2
Huang, Zi-Wei - W3A.7
Huangfu, Wei - Tu2I.3
Hudson, Darren D. - F1A.1
Huffaker, Diana L. - Th4H.5
Hung, Jui-Hung - W3A.36
Hung, Yu-Chueh - W4H.7
Huo, Dewang - W2B.2
Huo, Jiahao - Tu2I.3
Huo, Li - W2K.6
Hurst, Robert - Tu3F.4
Huyghebaert, Cedric - Th4G.3
Huynh, Hoa - Th2E.4
- I**
- Iadicicco, Agostino - Tu3K.2
Ihn, Yong Sup - F1D.5, Th4J.5
Iida, Masahiro - Tu3C.3
Iinuma, Masataka - Th3H.3
Iiyama, Koichi - Tu3L.6
Ikeda, Kohei - Th1C.4, Th4J.6, W2G.3
Ikisawa, Yoshihisa - W4F.2
Ikuta, Takuya - W2G.5
Ilday, F. Ömer - W1E.2, W4G.4
Ilday, Serim - W1E.2, W4G.4
Im, Dong-Gil - Th3H.2
Imajuku, Wataru - W3A.16, W3A.17, W3A.75, W3A.99
Imbrock, Joerg - Th1B.1
Improso, Wynn Dunn Gil - Th3K.5
Inagaki, Yoshizumi - W3A.43
Inoue, Shuichiro - Th4J.6, W3A.108
Inoue, Takuya - Th1H.4, W4H.6
Intes, Xavier - W1K.2
Iqbal, Md A. - F2F.2
Isaenko, Lyudmila - W3A.52
Isaku, Koji - Tu3A.6
Ishida, Rammaru - W3A.4
Ishihara, Kazumasa - W1D.2
Ishii, Hirotaka - F2A.2
Ishizaki, Kenji - Th1H.4
Ishizawa, Atsushi - W2F.5, W4B.5
Ismaeel, Rand M. - F1E.1
Isoda, Misaki - Tu3L.6
Ito, Hironori - Th4B.4
Ito, Takahiro - W4D.3
Itoigawa, Fumihiko - W2E.5, W3A.93
Iwasa, Torai - W2K.4, W3A.131
Iyer, Arjun N. - Tu3D.3
- J**
- Jackson, Stuart D. - F1A.1, Tu2A.1
Jacquot, Maxime - W1D.4
Jagadish, Chennupati - Th1H.5
Jaimés-Nájera, Alfonso I. - Th2A.4
Jain, Deepak - Th3D.5, Th2D
Jalali, Bahram - Tu1A.3, Tu2D.1
Janaszek, Bartosz - Th1F.2, Th1F.3
Janches, Diego - Tu3L.8
Jang, Heejin - W3A.77
Jang, Jin - W3A.53
Janjua, Bilal - W2J.5
Jantzen, Alex - Th4C.2
Jauregui, Cesar - Th4D.2, Tu2L.1
Jauregui, Luis A. - W2H.1
Jayakumar, Madhan P. - Tu2F.2
Jelinek, Michal - F2E.4, W3A.52, W3A.54, W3A.56
Jelínková, Helena - W3A.55, W3A.56
Jen, Alex - Th2J.5
Jeon, Jun Woo - W3A.135
Jerwick, Jason - W4K.4
Jha, Keshav Kumar - Th2H.3
Jhang, Y. W. - W4A.4
Ji, Dengxin - Th4E.4
Ji, Junhua - F1A.5
Ji, Lanting - W3A.103
Ji, Lingfei - W2E.2, W3A.95
Ji, Pengfei - W4B.3
Ji, Wei - Th1G.3
Ji, Wenbin - Th3L.1
Ji, Xue - W4I.2
Jia, Baohua - Th2G.4
Jia, Chenyang - W3A.69
Jia, Ping - Th2I.5
Jia, Yi - Th4G.4
Jian, Meng-Syuan - W3A.134
Jiang, Chen - Th1E.3, Th4L.3, Th4L.6
Jiang, Chenying - Th4I.4
Jiang, Chun - W1J.2
Jiang, Dapeng - F2E.4
Jiang, Haifeng - F2A.7, Tu2F.3
Jiang, Haowei - W3A.3
Jiang, Junfeng - W4L.5
Jiang, Lei - F1B.2
Jiang, Liwen - Th4E.7
Jiang, Ning - F2D.2, F2D.4, W3A.24
Jiang, Shoulin - Th2E.3
Jiang, X. - W3A.41
Jiang, Xiaoshun - Tu3H.3

Jiang, Yadong - F2B.5
 Jiang, Yang - W3A.34
 Jiang, Yijian - Th2H.6
 Jiang, Yunshan - Tu2D.1
 Jiang, Zhengyang - W4A.6
 Jiang, Zongfu - W3A.121
 Jiao, Hua - W2L.3
 Jiao, Yue - W3A.69
 Jia-Ruei, Nian - F1B.3
 Jie, Jiansheng - Th4G.1
 Jin, Jonghan - Tu3F.6
 Jin, Kuijuan - W1B, W2B.1
 Jin, Rui-Bo - Th3H.4
 Jin, Shengji - W4H.3
 Jin, Wei - Th2F.3, Th4I.2, Tu3E.5
 Jin, Xiaoxi - W3A.44, W3A.63
 Jin, Zhonghe - Th3L.4
 Jing, Feng - F1B.2, W1A.4
 Jing, Jietai - Th4J.2
 Jinno, Masahiko - F2D.5
 Jo, Gyu-Boong - Tu3G.4
 Jo, Jihun - W3A.132
 Johnsson, Mattias - Tu2G.3
 Joo, Ki-Nam - W3A.135, W3A.139, W3A.53
 Jost, John - W2F.1
 Ju, Cheng - Th4I.4
 Juan, Yen-Chia - Tu2B.3
 Jun, Ren - Th2G.4
 Jung, Jisung - W3A.109

K

K R, Kishore - W3A.147
 K, Ramesh - W3A.115
 Kaertner, Franz - F2A.1, Th3B.5, Tu3B.5, W2C.3
 Kakauridze, George - W3A.29
 Kakitsuka, Takaaki - Th2J.2
 Kakushi, Yuki - W3A.75
 Kalashnikov, Dmitry - Tu3F.7
 Kam, Pooi-Yuen - W4I.6
 Kamada, Naoki - W3A.117
 Kamimura, Tomosumi - W3A.43
 Kamioka, Naotaka - W4H.3
 Kamiya, Tatsuki - Tu3C.3
 Kang, Bong Joo - W4C.6
 Kang, Jiqiang - Th4A.3
 Kang, Jun - Th4B.3
 Kang, Myeongsoo - Th2H.2
 Kang, Soo-Min - Th2I.4
 Kang, Zhe - Th2B.5, W3A.30, W3A.33, W3A.35, W3A.149

Kannari, Fumihiko - Th1B.3, Th1D.3, Th4A.5, Tu3J.2, W1A.5, W3A.111
 Kanno, Atsushi - W4J.2
 Kantola, Emmi - W1A.3
 Kao, Hsuan-Yun - W3A.12
 Kapteyn, Henry C. - Th1A.1
 Kara, Dhiren - Tu3G.3
 Karpov, Maxim - W1B.2, W2F.1
 Kärtner, Franz X. - Tu3B.2, W1G.3, W2C.2
 Kasai, Keisuke - W1J.4
 Kasumie, Sho - W3A.156
 Katis, Ioannis N. - W1E.4
 Kato, Takashi - Th1C.5
 Kato, Yuki - - Tu3A.6
 Kawde, Trideep - W2H.2
 Ke, Li-Ann - Th3J.4
 Keathley, Phillip - W1G.3
 Keil, Norbert - W1L.2
 Kemel, Meriem - Th3A.1
 Kesim, Denizhan K. - W4G.4
 Kettlewell, Joshua A. - F1D.4
 Kfir, Ofer - Th1B.4
 Khaidarov, Egor - Th2F.2
 Khazanov, Efim A. - Th4B.2
 Khokhar, Ali - Th3C.2, Th3C.3, W1F.1, W2D.1
 Kieliszczyk, Marcin R. - Th1F.2, Th1F.3
 Kieninger, Clemens - W4J.1
 Kilosanidze, Barbara N. - W3A.29
 Kim, Chulki - W3A.88
 Kim, Dae Hee - W3A.139
 Kim, Dae Y. - W3A.88
 Kim, Daesuk - Tu2F.2
 Kim, Hoon - Tu2I.2, W4I.1
 Kim, Hyo-Suk - W3A.88
 Kim, Hyung M. - W3A.88
 Kim, Hyung-Sik - W3A.132
 Kim, Jae Hun - W3A.88
 Kim, Jin Sub - W3A.139
 Kim, Jin-Hun - F1D.5
 Kim, Jiung - Tu3F.6, W2B.6
 Kim, Junho - Tu2F.2
 Kim, Kwang Ok - W2I.2
 Kim, Kwan-Ho - W3A.150
 Kim, Kyungjo - W2B.6
 Kim, Jun - Th4B.3
 Kim, Philip - W2H.1
 Kim, Seok H. - W3A.88
 Kim, Seunghwan - W2I.2
 Kim, Sun-Je - W3A.146
 Kim, Won Tae - W4C.6

Kim, Yong-Su - W2G.4, W3A.109
 Kim, Yoon-Ho - F1D.5, Th3H.2, Th4J.5, W2G.4, W3A.109
 Kim, Yosep - Th3H.2, Th4J.5, W2G.4
 Kim, Yu J. - W3A.88
 Kim, Yunkyung - W3A.86
 Kimura, Shota - W4A.8
 Kinoshita, Kei - W4D.3
 Kippenberg, Tobias J. - Th2B.6, W1B.2, W2F.1
 Kishikawa, Hiroki - Th1L.2, W1D.2, W4J.7
 Kiss, Matyas - W3A.47
 Kistner, Caroline - Th1L.1
 Kitzler, Ondrej - F2A.4
 Kiwa, Toshihiko - Tu3C.3, Tu3C.5, Tu3C.6
 Klamkin, Jonathan - W1F.4
 Klarskov, Pernille - Tu3C.2
 Kleiner, Vladimir - W1H.1
 Klenke, Arno - W1A.1
 Knebl, Georg - Th1L.1
 Knigge, Andrea - W2J.2
 Knight, Jonathan C. - Th2E.1
 Knight, Peter L. - Tu2G.3
 Kobayashi, Masaki - Th1B.5, W2K.4, W3A.131
 Kobayashi, Nobuhiro - F2A.8
 Kobayashi, Yohei - Th4C.5, W4A.8
 Kobulashvili, Irina - W3A.29
 Kochetkov, Anton - Th4B.2
 Kodama, Takahiro - W3A.20
 Koeth, Johannes - Th1L.1
 Koilpillai, R David - Tu3D.4
 Kokubun, Futoshi - W4F.6
 Kolesnikov, Iliya - Th1G.2
 Kolker, Dmitry - W4B.6
 Komarov, Andrey - Th3A.1, Tu2A
 Kondo, Ken-Ichi - W4F.7
 Kong, Lingchao - W3A.121
 Kong, Youxue - F2C.4
 Konoplev, Oleg - Tu3L.8
 Konyashkin, Aleksey - W3A.137
 Koos, Christian - Th2J, W4J.1
 Koptyaev, Sergey - Th2H.7
 Korganbayev, Sanzhar - Tu3K.2
 Kormin, Dmitrii - Th3B.2
 Kosaka, Hideo - Th1C.4, Th4J.6, W2G.3
 Kost, Alan - W2A.3
 Kostyukova, Nadezhda - W4B.6
 Kovacevic, Goran - Th4A.7

Kovalenko, Nazar O. - W3A.55, W3A.56
 Kovalenko, Nikita - W3A.137
 Krainak, Michael A. - Tu3L.8, W2L.3
 Kränkel, Christian - Th4A.5, W4A.1
 Krishna, Lal - Th2H.3
 Krishnadas, Anjana - Tu3G.5
 Krishnan, Chirenjeevi - W3A.2, W3A.8
 Krivitsky, Leonid - F1D.3
 Krivitsky, Leonid A. - Tu3F.7
 Lee, Chun-Fu - W1G.3
 Krolkowski, Wieslaw - W2E.4
 Krueger, Sebastian - Th1L.1
 Kubecek, Vaclav - F2E.4, W3A.52, W3A.54
 Kucera, Courtney - Th2E.2
 Kulkhevsky, Sergei V. - W3A.47
 Kumagai, Kota - Th1K.1
 Kumagai, Yoshinoo - Th1B.2
 Kumar, Arun - Th1L.5
 Kumar, Pavan - W2B.6
 Kuo, Hao Chung - F1F.1
 Kuo, Hao-Chung - F1F.4, Th1K.3, W2J.6, W3A.12, W4A.7
 Kuramata, Akito - Th1B.2
 Kuroda, Keiji - W2K.3
 Kuroda, Taihei - Tu3C.5
 Kurtisiefer, Christian - Tu3G.2
 Kurus, Aleksey - W3A.52
 Kusano, Yuya - W3A.140
 Kutuvantavida, Yasar - W4J.1
 Kuyken, Bart - W2F.4
 Kuznetsov, Arseniy I. - Th2F.2
 Kuznetsov, Ivan - Th2D.4, Tu3A.4
 Kwon, Min Ki - W3A.81

L

Lacava, Cosimo - W2D.1
 Laha, Arnab - Tu3H.2
 Lai, Puxiang - W2K.5
 Lai, Wenn Jing - Th4D
 Lai, Xin-Ji - W3A.90
 Lai, Yinchieh - Tu2B.3
 Lam, Chi-Hang - Tu3J.5
 Lam, Ping Koy - Th1D.2
 Lan, Jia C. - W3A.45
 Lan, Mingying - W3A.101, W3A.105
 Lang, Ben - Th4H.5
 Lang, Tingting - W4J.5
 Larger, Laurent - W1D.4
 Larionov, Igor - W4B.7

Larochelle, Sophie - F2F.1
 Latawiec, Pawel - Tu3G.3
 Lau, Alan - Tu2I.3, W1I.2, W2I.6
 Laueremann, Matthias - W4J.1
 Lecomte, Steve - Th2B.1
 Lee, Andrew J. - Tu3C.4
 Lee, Byoungcho - F2B.2, W3A.143, W3A.146
 Lee, Chao-Kuei - W3A.45
 Lee, Cheng-Ling - Th4L.4
 Lee, Choonghwan - Tu3F.6
 Lee, Chun-Fu - Th1K.3
 Lee, Elizabeth M. - F1A.5
 Lee, Gun-Yeal - F2B.2, W3A.143
 Lee, Hanhyub - W2I.2
 Lee, Ho Wai H. - Th1F.4, Th3J, Tu3J
 Lee, Jun Ho - Tu3L.2
 Lee, Kang-Yuan - W3A.2
 Lee, Kyeoreh - Th1K.4
 Lee, Kyoung M. - W3A.88
 Lee, Kyuhyuk - W3A.77
 Lee, Po-Tsung - W2J.6
 Lee, Sang-Yun - W2G.4
 Lee, Yin-Wen - W4A.4
 Lei, Cheng - Th2K.3, Tu2F.1
 Lei, Dang Yuan - Th2F.3, Tu3J.5, W3A.141, W3A.142, W3A.144, W3A.145, Th3B
 Lei, Danguyan - Th4E, Tu2J
 Lei, Fuchuan - Th3L.3
 Lei, Weiwei - Th2G.4
 Leibfried, Dietrich - W1A.3
 Leitenstorfer, Alfred - W2C.1
 Leng, Jinyong - W3A.121, W3A.123
 Leng, Yuxin - Th1B.5, Th1H.1, Th2D.1, Th2H.5
 Leo, François - Th4B.1
 Leong, Shan-Fong - W3A.12
 Leong, Victor - F1D.3
 Leszczynski, Adam - Th4J.7, W2G.2
 Letellier, Vincent - Th1I.5
 Leuchs, Gerd - Th1G.2, Th4D.2
 Leung, Anthony C. - Th1D.2
 Leung, Chi Wah - W3A.144
 Leung, Ho M. - Th2F.3
 Lewis, Elfed - Tu2L.2
 Leykam, Daniel - Th4H.4
 Lezius, Matthias - W2F.6
 Li, Baihong - W3A.110
 Li, Bowen - Th1C, Th4A.3, Tu2D.4, Tu2D.5
 Li, Cai - W3A.13
 Li, Canyu - W4K.4

Li, Changlei - W2A.5
 Li, Chao - Th4F.5
 Li, Cheng - Th4E.6
 Li, Chung-Yi - Th4I.5, W2I.3
 Li, Chunlai - Th3B.2
 Li, Da - W3A.154
 Li, Feng - Th1A.5, Th2B.5, W3A.30, W3A.33, W3A.35, W3A.49, F2E
 Li, Gongqing - W3A.129
 Li, Guangcan - Th4E.3
 Li, Guang-Can - W3A.144
 Li, Guangrui - W4E.6
 Li, Guangyuan - Tu3J.3, Tu3J.4
 Li, Guanyu - Tu3H.3
 Li, Guixin - W2H.4
 Li, Guoxin - W2K.6
 Li, Hao - Th3B.3, W2B.7
 Li, Hua - Tu2C.4
 Li, Huanhao - W2K.5
 Li, Jensen - Th1F.1, Th2F
 Li, Jian - F1F.2, W3A.148
 Li, Jianfeng - F1A.3, F1A.6
 Li, Jie - Th4L.5, W4L.6
 Li, Jingnan - F2C.7
 Li, Jinyan - Th2D.5, W3A.123
 Li, Kaile - F2F.6, W4I.3
 Li, Liangchuan - W4I.4
 Li, Linjun - Th4G.6
 Li, Mengdi - W4L.5
 Li, Miao - W3A.123
 Li, Ming - F2C.1, Th3F.1, Tu2I.5, Tu3J.6, W1L
 Li, Mo - Th2H.4, W1J.3
 Li, Qian - Th1A.5, W1J.3
 Li, Ran - Tu3C.4
 Li, Ru - Th2H.4
 Li, Ruxin - Th2D.1
 Li, Shiguang - W4A.6
 Li, Shi-Ling - Th3E.4
 Li, Shiyu - W2B.5
 Li, Shuai - Th2D.1
 Li, Shuhui - W3A.100
 Li, Shuxiao - W1J.3
 Li, Si Q. - W3A.141
 Li, Simin - F1C, Th3F.2
 Li, Steven X. - Tu3L.8
 Li, Tianyu - Th3F.4, W3A.138, W3A.34
 Li, Ting - W3A.59, W4F.4
 Li, Wei - Th2I.5
 Li, Weihua - Tu2I.5
 Li, Weiwei - Th1A.2
 Li, Weizhong - Tu2I.4

- Li, Wenfang - Tu3G.5
 Li, Wenjing - Th2I.5
 Li, Wenqi - Th2D.1
 Li, Wenxue - F2A.5, Th2A.6, W4A.3
 Li, Xianbo - W3A.23
 Li, Xiang - Tu2I.4, W1I.4, W3A.13, W3A.15, W3A.22
 Li, Xiangping - Th1K.2, W1H, W2H, W2H.4, W2H.5
 Li, Xiaoting - W3A.91
 Li, Xin - Th2I.6, W4L.5
 Li, Xing-Ao - Th2K.4
 Li, Xingde - Tu2K.2
 Li, Xingliang - W3A.64
 Li, Xiujian - W3A.89
 Li, Xuan - Th1E.4
 Li, Xun - W4J.3
 Li, Yajie - Th2I.5
 Li, Yan - W4I.6
 Li, Yanfeng - Tu2C.3
 Li, Yao - W3A.1
 Li, Yin-Hai - W2G.7
 Li, Yitong - F2F.6, W4I.3
 Li, Yongrui - F1F.5
 Li, Yuan - W3A.69
 Li, Yuanyao - W4L.5
 Li, Yuhua - W3A.42
 Li, Yujia - Tu2B.4, W3A.38
 Li, Yusha - Tu3K.4, W1K.3
 Li, Yuwei - F1B.2
 Li, Yvonne Y. - Th3L.5
 Li, Zeli - W3A.33
 Li, Zhe - F2B.5
 Li, Zhengyang - F1F.3
 Li, Zhixian - W3A.124, W3A.51
 Li, Zhiyong - W3A.103
 Li, Zhuo - W1E.1
 Li, Zihao - W2K.5
 Liang, Hanxiao - W3A.3
 Liang, Shangyu - Th4I.6
 Liang, Song - W4C.3, W4C.4
 Liang, Xiaoyan - Th2D.1
 Liao, Meisong - W3A.98
 Liao, Mengya - W1F.2
 Liao, Ruoyu - W1G.2
 Liao, Xiao - Th2I.5
 Liao, Xiaolu - W1J.5
 Liao, Zhen-You - W2J.6
 Liaw, Shien-Kuei - Th1L.2, Tu3L.1
 Lihachev, Grigory - Th2H.7
 Lim, Ok Rak - W3A.81
 Lim, Ok-Rak - W3A.70, W3A.77
- Limpert, Jens - Th4D.2, Tu2L.1, W1A.1
 Lin, Aoxiang - F1B.2
 Lin, Bangjiang - Th4I.3
 Lin, Chien-Chung - F1F.4, Th3J.4, W4A.7
 Lin, Chi-Feng - Th4L.4
 Lin, Chih-Hao - F1F.1, Th1K.3
 Lin, Chun - Th4I.3
 Lin, Chung-Hsiang - W3A.2
 Lin, Di - Tu3A.5
 Lin, Gong-Ru - W3A.12, W4A.7
 Lin, Honghuan - W1A.4
 Lin, Huang-Yu - Th1K.3
 Lin, J. T. - W4A.4
 Lin, Jiachuan - W2D.2
 Lin, Li-Jyuan - W3A.7
 Lin, Qiang - W3A.3
 Lin, Shou-Tai - Tu2B.2
 Lin, Tianhua - Tu3L.7
 Lin, Tzu-Neng - W2J.6
 Lin, Y. C. - Th4B.7
 Lin, Yi - Th3L.4
 Lin, Yuanyao - W3A.31
 Lin, Yu-Chih - W3A.90
 Lin, Zhenyuan - W3A.95
 Lin, Zhiyang - W3A.37
 Linss, Sebastian - W2H.2
 Lipka, Michal - Th4J.7, W2G.2
 Little, Brent E. - Th3F.3, W3A.42
 Littlejohns, Callum - Th3C.2
 Liu, Ai-Qun - Th4H.1
 Liu, Bo - Th4G.6
 Liu, Bowen - F2E.2, F2E.5
 Liu, Dan - Th2G.4
 Liu, Deming - F2E.2, W4H.2
 Liu, Dong - W1E.1
 Liu, Fei - F1A.3, F1A.6
 Liu, Feng - W3A.14
 Liu, Guanyu - Th4A.2, W2A.4
 Liu, Guoqin - W4B.2
 Liu, Haiyi - W2G.6
 Liu, Hao - W2K.6
 Liu, Hongyao - Th4E.7
 Liu, How-Wei - Tu2B.2
 Liu, Huan - W2E.3
 Liu, Huiyun - Th1J.2, W1F.2
 Liu, Jianqiang - W3A.91
 Liu, Jiantao - Tu2E.3, Tu3I.4
 Liu, Jie - Th2I.1, W2I.6
 Liu, Jin - Tu3J.5
 Liu, Jun - W3A.57
 Liu, Junku - Th4G.4
- Liu, Junqiu - W2F.1
 Liu, Kai - W3A.129, W4J.6
 Liu, Kun - W4L.5
 Liu, Lanlan - Th2L.5
 Liu, Le - W3A.102, W3A.120, W3A.126, W3A.25
 Liu, Lei - F2F.4
 Liu, Lin - W4D.5
 Liu, Linbo - Th4K.2, W1K.4, W4G
 Liu, Liyuan - Tu3A.7
 Liu, Lu - F2B.5
 Liu, Meng - F2E.1
 Liu, Ningwen - F1F.2
 Liu, Qiang - W4D.4
 Liu, Qingwen - Th2L.1
 Liu, Ren-Young - Tu3L.1
 Liu, Sa - W1K.3
 Liu, Shan - W2E.4
 Liu, Shaozhen - W3A.62
 Liu, Shiliang - W3A.9
 Liu, Shi-Long - F1D.2
 Liu, Tao - F2E.2, Th2L.6, Th4J.3, W3A.106, W3A.57
 Liu, Tiegen - W4L.5
 Liu, Wei - Tu3B.2, W3A.22
 Liu, Weiqi - Th4A.8
 Liu, Wen-Fung - Th4L.4
 Liu, Wu - W1G.2, W3A.22
 Liu, Xiang J. - W2I.1
 Liu, Xingzhao - F2F.4
 Liu, Xinyu - Th4K.2
 Liu, Xiu - Th1L.6
 Liu, Xiuying - Th4H.3
 Liu, Xu - W3A.107
 Liu, Xueming - W3A.122
 Liu, Y. - W2E.3
 Liu, Yabing - W2K.6
 Liu, Yajing - Th4E.5
 Liu, Yang - F2A.5, Th1E.5, Th2A.6, W3A.154, W4A.3
 Liu, Yange - Th1E.2
 Liu, Yanqi - Th2D.1
 Liu, Yehui - W3A.123
 Liu, Yi - W4L.4
 Liu, Ying - Th1A.3
 Liu, Yizhou - W1G.3
 Liu, Yong - F1A.3, F1A.6, F2C.2, Th2J.6
 Liu, Yujie - W3A.149
 Liu, Yunqi - Th1E.3, Th4L.1, Th4L.3, Th4L.6, W2L, W3A.71
 Liu, Yin - Tu3J.5
 Liu, Z.w. - Th4K.1
 Liu, Zeng-Yong - W3A.76
- Liu, Zhangweiyi - Th4F.1
 Liu, Zhaojun - W3A.69
 Liu, Zhengtong - Th2F.2
 Liu, Zheng-Yong - W4L.6
 Liu, Zhengzheng - Th1B.5, Th1H.1, Th2H.5
 Liu, Zhijun - F2B.5
 Liu, Zhu - Th2I.5
 Liu, Zizhuo - W1F.2
 Liu, Zuyao - W3A.71
 Lo, Hsin Pin - W2G.5
 Lo, Mu-Chieh - W1L.2, W2J.4
 Lo, Tsz Wing - Tu3J.5, W3A.142
 Loh, Kianping - Th4G.6
 Loiko, Pavel - Th2G.1, W4A.2
 Loncar, Marko - Tu3G.3
 Long, J. - W2E.3
 Long, Keping - Tu2I.3
 Longdell, Jevon J. - Tu2G.2
 Loo, Roger - Th3C.1
 Lou, Shuqin - Th2E.5
 Lou, Yijie - Tu2J.2
 Lu, Benquan - Tu3G.6
 Lu, Bingbing - Th1A.4
 Lu, C.c.f. - W2E.3
 Lu, Chao - Th2L.4, Tu2I.3, W1I.2, W2I.6
 Lu, Chaoyang - Tu3G.1
 Lu, Fanfan - Th4E.6
 Lu, Hai-Han - F2D, Th4I.5, W2I.3
 Lu, Huafeng - Th4L.2
 Lu, Jiao - Th4L.2
 Lu, Liangjun - W4D.6
 Lu, Luluzi - W4H.2
 Lu, Qiaoyin - W1J.2
 Lu, Qichao - W3A.5
 Lu, Rongguo - Th2J.6
 Lu, Ting-Hua - W3A.60
 Lu, Tsung-Yu - Tu3L.1
 Lu, Xinchao - Th4E.7
 Lu, Yaojie - Tu3C.4
 Lu, Yeng-Hong - Tu3L.1
 Lu, Ying - W1F.2
 Lu, Yonghua - W2J.3
 Lu, Yuanfu - Tu3J.4
 Lu, Yudong - Th1K.2, W2H.5
 Lu, Zhen-Da - W3A.76
 Lu, Zhong - W2L.4
 Lucas, Erwan - W1B.2, W2F.1
 Lucidi, Massimiliano - W1K.1
 Lukashchuk, Anton - W2F.1
 Luo, Aiping - F2E.1
 Luo, Bin-Bin - Th4L.2
- Luo, Cheng-Jih - Tu2B.3
 Luo, Ciwei - F2D.3
 Luo, Daping - F2A.5, Th2A.6, W4A.3
 Luo, Hongyu - F1A.3, F1A.6
 Luo, Huiwen - W2J.3
 Luo, Jiaqi - F1A.5
 Luo, Jie - Tu2I.5
 Luo, Jingdong - Th2J.5
 Luo, Ming - Tu2I.4, W1I.4, W3A.13, W3A.15
 Luo, Rui - W3A.3
 Luo, Site - W2K.6
 Luo, Songjie - Th2A.4
 Luo, Xiao - W2I.5
 Luo, Yanbin - W3A.5
 Luo, Yiyang - F2E.2, F2E.5
 Luo, Yufei - Th2I.7
 Luo, Zhengqian - Th1A.2, Th2G.3
 Luo, Zhi-Chao - F2E.1, Th1A, Th4A, Tu2F
- M**
- M S, Aruna Gandhi - W3A.80
 Ma, Chuang - Th3F.4, Th3I.5, W3A.138, W3A.34
 Ma, Fengkai - F2E.4
 Ma, Guangjin - Th3B.2
 Ma, Huilian - Th3L.4
 Ma, Jian - W3A.41
 Ma, Jie - Th3I.1
 Ma, Lin - Th2E.3
 Ma, Ming - Th2C.3
 Ma, Peng - Th4L.5
 Ma, Qi Chang - W3A.148
 Ma, Xiang - W1J.2
 Ma, Xiuhua - W4A.6
 Ma, Xiuquan - Th2D.5
 Ma, Yutao - W4K.4
 Ma, Yuxuan - F2A.2, Th4A.4
 Macfarlane, Duncan - W4J
 Macfarlane, Duncan L. - Th2J.1
 Machida, Tomoki - W4D.3
 Mackonis, Paulius - Th2D.3
 Maeda, Yoshinobu - W3A.75
 Maeno, Kenichi - W4D.3
 Maguid, Elhanan - W1H.1
 Mahnke, Christoph - Th2B.4
 Mainz, Roland E. - F2A.1, Th3B.5, Tu3B.5
 Majewski, Matthew - F1A.1
 Makey, Ghaith - W4G.4
 Mäki, Mika - W1A.3
- Makino, Tomohiro - Th1B.5, W4F.2
 Maktoobi, Sheler - W1D.4
 Malasuk, Chacriya - W3A.79
 Mamakos, William A. - Tu3A.2
 Mamuti, Roukuya - Th3A.2
 Man, Tianlong - W4G.3
 Manshina, Alina A. - Th1G.2
 Maram, Reza - Th1C.1
 Marchev, Georgi - W4B.6
 Marquardt, Christoph - Th4D.2, Th4J.4
 Marsan, Marco - W1K.1
 Marsh, John - W4C.3, W4C.4
 Martin-Mateos, Pedro - W4F.1
 Martin-Monier, Louis - W1C.2
 Maruyama, Ayumu - Tu3A.6
 Mashanovich, Goran - Th3C.2
 Masoudi, Ali - F1E.1
 Massa, Francesco - F1D.4
 Mastronardi, Lorenzo - Th3C.2
 Masuda, Hiroji - W4I.5
 Masuda, Kota - Tu3A.6
 Masuda, Shin - Th2J.5
 Masuoka, Takashi - Tu2L.5
 Mateos, Xavier - Th2G.1, Tu2B.5, W4A.2
 Matsuda, Nobuyuki - W2G.5
 Matsumoto, Atsushi - W4J.2
 Matsumoto, Masayuki - Th3I.3
 Matsuo, Shinji - Th2J.2
 Matsuo, Leo - W3A.140, W3A.73
 Matsushima, Isao - F2A.2
 Matsuura, Motoharu - F2C, Th4F.2
 Mazelanik, Mateusz - Th4J.7, W2G.2
 Mazzotti, Davide - W2C.4
 McClean, Jarrod - Th1D.4
 Mclean, Russell - W3A.113
 Mei, Chao - Th2B.5, W3A.30, W3A.35
 Mei, Ting - Th4E.6
 Melikyan, Argishti - W4J.1
 Men, Hongyun - W3A.148
 Mendinueta, José M. - Tu3I.3
 Meng, Lingheng - Tu2I.5
 Meng, Yichang - Th3A.1
 Meng, Yongjun - W3A.144
 Meng, Yuan - Th2J.6
 Menon, Sruti - Th2H.3
 Merano, Michele - Th1G.4, Th2F.4
 Mercier, Thomas - W3A.2
 Mercier, Thomas M. - W3A.8
 Merklein, Moritz - Th3B.1
 Mero, Mark - Th2G.1, Tu2B.5

Merritt, Scott A. - W2L.3
 Messaddeq, Younes - F2F.1
 Micalizzi, Frankie - W2L.3
 Michailovas, Andrejus - W2A.2
 Michalska, Maria - W3A.46
 Midorikawa, Katsumi - Th3B.4, Th4B.7
 Miguel, Martin - Th2E.3, Tu3A.5
 Mildren, Richard P. - F2A.3, F2A.4, Th4D.6
 Milosevic, Milan M. - Th3C.3
 Minaev, Nikita - Th4C.4
 Minamikawa, Takeo - Tu2L.4, Tu2L.5, W3A.130, W4F.3
 Ming, Hai - Th3A.3
 Minoshima, Kaoru - F2A.2, F2A.6, F2E.3, Th1C.3, Th1C.5, Tu2L.4, Tu2L.5, Tu3A.3, W4F.2, W4F.7
 Miroshnichenko, Andrey E. - W3A.6
 Misawa, Kazuhiko - Th1B.2, Th4B.4
 Mitchell, Arnan - Th3F.3
 Mitetelo, Nikolai - Th1G.2
 Mitschke, Fedor - Th2B.4
 Mitsunaga, Yasushi - W3A.75
 Mittal, Sunil - Th4H.4
 Mittleman, Daniel - Tu2C
 Mittleman, Daniel M. - Tu3C.2
 Miyakawa, Takahiro - W4C.5
 Miyamoto, Katsuhiko - F1A.2, Th3A.2, Th3A.5, W4C.5, W4C.6
 Mizaikoff, Boris - Tu3F.1
 Mizuno, Shota - Tu3A.6
 Mizuno, Takahiko - W4F.3
 Mo, Jinyu - F2D.1
 Moein, Tania - Th2C.2
 Mohan, Gurusamy - W4I.6
 Molardi, Carlo - Tu3K.2
 Mondal, Partha - F1B.5
 Monemar, Bo - Th1B.2
 Monro, Tanya - W1I.2
 Montblanch, Alejandro - Tu3G.3
 Mookherjee, Shayan - W2D.3, W4H.1
 Moon, Sung - W2G.4, W3A.109
 Moqanaki, Amir - F1D.4
 Morandotti, Roberto - Th3F.3
 Mori, Kunihiko - W3A.16, W3A.17, W3A.99
 Mori, Yojiro - W4I.7
 Morimoto, Taiga - Tu3C.5
 Morita, Kinichi - W3A.79
 Morita, Ryohei - Th1H.4, W4H.6
 Moriwaki, Atsuto - Th4K.4

Moriya, Rai - W4D.3
 Morley-Short, Sam - Th1D.4
 Moser, Christophe - Th3E.3
 Moslemi, Parisa - F1C.5
 Moss, David - Th2C.2, Th3F.3
 Moteki, Yuta - F2A.8
 Mou, Chengbo - Th1A.4, Th1E.3, Th2A.3, Tu3A, Tu3A.7, W2A.3, W3A.58, W3A.71, W3A.74, W4A.5
 Mroczynski, Robert - Th1F.2
 Mu, Ganggang - W1K.4
 Mu, Xin - W3A.153
 Mücke, Oliver D. - Tu3B.5
 Muehlbrandt, Sascha - W4J.1
 Mueller, Christian R. - Th4D.2, Th4J.4
 Muir, Jack - W3A.113
 Mukhin, Ivan - Th2D.4, Tu3A.4
 Müller, Michael - W1A.1
 Mun, Kyoung-Hak - Th2I.4
 Mun, Sang-Eun - W3A.146
 Murakami, Hisashi - Th1B.2
 Murdoch, Stuart G. - Th2B.3, Th4B.1
 Murnane, Margaret M. - Th1A.1
 Murzina, Tatiana - Th1G.2
 Myslivets, Yauheni - Tu2D.6

N

N, Aparna - Tu3L.3
 Nabekawa, Yasuo - Th4B.7
 Nacher-Castellet, Victor - Th4F.4
 Nagai, Kosuke - Tu2L.4
 Naing, May Win - W4K.6
 Nakagawa, Hiroki - W1D.2
 Nakajima, Yoshiaki - F2A.2, F2A.6, F2E.3, Th1C.3, Tu2L.4, Tu2L.5, Tu3A.3, W4F.2
 Nakakubo, Keisuke - W3A.79
 Nakamoto, Atsushi - Tu3L.6
 Nakamura, Kei-Ichiro - W4K.3
 Nakamura, Ryosuke - W3A.43
 Nakamura, Takuma - W4A.8
 Nakano, Masayuki - Th3H.3
 Nakano, Shota - W4F.3
 Nakarmi, Bikash - F2C.6
 Nakashima, Yuta - W3A.79
 Nakazawa, Masataka - W1J.4
 Nakkeeran, K. - W3A.83
 Nam, Sae Woo - Th4J.1
 Namekata, Naoto - Th4J.6, W3A.108

O

Nemani, Arun - W1K.2
 Nemoto, Hirofumi - Th1B.3
 Neugebauer, Martin - Th1G.2
 Ng, Doris K. T. - W2B.4
 Ng, Tien Khee - W2J.5
 Nguyen, Thach - Th3F.3
 Nguyen-Dang, Tung - W1C.2
 Ni, Feng Chao - W3A.148
 Ni, Kai - W4F.5
 Ni, Li - F1B.2
 Nic Chormaic, Sile - Th3L.3, Tu3G.5, W3A.156
 Nicholson, Jeffrey W. - Tu3A.2
 Nie, Qianwen - W3A.89
 Nie, Zhonghui - W3A.1
 Nieddu, Thomas - Tu3G.5
 Nielsen, Alexander U. - Th2B.3
 Niimura, Shintaro - Th1D.3, W3A.111
 Niizeki, Kazuya - Th4J.6
 Nilsson, Johan - W1G.1
 Ning, Yuan - W4K.4
 Nirmalathas, Ampalavanapillai - Th4E.5
 Nishikawa, Tadashi - W2F.5, W4B.5
 Nishimura, Kotaro - Th3B.4
 Nishiya, Noritaka - W3A.140
 Nishiyama, Akiko - Th1C.3
 Nishiyama, Nobuhiko - Tu2H.5
 Niu, Sujian - F1A.2
 Niu, Yongjiao - F2D.3
 Noda, Susumu - Th1H.2, Th1H.4, Tu1A.4, W4H.6
 Noguchi, Shun - W3A.99
 Nomura, Junia - Th1C.2, Th4A.1
 Norman, Justin - Th2J.3
 Numata, Kenji - Tu3A.2, Tu3L.8, W2L.3

O'Brien, Jeremy - Th1D.4
 O'keefe, Nicholas - Th4E.5
 Obara, Yuki - Th1B.2
 Obrzud, Ewelina - Th2B.1
 Odbayar, Nyam-Erdene - W4J.7
 Oe, Ryo - Tu2L.4
 Oguchi, Kenichi - W3A.68
 Ogura, Takashi - Tu2L.5
 Oh, Juyeong - W3A.88
 Oh, Kyunghwan - W3A.109
 Oh, Sang Soon - Th4H.5
 Ohta, Keisuke - W4K.3

Okamura, Kotaro - Th4J.6, W2G.3
 Okamura, Taku - W4H.3
 Okano, Makoto - Th1H.2, Th4K.4, W3A.68, W4D.3
 Okano, Yu - Th1B.2
 Oki, Yuji - W3A.79
 Omatsu, Takashige - F1A.2, Th3A.2, Th3A.5, W4C.5, W4C.6
 Omi, Akihito - Th1D.3, W3A.111
 Ong, Jesslyn - W4K.6
 Ono, Shingo - W2E.5, W3A.66, W3A.93
 Onuki, Yuya - W3A.117
 Oo, Swe Z. - W1F.1
 Ooi, Boon - W2J.5
 Ooi, Kelvin J. - W2B.4
 Ooka, Yuta - W4H.3
 Oppo, Gian-Luca - Th4B.1
 Osiko, Vjatcheslav - W3A.56
 Ou, Yangcheng - F2A.5
 Ouyang, Lie - W1A.4
 Oxenlowe, Leif K. - Tu3D.2
 Ozcan, Aydogan - Tu3K.3
 Ozeki, Yasuyuki - Th2K.3

P

Padilla, Willie - Tu3C
 Padilla, Willie J. - Tu2C.1
 Paesani, Stefano - Th1D.4
 Page, Alexis G. - W1C.2
 Pai, Yung-Min - F1F.1, Th1K.3
 Palacios-Berraquero, Carmen - Tu3G.3
 Palashov, Oleg - Tu3A.4
 Palomba, Stefano - Tu3J.3
 Pan, Ci-Ling - F2E.6
 Pan, Guanzhong - W2A.6
 Pan, Jisheng - W3A.127
 Pan, Shilong - F2C.6, Th3F.2
 Pan, Shu - W1F.2
 Pan, Zhongben - Th2G.1, Tu2B.5, W4A.2
 Pandey, Awanish - F1C.4, W2D.4
 Paniagua-Domínguez, Ramón - Th2F.2
 Pant, Ravi - F1C.3, F2F.5
 Pantouvaki, Marianna - Th3C.1, Th4G.3
 Panusa, Giulia - Th3E.3
 Panyutin, Vladimir - W4B.6
 Park, Hyo Mi - W3A.135
 Park, Hyoung-Joon - Th4F.3

Park, Jae-Seong - W1F.2
 Park, Jin-Hong - W3A.150
 Park, Jongchan - Th1K.4
 Park, Ju Eun - Tu3F.6
 Park, Jung-Hoon - Th2K, Th4K.3
 Park, Subeen - W3A.88
 Park, Taejun - W3A.77
 Park, Yongkeun - Th1K.4

Parmigiani, Francesca - W2D.1
 Parniak, Michal - Th4J.7, W2G.2
 Parsons, Joshua - Th2E.2
 Paterova, Anna - Tu3F.7
 Pathak, Anisha - Th3D.2, Tu2L.3
 Paul, Karun - Th1D.2
 Paul, M. C. - W4A.4
 Pavlov, Nikolay G. - Th2H.7
 Peacock, Anna C. - W1F.1, W4E.1
 Pecci, Pascal - Th1I.5
 Peng, Chun-Yen - W3A.12, W4A.7
 Peng, Hao - F2B.5
 Peng, Jiahui - W3A.62
 Peng, Kun - F1B.2
 Peng, Lung-Han - W3A.36
 Peng, Qixian - F1F.2
 Peng, Zhigang - Tu3B.4
 Penttinen, Jussi-Pekka - W1A.3
 Perevezentsev, Evgeny - Tu3A.4
 Perez-Galacho, Diego - Th4F.4
 Periyanyagam, Gandhi Kallarasan - W3A.117
 Perrone, Guido - Tu3K.2
 Pertsch, Thomas - W2H.2
 Petra, Rafidah - W1F.1
 Petropoulos, Periklis - W2D.1
 Petrov, Valentin - Th2G.1, Tu2B.5, W4A.2, W4B.6
 Petrov, Yuriy - Th1G.2
 Peucheret, Christophe - W4E.4
 Peuntinger, Christian - Th4J.4
 Peyghambarian, Nasser - W2B.6
 Pfeiffer, Martin H. - Th2B.6, W1B.2, W2F.1
 Pfenning, Andreas - Th1L.1
 Ping, Junyu - W1K.3
 Pizzuto, Angela - Tu3C.2
 Plantady, Philippe - Th1I.5
 Png, C. E. - W2B.4
 Png, Ching Eng - Th2F.2
 Poon, Andrew - Tu3H, W4H
 Poon, Joyce - Th2H
 Poon, Joyce K. - Th1J.1
 Porret, Clement - Th3C.1
 Prabaswara, Aditya - W2J.5

Priante, Davide - W2J.5
 Pryde, Geoffrey - Th4J.1
 Psaltis, Demetri - Th3E.3
 Pu, Jixiong - Th2A.4
 Pu, Ye - Th3E.3
 Puttnam, Benjamin - Tu3I.3

Q

Qaraqe, Khalid - F2D.6
 Qasymeh, Montasir - W3A.67
 Qi, Chen - F2B.4
 Qi, Shuxian - F1A.4, Th1A.3
 Qin, Peng - F2E.7, Th4A.6
 Qin, Shuchao - W3A.1
 Qin, Xuanchao - W3A.62
 Qin, Yingxiong - F2E.5
 Qin, Zengguang - W3A.69
 Qin, Zhipeng - Th2G.2
 Qiu, Chengwei - Th3G.1
 Qiu, Cheng-Wei - F1F.6, W1H.2
 Qiu, Feng - Tu3E.3
 Qiu, Huaqing - W3A.158
 Qiu, Jifang - W4I.2
 Qiu, Josephine Yi - W3A.32
 Qiu, Kun - F2D.2, F2D.4, Th2B.2, Th2I.8, Th4I.2, W1I.5, W2F.2, W3A.24
 Qiu, Meng - Th2F.3, Tu3J.5, W3A.144
 Qiu, Min - Tu2J.2
 Qiu, Xingzhi - Tu2J.3
 Qu, Yunpeng - W1C.2
 Quan, Runai - Th4J.3

R

Radic, Stojan - Tu2D.6
 Raghunathan, Varun - Th2H.3
 Rahaman, Nafia - W3A.113
 Rahimzadegan, Aso - W2H.2
 Rahman, Aziz, B. M. - W4D.6
 Rahubadde, Udaya S. - W1C.3
 Raja, Arslan - W2F.1
 Rajasree, Krishnapriya S. - Tu3G.5
 Ramalingam, Vincent Larry - F1A.5
 Ramesh Babu, P. - W3A.83
 Ramírez-Martínez, N. J. - Tu3A.5
 Ran, Maojie - F1F.2
 Ran, Qiandong - W2B.7
 Ran, Yang - W2L.4
 Randel, Sebastian - W4J.1
 Ranta, Sanna - W1A.3
 Rao, Bingjie - F2A.7

- Rao, Yunjiang - Th2L.2, W3A.50
Rauschenbeutel, Arno - Th3G, W2G.1
Ravi, Koustuban - W2C.3
Ray, Tridib - Tu3G.5
Razinskas, Gary - F2B.3
Reed, Graham - Th3C.3, W1F.1
Ren, Jie - Th3H.5
Ren, Xiaomin - W3A.129, W3A.5, W4J.6
Ren, Xifeng - Th1F, Tu3J.6
Ren, Zejian - Tu3G.4
Richardson, David J. - Tu3L.1, W2D.1
Richardson, Martin - W1C.1, W2C
Rochette, Martin - F1C.5
Rockstuhl, Carsten - W2H.2
Rodin, Aleksej - Th2D.3, W2A.2
Rodriguez, Michael R. - Tu3A.2
Romero Cortes, Luis - Th1C.1
Ropers, Claus - Th1B.4
Rossi, Giulio Maria - F2A.1, Th3B.5, Tu3B.5
Rotermund, Fabian - Th2G.1, Tu2B.5, W4A.1, W4C.6
Rothmayr, Florian - Th1L.1
Rozhin, Aleksey - Th1A.4, W3A.58, W4A.5
Ruan, Shuangchen - Th4A.8
Ruan, Tiantian - Th3A.4
Ruan, Zhichao - Tu2J.2
Rubin, Noah A. - W1H.2
Run Ai, Quan - W3A.106
Rusch, Leslie - F2F.1, W2D.2, W4I
Russell, Philip S. - Tu2E.1
Rutirawut, Teerapat - Th3C.2
- S**
- S N, Shiva N. - Tu3L.4
Saba, Matthias - Th4H.5
Sabella, Alexander - Th4D.6
Sachkou, Yauhen - Tu3F.3
Saha, Nabarun - Th1L.5
Sahin, Ezgi - W2B.4
Sahu, Jayanta K. - Th2E.3, Tu3A.5
Saito, Yuma - Th4B.4
Sakai, Kenji - Tu3C.3, Tu3C.5, Tu3C.6
Sakamoto, Takahide - F2A.8, F2F.3
Sakaue, Takuya - W3A.130
Saleh, Mohammed F. - W2B.3
Sales, Salvador - Th4F.4, Tu3K.2
Salhi, Mohamed - Th3A.1
Sanchez, Francois - Th3A.1
Sander, Michelle - Tu3B
Sander, Michelle Y. - Tu2B.1
Sang, Xinzhu - F1F.5, Th2B.5, W3A.30, W3A.33, W3A.35
Santagati, Raffaele - Th1D.4
Saraceno, Clara - W4A.1
Sarang, Soumya - F2A.3, F2A.4, Th4D.6
Sasada, Hiroyuki - W3A.136
Sato, Kazuhide - Tu3F.2
Sato, Kazuo - W3A.36
Sato, Ken-Ichi - W4I.7
Sato, Masayasu - Th1L.2
Sawadsky, Andreas - Tu3F.3
Sayem El-Daher, Moustafa - W4G.4
Scalari, Giacomo - W2C.4
Schaarschmidt, Kay - Th1E.1
Schade, Anne - Th1L.1
Scheiba, Fabian - F2A.1, Th3B.5, Tu3B.5
Scheibinger, Ramona - Th1E.1
Schena, Emiliano - Tu3K.2
Schibli, Thomas - F2A.2
Schimpf, Damian - W1G.3
Schirrmacher, Andre - W4B.6
Schmidt, Markus - Th1E.1, Th2E, W4E.6
Scholl, Senta - Th4C.2
Schreiber, Karl U. - Tu3F.4
Schreiber, Thomas - Th4D.2
Schülzgen, A. - W4L.2
Schunemann, Peter - W4B.6
Sedlmeir, Florian - Th4D.2
Seeds, Alwyn - W1F.2
Seghilani, Mohamed - Th1C.1
Segovia, Daniel - W1L.2
Seki, Atsushi - Th2J.5
Selvaraj, Ramya - Tu3L.4
Selvaraja, Shankar K. - F1C.4, W2D.4
Semaan, Georges - Th3A.1
Semwal, Vivek - Th3D.1, Th3D.2
Senthilnathan, K. - W3A.83
Seo, Gyeongseo - W3A.70, W3A.77, W3A.81
Sepehrian, Hassan - W2D.2
Sergaeva, Olga - W4B.3
Serres, Josep - Tu2B.5, W4A.2
Seshadreesan, Kaushik P. - Th4J.4
Seshadri, S - Tu3L.3
Set, Sze - W2A
- Set, Sze Y. - Th4A.7
Sfendla, Yasmine - Tu3F.3
Shadbolt, Peter - Th1D.4
Shafi, K. Muhammad - W4E.2
Shalm, Lynden - Th4J.1
Shan, Zhang - W3A.155
Shang, Aixue - W3A.145
Shang, Qisong - Th1I.1
Shao, Qiongchan - W2L.6
Shao, Zengkai - W4D.5
Shapolov, Anatolij A. - W3A.47
Shebarshina, Irina - W3A.137
Shen, Changyu - W4L.3
Shen, Lei - F1B.4
Shen, Li - W3A.100
Shen, Xiao - Th2K.4
Shen, Yijie - Th2J.6
Shen, Ying - W2L.5
Sheng, Yan - W2E.4
Sheng, Zicheng - Tu2E.3
Shi, Baosen - W2G.7
Shi, Bao-Sen - F1D.2
Shi, Chen - Th3D.4
Shi, Fulong - W4H.4
Shi, Jindan - Tu3B.3
Shi, Liu - W2H.5
Shi, Shenghui - Th4L.2
Shi, Tongchao - Th1B.5, Th1H.1
Shi, Wei - W2D.2
Shi, Yaocheng - Th2C.4
Shi, Yi - W1A.4
Shi, Yitong - Th1L.3
Shi, Yiwen - F1A.3, F1A.6
Shibuya, Kyuki - Tu2L.5
Shieh, William - Tu2I.1
Shim, Jeawoo - W3A.150
Shimizui, Ryosuke - Th3H.4
Shimomura, Kazuhiko - W3A.117
Shin, Don Jin - W1C.1
Shin, Heedeuk - F1D.5
Shioda, Tatsutoshi - Tu2F.4, Tu2F.5, W4F.6
Shiozaki, Risa - W3A.116
Shirahata, Takuma - Th4A.7
Shirasaki, Hikari - W2K.3
Shriakawa, Akira - W1A.2
Shu, Chester C.t. - Th2L.4
Shu, Chester C.t. - Tu3D
Shu, Lei - W4E.5
Shuhei, Tamura - W2G.3
Shum, Perry P. - W4L.3
Shy, Jow-Tsong - W3A.78
- Silverstone, Joshua - Th1D.4
Sincore, Alex - W1C.1
Sivis, Murat - Th1B.4
Slim, Joseph C. - W4E.4
Slussarenko, Sergei - Th4J.1
Smetanin, Sergei - W3A.52, W3A.54
Smith, Peter - Th4C.2
Sobhanan, Aneesh - Tu3D.3, Tu3D.4
Sogawa, Tetsuomi - W2F.5
Someya, Mayu - W4B.5
Sones, Collin L. - W1E.4
Song, Bo - Tu3G.4
Song, Congcong - W3A.14
Song, Da In - Th2H.2
Song, Daohong - Th4H.3
Song, Jiabin - W3A.44, W3A.63
Song, Kui Y. - Th4D.5
Song, Liwei - Tu3B.5
Song, Qinghai - Th1H.3
Song, Wei-Heng - W3A.45
Song, Youjian - Th4A.4
Sonoyama, Yutaro - W3A.73
Sorel, Marc - W2D.1
Sorin, Fabien - W1C.2, W4C
Spence, David J. - F2A.3, F2A.4, Th4D.6
Srinivasan, Balaji - W3A.27
Srinivasan, Srinivasan Ashwyn - Th3C.1
Srivastava, Manas - W3A.27
Stanciu, George A. - Th3K.4
Stanciu, Stefan G. - Th3K.4
Stark, Henning - W1A.1
Staude, Isabelle - W2H.2
Stefania, Campopiano - Tu3K.2
Stephen, Mark A. - Tu3A.2
Stiller, Birgit - Th3B.1, Th4B
Stoichita, Catalin - Th3K.4
Su, Chung-Wei - W2L.3
Su, Haibin - W3A.127
Su, Liangbi - F2E.4
Su, Lin-Yun - Tu3K.5
Su, Yikai - Th2C.1
Suda, Akira - Th3B.4
Sudo, Masaaki - W2E.5, W3A.66, W3A.93
Sugie, Toshihiko - W4I.5
Sugiyama, Hirokazu - W3A.117
Šulc, Jan - W3A.55, W3A.56
Sumpf, Bernd - W2J.2
Sun, Biao - F1A.5
Sun, Chuanbowen - Tu2I.1
Sun, Dechuan - Th4E.5
- Sun, Fangling - Th3A.3
Sun, Fang-Wen - Th4J
Sun, Jiahui - F2D.7
Sun, Lin - Th3K.2, W3A.10
Sun, Li-Peng - Th4L.5, W4L.6
Sun, Meizhi - Th4B.3
Sun, Pengshuai - Tu3L.5
Sun, Qizhen - F2E.2, F2E.5
Sun, Shanyong - Th1I.2, Th1I.4
Sun, Song - Th2F.2, Th2H.4
Sun, Xiankai - W4D.2
Sun, Xiaolan - Tu3A.7, W2A.3
Sun, Xiaoqiang - W3A.103
Sun, Xuqing - Th4E.7
Sun, Yizhi - W4E.3
Sung, Jangwoon - F2B.2, W3A.143
Suzuki, Chihiro - W3A.73
Suzuki, Kenta - W3A.68
Suzuki, Ryo - Tu3H.4, W1B.3
Suzuki, Takakazu - Th1B.3
Suzuki, Yutaro - Th3H.3
Svejkar, Richard - W3A.55
Svyakhovskiy, Sergey E. - Th4C.4
Swiderski, Jacek - W3A.46
Switkowski, Krzysztof - W2E.4
Szatmari, Sandor - W3A.47
Szczepanski, Pawel - Th1F.2, Th1F.3
- T**
- Tada, Akiko - W3A.108
Taglietti, Bruno - Th2C.3
Taguchi, Kaho - Th1C.2
Tai, Zhaoyang - Tu2F.3
Takada, Kazumasa - F2A.8
Takahashi, Eiji J. - Th3B.4
Takahashi, Yasushi - Th1H.2, W3A.116, W4D.3
Takeda, Koji - Th2J.2
Takeda, Shinogu - Th3I.3
Takei, Nobuyuki - Th4J.6
Takemura, Takuya - W3A.99
Takenaka, Mitsuru - Th3C.4
Takesue, Hiroki - W2G.5
Takeuchi, Mahiro - W3A.66
Talataisong, Wanvisa - F1E.1
Tam, Hwa-Yaw - F1E.3, W4L.4, W4L.6
Tamagnone, Michele - W2H.1
Tamiaki, Hitoshi - Th1B.5
Tamma, Vincenzo - Th4J.5
Tan, Dawn T. - W2B.4, W4B.1
Tan, Fangzhou - Th1A.3
Tan, Mingming - F2F.2
Tan, Zhiyong - Tu2C.4
Tanabe, Takasumi - Tu3H.4, W1B.3, W3A.4, W4H.3
Tanaka, Hiroki - Th4A.5, W1A.5
Tanaka, Yoshinori - Th1H.4, W4H.6
Tanaka, Yurina - Th1C.5
Tang, Chung-Po - W3A.31
Tang, Liqin - Th4H.3
Tang, Mingchu - W1F.2
Tang, Ni - W3A.51
Tang, Song - W4C.3
Tang, Wusheng - W3A.89
Tang, Xiahui - F2E.5
Tang, Xianfeng - Th1I.1, Th2I.2
Tang, Xiaosheng - Th1H.1, Th2H.5
Tang, Xuan - Th4I.3
Tang, Yanni - W3A.125
Tang, Ying - Th2I.6
Tang, Zhenzhou - F2C.5
Tangi, Malleswararao - W2J.5
Tani, Shuntaro - W4A.8
Tao, Jin - W3A.148
Tao, Long - Th1F.4
Tapang, Giovanni A. - Th3K.5
Tarazona, Antulio - W1F.1
Tariq, Unaiza - Th2I.1
Taue, Shuji - Tu2L.4
Tawfiq, Mahmoud - W2J.2
Taximaiti, Yusufu - F1A.2
Tei, Kazuyoku - Tu3A.6, Tu3F.2
Teng, Jinghua - Th2F.1
Teng, Yuan-He - F2E.6
Terakawa, Shusaku - W2E.5
Tereshchenko, Dmitriy - W3A.54
Tetsumoto, Tomohiro - W4H.3
Tew, Xuan - Th1D.4
Thirkettle, Robert - Tu3F.4
Thompson, Mark - Th1D.4
Thomson, David - Th3C.3
Tian, Changyong - W3A.97
Tian, Chunxiu - Tu2C.3
Tian, Haochen - Th4A.4
Tian, Wenjing - W4B.4
Tian, Xiangjun - W1E.1
Ting, Lei - W3A.155
Tjin, Sweechuan - Th3L.1
Tokel, Onur - W1E.2, W4G.4
Tomita, Keita - Tu3J.2
Tomita, Masaya - Th1D.3, W3A.111
Tomomatsu, Yasunori - W1J.4
Tong, Limin - F2B.6, Th4G.2, W4H.5
Tong, Zhengrong - Tu2H.3

Torisawa, Shinsuke - W3A.75
 Tosi, Daniele - Tu3K.2, W4K
 Toumi, Johnny - W4G.4
 Tranca, Denis E. - Th3K.4
 Tränkle, Günther - W2J.2
 Tranter, Aaron - Th1D.2
 Travers, John C. - W2A.1
 Tsai, Cheng-Ting - W3A.12
 Tsai, Din Ping P. - W2H.3
 Tsai, Ding-Zhang - W3A.134
 Tsai, Meng-Zhe - F1E.2
 Tsai, Wen-Shing - Th4I.5
 Tsang, Hon - W1F
 Tsang, Hon K. - Th3C.4
 Tsang, Peter - W4G.1
 Tsia, Kevin K. - Th4B.5, Th4B.6, W3A.32
 Tsuchizawa, Tai - Th2J.2
 Tsukada, Keiji - Tu3C.3, Tu3C.5, Tu3C.6
 Tsukijima, Saki - W4K.3
 Tsuru, Shota - W3A.79
 Tu, Han-Yen - W3A.28, W3A.90
 Tu, Jih-Hu - W3A.31
 Tu, Jiajing - Tu2I.3, Th3A
 Tuennermann, Henrik - W1A.2
 Tuggle, Matthew - Th2E.2
 Tünnermann, Andreas - Th4D.2, Tu2L.1, W1A.1
 Turnali, Ahmet - W1E.2, W4G.4
 Twamley, Jason - Tu2G.3
 Tyrtyschnyy, Valentin - W4B.7
 Tyszka-Zawadzka, Anna - Th1F.2, Th1F.3
 Tzou, An-Jye - W2J.6

U

Uchida, Kazuki - W3A.117
 Uchida, Megumi - Th1C.5
 Uddin, Hemayet - Th4E.5
 Ullah, Rahat - W4E.5
 Umemura, Nobuhiro - W3A.43
 Umezawa, Toshimasa - W4J.2
 Ummethala, Sandeep - W4J.1
 Umnikov, Andrey - Tu3A.5
 Unnithan, Ranjith R. - Th4E.5
 Upendar, Swaathi H. - W4E.6

V

Vahala, Kerry J. - Tu1A.1
 Van Campenhout, Joris - Th3C.1, Th4G.3

Vanholsbeeck, Frederique - Tu2B
 Vanthourhout, Dries - Th3C.1, Th4G.3
 Varshney, R. K. - Tu3H.2
 Varshney, Shailendra - F1B.5, W3A.104
 Vasa, N J. - Tu3L.3, Tu3L.4
 Veisz, Laszlo - Th3B.2
 Venkatasubramani, Lakshmi Narayanan - Tu3D.4
 Venkitesh, Deepa - Tu2D, Tu3D.3, Tu3D.4, W3A.27
 Verma, Varun - Th4J.1
 Vernaz-Gris, Pierre - Th1D.2
 Vieker, Henning - F2B.3
 Villatoro, J. - W4L.2
 Vissers, Ewoud - Th3C.1
 Volkov, Mikhail - Tu3A.4
 Volkov, Mikhail R. - Th2D.4
 Vollmer, Frank - Tu3H.1
 Voloshin, Andrey - Th2H.7
 Volz, Jürgen - W2G.1
 Vyhlidal, David - F2E.4, W3A.56

W

Wada, Naoya - Tu3I.3
 Wai, P K A - Th1A.5
 Wai, Ping Kong A. - F1E.3, Th2B.5, Tu3H.5, W3A.35, W3A.49
 Walmsley, Ian - Tu3B.1
 Walsler, Stefan - W2G.1
 Walther, Philip - F1D.4
 Wan, Hongdan - Th3A.4, W2A.7
 Wan, Wenjian - Tu2C.4
 Wan, Yuhang - Th1L.3
 Wan, Yuhong - W4G.3
 Wang, Aimin - Th4A.2, W2A.4
 Wang, Anting - Th3A.3, W1A, W4A
 Wang, Bo - W1H.1
 Wang, Can S. - W3A.23
 Wang, Chang - Tu2C.4
 Wang, Chao - F2A.5, F2D.4, Th2A.6, W2B.2, W3A.24, W4A.3, W4L.5
 Wang, Cheng - Th2D.1, Tu2H.4, W1C, W3A.128, W4C.2
 Wang, Chingyue - W1G.2
 Wang, Dan - W2K.6
 Wang, Dayong - F2C.7
 Wang, Dongdong - Th1I.2, Th1I.4
 Wang, Fei - W3A.103
 Wang, Feng - Th2L.6
 Wang, Fengqiu - W3A.1, W3A.149
 Wang, Gao - W3A.85
 Wang, Guanghui - Th3L.1
 Wang, Guanjun - W3A.85
 Wang, Guanling - W3A.119
 Wang, Hailin - W3A.61
 Wang, Heng - F2C.2
 Wang, Hong - Th3C.5, W4B.2
 Wang, Honghai - Tu2I.5
 Wang, Hongjian - Th1A.2
 Wang, Hsiang - Tu3L.1
 Wang, Huachun - F1F.5
 Wang, Huai-Yung - W3A.12
 Wang, Huaming - W1E.1
 Wang, Hui - W3A.24
 Wang, Jia - Th3K.2, W3A.10
 Wang, Jian - Th2L.5, W2D, W3A.100
 Wang, Jianfang - F2B.1
 Wang, Jianhuan - Th4G.5
 Wang, Jianjun - F1B.2, W1A.4
 Wang, Jianwei - Th1D.4
 Wang, Jie - Th3A.4, W2A.7
 Wang, Jieping - Th3E.3
 Wang, Jin - W3A.91
 Wang, Jinghao - Th3A.3
 Wang, Jinzhang - Th4A.8
 Wang, Ju - Th3F.4, Th3I.5, W3A.138, W3A.34
 Wang, Jun - Th1G.1
 Wang, Kai - W4E.5
 Wang, Kaijie - Th1A.2
 Wang, Kairu - F1F.5, Th2B.5, W3A.30, W3A.33, W3A.35
 Wang, Lei - W3A.89
 Wang, Li - W3A.23, W4B.6
 Wang, Liang - Th1J, Th2L.4, W2J.3
 Wang, Lifeng - Th3B.3, W2B.7
 Wang, Liqian - Th1I.2, Th1I.4
 Wang, Lon - F1B.3, W3A.82
 Wang, Lu - W2C.3
 Wang, Meng - W3A.102, W3A.120, W3A.126, W3A.25
 Wang, Mengke - F2C.2
 Wang, Nanshuo - Th4K.2
 Wang, Pei - W2J.3
 Wang, Peng - F1F.5
 Wang, Pengfei - W1I.1
 Wang, Ping - W3A.89
 Wang, Pu - F1A.4, Th1A.3, Th2G.4, Tu2E.2, Tu3B.4
 Wang, Qi - W4J.6
 Wang, Qijie - F1A.5, Th3J.1, Tu2H
 Wang, Qiu - Tu2C.3

Wang, Rui - W3A.84
 Wang, Rundong - W4L.5
 Wang, Shaohao - Tu3H.5
 Wang, Shaojie - F2D.3
 Wang, Sheng - Tu2D.5
 Wang, Shuai - Th2L.1
 Wang, Shuaishuai - Th3F.4, W3A.34
 Wang, Shuang - W4L.5
 Wang, Shuxin - W4J.5
 Wang, Sijia - F2E.7, Th4A.6
 Wang, T - W1J, W2J.1
 Wang, Teng - Tu3I.4
 Wang, Tianxing - Th2A.3, W2A.3, W3A.58, W4A.5
 Wang, Ting - Th4G.5, W1F.3
 Wang, Tingyun - Th1E.3, Th4L.3, Th4L.6, Tu3A.7, W2A.3
 Wang, Weitao - W3A.69
 Wang, Wen - Tu3E.5
 Wang, Xian - Tu3I.4
 Wang, Xianghong - Th4K.2
 Wang, Xiaocheng - Th4F.1
 Wang, Xiaocong - Tu3B.4
 Wang, Xiaofang - W4K.4
 Wang, Xiaolin - Th3D.4, W3A.44
 Wang, Xiaolong - F1B.2
 Wang, Xibin - W3A.103
 Wang, Xin - Th2E.5
 Wang, Xing-Guang - W3A.128
 Wang, Xiong - W3A.44
 Wang, Xiulin - W3A.84
 Wang, Xu - F2C.1, W3A.157
 Wang, Xudong - F2C.4, W2L.4
 Wang, Xuechun - Tu3K.4
 Wang, Yadong - Th4B.1
 Wang, Yan - Th4A.4
 Wang, Yaoting - W4E.3
 Wang, Yarong - Tu3K.6
 Wang, Yebing - Th3H.5, Tu3G.6
 Wang, Yi - W2B.5, W4B.2
 Wang, Yicheng - Th2G.1, Tu2B.5, W4A.2
 Wang, Yihong - W4K.4
 Wang, Ying Y. - F1B.2
 Wang, Ying-Bin - Tu3K.5
 Wang, Yingying - Tu2E.2, Tu3B.4
 Wang, Yi-Ran - W3A.45
 Wang, Yiyi - W4E.5
 Wang, Yong - Tu2L.2, W2J.3
 Wang, Yue - W4F.7
 Wang, Yunfeng - W3A.141
 Wang, Yunlong - Th4L.3
 Wang, Yunxin - F2C.7

Wang, Zefeng - W3A.102, W3A.120, W3A.124, W3A.126, W3A.25, W3A.51
 Wang, Zhen-Han - Th4I.5, W2I.3
 Wang, Zhi - Th1E.2, Th2L.5
 Wang, Zhiqiang - Th2A.2
 Wang, Zifei - Th2C.3
 Wang, Zihao - W3A.105
 Wang, Zinan - Th2L.2, W3A.50, W4L
 Wang, Zixiong - F2D.7, Th3I.5, W3A.138
 Ward, Jonathan - Th3L.3, W3A.156
 Wasilewski, Wojciech - Th4J.7, W2G.2
 Watanabe, Shinichi - Th4K.4, W3A.68
 Wei, Chengli - Tu3B.3
 Wei, Pu - W3A.72
 Wei, Qi - W4J.6
 Wei, Wei - Th4F.1
 Wei, Wenqi - Th4G.5
 Wei, Xiaoming - Th4B.5, Th4B.6, W3A.32
 Wei, Xunbin - W2K.1
 Wei, Yuan - Tu2D.4
 Wei, Zheng - W3A.84
 Wei, Zixian - W3A.153
 Weiss, Thomas - W4E.6
 Wells, Jon-Paul - Tu3F.4
 Wen, Jing - W1A.4, W3A.9
 Wen, Weifeng - F1F.2
 Weng, Wenle - Th2B.6, W2F.1
 Wenzel, Hans - W2J.2
 Weston, Morgan - Th4J.1
 Weyers, Markus - W2J.2
 White, Tommi - W4B.3
 Wiebe, Nathan - Th1D.4
 Wilkowski, David - Th4E.2
 Williams, Robert J. - F2A.3, F2A.4, Th4D.6
 Willner, Alan E. - Tu3D.1
 Wilson, William - W2H.1
 Wolf, Stefan - W4J.1
 Wong, Chee Wei - F2D.3
 Wong, Kam Sing - Th1K.5
 Wong, Kenneth Kin-Yip - Th4A.3, Th4B.5, Th4B.6, Tu2D.4, Tu2D.5, W2F, W3A.32
 Woodward, Robert I. - F1A.1
 Worschech, Lukas - Th1L.1
 Wu, Baojian - Th2B.2, Th2I.8, W2F.2
 Wu, Chao-Hsin - W3A.12, W4A.7
 Wu, Chongqing - Th2L.5

Wu, Chuang - Th4L.5, W4L.6
 Wu, Chunzhou - Th3L.2
 Wu, Danlei - Th4A.2
 Wu, Dong - W3A.69
 Wu, Guanhao - W4F.2, W4F.5
 Wu, Han - W3A.50
 Wu, Hao - W3A.22
 Wu, Hsiao-Hua - F2E.6
 Wu, Huan - Th2L.4
 Wu, Jia-Gui - F2D.3
 Wu, Jian - W4I.2
 Wu, Jiang - W1F.2
 Wu, Jianglai - Th4B.5, Th4B.6
 Wu, Jiayang - Th2C.2, Th3F.3
 Wu, Jieyun - Th1E.5
 Wu, Junyi - W3A.114
 Wu, Jushuai - Th4H.6
 Wu, Kaiquan - Th3I.4
 Wu, L.f. - Th4K.1
 Wu, Meng-Shan - Th4L.4
 Wu, Ming-Wei - W4I.6
 Wu, Nishan - W1C.3
 Wu, Stewart T. - Tu3A.2
 Wu, Xiaofei - F2B.3
 Wu, Xingbang - Th4I.6
 Wu, Xiong - Th2I.1, W2I.6
 Wu, Yao - W3A.5
 Wu, You-Ruei - Th4I.5, W2I.3
 Wu, Yue - W4J.5
 Wu, Yuehan - W4F.4
 Wu, Zeru - W4D.5
 Wu, Zheng-Mao - W1D.3

X

Xi, Lixia - Th1E.4, Th1I.1, Th2I.2, W4I.4
 Xi, Peng - W4K.2, W1K
 Xi, Xiaoming - W3A.126, W3A.25
 Xia, Changming - Tu2E.3
 Xia, Guang-Qiong - W1D.3
 Xia, Hua - Tu3L.5
 Xia, Jinsong - Tu2J.3, W4D.4
 Xia, Keyu - Tu2G.3
 Xia, Li - W1C.3
 Xia, Ouyang - F1E.3, Th4H.6
 Xia, Shiqi - Th4H.3
 Xiang, Changqing - Th3I.4
 Xiang, Qian - Th2I.3, W3A.19
 Xiang, Xiao - Th4J.3
 Xiang, Yang - F2E.2, F2E.5
 Xiao, Hu - W3A.44

- Xiao, Lin - Th4G.4
 Xiao, Longfu - Tu3H.3
 Xiao, Min - Tu3H.3
 Xiao, Peng - W2L.4
 Xiao, Ting-Hui - Th3C.4
 Xiao, Xi - W3A.158
 Xiao, Yang - Tu3I.4
 Xiao, Yaoqiang - Th3I.4
 Xiao, Yin - Th4K.5
 Xie, Chen - W1G.2
 Xie, Guoqiang - Th2G.2
 Xie, Huikai - W2K.6
 Xie, Huimin - Th4K.1
 Xie, Shouyi - W2H.5
 Xie, Tianyuan - Th3F.4, Th3I.5, W3A.138, W3A.34
 Xie, Wei - W4A.6
 Xie, Weilin - Th4F.1
 Xie, Xinglong - Th4B.3
 Xie, Xiuping - Th4J.6
 Xie, Yiyang - W2A.6
 Xie, Youpeng - W3A.155
 Xie, Ze T. - W3A.148
 Xin, Chenguang - W4H.5
 Xin, Ming - Tu3B.2
 Xing, Cheng - Th2H.6
 Xing, Da - W4K.1
 Xing, Xin - Th1H.1
 Xing, Zhen - Th2E.5
 Xiong, Ji - Th2L.2
 Xiong, Shilin - W4F.5
 Xiong, Wei - Th4E.7, W1E, W2E.3
 Xu, Bairu - W3A.40
 Xu, Bo - F2A.2, Th2I.8, W3A.23
 Xu, Chen - W2A.6
 Xu, Fei - Th3J.2, W3A.76
 Xu, Feng - W3A.30
 Xu, Guanjun - W3A.57
 Xu, Haiyang - W3A.63
 Xu, Hengying - Th1I.1
 Xu, Hongnan - Th2C.4
 Xu, Jiahao - F2C.7
 Xu, Jian - Tu2I.5
 Xu, Jiangming - W3A.63
 Xu, Jimmy - F2B.5
 Xu, Jingjiang - Th4B.5, Th4B.6
 Xu, Jingjun - Th4H.3
 Xu, Jin-Shi - Th3H
 Xu, Jun - Th2G.1
 Xu, Ke - Th3E.1
 Xu, Kun - W3A.18
 Xu, Pengfei - W3A.118
 Xu, Qijia - Th1I.2, Th1I.4
- Xu, Qinfang - Th3H.5, Tu3G.6
 Xu, Quan - Tu2C.3
 Xu, Rui - W3A.1
 Xu, Shengyao - F1F.3
 Xu, Tao - W4K.4
 Xu, Wei - W2L.5, W4K.5
 Xu, Wen-Cheng - F2E.1
 Xu, Xiaodong - Th2G.1
 Xu, Xiaojun - Th3D.4, W3A.102, W3A.120
 Xu, Xingyuan - Th2C.2, Th3F.3
 Xu, Yan - W3A.103
 Xu, Yao - F1A.3
 Xu, Yi - W3A.6
 Xu, Yin - Th2B.5, W3A.35
 Xu, Yiqing - Th4B.5, Th4B.6, W3A.32
 Xu, Yitong - F2D.7
 Xu, Zhe - W3A.100
 Xu, Zhengyuan - Th4F.5
 Xu, Zhizhan - Th2D.1
 Xu, Zihan - W4D.5
 Xue, Chenpeng - F2D.2
 Xue, Daojun - Tu2I.4
 Xue, Lei - Th4I.1
- Y**
- Yada, Hiromu - W3A.117
 Yalla, Ramachandrarao - W4E.2
 Yamada, Hirohito - W3A.36
 Yamada, Koji - W4D.3
 Yamada, Yuko - W2F.3
 Yamaguchi, Shigeru - Tu3A.6, Tu3F.2
 Yamaguchi, Yuki - Th1B.3
 Yamakoshi, Shigenobu - Th1B.2
 Yamamoto, Hirotsugu - W4F.3
 Yamamoto, Naokatsu - W4J.2
 Yamamoto, Yoshihisa - W1D.1
 Yamamura, Munenori - W4K.3
 Yamaoka, Shuhei - W4I.7
 Yamaoka, Yoshihisa - Tu2L.5
 Yamashita, Kosuke - F2D.5
 Yamashita, Shinji - Th4A.7
 Yamaski, Tomohito - W4C.5
 Yamauchi, Yukiko - Th1H.2
 Yan, Banban - W3A.33
 Yan, Binbin - F1F.5, Th2B.5, W3A.30, W3A.35
 Yan, Guofeng - Th3L.2
 Yan, He-Jie - W3A.36
 Yan, Jikun - W3A.62
 Yan, Jin-Yi - Tu2H.4
- Yan, Lulu - F2A.7, Tu2F.3
 Yan, Peiguang - Th4A.8, W3A.151
 Yan, Shao-Cheng - W3A.76
 Yan, Shibo - Th2E.5
 Yan, Wei - W1C.2
 Yan, Xin - W3A.5
 Yan, Yinzhou - Th2H.6
 Yan, Zhijun - F2E.2, F2E.5, Th1A.4, Th2A.3
 Yanagiya, Shin-Ichiro - Th1L.2
 Yang, Baolai - Th3D.4
 Yang, Bo - W3A.87
 Yang, Cao - W3A.75
 Yang, Ce - Th1D.5
 Yang, Chao - W4A.3
 Yang, Chuanchuan - W1I.1
 Yang, Chunchuan - W4D.5
 Yang, Decheng - W3A.141
 Yang, Dengcai - F2C.7
 Yang, Feng - F2C.7
 Yang, Guangyao - Th2L.1
 Yang, Hongzhi - Tu3F.7
 Yang, Jingyi - Th1F.4
 Yang, Jin-Kyu - F2B.7
 Yang, Kang - Th1E.2
 Yang, Kangwen - Th2A.5
 Yang, Lan - W1B.1, W2B
 Yang, Li - W4H.7
 Yang, Lin - W4B.4
 Yang, Lingxiao - Tu2D.5
 Yang, Minghong - Th4L.7, Tu2L.2
 Yang, Mingrui - W3A.22
 Yang, Ning - W4B.2
 Yang, Ningning - Th2B.7
 Yang, Qi - Tu2I.1
 Yang, Qingwei - Th4B.3
 Yang, Shang-Lin - W3A.31
 Yang, Shiwen - Th4L.7
 Yang, Sigang - W3A.87
 Yang, Sihua - W4K.1
 Yang, Tao - F1F, Th2K.4, W2I.5, W3A.65
 Yang, Wan - Th4A.2
 Yang, Wei - Th2L.3
 Yang, Yanfu - Th2I.3, W3A.19
 Yang, Yong - W3A.156
 Yang, Yuanhong - Th2L.3, Th4D.5
 Yang, Yuanjie - W3A.48
 Yang, Yudong - F2A.1, Th3B.5, Tu3B.5
 Yang, Yue-De - F2C.3
 Yang, Zhenjun - W3A.64
 Yannai, Michael - W1H.1
- Yao, Jianping - W1L.1
 Yao, Junna - Th3A.3
 Yao, Mian - F1E.3
 Yao, Wenming - W2A.5
 Yao, Xin - W3A.107
 Yao, Yong - Th2I.3, W3A.19
 Yao, Yuan - Tu2H.3
 Yao, Yuhan - W3A.158
 Yao, Zijun - Th1L.3, W3A.59, W4F.4
 Yao-Yang, Tsai - F1B.3
 Yap, Stephanie H. - Th3L.1
 Yasui, Takeshi - Tu2L.4, Tu2L.5, W3A.130, W4F.3
 Yasuno, Yoshiaki - W2K.2
 Yatagai, Toyohiko - Th1K, W4G.2
 Yavuz, Özgün - W4G.4
 Ye, Hui - Tu2J.2
 Ye, Jian - Tu3J.1
 Ye, Pengbo - Th2A.5
 Ye, Shengwei - Th2J.6
 Yi, Lilin - Th4I.1, W1D
 Yi, Wenjun - W3A.89
 Yi, Xingwen - Th1I.3, W1I.5
 Yi, Yasha - W4D.1
 Yin, Feifei - W3A.18
 Yin, Jianzhao - W4E.5
 Yin, Jinde - W3A.151
 Yin, Mojuan - Th3H.5, Tu3G.6
 Yin, Yj. - Th4K.1
 Yin, Zhengkun - Th4H.6
 Ying, Xiangxiao - F2B.5
 Yodh, Arjun G. - Tu2K.1
 Yokoyama, Hiroyuki - W3A.36
 Yokoyama, Shiyoshi - Tu3E.3
 Yong, Derrick - W4K.6
 Yong, Ken Tye - Th3L.1
 Yoshida, Masahiro - W4H.6
 Yoshii, Kazumichi - Th1C.2, Th1C.4, Th4A.1, W2F.3, W2G.3
 Yoshikuni, Yuzo - W2K.3
 Yoshimura, Yoshiharu - W3A.73
 Yoshioka, Hiroaki - W3A.79
 You, Li - Th4J, F1D.1
 You, Pei - W3A.100
 You, Quan - W3A.15
 You, Shanhong - W2L.5, W3A.22
 Yu, Anthony W. - Tu3A.2, Tu3L.8, W2L.3
 Yu, Binbin - W3A.9
 Yu, Changyuan - F1F.6, F2D.7, Tu2I.3, W2L.5, W4I.6, W4K.5, W4L.4
 Yu, Cheungchuen - W2L.5, W4K.5
- Yu, Chongxiu - Th2B.5, W3A.30, W3A.33, W3A.35
 Yu, Chung-Ping - F1F.4, Th3J.4
 Yu, Chunlei - Th3D.3
 Yu, Fei - Th2E.1
 Yu, Haihu - W3A.41
 Yu, Haohai - Th2G.1, Tu2B.5
 Yu, Honggang - W1K.4
 Yu, Jianguo - F2F.6, W4I.3
 Yu, Jiekui - Tu2I.5
 Yu, Jinlong - F2D.7, Th3F.4, Th3I.5, W3A.138, W3A.34
 Yu, Lianghong - Th2D.1
 Yu, Nanjie - Th2E.2
 Yu, Runqing - Tu3L.5
 Yu, Siu Fung - W3A.141
 Yu, Siyuan - Th2I.1, W2I.6, W3A.118, W4D.5
 Yu, Song - W3A.101, W3A.105
 Yu, Xi - W2E.5, W3A.66, W3A.93
 Yu, Xia - F1A.5, Th4C.1
 Yu, Xiaojun - W1K.4
 Yu, Xiaosong - Th2I.5
 Yu, Xuechao - Th3J.1
 Yu, Yang - Th3F.4, Th3I.5, W3A.138, W3A.34
 Yu, Ying - Th4A.3, Th4B.5, Th4B.6
 Yu, Yuan - W3A.158
 Yu, Zejie - W4D.2
 Yu, Zhipeng - W2K.5
 Yuan, Hualei - W4A.2
 Yuan, Jinhui - F1F.5, Th2B.5, Tu2I.3, W3A.30, W3A.33, W3A.35, W3A.49, F1A
 Yuan, Pengtao - Th4A.7
 Yuan, Quan - Th2L.6
 Yuan, Ru - Tu2F.3
 Yuan, Shuai - Tu2J.3
 Yuan, Xiaocong L. - Th4E.1, W3A.155
 Yuan, Xiaolong - Th1A.5
 Yuda, Leona - Tu2F.5
 Yue, Chik P. - W3A.23
- Z**
- Zafeiropoulou, Angeliki - F1E.1
 Zang, Jie - W3A.69
 Zang, Siyao - F1F.3
 Zang, Tianyang - W2J.3
 Zarzuelo Garcia, Alberto - W1L.2
 Zayats, Anatoly - Tu2J.1
 Zayko, Sergey - Th1B.4
- Zeng, Heping - Th2A.5
 Zeng, Jun - W3A.48
 Zeng, Qihang - W4K.5
 Zeng, Tao - Tu2I.5
 Zeng, Xianxu - W4K.4
 Zhai, Yiwei - W3A.106
 Zhan, Huan - F1B.2
 Zhan, Qiwen - Tu2A.2
 Zhan, Sui - Th3D
 Zhang, A. Ping - F1E.3, Th4H.6
 Zhang, Ailing - Tu2H.3
 Zhang, Bin - Th4G.5
 Zhang, Chengyun - W3A.40
 Zhang, Chi - Th2B.7, Th3K.3, Tu2D.2, Tu2D.3, Tu2D.5, W4B.2
 Zhang, Chongfu - Th4I.2
 Zhang, Daming - W3A.103
 Zhang, Dao Hua - Th4H.2, W3A.127
 Zhang, Dawei - W3A.9
 Zhang, Fan - Th1I, W1I.1
 Zhang, Guofeng - F1D, Th1D, Tu2G
 Zhang, Haiguang - Th4I.3
 Zhang, Han - Th1G, Th2G, Th4G
 Zhang, Hanwei - Th3D.4, W3A.63
 Zhang, Hanyu - W4D.6
 Zhang, Hongwei - Th1E.2
 Zhang, Hu - Th1E.4
 Zhang, Huajin - Th2G.1, Tu2B.5
 Zhang, Hui - W1J.3
 Zhang, Jian - W1J.3
 Zhang, Jianjun - Th4G.5, W1F.3
 Zhang, Jie - Th2I.5
 Zhang, Jieyin - Th4G.5
 Zhang, Jing - F2D.4, Th1I.3, W1I.5, W3A.24
 Zhang, Jingwen - W2B.2
 Zhang, Junwei - Th2I.1, W2I.6
 Zhang, Junxuan - W4A.6
 Zhang, Lei - Tu2D.2, Tu2D.3, Tu2I.5, W4B.4
 Zhang, Lin - Th2A.3, Th3A.4
 Zhang, Linbo - W3A.57
 Zhang, Linlin - W4K.4
 Zhang, Lu - Th2I.6, W3A.112
 Zhang, Meng - Th2A, Th3G.2
 Zhang, Mengyu - W3A.151
 Zhang, Min - Th2I.8
 Zhang, Minming - W4H.2
 Zhang, Na - W2L.5, W4K.5
 Zhang, Nannan - Th1I.1
 Zhang, Pan - F2A.7, Tu2F.3
 Zhang, Q. - Th4K.1
 Zhang, Qian - F1A.4

- Zhang, Qiang - W3A.144
 Zhang, Qun - Th2I.3, W3A.19
 Zhang, Shang Jian - F2C.2
 Zhang, Shaojun - W3A.69
 Zhang, Shougang - F2A.7, Th4J.3, Tu2F.3, W3A.106, W3A.57
 Zhang, Shuai - W3A.129
 Zhang, Shumin - W3A.64
 Zhang, Songlin - Th4A.8
 Zhang, Tiantian - W3A.154
 Zhang, Wanying - Th1E.5
 Zhang, Wei - W3A.107
 Zhang, Weili - Tu2C.3
 Zhang, Wenbo - Th1I.1, Th2I.2, W4I.4
 Zhang, Wenchao - W4A.3
 Zhang, Wending - F2B, Th4E.6
 Zhang, Wenjing - Th1I.3
 Zhang, Wenqi - W1I.2
 Zhang, Xia - W3A.5
 Zhang, Xiang - Th2F.6
 Zhang, Xianting - Th2B.5, W3A.35, W3A.49
 Zhang, Xiao L. - Th4I.2
 Zhang, Xiaohan - W4K.4
 Zhang, Xiaoguang - Th1E.4, Th1I.1, Th2I.2, W4F, W4I.4
 Zhang, Xin - Tu2E.2
 Zhang, Xingyu - W3A.69
 Zhang, Xinliang - F1B.4, Th2B.7, Th3K.3, Tu2D.2, Tu2D.3, W3A.157, W3A.158
 Zhang, Xixiang - Tu2C.3
 Zhang, Xu - W3A.13
 Zhang, Xuexia - Th4D.5
 Zhang, Xuezhai - W4L.5
 Zhang, Xuming - Th1H, Th4H
 Zhang, Xuping - Th2L.6, Th3L.1, Th2L
 Zhang, Yali - F2C.2
 Zhang, Yanfeng - W3A.118, W4D.5
 Zhang, Yang - Th1L.4
 Zhang, Yanting - W3A.84
 Zhang, Yanyan - F2A.7, Tu2F.3
 Zhang, Yazhen - Tu3H.5
 Zhang, Yi Xin - Th3L.1
 Zhang, Yinan - W2H.5
 Zhang, Ying - Th3B.3, W2B.7
 Zhang, Yu - Th1L.3, W3A.59
 Zhang, Yusheng - W3A.122
 Zhang, Yuwen - W4B.3
 Zhang, Zeyu - Th1B.5, Th1H.1, W3A.39
- Zhang, Zhan - W4K.4
 Zhang, Zhaoyu - Th1L.6
 Zhang, Zhigang - F2A.2, Th4A.2, Th4A.4, W2A.4
 Zhang, Zhiguo - Th4I.4
 Zhang, Zhirong - Tu3L.5
 Zhang, Zhiyao - F2C.2
 Zhang, Zuxing - Th2A.2, Th3A.4, W2A.7
 Zhanghao, Karl - W4K.2
 Zhao, Anke - F2D.2, F2D.4, W3A.24
 Zhao, Bin-Bin - W3A.128
 Zhao, Chao - W2J.5
 Zhao, Chengliang - W3A.48
 Zhao, Fang - W1K.3
 Zhao, Hua - W2B.2
 Zhao, Hui - W2K.6
 Zhao, Jian - Th3I
 Zhao, Jianguo - W3A.42
 Zhao, Lei - W1A.4
 Zhao, Mingfu - Th4L.2
 Zhao, Nan - W3A.123
 Zhao, Peng - Th2A.5
 Zhao, Ruixuan - W3A.100
 Zhao, Wei - Tu3A.7, W2A.3
 Zhao, Weijie - Th4G.6
 Zhao, Wenguang - W3A.61
 Zhao, Xiaoyan - F2D.2
 Zhao, Xin - W3A.59, W4F.4
 Zhao, Xin Cai - F1F.2
 Zhao, Yongguang - Th2G.1, Tu2B.5, W4A.2
 Zhao, Yongli - Th2I.5
 Zhao, Yunhe - Th1E.3, Th4L.6
 Zhao, Yuxuan - Tu3K.6
 Zhao, Zhigang - Th4C.5
 Zhao, Zhiyong - F1E, Th2L.4
 Zhao, Ziqiang - Th3C.4
 Zheludev, Nikolay - Th4E.2
 Zheng, Chen - Tu2D.3
 Zheng, Fusheng - Tu2I.5
 Zheng, Gaige - W3A.152
 Zheng, Mingyang - Th4J.6
 Zheng, Ruiqi - F2C.4
 Zheng, Shilie - F1C.1
 Zheng, Xiaorui - Th2G.4
 Zheng, Xu - Tu2H.5
 Zheng, Yu - W3A.41
 Zheng, Zheng - Th1L.3, Tu3F, W3A.59, W4F.4
 Zheng, Zibo - Th1I.1, Th2I.2, W4I.4
 Zhong, Kangping - Tu2I.3, W3A.30
 Zhong, Tianting - W2K.5
- Zhong, Xin - F2C.7
 Zhong, Xuexiang - Th4L.7
 Zhou, Bin - W2A.3
 Zhou, Changhe - Th4H.6
 Zhou, Chao - Th2K.2, W2K, W4K.4
 Zhou, Chaobiao - W2B.5
 Zhou, Feng - Th3L.5, W3A.157, W3A.158
 Zhou, Gengji - Tu3B.2
 Zhou, Guiyao - Tu2E.3, Tu3I.4, Th3L
 Zhou, Haidong - Th2B.7
 Zhou, Hailong - F1B.4
 Zhou, Heng - Th2B.2, W2F.2
 Zhou, Honghang - W4I.2
 Zhou, Hongqiang - W4G.3
 Zhou, Hongyan - Tu2I.5
 Zhou, Jie - Th1L.6
 Zhou, Kaiming - Th2A.3
 Zhou, Lei - Th2F.5, Tu2I.4
 Zhou, Linjie - Th3C, W3A.157, W4D.6
 Zhou, Minglai - W3A.22
 Zhou, Pu - Th3D.4, Th4D.1, W3A.121, W3A.44, W3A.63, W1G
 Zhou, Qian - W4F.5
 Zhou, Renjie - Th3K.1
 Zhou, Siyu - W4F.5
 Zhou, Tao - F2C.7
 Zhou, Taojie - Th1L.6
 Zhou, Wen - Th3C.4
 Zhou, Wenjing - Th1I.3
 Zhou, Xi - Th2B.7, Th3K.3, Tu2D.2, Tu2D.3
 Zhou, Xian - Tu2I.3, W1I, W3A.30, W3A.35
 Zhou, Xiaoqi - Th1D.4
 Zhou, Yihan - Tu2J.2
 Zhou, Yue-Guang - Tu2H.4
 Zhou, Zhenlei - Th4I.3
 Zhou, Zhihua - Th3I.2
 Zhou, Zhiping - Th3B.2
 Zhou, Zhi-Yuan - F1D.2, W2G.7
 Zhou, Zhiyue - W3A.51
 Zhu, Baohua - W3A.91
 Zhu, Chengjie - Tu3F.5
 Zhu, Chunhui - W3A.149
 Zhu, Dan - F2C.5, Tu3K.4, W1K.3
 Zhu, Eric Y. - Th3L.5
 Zhu, Guangzhi - W3A.61
 Zhu, Haidong - Th4B.3
 Zhu, Jianqiang - Th4B.3
- Zhu, Kun - Th4F
 Zhu, Lanxin - Tu3K.4
 Zhu, Luyao - Tu3I.4
 Zhu, Mengjun - W3A.89
 Zhu, Mengmeng - Tu3I.4
 Zhu, Ming - W4E.3
 Zhu, Mingyue - Th4I.2, W1I.5
 Zhu, Ping - Th4B.3
 Zhu, Qihua - Th2D.2
 Zhu, Ruijie - Th2I.5
 Zhu, Shicheng - Th2D.5
 Zhu, Shining - W3A.1
 Zhu, Tao - F1B, Tu2B.4, W3A.38
 Zhu, Tengfeng - Tu2J.2
 Zhu, Weiming - W2B.7
 Zhu, Wenjie - Tu2L.2
 Zhu, Xiao - W3A.61
 Zhu, Xiaolei - W4A.6
 Zhu, Xuehua - W3A.119
 Zhu, Yixiao - W1I.1
 Zhu, Yong-Yuan - W3A.65
 Zhu, Zebin - W4F.5
 Zhu, Zhiwei - F2A.5, Th2A.6
 Zi, Jianchen - Tu2C.3
 Zichi, Julien - W2G.6
 Zou, Chuanhang - Th1A.4, Th2A.3, Tu3A.7, W2A.3, W3A.58, W4A.5
 Zou, Fang - Th4L.3
 Zou, Jun - Th1L.4
 Zou, Kai - W2G.6
 Zou, Pu - W2F.6
 Zou, Xinhai - F2C.2
 Zou, Xiujian - W3A.152
 Zoysa, Menaka D. - Th1H.4, W4H.6
 Zubia, J. - W4L.2
 Zuo, Chao - Th2K.1, Th3K
 Zuo, Chengliang - W4J.3
 Zwickel, Heiner - W4J.1
 Zwiller, Val - W2G.6

CLEO Pacific Rim 2018 Post-deadline Session (Room S421, 18:30-20:45, 2 August, 2018)

Presider: Changyuan Yu, The Hong Kong Polytechnic University

Time

PDP.1	<p>Fiber-based high-dimensional quantum key distribution with twisted photons Daniele Cozzolino¹, Davide Bacco¹, Beatrice Da Lio¹, Kasper Ingerslev¹, Yunhong Ding¹, Kjeld Dalgaard¹, Poul Kristensen², Michael Galili¹, Karsten Rottwitz¹, Siddharth Ramachandran³, Leif Katsuo Oxenløwe¹ ¹CoE SPOC, DTU Fotonik, Dep. Photonics Eng., Technical University of Denmark, Denmark ²OFS-Fitel, Denmark ³Electrical and Computer Engineering Department, Boston University, USA We implement the first fiber-based orbital angular momentum (OAM) state highdimensional quantum key distribution protocol using four OAM modes, and demonstrate the highest secret key rate and longest transmission distance for OAM presented to date.</p>	18:30-18:45
PDP.2	<p>Image Classification and Reconstruction through Multimode Fibers by Deep Neural Networks Kakkava E.¹, Borhani N.¹, Pu. Y.¹, Moser C.², Psaltis D.¹ ¹Optics Laboratory, School of Engineering, Ecole Polytechnique Fédérale De Lausanne, Switzerland ²Laboratory of Applied Photonic Devices, School of Engineering, Ecole Polytechnique Fédérale De Lausanne, Switzerland A VGG-type classifier and a U-net deep neural network were used to classify and restore the input image on a multimode fiber from the intensity only image of the speckle pattern at the output.</p>	18:45-19:00
PDP.3	<p>Self-organized nonlinear gratings for ultrafast nanophotonics Daniel D. Hickstein¹, David R. Carlson¹, Haridas Mundoor², Jacob B. Khurgin³, Kartik Srinivasan⁴, Daron Westly⁴, Abijith Kowligy¹, Ivan Smalyukh², Scott A. Diddams^{1,5}, and Scott B. Papp^{1,5} ¹National Institute of Standards and Technology, U.S.A. ²Department of Physics and Soft Materials Research Center, University of Colorado, U.S.A. ³Department of Electrical and Computer Engineering, Johns Hopkins University, U.S.A. ⁴Center for Nanoscale Science and Technology, NIST, U.S.A. ⁵Department of Physics, University of Colorado, U.S.A. We show how reconfigurable, self-organizing grating structures can be written in silicon nitride nanophotonic waveguides, using femtosecond pulses. These gratings provide simultaneous phase- and group-velocity matching for efficient broadband second-harmonic generation.</p>	19:00-19:15
PDP.4	<p>Optical SNR Engineering using Warped Stretch Jacky C.K. Chan, Bahram Jalali Department of Electrical and Computer Engineering, UCLA, USA We introduce a method for reversible engineering of signal to noise ratio of optical waveforms and discuss its potential for optical encryption and context-aware detection of weak signals in noisy environments.</p>	19:15-19:30

PDP.5	<p>Polarization Insensitive Silicon-Indium Tin Oxide Based Electro-Absorption Modulator <u>Yin Xu</u>^{1,2}, Feng Li^{2,3}, Jinhui Yuan^{3,4}, Zhe Kang³, Dongmei Huang³, Xianting Zhang³, and P. K. A. Wai³ ¹Department of Electrical Engineering, The Hong Kong Polytechnic University, Hong Kong, China ²The Hong Kong Polytechnic University Shenzhen Research Institute, China ³Department of Electronic and Information Engineering, The Hong Kong Polytechnic University, Hong Kong, China ⁴State Key Laboratory of Information Photonics and Optical Communications, Beijing University of Posts and Telecommunications, China We propose a highly-efficient, low-loss, and polarization insensitive silicon-indium tin oxide electro-absorption modulator. High modulation efficiency of ~3.18 dB/μm and low insertion loss of <0.3 dB are achieved in a length of 8 μm.</p>	19:30-19:45
PDP.6	<p>16nm resolution lithography using ultra-small gap bowtie apertures <u>Jin Qin</u>, Liang Wang Department of Optics and Optical engineering, University of Science and Technology of China, China Here, we report a novel method to fabricate bowtie aperture with sub-15 nm gap. Utilizing a passive flexure stage for contact control, we present our recent lithography results with a record 16 nm resolution (FWHM).</p>	19:45-20:00
PDP.7	<p>Bragg solitons in CMOS-compatible platform <u>Ezgi Sahin</u>^{1,2}, Andrea Blanco-Redondo³, Peng Xing¹, Doris K. T. Ng⁴, Ching E. Png², Dawn T. H. Tan¹, Benjamin J. Eggleton³ ¹Photonics Devices and Systems Group, Singapore University of Technology and Design, Singapore ²Institute of High Performance Computing, Agency for Science, Technology and Research, Singapore ³Institute of Photonics and Optical Science (IPOS), The Sydney Nano Institute, School of Physics, The University of Sydney, Australia. ⁴Institute of Microelectronics, A*STAR, Singapore We demonstrate Bragg soliton dynamics on CMOS-compatible platform for the first time. We provide complete time-resolved measurements of record high-order soliton compression and show third-order dispersion induced fission in an ultra-silicon-rich nitride cladding-modulated Bragg grating.</p>	20:00-20:15
PDP.8	<p>Versatile mid-infrared mode-locked fiber laser, electronically tunable from 2.97 to 3.30 μm <u>R. I. Woodward</u>, M. R. Majewski, S. D. Jackson MQ Photonics Research Centre, Macquarie University, Australia We demonstrate the first dysprosium mode-locked laser: the longest wavelength and most widely tunable mode-locked fiber laser to date. Picosecond pulses are generated by a novel frequency-shifted feedback mechanism using an intracavity acousto-optic tunable filter.</p>	20:15-20:30
PDP.9	<p>High-resolution Accurate Mosaic Imaging Technique for Laser Micro-fabrication using Motion-blur Compensation Jerome de Leon¹, Kenichi Murakami², <u>Tomohiko Hayakawa</u>³, Masatoshi Ishikawa^{2,3} ¹Department of Astronomy, Graduate School of Science, University of Tokyo, Japan ²Department of Creative Informatics, University of Tokyo, Japan ³Department of Information Physics and Computing, University of Tokyo, Japan In this paper, high-resolution and accurate imaging and mosaicing techniques for laser micro-fabrication target are described. The effectiveness of methods are validated for capturing 0.5 μm/pixel images and mosaicing with featureless patterned images.</p>	20:30-20:45

港鐵路綫圖 MTR system map

